TRANSFORMATION OF PHENOLIC COMPOUNDS OF PYROLYSIS BIO-OIL TO HIGH-VALUE CHEMICALS BY CATALYTIC HYDROTREATMENT

HODA SHAFAGHAT

**THESIS SUBMITTED IN FULFILLMENT
OF THE REQUIREMENTS FOR THE DEGREE OF
DOCTOR OF PHILOSOPHY**

**FACULTY OF ENGINEERING
UNIVERSITY OF MALAYA
KUALA LUMPUR**

2016

UNIVERSITI MALAYA

ORIGINAL LITERARY WORK DECLARATION

Name of Candidate: Hoda Shafaghat

Registration/Matric No: KHA110100

Name of Degree: DOCTOR OF PHILOSOPHY

Title of Project Paper/Research Report/Dissertation/Thesis ("this Work"):

TRANSFORMATION OF PHENOLIC COMPOUNDS OF PYROLYSIS BIO-OIL TO HIGH-VALUE CHEMICALS BY CATALYTIC HYDROTREATMENT

Field of Study: Reaction Engineering

I do solemnly and sincerely declare that:

(1) I am the sole author/writer of this Work;
(2) This Work is original;
(3) Any use of any work in which copyright exists was done by way of fair dealing and for permitted purposes and any excerpt or extract from, or reference to or reproduction of any copyright work has been disclosed expressly and sufficiently and the title of the Work and its authorship have been acknowledged in this Work;
(4) I do not have any actual knowledge nor ought I reasonably to know that the making of this work constitutes an infringement of any copyright work;
(5) I hereby assign all and every rights in the copyright to this Work to the University of Malaya ("UM"), who henceforth shall be owner of the copyright in this Work and that any reproduction or use in any form or by any means whatsoever is prohibited without the written consent of UM having been first had and obtained;
(6) I am fully aware that if in the course of making this Work I have infringed any copyright whether intentionally or otherwise, I may be subject to legal action or any other action as may be determined by UM.

Candidate's Signature **Date: 30 May 2016**

Subscribed and solemnly declared before,

Witness's Signature **Date: 30 May 2016**

Name: Pouya Sirous Rezaei
Designation: Department of Chemical Engineering,
Faculty of Engineering, University of Malaya

ABSTRACT

Pyrolysis bio-oil is recognized as a renewable and carbon-neutral fuel which could be potential alternative for depleting fossil fuels. However, bio-oil is highly oxygenated and needs to be upgraded prior to be used as fuel/fuel additive. Catalytic hydrodeoxygenation (HDO) is an efficient technique for bio-oil upgrading. The reaction pathway for HDO of bio-oil is unknown since it is a mixture of hundreds of different compounds. The study on mechanism of transformation of these compounds could be helpful to propose an overall pathway for HDO of bio-oil. Phenols which are derived from pyrolysis of lignin fraction of biomass are considered as attractive model compounds for study of bio-oil HDO since they are highly stable in HDO reaction. Reaction pathway and product selectivity in HDO of phenols are highly affected by catalyst type and process conditions. Bifunctional catalysts consisting of metal and acid sites are usually used for transformation of bio-oil/bio-oil model compounds to valuable hydrocarbons. Metal and acid sites are generally involved in hydrogenation/hydrogenolysis and dehydration/hydrocracking/dealkylation/alkylation/isomerization reaction mechanisms, respectively. In this work, product selectivity of hydrogenation of phenol, *o*-cresol, *m*-cresol and guaiacol (the most abundant phenolics of bio-oil) was investigated over combined catalysts of Pd/C with zeolite solid acids of HZSM-5 (Si/Al of 30, 50 and 80) and HY (Si/Al of 30 and 60) in an autoclave batch reactor. Catalytic activity and product distribution were affected by density and strength of zeolite acid sites. Meanwhile, bifunctional metal/acid catalysts of 5 wt% Ni/HBeta, 5 wt% Fe/HBeta, 2.5 wt% Ni-2.5 wt% Fe/HBeta (NiFe-5/HBeta) and 5 wt% Ni-5 wt% Fe/HBeta (NiFe-10/HBeta) were used for HDO of a phenolic bio-oil simulated by mixing phenol, *o*-cresol and guaiacol. Cycloalkanes and aromatic hydrocarbons were the dominant hydrocarbons obtained over monometallic catalysts of Ni/HBeta and Fe/HBeta, respectively. Bimetallic catalyst of NiFe/HBeta showed enhanced HDO efficiency compared with monometallic catalysts of

Ni/HBeta and Fe/HBeta due to the synergistic effect between the two metals. The effect of reaction temperature on HDO efficiency of NiFe-10/HBeta catalyst was investigated. Replacement of water with methanol as solvent in HDO of the simulated phenolic bio-oil over NiFe-10/HBeta remarkably reduced the selectivity towards hydrocarbons. High flammability of hydrogen gas in contact with air leads to difficult control of high pressurized hydrogen gas in large-scale systems. Meanwhile, molecular hydrogen production is a costly industrial process. Thus, hydrogenation study using hydrogen donor (H-donor) material as alternative for hydrogen gas could be useful in terms of cost and safety control. In this study, the potential of decalin and tetralin for use as hydrogen source was investigated in transfer hydrogenation of renewable lignin-derived phenolic compounds (phenol, *o*-cresol and guaiacol) and a simulated phenolic bio-oil over Pd/C and Pt/C catalysts. Reaction mechanisms of H-donor dehydrogenation and phenolics hydrogenation were studied. Furthermore, the influence of water content on transfer hydrogenation activity was studied by employing the water to donor ratios of 0/100, 25/75, 50/50 and 75/25 g/g. The catalysts used in this research were characterized by N_2 adsorption, XRF, XRD, NH_3-TPD, H_2-TPD and TGA, and liquid products were analyzed using GC-MS.

ABSTRAK

Pirolisis bio-minyak diiktiraf sebagai bahan api yang boleh diperbaharui dan bebas karbon yang boleh menjadi potensi alternatif untuk bahan api fosil yang semakin berkurangan. Walau bagaimanapun, bio-minyak adalah sangat beroksigen dan perlu dinaik taraf sebelum digunakan sebagai bahan tambahan bahan api/bahan api. Hydrodeoxygenation pemangkin (HDO) adalah satu teknik berkesan untuk peningkatan bio-minyak. Tengah-tengah jalan reaksi untuk HDO bio-minyak adalah tidak diketahui kerana ia adalah campuran beratus-ratus sebatian yang berbeza. Kajian ke atas mekanisme transformasi sebatian ini boleh menjadi berguna untuk mencadangkan satu laluan keseluruhan untuk HDO bio-minyak. Fenol yang diperolehi daripada pirolisis pecahan lignin biojisim adalah dianggap sebatian model yang menarik untuk kajian HDO bio-minyak kerana mereka adalah sangat stabil dalam tindak balas HDO. Laluan reaksi dan pemilihan produk dalam HDO fenol adalah sangat dipengaruhi oleh jenis pemangkin dan proses syarat. Pemangkin Bifunctional terdiri daripada logam dan asid laman biasanya digunakan untuk transformasi sebatian model bio-minyak/bio-minyak untuk hidrokarbon berharga. Logam dan asid laman umumnya terlibat dalam penghidrogenan/hydrogenolysis dan dehidrasi/hidrocracking/dealkilasi/alkilasi/ isomerisasi tindak balas mekanisme, masing-masing. Dalam karya ini, pemilihan produk penghidrogenan fenol, o-cresol, m-cresol dan guaiacol (yang phenolic paling banyak bio-minyak) telah disiasat berhubung pemangkin gabungan Pd/C dengan asid pepejal zeolite daripada HZSM-5 (Si/Al: 30, 50 dan 80) dan HY (Si/Al: 30 dan 60) dalam reaktor kumpulan autoklaf. Aktiviti mangkin dan pengedaran produk terjejas oleh ketumpatan dan kekuatan tapak asid zeolit. Sementara itu, bifunctional logam/asid pemangkin 5 w% Ni/HBeta, 5 w% Fe/HBeta, 2.5 w% Ni-2.5 w% Fe/HBeta (NiFe-5/HBeta) dan 5 w% Ni-5 w% Fe/HBeta (NiFe-10/HBeta) telah digunakan untuk HDO daripada fenolik bio-minyak simulasi dengan mencampurkan fenol, o-cresol dan guaiacol. Sikloalkana dan

hidrokarbon aromatik adalah hidrokarbon dominan diperolehi lebih pemangkin monometallic Ni/HBeta dan Fe/HBeta, masing-masing. Pemangkin Bimetallic daripada NiFe/HBeta menunjukkan peningkatan kecekapan HDO berbanding monometallic pemangkin Ni/HBeta dan Fe/HBeta disebabkan oleh kesan sinergi antara kedua-dua logam. Kesan suhu tindak balas kepada kecekapan HDO daripada NiFe-10/HBeta pemangkin telah dikaji. Penggantian air dengan metanol sebagai pelarut dalam HDO daripada fenolik simulasi bio-minyak lebih NiFe-10/HBeta amat dikurangkan pemilihan ke arah hidrokarbon. Kemudahbakaran tinggi gas hidrogen dalam hubungan dengan udara membawa kepada kawalan sukar tinggi gas hidrogen bertekanan dalam sistem berskala besar. Sementara itu, pengeluaran hidrogen molekul adalah proses industri mahal. Oleh itu, kajian penghidrogenan menggunakan hidrogen penderma (H-penderma) bahan sebagai alternatif bagi gas hidrogen boleh menjadi berguna dari segi kos dan keselamatan kawalan. Dalam kajian ini, potensi decalin dan tetralin untuk digunakan sebagai sumber hidrogen telah disiasat dalam pemindahan penghidrogenan diperbaharui sebatian lignin yang diperolehi fenolik (fenol, o-cresol dan guaiacol) dan fenolik simulasi bio-minyak lebih Pd/C dan Pt/C pemangkin. Mekanisme tindak balas nyahhidrogenan H-penderma dan fenolik penghidrogenan telah dikaji. Tambahan pula, pengaruh kadar air terhadap aktiviti pemindahan penghidrogenan telah dikaji dengan menggunakan air dengan nisbah penderma 0/100, 25/75, 50/50 dan 75/25 g/g. Pemangkin yang digunakan dalam kajian ini telah disifatkan oleh N_2 penjerapan, XRF, XRD, NH_3-TPD, H_2-TPD dan TGA, dan produk cecair dianalisis dengan menggunakan GC-MS.

ACKNOWLEDGEMENTS

I would like to express my sincere gratitude to my advisor Prof. Dr. Wan Mohd Ashri Bin Wan Daud for giving me the opportunity to carry out the PhD within a great project and great research group. His patience and kindness have left a lasting impression on me.

I would like to thank all the people I met here at University of Malaya who made my PhD career happy and memorable. I want to give my special thanks to my beloved husband, Pouya Sirous Rezaei, for his unconditional love, continuous encouragement and devotion. He was also my friend and colleague during the study at UM. Numerous discussions with Pouya and his valuable insights and efforts were a great help in this study and are appreciatively acknowledged. I also would like to thank Masoud Asadieraghi for his friendly supports and helps during my research at chemical engineering department.

I owe a special gratitude to my family who always supported and believed in me. Their encouragement and unconditional love made possible what I have today.

TABLE OF CONTENTS

TITLE PAGE……..…..i

ORIGINAL LITERARY WORK DECLARATION FORM…….….ii

ABSTRACT……iii

ABSTRAK…….....v

ACKNOWLEDGEMENTS……..vii

TABLE OF CONTENTS.....viii

LIST OF FIGURES…….....……xiii

LIST OF SCHEMES…….....……..xiv

LIST OF TABLES…….....……...xvi

LIST OF SYMBOLS AND ABBREVIATIONS…….....…...xix

CHAPTER 1: INTRODUCTION…….……..1

1.1 General……....……1

1.2 Bifunctional metal/acid catalysts for HDO of phenolic compounds of pyrolysis bio-oil…….6

1.3 Transfer hydrogenation of phenolic compounds of pyrolysis bio-oil…….....9

1.4 Thesis objectives…….……9

1.5 Thesis organization…….....……...10

CHAPTER 2: LITERATURE REVIEW……..……...13

2.1 HDO mechanism of phenolic compounds…….……13

2.1.1 HDO mechanism of phenol……...……...…13

2.1.2 HDO mechanism of cresol……..……..…24

2.1.3 HDO mechanism of guaiacol ……..……31

2.1.4 HDO mechanism of anisole……...…..…….....42

2.2 Effective parameters on reaction selectivity of catalytic HDO of phenol, cresol, guaiacol and anisole…….…….46

2.2.1 Catalyst promoters…….……...…...46

2.2.1.1 Effect of promoters on catalyst structure……47

2.2.1.2 Effect of promoters on catalyst active site……..49

2.2.2 Catalyst support……...……...….52

2.2.3 Solvent……....61

2.2.4 Catalyst preparation procedure……63

2.2.5 Operating conditions……...69

2.2.6 Co-feeding……...73

2.3 Deactivation of HDO catalysts……..77

2.3.1 Deactivation caused by coke……78

2.3.2 Deactivation caused by poisoning……82

2.3.3 Deactivation caused by thermal degradation……84

2.3.4 Deactivation caused by desulfurization……85

2.4 Transfer hydrogenation of phenol……86

CHAPTER 3: MATERIALS AND METHODS……..91

3.1 Materials…….……..91

3.2 Commercial catalysts……..…….....…...91

3.3 Modified catalysts…..…….....……..91

3.4 BET surface area and porosity analysis.…….....92

3.5 X-ray flouresence (XRF) analysis……..…….....92

3.6 X-ray diffraction (XRD) analysis……..92

3.7 Temperature-programmed desorption of ammonia (NH_3-TPD)……93

3.8 Temperature-programmed desorption of hydrogen (H_2-TPD)……..93

3.9 Catalytic activity measurement…….....93

3.9.1 Catalytic hydrogenation of phenol, cresol and guaiacol over physically mixed catalysts of Pd/C and zeolite solid acids…….....93

3.9.2 Catalytic HDO of simulated phenolic bio-oil over bifunctional metal/acid catalysts of Ni/HBeta, Fe/HBeta and NiFe/HBeta…….....95

3.9.3 Using decalin and tetralin as hydrogen source for transfer hydrogenation of renewable lignin-derived phenolics over Pd/C and Pt/C catalysts…..96

3.10 Product analysis...……....……...97

3.11 Catalyst regeneration……...98

3.12 Coke quantification…….....99

CHAPTER 4: RESULTS AND DISCUSSION…….....100

4.1 Catalytic hydrogenation of phenol, cresol and guaiacol over physically mixed catalysts of Pd/C and zeolite solid acids.…….....…100

4.1.1 Physicochemical characteristics of catalysts…….....…100

4.1.2 Catalytic hydrogenation of phenol.…….....…104

4.1.3 Catalytic hydrogenation of cresol……..107

4.1.4 Catalytic hydrogenation of guaiacol……..111

4.2 Catalytic hydrodeoxygenation of simulated phenolic bio-oil to cycloalkanes and aromatic hydrocarbons over bifunctional metal/acid catalysts of Ni/HBeta, Fe/HBeta and NiFe/HBeta.…….....…..113

4.2.1 Physicochemical characteristics of catalysts.…….....113

4.2.2 HDO of simulated phenolic bio-oil over Ni/HBeta, Fe/HBeta and NiFe/HBeta……..117

4.2.3 Temperature dependence of product distribution of simulated bio-oil HDO over NiFe-10/HBeta…….……....….125

4.2.4 Effect of methanol solvent on HDO of simulated phenolic bio-oil over NiFe-10/HBeta…….127

4.3 Using decalin and tetralin as hydrogen source for transfer hydrogenation of renewable lignin-derived phenolics over activated carbon supported Pd and Pt catalysts……...…….....….129

4.3.1 Physicochemical characteristics of catalysts…….....129

4.3.2 Mechanism of dehydrogenation of decalin and tetralin…….131

4.3.3 Transfer hydrogenation of phenol, *o*-cresol and guaiacol……..134

4.3.4 Kinetic study of hydrogenation/transfer hydrogenation of phenol, *o*-cresol and guaiacol over Pt/C catalyst……142

4.3.5 Role of water solvent in transfer hydrogenation of phenol using decalin and tetralin over Pt/C catalyst……...145

4.3.6 Transfer hydrogenation of simulated bio-oil consisting of phenol, *o*-cresol and guaiacol…….146

CHAPTER 5: CONCLUSIONS AND RECOMMANDATIONS FOR FUTURE STUDIES…….....……...148

5.1 Conclusions…….....…….148

5.1.1 Effective parameters on selective catalytic hydrodeoxygenation of phenolic compounds of pyrolysis bio-oil to high-value hydrocarbons……148

5.1.2 Catalytic hydrogenation of phenol, cresol and guaiacol over physically mixed catalysts of Pd/C and zeolite solid acids…..…….....……149

5.1.3 Catalytic hydrodeoxygenation of simulated phenolic bio-oil to cycloalkanes and aromatic hydrocarbons over bifunctional metal/acid catalysts of Ni/HBeta, Fe/HBeta and NiFe/HBeta...……150

5.1.4 Using decalin and tetralin as hydrogen source for transfer hydrogenation of renewable lignin-derived phenolics over activated carbon supported Pd and Pt catalysts……...…….....151

5.2 Recommendations for future studies…….....152

REFERENCES……...……..154

LIST OF PUBLICATIONS……..……...175

LIST OF FIGURES

Figure 3.1: Autoclave batch reactor used for hydrotreatment of phenolic model compounds of bio-oil……94

Figure 4.1: Nitrogen adsorption-desorption isotherms of Pd/C, HY and HZSM-5 catalysts……..101

Figure 4.2: Pore size distribution (from BJH desorption data); Halsey plot with Faas correction: (a) Pd/C and HY zeolites (b) HZSM-5 zeolites…..……...101

Figure 4.3: NH_3-TPD curves of HZSM-5 and HY zeolites with different Si/Al ratios……...103

Figure 4.4: XRD patterns of HBeta, Ni/HBeta, Fe/HBeta and NiFe/HBeta……...115

Figure 4.5: NH_3-TPD curves of HBeta, Ni/HBeta, Fe/HBeta and NiFe/HBeta…….116

Figure 4.6: H_2-TPD profiles of Ni/HBeta, Fe/HBeta and NiFe/HBeta……..117

Figure 4.7: Pressure dependency of phenol conversion and (cyclohexane + methylcyclopentane)/benzene ratio over Ni/HBeta and Fe/HBeta catalysts. Reaction conditions: phenol, 2 g; water, 100 ml; catalyst, 2 g; temperature, 300 °C; reaction time, 4 h and rpm, 800…….123

Figure 4.8: XRD patterns of fresh and five times used NiFe-10/HBeta catalyst……125

Figure 4.9: Nitrogen adsorption-desorption isotherms of Pd/C and Pt/C catalysts…130

Figure 4.10: XRD patterns of Pd/C and Pt/C catalysts……...131

Figure 4.11: Catalytic conversion (a) and cyclohexanone selectivity (b) in hydrogenation/transfer hydrogenation of phenol over Pt/C catalyst……...144

Figure 4.12: Catalytic conversion (a) and methylcyclohexanone selectivity (b) in hydrogenation/transfer hydrogenation of *o*-cresol over Pt/C catalyst……144

Figure 4.13: Catalytic conversion (a) and cyclohexanone selectivity (b) in hydrogenation/transfer hydrogenation of guaiacol over Pt/C catalyst……144

LIST OF SCHEMES

Scheme 2.1: General reaction scheme for HDO of phenol……...14

Scheme 2.2: Reaction pathway for conversion of phenol to bicyclic compounds over Pd/HBeta and Pt/HY catalysts……..15

Scheme 2.3: HDO mechanism of phenol over Co–Mo–O–B amorphous catalyst…...15

Scheme 2.4: Simple reaction scheme of HDO of *p*-cresol……25

Scheme 2.5: General scheme of guaiacol conversion pathways……...32

Scheme 2.6: Proposed reaction pathway for conversion of guaiacol to cyclohexane over Pt, Rh, Pd, and Ru catalysts supported on Al_2O_3, SiO_2-Al_2O_3, and NAC……33

Scheme 2.7: HDO network of anisole……..42

Scheme 2.8: Phenol hydrotreating mechanism for formation of cyclohexylbenzene, cyclohexylphenol and benzene over CoMo/MgO……52

Scheme 2.9: Principal reaction network for guaiacol HDO occurring on (a) CoMoS/Al_2O_3; (b) CoMoS/TiO_2; (c) CoMoS/ZrO_2……54

Scheme 2.10: Non-planar adsorption of phenol producing cyclohexanone (a); Co-planar adsorption of phenol producing cyclohexanol (b)……..55

Scheme 2.11: Proposed reaction network for *m*-cresol conversion over Pt/Al_2O_3…...56

Scheme 2.12: Proposed reaction pathways of anisole HDO over (a) HBeta; (b) 1% Pt/SiO_2; (c) 1% Pt/HBeta……..60

Scheme 2.13: Proposed reaction mechanisms for hydroprocessing of *p*-cresol in polar solvent (I) and non-polar solvent (II)……63

Scheme 2.14: Hydrogenation of cyclohexanol to form cyclohexene and cyclohexanethiol by elimination (E_1 and E_2) and nucleophilic substitution (S_N1 and S_N2) reactions, respectively……..75

Scheme 2.15: *p*-Cymene formation due to reduction of vanadium by *α*-terpinene (a); The adsorption of oxygen atom of catechol by V(III) (b); The total scheme of guaiacol HDO on V_2O_5/Al_2O_3 catalyst (c)……..76

Scheme 4.1: Reaction pathways of phenol hydrogenation over Pd/C and Pd/C mixed with HZSM-5 or HY zeolites; HDO: hydrodeoxygenation, HYD: hydrogenation, DHY: dehydration, EAS: electrophilic aromatic substitution……107

Scheme 4.2: Mechanisms of hydrogenation of *o*-cresol over combined catalysts of Pd/C and zeolite solid acids……110

Scheme 4.3: Mechanisms of hydrogenation of *m*-cresol over combined catalysts of Pd/C and zeolite solid acids……111

Scheme 4.4: Reaction mechanisms of guaiacol hydrogenation over 10 wt% Pd/C catalyst and combined catalysts of Pd/C and zeolite solid acids……113

Scheme 4.5: Proposed reaction mechanism for catalytic HDO of simulated phenolic bio-oil over Ni/HBeta, Fe/HBeta and NiFe/HBeta catalysts; HYD: hydrogenation, DDO: direct deoxygenation (hydrogenolysis), DMO: demethoxylation, DME: demethylation, AL: alkylation, DHY: dehydration……122

Scheme 4.6: Acetal reaction occurred during catalytic HDO of simulated phenolic bio-oil over NiFe-10/HBeta using methanol as solvent……129

Scheme 4.7: Reaction mechanism of phenol hydrogenation over Pt/C and Pd/C using H_2 gas, decalin and tetralin as hydrogen source; HYD: hydrogenation……...139

Scheme 4.8: Reaction mechanism of *o*-cresol hydrogenation over Pt/C and Pd/C using H_2 gas, decalin and tetralin as hydrogen source; HYD: hydrogenation, HDO: hydrodeoxygenation……...140

Scheme 4.9: Reaction mechanism of guaiacol hydrogenation over Pt/C and Pd/C using H_2 gas, decalin and tetralin as hydrogen source; DMO: demethoxylation, HYD: hydrogenation, DME: demethylation……141

LIST OF TABLES

Table 2.1: Overview of catalysts and operating conditions applied in HDO processing of phenol……..16

Table 2.2: Overview of catalysts and operating conditions applied in HDO processing of cresols……26

Table 2.3: Overview of catalysts and operating conditions applied in HDO processing of guaiacol……34

Table 2.4: Overview of catalysts and operating conditions applied in HDO processing of anisole……..43

Table 2.5: Transfer hydrogenation of phenol at different conditions……...90

Table 4.1: Textural properties of 10 wt% Pd/C and zeolite solid acids……..100

Table 4.2: Ammonia desorption temperature and amount of desorbed ammonia from zeolite acid sites obtained by TPD analysis……103

Table 4.3: Hydrogenation of phenol over mixed catalysts of Pd/C and zeolite solid acids……...106

Table 4.4: Hydrogenation of *o*-cresol over mixed catalysts of Pd/C and zeolite solid acids……...110

Table 4.5: Hydrogenation of *m*-cresol over mixed catalysts of Pd/C and zeolite solid acids……...110

Table 4.6: Hydrogenation of guaiacol over mixed catalysts of Pd/C and zeolite solid acids……...112

Table 4.7: Physicochemical properties of HBeta, Ni/HBeta, Fe/HBeta and NiFe/HBeta catalysts……..114

Table 4.8: Catalytic performance of Ni/HBeta, Fe/HBeta and NiFe/HBeta in HDO of simulated bio-oil……121

Table 4.9: Selectivity of phenolic and oxygen-free products of fresh and reused NiFe-10/HBeta as well as physical properties of regenerated NiFe-10/HBeta……125

Table 4.10: Temperature dependence of products selectivity and coke formation over NiFe-10/HBeta in HDO of simulated phenolic bio-oil……...126

Table 4.11: The effect of solvent type on product distribution of HDO of simulated phenolic bio-oil over NiFe-10/HBeta. Reaction conditions: simulated bio-oil, 4 g; solvent, 100 ml; catalyst, 4 g; temperature, 300 °C; reaction time, 4 h and rpm, 800…….128

Table 4.12: Chemical and textural properties of Pd/C and Pt/C catalysts: specific surface area (S_{BET}), micropore surface area (S_{micro}), micropore and mesopore volume (V_{micro} and V_{meso}), total pore volume (V_{total}), average pore width (D) and metal content……130

Table 4.13: Product selectivity of dehydrogenation of decalin and tetralin over Pd/C and Pt/C catalysts. Reaction conditions: H-donor, 50 g; water, 50 g; catalyst, 0.6 g; temperature, 275 °C; reaction time, 4 h and rpm, 500……133

Table 4.14: Product selectivity (mol%) and dehydrogenation conversion (mol%) of decalin and tetralin over Pt/C and Pd/C catalysts in presence of phenol, *o*-cresol and guaiacol. Reaction conditions: H-donor, 50 g; water, 50 g; phenolic compounds, 12 g; catalyst, 0.6 g; temperature, 275 °C; reaction time, 4 h and rpm, 500……134

Table 4.15: Product selectivity obtained from hydrogenation of phenol, *o*-cresol and guaiacol in absence of catalyst. Reaction conditions: H_2 gas, 16 bar; H-donor, 50 g; water, 100 g for hydrogenation and 50 g for transfer hydrogenation; phenolic compounds, 12 g; temperature, 275 °C; reaction time, 4 h and rpm, 500……136

Table 4.16: Product selectivity obtained from hydrogenation/transfer hydrogenation of phenol over Pt/C and Pd/C catalysts……..138

Table 4.17: Product selectivity obtained from hydrogenation/transfer hydrogenation of *o*-cresol over Pt/C and Pd/C catalysts……139

Table 4.18: Product selectivity obtained from hydrogenation/transfer hydrogenation of guaiacol over Pt/C and Pd/C catalysts……141

Table 4.19: Impact of water content on catalytic activity of Pt/C in transfer hydrogenation of phenol. Reaction conditions: Pt/C, 0.6 g; phenol, 12 g; total weight of water and decalin/tetralin, 100 g; temperature, 275 °C; reaction time, 4 h and rpm, 500…….145

Table 4.20: Product selectivity obtained from hydrogenation/transfer hydrogenation of bio-oil over Pd/C and Pt/C catalysts. Reaction conditions: simulated bio-oil, 12 g; catalyst, 0.6 g; water, 50 g; H-donor, 50 g; temperature, 275 °C; reaction time, 4 h and rpm, 500…….147

LIST OF SYMBOLS AND ABBREVIATIONS

AC	Activated carbon
AHM	Ammonium hepta molybdate
AL	Alkylation
ASA	Amorphous silica alumina
BET	Brunauer, Emmett and Teller
BJH	Barrett-Joyner-Halenda
C	Carbon
CCA	Carbon-coated alumina
Conv.	Conversion
DDO	Direct deoxygenation
DHY	Dehydration
DME	Demethylation
DMO	Demethoxylation
E_a	Activation energy
EAS	Electrophilic aromatic substitution
GC	Gas chromatograph
GHG	Greenhouse gas
H	Hydrogen
HDO	Hydrodeoxygenation
HDS	Hydrodesulfurization
HPS	Hypercrosslinked polystyrene
HYD	Hydrogenation
LHSV	Liquid hourly space velocity
MoNaph	Molybdenum naphthenate

MS	Mass spectrometer
N	Nitrogen
NAC	Nitric acid treated carbon black
NIST	National Institute of Standards and Technology
P	Pressure
SRGO	Straight run gas oil
t	Time
T	Temperature
TCD	Thermal conductivity detector
TDM-D	Exfoliated MoS_2 dispersed in decalin
TDM-W	Exfoliated MoS_2 dispersed in water
TGA	Thermogravimetric analysis
TOF	Turnover frequency
TPD	Temperature-programmed desorption
XRD	X-ray diffraction
XRF	X-ray flouresence
θ	Bragg angle
λ	X-ray wavelength

CHAPTER 1: INTRODUCTION

1.1 General

Approximately 80% of the world total primary sources of energy are provided by the fossil fuels such as petroleum, coal and natural gas (Wiggers, Meier, Wisniewski, Barros, & Maciel, 2009). In accord with the United Nations Intergovernmental Panel on Climate Change (IPCC), increase of the greenhouse gas (GHG) emission causes the climate change and the increase in global average temperature. Power generating plants based on fossil fuels are the main sources of GHG emissions. In general, increase of energy request, depletion of fossil fuel resources as well as growing environmental concerns have raised the importance of finding renewable and environmentally friendly fuel resource alternatives. Lignocellulosic biomass consisting of cellulose, hemicellulose and lignin is a significant source for production of fuels and valuable chemicals (Yoshikawa et al., 2014; Yoshikawa et al., 2013). Fuels from biomass (bio-fuels) have, in principle, lower carbon emissions because they are produced within the short-term carbon cycle, and their combustion only returns as much CO_2 to the atmosphere as plant growth has taken out. Hence, unlike the burning of fossil fuels, the combustion of bio-fuels has the potential to be carbon neutral (Wiggers, Wisniewski, Madureira, Barros, & Meier, 2009).

There are two main routes available for producing liquid bio-fuels from biomass; one involves thermochemical processing and the other biochemical processing. Thermochemical processing defines the conversion of biomass into a range of products by thermal decay and chemical reformation, and essentially involves heating biomass in the presence of different concentrations of oxygen. The exclusion of oxygen during heating is a process named pyrolysis, which produces various organic liquids (bio-oil), combustible gas and solid char (Xu, Ferrante, Briens, & Berruti, 2009). Fast pyrolysis of biomass is a highly favorable technology for production of high yield of liquid fuel (up

to 70 wt%) (González-Borja & Resasco, 2011; Romero, Richard, Renème, & Brunet, 2009; Wildschut, Arentz, Rasrendra, Venderbosch, & Heeres, 2009; Wildschut et al., 2010; Wildschut, Mahfud, Venderbosch, & Heeres, 2009; Wildschut, Melián-Cabrera, & Heeres, 2010). The liquid bio-oil has a higher bulk and energy density and is easier to transport and store than the original biomass. Furthermore, the bio-oil comprises valuable organic components which can be extracted for other applications before the rest is used as a fuel (Xu et al., 2009). It has been observed that by adding bio-fuels to the petrodiesel fuels, the properties related to the injection and lubrication of the fuel in the engines were enhanced (Sharma, Suarez, Perez, & Erhan, 2009).

Due to the high oxygen content of biomass (around 50 wt%), bio-oil obtained from pyrolysis of biomass is highly oxygenated (He, Zhao, & Lercher, 2014). Pyrolysis bio-oil has high contents of water (15-30 wt%) and oxygen (40-55 wt%) which cause some undesirable properties such as poor chemical and thermal stability, high viscosity (poor storage stability), corrosiveness (high acidity) and low heating value (Busetto et al., 2011; Elliott & Hart, 2009; Joshi & Lawal, 2012; Romero et al., 2009; Şenol, Viljava, & Krause, 2007; Xiong, Fu, Zeng, & Guo, 2011). These negative properties of bio-oil can be removed by elimination of its oxygen content through an upgrading process. Bio-fuel derived via deoxygenation reactions is more environmental friendly and more suitable for blending with petrodiesel fuels.

Catalytic hydrodeoxygenation (HDO) and zeolite cracking are considered as the two general techniques for bio-oil upgrading. HDO is a noteworthy method for bio-oil upgrading performed in a heterogeneous system including solid catalyst, hydrogen gas and liquid bio-oil under severe conditions (150-450 °C, 50-250 bar) (Mercader, Koehorst, Heeres, Kersten, & Hogendoorn, 2011; Elliott, 2007; Fisk et al., 2009; Joshi & Lawal, 2012; Kobayashi, Ohta, & Fukuoka, 2012; Mortensen, Grunwaldt, Jensen, Knudsen, & Jensen, 2011; Wang, Fang, He, Hu, & Wu, 2011; Wildschut et al., 2009; Wildschut et al.,

2010; Wildschut et al., 2009; Wildschut et al., 2010; Yang, Gilbert, & Xu, 2009). In catalytic HDO of bio-oil, oxygen is eliminated as water and/or carbon oxides giving a high grade oil product equivalent to crude oil (Joshi & Lawal, 2012; Romero, Richard, & Brunet, 2010; Wildschut et al., 2009; Wildschut et al., 2010). Supported and/or unsupported conventional desulfurization catalysts, noble metal and transition metal catalysts have been applied in catalytic HDO process. Zeolite cracking is an alternative path, where zeolites, i.e. HZSM-5, are used as catalysts for the deoxygenation reaction. In these systems hydrogen is not a requirement, so operation is performed at atmospheric pressure. Overall, oil from zeolite cracking is of a low grade, with heating values approximately 25% lower than that of crude oil. Among the two mentioned techniques, HDO appears to be an appropriate choice for producing sustainable fuels, because of the high carbon efficiency and thereby a high production potential, as zeolite cracking cannot produce fuels of acceptable grade for the current infrastructure (Mortensen et al., 2011).

In bio-oil upgrading through HDO process, use of hydrogen leads to the mechanisms of removing oxygen and saturating double bounds. The principal reaction for HDO is hydrodeoxygenation and can be generally written as Eq. (1-1) (Mortensen et al., 2011):

$$CH_{1.4}O_{0.4} + 0.7\,H_2 \rightarrow 1\ \text{“}CH_2\text{”} + 0.4\,H_2O \quad (1.1)$$

where “CH_2” symbolizes an undetermined hydrocarbon product. As shown in this conceptual reaction, water is produced in HDO mechanism, so it is expected that at least two liquid phases of organic and aqueous are observed as product. Based on the stoichiometry of Eq. (1-1), maximum oil yield of 56-58 wt% could be obtained by the complete deoxygenation. However, the complete deoxygenation indicated by Eq. (1-1) is rarely achieved due to the span of reactions taking place; instead a product with residual oxygen will often be formed (Mortensen et al., 2011). High pressure of hydrogen which is generally used in HDO process causes a higher solubility of hydrogen in the oil and

thus a higher availability of hydrogen in the catalyst vicinity. High avalibility of hydrogen on catalytic active sites increases the reaction rate and decreases coking in the reactor.

A pronounced problem in HDO process is catalyst deactivation which can occur via catalyst poisoning by water, catalyst sintering, metal deposition and/or coking. The extent of these phenomena depends on the catalyst type, but coke formation has proven to be a general problem and the main cause for deactivation of catalyst. Carbon is essentially produced through polycondensation and polymerization mechanisms on catalyst surface, forming polyaromatic species. Coke generation leads to the blockage of catalytic active sites by filling up the catalyst pore volume during the start-up of the system. The rates of carbon formation reactions could be considerably controlled by the type of feed injected into the system, but process conditions also play an important role. Coke formation increases by increasing catalyst acidity. Temperature also affects coke formation; at elevated temperatures, the increase of dehydrogenation rate leads to the increase in polycondensation rate. Generally, rising the reaction temperature leads to the enhanced carbon formation (Mortensen et al., 2011).

Selection of a suitable catalyst is the main focus of researchers for efficient hydrotreating of bio-oil. Many studies have been conducted to develop catalysts with high catalytic activity and stability, low hydrogen consumption and high selectivity towards direct removal of oxygen (Ghampson et al., 2012). So far, supported and/or unsupported conventional desulfurization catalysts, noble metal and transition metal catalysts have been applied in catalytic HDO (Bui, Laurenti, Afanasiev, & Geantet, 2011; Busetto et al., 2011; Elliott & Hart, 2009; Joshi & Lawal, 2012; Romero et al., 2009; Wang, Yang, Luo, Hu, & Liu, 2011; Wang et al., 2011; Whiffen & Smith, 2010; Wildschut et al., 2009; Wildschut et al., 2010). Carbon (Mercader et al., 2011; Elliott & Hart, 2009; Wildschut et al., 2009), alumina (Joshi & Lawal, 2012; Romero et al., 2010; Romero et al., 2009; Şenol, Viljava, et al., 2007; Wang et al., 2011), zeolites (Nimmanwudipong, Runnebaum,

Block, & Gates, 2011b; Runnebaum, Nimmanwudipong, Block, & Gates, 2010; Wang et al., 2011; Wang, He, Liu, Wu, & Fang, 2012; Xiong et al., 2011), silica (Bykova et al., 2011; Bykova et al., 2012; Li, Wang, & Chen, 2011; Yakovlev et al., 2009; Zhao, He, Lemonidou, Li, & Lercher, 2011; Zhao, Li, Bui, & Oyama, 2011), zirconia (Bui, Laurenti, Delichère, & Geantet, 2011; Bykova et al., 2011; Bykova et al., 2012; Fisk et al., 2009; Gutierrez, Kaila, Honkela, Slioor, & Krause, 2009) and titania (Bui, Laurenti, Delichère, et al., 2011; Fisk et al., 2009; Wildschut et al., 2009) are the common materials used as catalyst support in HDO.

The reaction pathway for HDO of bio-oil is still unknown since it contains several hundreds of various organic compounds like acids, alcohols, aldehydes, esters, ketones, sugars, phenols and phenol derivatives resulting in hundreds of concurrent reactions during HDO of bio-oil (Fisk et al., 2009; Joshi & Lawal, 2012; Romero et al., 2010; Romero et al., 2009; Şenol, Viljava, et al., 2007; Wildschut et al., 2010). Therefore, investigation on the transformation of bio-oil model compounds seems to be necessary in order to attain sufficient knowledge for prediction of an overall reaction pathway for bio-oil HDO (Joshi & Lawal, 2012; Wildschut et al., 2010). Generally, model compounds are selected among the most reactive bio-oil compounds which lead to bio-oil instability (Busetto et al., 2011). Since reactive phenolic compounds which are mainly formed through pyrolysis of lignin fraction of biomass, lignin is a phenol based polymer, (Yoshikawa et al., 2014; Zhao, Camaioni, & Lercher, 2012; Zhao & Lercher, 2012) constitute the main fraction of bio-oil (Li et al., 2011; Wan, Chaudhari, & Subramaniam, 2012; Wang, Yang, Luo, Peng, & Wang, 2011; Whiffen & Smith, 2010; Yoosuk, Tumnantong, & Prasassarakich, 2012a; Zhao et al., 2011) and the cleavage of $C_{aromatic}$-OH bond in these compounds is difficult (Wang, Yang, Luo, & Liu, 2010; Wang, Yang, Luo, Peng, et al., 2011), many researches have been conducted in order to find suitable catalytic systems for HDO of phenols. Furthermore, phenolic compounds of bio-oil are

the major cause for formation of coke precursors and catalyst deactivation during the upgrading process (Ibáñez, Valle, Bilbao, Gayubo, & Castaño, 2012; Wildschut et al., 2010). Therefore, hydrodeoxygenation of bio-oil phenolic compounds to value-added chemicals is a research field of great significance.

Generally, HDO of phenolic compounds leads to formation of aromatic and alicyclic products through direct hydrogenolysis and combined hydrogenation-hydrogenolysis reaction pathways, respectively (Massoth et al., 2006; Viljava, Komulainen, & Krause, 2000). Benzene, toluene and xylene (used as octane enhancer) are three typical aromatic compounds produced from HDO of phenols. They have several applications; apart from being used as fuel additives and solvents, they can be implemented for manufacture of various high value-added chemicals (Jae et al., 2011; Olcese et al., 2012; Zakzeski, Bruijnincx, Jongerius, & Weckhuysen, 2010). Cycloalkanes, cycloalcohols and cycloketones are also valuable alicyclic chamicals produced from HDO of phenolic compounds. Different parameters such as operating conditions, type of phenolic compound and catalyst properties affect reaction pathway and product selectivity in HDO of phenols (Mahfud, Ghijsen, & Heeres, 2007; Zhao et al., 2011).

1.2 Bifunctional metal/acid catalysts for HDO of phenolic compounds of pyrolysis bio-oil

Removal of hydroxyl functional group (-OH) of phenolic compounds could occur through two different reaction pathways: (i) direct deoxygenation or direct hydrogenolysis which is the cleavage of $C_{aromatic}$-OH bond to produce aromatic hydrocarbons; (ii) hydrogenation of aromatic ring which leads to formation of cycloalcohols as intermediate, followed by dehydration and further hydrogenation to form cycloalkenes and cycloalkanes, respectively. Reaction selectivity and degree of deoxygenation in catalytic conversion of phenolics is highly affected by the type and characteristics of catalyst. Noble metal

catalysts are recognized to be highly efficient for conversion of phenolic compounds into hydrocarbons. Pd, Ru, Pt and Rh supported on C, Al_2O_3, and ZrO_2 have been the most commonly used noble metal catalysts for HDO of phenolic model compounds of bio-oil to produce aromatic hydrocarbons and saturated cyclic compounds through hydrogenolysis and hydrogenation mechanisms, respectively (Gutierrez et al., 2009; Nimmanwudipong et al., 2011b; Wan et al., 2012; Wildschut et al., 2010; C. Zhao, Kou, Lemonidou, Li, & Lercher, 2009; Zhao et al., 2011). However, high cost of these catalysts makes them useless for industrial applications. Transition metal catalysts could be suitable replacement for expensive noble metal catalysts due to their high activity in reactions including hydrogen, and have been vastly used for hydrodeoxygenation of phenolic compounds. $NiCu/Al_2O_3$, $CoMo/Al_2O_3$, Ni_2P/SiO_2, Fe_2P/SiO_2, MoP/SiO_2, Co_2P/SiO_2, Co-Ni-Mo-B, Ni-W-B, La-Ni-W-B, Mo-S and Ni-Mo-S are the transition metal catalysts studied for HDO of phenolic compounds (Ardiyanti, Khromova, Venderbosch, Yakovlev, & Heeres, 2012; Wandas, Surygala, & Śliwka, 1996; Wang, Yang, Luo, & Liu, 2010; Wang, Yang, Luo, Peng, et al., 2011; Yoosuk et al., 2012a; Zhao et al., 2011).

Catalysts including both metal and acid functions are highly efficient for hydrotreating of bio-oil/bio-oil model compounds. Metal and acid sites accomplish hydrotreating reaction through hydrogenation/hydrogenolysis and dehydration/isomerization/alkylation/ condensation mechanisms, respectively (Echeandia et al., 2014; He et al., 2014; Procházková, Zámostný, Bejblová, Červený, & Čejka, 2007). Since dehydration of alcoholic intermediates proceeded by catalytic acid sites is one of the reaction steps in HDO of phenolics, the presence of acid sites is effective for enhanced deoxygenation through hydrogenation of phenolic compounds. The metal/acid dual functional catalysts are generally prepared by embedding metals into acidic supports. As an alternative to dual functional catalysts, supported or unsupported metal catalysts such as Pd/C and RANEY

Ni could be physically mixed with liquid (H_3PO_4) and/or solid acids (HZSM-5, sulfated zirconia, Nafion/SiO_2, Amberlyst 15) and used for hydrogenation of phenolic compounds of bio-oil (He et al., 2014; Zhao et al., 2009; Zhao, Kou, Lemonidou, Li, & Lercher, 2010; Zhao & Lercher, 2012). Zhao et al. (2010) reported that substituting liquid acid with solid acid enhances the hydrotreating efficiency of the mixed catalyst system. Brønsted acids are appropriate for hydrotreatment of oxygenated compounds due to the presence of H^+ sites in their structure which promote dehydration reaction. Zeolites contain Brønsted acid sites and have high shape selectivity and thermal/hydrothermal stability, and could be a suitable selection to proceed the acid-catalyzed reactions in HDO of phenolic compounds. Zeolites with optimum density and strength of acid sites seem to be suitable for hydrodeoxygenation of bio-oil/bio-oil model compounds. The structural framework of zeolite includes the atoms of silicon and/or aluminium having tetrahedral coordination to four oxygen atoms (Primo & Garcia, 2014; Smit & Maesen, 2008). A zeolite consisting of only SiO_4 is electrically neutral but the presence of each AlO_4 in zeolite framework makes a negative charge which can be compensated by a cation (Primo & Garcia, 2014; Smit & Maesen, 2008). The presence of AlO_4 species and cations in zeolite structure changes catalytic properties of zeolites. By compensating the negative charges with protons, zeolites become strong solid acids. Complete conversion of phenol to cycloalkanes was obtained over physically mixed catalysts of Pd/C and HZSM-5 which were used for hydrogenation and dehydration functions, respectively (Zhao & Lercher, 2012). Catalytic transformation of phenol over Ni/HZSM-5 was carried out through hydrogenation and dehydration mechanisms promoted by Ni metal and HZSM-5 acidic support, respectively (Song, Liu, Baráth, Zhao, & Lercher, 2015). Use of bifunctional catalyst of Pt/HBeta and monofunctional catalysts of HBeta and Pt/SiO_2 in HDO of anisole showed that catalytic activity of Pt/HBeta was higher than that of HBeta and Pt/SiO_2 in both transalkylation and hydrodeoxygenation of anisole (Zhu, Lobban,

Mallinson, & Resasco, 2011). Furthermore, remarkable degree of deoxygenation (above 93%) was achieved in HDO of mixed isomers of cresol over bifunctional catalyst of Pt/ZSM-5 (Wang et al., 2012).

1.3 Transfer hydrogenation of phenolic compounds of pyrolysis bio-oil

High-pressure hydrogen gas is commonly used for catalytic hydrogenation of bio-oil/bio-oil model compounds. High cost of hydrogen gas as well as difficult control of hydrogen pressurized systems due to its high flammability in contact with air necessitate the use of hydrogen donor (H-donor) compounds as alternative source of hydrogen. Hydrogen released from H-donor compounds could be reacted with hydrogen acceptors on catalytic active sites. Catalytic reduction of a molecule using hydrogen atom transferred from donor molecule is called transfer hydrogenation (Wang & Rinaldi, 2012). Transfer hydrogenation occurs at less severe operating condition compared with hydrogenation using explosive hydrogen (Liu et al., 2013; Vilches-Herrera, Werkmeister, Junge, Börner, & Beller, 2014). The exact mechanism of transfer hydrogenation reaction depends on type of H-donor and catalyst (Wei, Liu, Yang, & Deng, 2014). An efficient catalyst for transfer hydrogenation reaction should have high potential for adsorption of both hydrogen donor and acceptor molecules (Zhang, Ye, Xue, Guan, & Wang, 2014). Generally, it is supposed that both the reactions of hydrogen liberation from H-donor and hydrogen consumption by acceptor occur on the same catalytic active sites.

1.4 Thesis objectives

The main aim of this thesis is to study the transformation of phenolic model compounds of pyrolysis bio-oil to high-value components through catalytic hydrotreatment in a high-pressure batch reactor. This aim is precisely achieved through the following specific objectives:

- To investigate the importance of metal and catalytic acid site in product selectivity of catalytic hydrodeoxygenation of lignin-derived phenolics
- To design a bifunctional metal/acid catalyst efficient for selective catalytic hydrodeoxygenation of phenolic model compounds of bio-oil
- To study the feasibility of replacing hydrogen gas with liquid hydrogen donors for transfer hydrogenation of renewable lignin-derived phenolics

1.5 Thesis organization

The present thesis comprises five chapters including this introductory chapter which provides a general introduction to the subject. The remainder of the thesis is organized as follows. Chapter 2 gives a comprehensive literature overview on recently used catalysts in HDO of phenol, cresol isomers, guaiacol and anisole in order to find out how catalyst type and reaction conditions could affect product selectivity of the reaction. Reaction pathway and product selectivity in HDO of the phenolics are highly affected by type of catalyst promoters and supports, catalyst preparation procedure, solvent type, chemicals used as co-feed and operating conditions (i.e., temperature and pressure). The effects of these factors on selective production of high-value hydrocarbons of aromatics and alicyclics from HDO of phenol, cresol, guaiacol and anisole are discussed in chapter 2. Chapter 3 describes all the experimental methods used through this thesis for catalyst preparation and modification, catalyst analysis and characterization and catalytic hydrotreatment of phenolic compounds. Meanwhile, brief details of raw materials, analysis instruments and experimental setup are given in chapter 3. Results obtained from experimental works and discussions about the experimental data are presented in chapter 4 which includes three parts. In part 1, the reaction mechanisms of hydrogenation of phenols over physically mixed catalysts containing metal and acid active sites are investigated. Phenol, *o*-cresol, *m*-cresol and guaiacol (the most abundant phenolic

compounds of bio-oil) are used as model compounds to investigate the hydrogenation activity of 10 wt% Pd/C and combined catalysts of 10 wt% Pd/C with HZSM-5 or HY zeolites. Effects of metal and acid active sites on catalytic activity and product selectivity of hydrogenation process are studied. The dependency of catalytic properties of zeolite on its aluminium content is investigated by the use of HZSM-5 and HY with different Si/Al ratios of 30;50;80 and 30;60, respectively. The main purpose of part 2 is to develop a bifunctional metal/acid catalyst which is efficient for both hydrogenolysis and hydrogenation of phenolic compounds. Inexpensive mono- and bimetallic catalysts of 5 wt% Ni/HBeta, 5 wt% Fe/HBeta, 2.5 wt% Ni-2.5 wt% Fe/HBeta (NiFe-5/HBeta) and 5 wt% Ni-5 wt% Fe/HBeta (NiFe-10/HBeta) are used in hydrodeoxygenation of a simulated phenolic bio-oil consisting of phenol, *o*-cresol and guaiacol. Products selectivity of HDO of the simulated bio-oil over these bifunctional catalysts is determined. Meanwhile, reusability of bimetallic catalyst of NiFe-10/HBeta is examined for simulated bio-oil HDO. Reaction selectivity of NiFe-10/HBeta catalyst is evaluated in temperature range of 220-340 °C using water as solvent. Furthermore, the effect of using methanol as solvent on HDO efficiency of NiFe-10/HBeta catalyst is investigated. In part 3, catalytic transfer hydrogenation of phenol, *o*-cresol, guaiacol and simulated bio-oil consisting of phenol, *o*-cresol and guaiacol is investigated using oxygen-free H-donors of decalin and tetralin over Pd/C and Pt/C catalysts. The efficiency of decalin and tetralin is compared with that of H_2 gas. By the use of these hydrogen sources, the process yielded products similar to those generated by the gas-based hydrogenation system; unsaturated phenolic compounds were converted to saturated cycloketones and cycloalcohols. Meanwhile, kinetic study of transformation of phenol, *o*-cresol and guaiacol over Pt/C catalyst is carried out and the dependency of reaction rate on hydrogen source and reactant type is investigated. In addition, the influence of non-donor solvent of water on transfer hydrogenation of phenol over Pt/C is studied. Finally, chapter 5 provides a part-by-part

summary of our works and conclusions and gives suggestions for future research directions.

CHAPTER 2: LITERATURE REVIEW

2.1 HDO mechanism of phenolic compounds

2.1.1 HDO mechanism of phenol

Due to the very simple structure of phenol, it has extensively been applied as a model compound of bio-oil in hydrodeoxygenation process to study the reaction selectivity of different catalysts at various operating conditions. Hydroxyl functional group (-OH) is the only oxygen-containing group of phenol. Therefore, breaking the $C_{aromatic}$-OH bond is the main objective of phenol deoxygenation process. Indeed, due to the high dissociation energy of Ar-OH bond (468 kJ/mol) (Wang, Male, & Wang, 2013), removal of the oxygen atom of hydroxyl group is very difficult which is needed to be conducted at severe operating conditions (Wang, Yang, Luo, Hu, & Liu, 2010; Wang, Yang, Luo, Peng, & Wang, 2011). Generally, the cleavage of $C_{aromatic}$-OH bond can occur by dehydration or hydrodeoxygenation reactions. Dehydration is an acid-catalyzed elimination reaction which can occur when both α- and β-carbon atoms with respect to the oxygen atom are saturated (Şenol, Ryymin, Viljava, & Krause, 2007). Since none of these two carbon atoms are saturated in phenol molecule, dehydration reaction does not occur to eliminate the oxygen atom of phenol. In fact, catalytic hydrodeoxygenation of phenol generally proceeds in two parallel reaction pathways (Scheme 2.1). The first path is direct deoxygenation (DDO) or direct hydrogenolysis involving the cleavage of $C_{aromatic}$-OH bond to produce benzene as an aromatic product. The second path entails the hydrogenation of aromatic ring (HYD) which leads to the formation of cyclohexanol as an intermediate, followed by a rapid dehydration and further hydrogenation to form cyclohexene and cyclohexane, respectively. Meanwhile, in catalytic hydrogenation of phenol over Pd and Pt supported on zeolites of HBeta (Zhao, Camaioni, & Lercher, 2012) and HY (Hong, Miller, Agrawal, & Jones, 2010), phenol alkylation by cyclohexanol

intermediate occurred over zeolite acid sites leading to the formation of bicyclic compounds (Scheme 2.2). Phenol and hydrogen molecules are activated by catalytic functional groups to participate in deoxygenation process. It was reported by Wang et al. (2011) that in HDO of phenol over Co-Mo-B catalyst, the oxygen of phenol is adsorbed on Mo^{4+} Brønsted acid sites and $C_{aromatic}$-O bond is polarized and ruptured by nucleophilic attack of dissociative hydrogen adsorbed on the near Co active sites (Scheme 2.3). The free hydrogen adsorbed on the active sites of Co can contribute to deoxygenation of phenol by DDO or HYD reaction pathways. Several types of catalysts have been examined for HDO of phenol. Table 2.1 presents a summary of previous studies in HDO of phenol describing the effects of different catalysts and operating conditions on product selectivity.

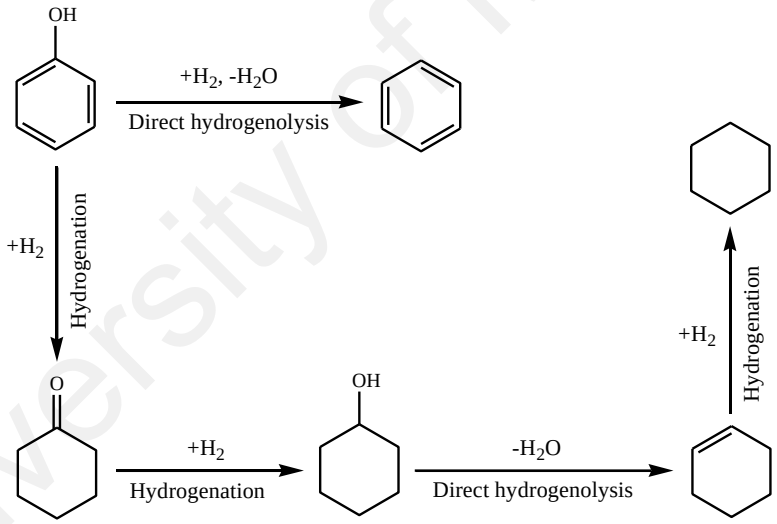

Scheme 2.1: General reaction scheme for HDO of phenol (Wang, Yang, Luo, & Liu, 2010).

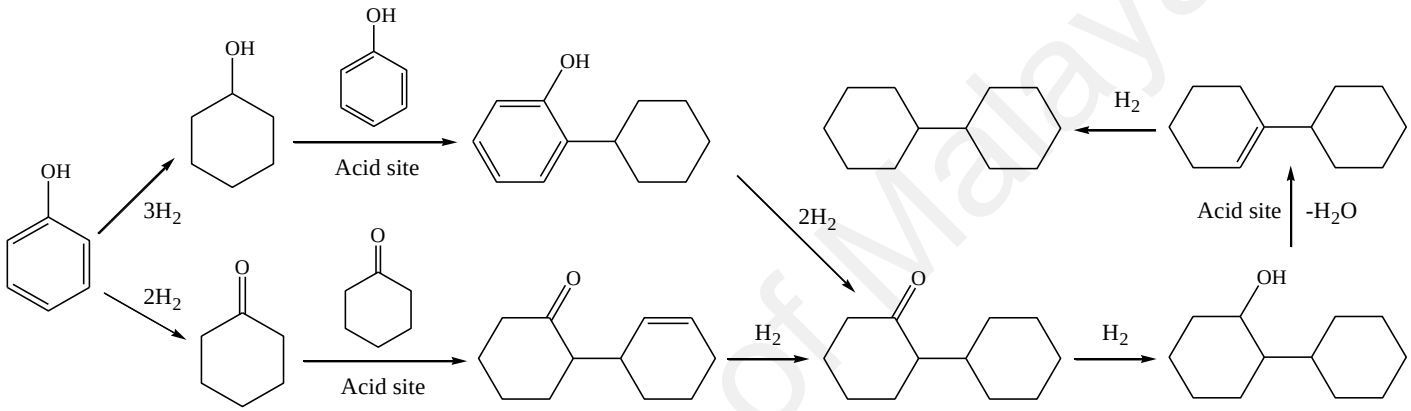

Scheme 2.2: Reaction pathway for conversion of phenol to bicyclic compounds over Pd/HBeta and Pt/HY catalysts (Hong, Miller, Agrawal, & Jones, 2010; Zhao, Camaioni, & Lercher, 2012).

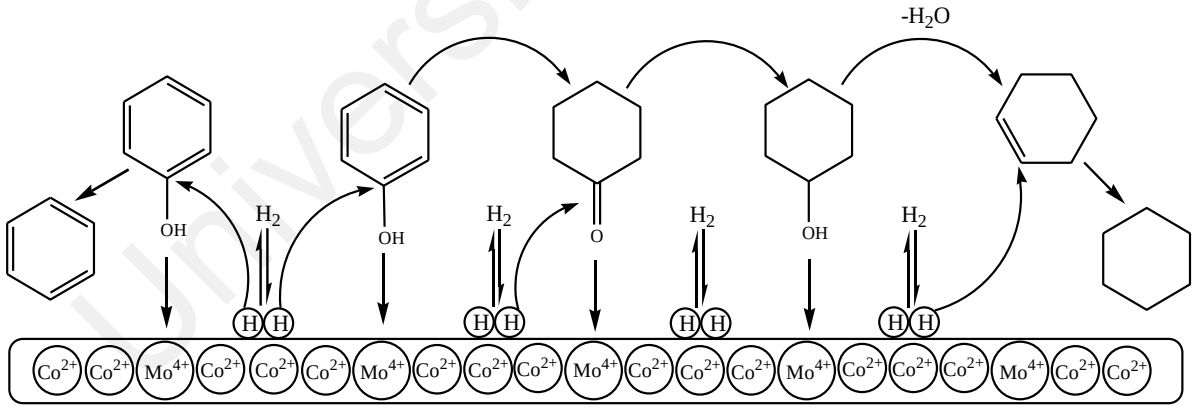

Scheme 2.3: HDO mechanism of phenol over Co–Mo–O–B amorphous catalyst (Wang, Yang, Luo, Hu, & Liu, 2010).

Table 2.1: Overview of catalysts and operating conditions applied in HDO processing of phenol.

Entry	Catalyst	S_{BET} (m^2/g)	Reactor	T (°C)	P (bar)	t[a] (h)	Solvent	Conv.[b] (%)	Product Selectivity	Ref.
1	Amorphous CoMoB (Mo/Co molar ratio of 3)	18.4	Batch	250	40	10	Dodecane	100	Cyclohexane (68.3 mol%) Cyclohexanol (27.8) Cyclohexene (2.2) Benzene (0.8) Cyclohexanone (0.7)	(Wang, Yang, Luo, Hu, & Liu, 2011)
2	Amorphous CoMoB (Mo/Co molar ratio of 3)	18.4	Batch	275	40	10	Dodecane	100	Cyclohexane (98.2) Benzene (1.5) Cyclohexene (0.3)	
3	Amorphous NiMoS (Ni/(Mo+Ni) molar ratio of 0.3)	268	Batch	350	28[c]	1	*n*-Decane	96.2	Cyclohexane (52.4 mol%) Benzene (30.4) Cyclohexene (9.8) Cyclohexanone (7.4)	(Yoosuk et al., 2012a)
4	Pd/C (5 wt% Pd)	845	Batch	200	50	0.5	Water	100	Cyclohexanol (98 C%) Cyclohexanone (2)	(Zhao et al., 2011)
5	Pd/C (5 wt% Pd)	845	Batch	200	50	0.5	Sodium hydroxide-water	100	Cyclohexanol (97) Cyclohexanone (3)	
6	Pd/C (5 wt% Pd)	845	Batch	200	50	0.5	Acetic acid-water	100	Cyclohexane (75) Cyclohexanol (20) Cyclohexanone (2)	
7	Pd/C (5 wt% Pd)	845	Batch	200	50	0.5	Phosphoric acid-water	99	Cyclohexane (85) Cyclohexanol (10) Cyclohexanone (4)	
8	Pd/C (5 wt% Pd)	845	Batch	250	50	0.5	Phosphoric acid-water	100	Cyclohexane (98) Cyclohexanol (1)	
9	Pd/C (5 wt% Pd)	845	Batch	150	50	0.5	Phosphoric acid-water	100	Cyclohexanol (74) Cyclohexanone (25)	
10	Pd/C (5 wt% Pd)	845	Batch	150	50	1	Phosphoric acid-water	100	Cyclohexanol (94) Cyclohexanone (4)	
11	Pd/Al_2O_3 (2 wt% Pd)	92	Batch	200	50	0.5	Water	82	Cyclohexanol (72) Cyclohexanone (28)	

'**Table 2.1,** continued'

Entry	Catalyst	S_{BET} (m^2/g)	Reactor	T (°C)	P (bar)	t[a] (h)	Solvent	Conv.[b] (%)	Product Selectivity	Ref.
12	Pd/Al_2O_3 (2 wt% Pd)	92	Batch	200	50	0.5	Sodium hydroxide-water	72	Cyclohexanol (69) Cyclohexanone (31)	
13	Pd/Al_2O_3 (2 wt% Pd)	92	Batch	200	50	0.5	Acetic acid-water	88	Cyclohexanone (56) Cyclohexane (20) Cyclohexanol (20)	
14	Pd/SiO_2 (2 wt% Pd)	174	Batch	200	50	0.5	Water	87	Cyclohexanol (62) Cyclohexanone (38)	
15	Pd/SiO_2 (2 wt% Pd)	174	Batch	200	50	0.5	Sodium hydroxide-water	55	Cyclohexanol (53) Cyclohexanone (47)	
16	Pd/SiO_2 (2 wt% Pd)	174	Batch	200	50	0.5	Acetic acid-water	95	Cyclohexanone (64) Cyclohexane (20) Cyclohexanol (13)	
17	Pd/ASA[d]	269	Batch	200	50	0.5	Water	96	Cyclohexanol (73) Cyclohexanone (27)	
18	Pd/ASA	269	Batch	200	50	0.5	Sodium hydroxide-water	72	Cyclohexanol (64) Cyclohexanone (36)	
19	Pd/ASA	269	Batch	200	50	0.5	Acetic acid-water	100	Cyclohexanone (53) Cyclohexanol (24) Cyclohexane (21)	
20	Pt/C (5 wt% Pt)	-	Batch	200	50	0.5	Phosphoric acid-water	100	Cyclohexane (86) Cyclohexanol (13)	
21	Rh/C (5 wt% Rh)	-	Batch	200	50	0.5	Phosphoric acid-water	100	Cyclohexane (92) Cyclohexanol (7)	
22	Ru/C (5 wt% Ru)	-	Batch	200	50	0.5	Phosphoric acid-water	100	Cyclohexane (88) Cyclohexanol (10) Cyclohexanone (1)	

‘**Table 2.1,** continued’

Entry	Catalyst	S_{BET} (m^2/g)	Reactor	T (°C)	P (bar)	t[a] (h)	Solvent	Conv.[b] (%)	Product Selectivity	Ref.
23	Ru/C (5 wt% Ru)	717	Batch	250	100	4.3	-	-	Cyclohexane (~45 wt%) Cyclohexanol (~43)	(Wildschut et al., 2010)
24	Ru/C prepared from $Ru(acac)_3$ 1%	-	Batch	250	100	4.3	-	-	Cyclohexane (~4) Cyclohexanol (~72) Phenol (~12)	
25	Ru/C prepared from $Ru(acac)_3$ 3%	-	Batch	250	100	4.3	-	-	Cyclohexane (~2) Cyclohexanol (~98)	
26	Ru/C prepared from $Ru(acac)_3$ 5%	774	Batch	250	100	4.3	-	-	Cyclohexane (~42) Cyclohexanol (~47)	
27	Ru/C prepared from $RuCl_3$ 1%		Batch	250	100	4.3	-	-	Cyclohexane (~9) Cyclohexanol (~81)	
28	Ru/C prepared from $RuCl_3$ 3%	-	Batch	250	100	4.3	-	-	Cyclohexane (~42) Cyclohexanol (~58)	
29	Ru/C prepared from $Ru(NO_3)_3$ 3%	-	Batch	250	100	4.3	-	-	Cyclohexane (~12) Cyclohexanol (~82)	
30	Ru/C prepared from $Ru(NO_3)_3$ 5%	-	Batch	250	100	4.3	-	-	Cyclohexane (~15) Cyclohexanol (~75)	
31	$CoMoS/Al_2O_3$	235	Continuous	300	28.5	-	*n*-Heptane or *n*-decane	30	Aromatic/hydrogenated compounds ratio (~0.2)	(Massoth et al., 2006)
32	$CoMoS/Al_2O_3$	-	Batch	300	50	4	Dodecane	27	Benzene (37 mol% of product) Cyclohexene, cyclohexanol, methylcyclohexane, and methylcyclohexene (4)	(Jongerius, Jastrzebski, Bruijnincx, & Weckhuysen, 2012)
33	Amorphous NiMoB	-	Batch	250	40	10	Decane	98.5	Cyclohexanol (72.5%) Cyclohexanone (0.7) Benzene (5) Cyclohexane (21.3) Cyclohexene (0.4)	(Wang, Yang, Luo, & Liu, 2010)

'**Table 2.1,** continued'

Entry	Catalyst	S_{BET} (m^2/g)	Reactor	T (°C)	P (bar)	t[a] (h)	Solvent	Conv.[b] (%)	Product Selectivity	Ref.
34	Amorphous CoNiMoB (Co molar ratio of 150)	-	Batch	250	40	10	Decane	98	Cyclohexanol (6.5) Cyclohexanone (0.3) Benzene (3.2) Cyclohexane (89.8) Cyclohexene (0.1)	
35	Amorphous CoNiMoB (Co molar ratio of 225)	-	Batch	250	40	10	Decane	98.5	Cyclohexanol (19.3) Cyclohexanone (1.2) Benzene (0.5) Cyclohexane (76.8) Cyclohexene (2.2)	
36	Amorphous CoNiMoB (Co molar ratio of 300)	-	Batch	250	40	10	Decane	62.3	Cyclohexanol (12.5) Cyclohexanone (1.4) Benzene (0.5) Cyclohexane (40.4) Cyclohexene (45.2)	
37	$CoMoS/Al_2O_3$	-	Continuous	250	15	24	-	36.4	Benzene (92.9%) Cyclohexane and cyclohexene (7.1)	(Viljava et al., 2000)
38	$CoMoS/Al_2O_3$	-	Continuous	300	15	7	-	71.9	Benzene (86.4) Cyclohexane and cyclohexene (13.6)	
39	$CoMoO/Al_2O_3$	-	Continuous	250	15	6	-	0.12	Benzene (100)	
40	Amorphous NiWB	40.2	Batch	225	40	4	Dodecane	100	Cyclohexanol (76.4 mol% of product) Cyclohexanone (1.2) Cyclohexane (22.3) Cyclohexene (0.1)	(Wang, Yang, Luo, Peng, & Wang, 2011)
41	Amorphous LaNiWB (La molar ratio of 50)	54.7	Batch	225	40	4	Dodecane	97.3	Cyclohexanol (40.6) Cyclohexanone (0.8) Cyclohexane (37.2) Cyclohexene (21.3)	

'**Table 2.1,** continued'

Entry	Catalyst	S_{BET} (m^2/g)	Reactor	T (°C)	P (bar)	t[a] (h)	Solvent	Conv.[b] (%)	Product Selectivity	Ref.
42	Amorphous LaNiWB (La molar ratio of 150)	25.5	Batch	225	40	4	Dodecane	69	Cyclohexanol (11.8) Cyclohexanone (9.1) Cyclohexane (22.9) Cyclohexene (56.2)	
43	CoMoS/MgO	45.5	Batch	350	50[c]	1	Supercritical hexane	16.74	Benzene (0.01 GC area%) Cyclohexanol (1.12) Cyclohexanone (0.75)	(Yang et al., 2009)
44	CoMoPS/MgO	51.1	Batch	350	50[c]	1	Supercritical hexane	35.16	Benzene (13.23)	
45	Raney Ni with Nafion/SiO_2	140	Batch	300	40	2	Water	100	Cyclohexane (93 C%) Cyclohexene (3.9) Benzene (2.9)	(Zhao et al., 2010)
46	Amorphous CoMoOB (2.5 h preparation time)	22.3	Batch	275	40	10	Dodecane	97.9	Cyclohexanol (~5 mol%) Cyclohexanone (~2) Cyclohexane (~80) Benzene (~3) Cyclohexene (~10)	(Wang, Yang, Luo, Hu, & Liu, 2010)
47	Amorphous CoMoOB (4 h preparation time)	20.5	Batch	275	40	10	Dodecane	99.5	Cyclohexanol, cyclohexanone and cyclohexene (~3) Cyclohexane (~95) Benzene (~2)	
48	Amorphous CoMoOB (5 h preparation time)	17.2	Batch	275	40	10	Dodecane	100	Cyclohexanol, cyclohexanone and cyclohexene (~2) Cyclohexane (~96) Benzene (~2)	
49	Oxide NiWP/AC	1099	Continuous	150	15	-	*n*-Octane	56	Cyclohexane (~78%) Cyclohexene (~3) Cyclohexanol (~19)	(Echeandia, Arias, Barrio, Pawelec, & Fierro, 2010)
50	Oxide NiWP/AC	1099	Continuous	300	15	-	*n*-Octane	98	Cyclohexane (~95) Benzene (~4) Methylcyclopentane (~1)	

'**Table 2.1,** continued'

Entry	Catalyst	S_{BET} (m^2/g)	Reactor	T (°C)	P (bar)	t[a] (h)	Solvent	Conv.[b] (%)	Product Selectivity	Ref.
51	Oxide NiWSi/AC	1071	Continuous	150	15	-	*n*-Octane	56	Cyclohexane (~86) Cyclohexene (~3) Cyclohexanol (~11)	
52	Oxide NiWSi/AC	1071	Continuous	300	15	-	*n*-Octane	98	Cyclohexane (~90) Benzene (~6.5) Methylcyclopentane (~3.5)	
53	Amorphous NiMoB (Mo/Ni molar ratio of 1)	143.5	Batch	225	40	7	Dodecane	100	Cyclohexanol (74 mol%) Cyclohexanone (0.1) Benzene (5.3) Cyclohexane (20.6)	(Wang, Yang, Bao, & Luo, 2009)
54	Amorphous NiMoB (Mo/Ni molar ratio of 2)	122.4	Batch	225	40	7	Dodecane	72.1	Cyclohexanol (19.2) Cyclohexanone (0.7) Benzene (8.9) Cyclohexene (0.1) Cyclohexane (71)	
55	Amorphous NiMoB (Mo/Ni molar ratio of 3)	38.4	Batch	225	40	7	Dodecane	94.9	Cyclohexanol (86.2) Cyclohexanone (0.8) Benzene (3.8) Cyclohexene (0.1) Cyclohexane (9.1)	
56	Pd/C	845	Batch	80	50	7	Phosphoric acid-water	~45	Cyclohexanol (~98 C%) Cyclohexanone (~2)	(Zhao et al., 2009)
57	Pd/C with HZSM-5	1062	Batch	200	50	2	Water	100	Cycloalkanes (100 C%)	(Zhao & Lercher, 2012)
58	Crystalline MoS	11	Batch	350	28[c]	1	*n*-Decane	30	Cyclohexanone (16.2 mol%) Benzene (20.3) Cyclohexane (34.5) Cyclohexene (29)	(Yoosuk, Tumnantong, & Prasassarakich, 2012b)
59	Amorphous MoS	368	Batch	350	28[c]	1	*n*-Decane	71	Cyclohexanone (4.5) Benzene (65.6) Cyclohexane (22) Cyclohexene (7.9)	

‘**Table 2.1,** continued’

Entry	Catalyst	S_{BET} (m^2/g)	Reactor	T (°C)	P (bar)	t[a] (h)	Solvent	Conv.[b] (%)	Product Selectivity	Ref.
60	Amorphous CoMoS (Co/(Mo+Co) molar ratio of 0.2)	275	Batch	350	28[c]	1	*n*-Decane	98.2	Cyclohexanone (3.2) Benzene (80.3) Cyclohexane (12) Cyclohexene (4.5)	
61	Pd/CeO_2 (1 wt% Pd)	229	Continuous	180	1	1	Benzene	50.2	Cyclohexanone (72.3%) Cyclohexanol (25.4) Cyclohexane (2.3)	(Velu, Kapoor, Inagaki, & Suzuki, 2003)
62	Pd/CeO_2 (1 wt% Pd)	229	Continuous	180	1	1	Toluene	52.8	Cyclohexanone (73.3) Cyclohexanol (23.9) Cyclohexene (2.8)	
63	Pd/CeO_2 (3 wt% Pd)	166	Continuous	180	1	1	Benzene	81.4	Cyclohexanone (46.2) Cyclohexanol (34.8) Cyclohexane (19)	
64	Pd/CeO_2 (3 wt% Pd)	166	Continuous	180	1	1	Toluene	81.8	Cyclohexanone (46.3) Cyclohexanol (48.9) Cyclohexene (4.8)	
65	Pd/CeO_2 (3 wt% Pd)	166	Continuous	180	1	1	Cyclohexane	93.7	Cyclohexanone (47) Cyclohexanol (53)	
66	Pd/CeO_2 (3 wt% Pd)	166	Continuous	180	1	1	Ethanol	28	Cyclohexanone (86.8) Cyclohexanol (13.2)	
67	Pd/ZrO_2 (1 wt% Pd)	269	Continuous	180	1	1	Benzene	52.7	Cyclohexanone (92.2) Cyclohexanol (5.1)	
68	Pd/ZrO_2 (3 wt% Pd)	254	Continuous	180	1	1	Benzene	62.9	Cyclohexanone (93) Cyclohexanol (3.5) Cyclohexane (2.7)	
69	Pd/MgO (1 wt% Pd)	-	Continuous	180	1	1	Benzene	77	Cyclohexanone (90.5) Cyclohexanol (4.9) Cyclohexane (0.6)	
70	Pd/Al_2O_3 (1 wt% Pd)	-	Continuous	180	1	1	Benzene	10	Cyclohexanone (100)	
71	Pd/TiO_2 (3 wt% Pd)	-	Continuous	180	1	1	Benzene	16.7	Cyclohexanone (98.8) Cyclohexanol (1.2)	

'**Table 2.1,** continued'

Entry	Catalyst	S_{BET} (m^2/g)	Reactor	T (°C)	P (bar)	t[a] (h)	Solvent	Conv.[b] (%)	Product Selectivity	Ref.
72	5% w/w Pd/SiO_2 prepared from $Pd(NO_3)_2$[e]	Surface area of SiO_2 > 200	Continuous	150	1	-	-	0.27[f]	Cyclohexanone/cycloxanol ratio (1.9)	(Shore, Ding, Park, & Keane, 2002)
73	5% w/w Pd/SiO_2 prepared from $Pd(NO_3)_2$[g]	Surface area of SiO_2 > 200	Continuous	150	1	-	-	0.13[f]	Cyclohexanone/cycloxanol ratio (2.1)	
74	5% w/w Pd/SiO_2 prepared from $Pd(C_2H_3O_2)_2$[e]	Surface area of SiO_2 > 200	Continuous	150	1		-	0.17[f]	Cyclohexanone/cycloxanol ratio (10.6)	
75	5% w/w Pd/SiO_2 prepared from $Pd(C_2H_3O_2)_2$[g]	Surface area of SiO_2 > 200	Continuous	150	1	-	-	0.06[f]	Cyclohexanone/cycloxanol ratio (46.6)	
76	Pd-Yb/SiO_2[e]	Surface area of SiO_2 > 200	Continuous	150	1	-	-	0.86[f]	Cyclohexanone/cycloxanol ratio (0.7)	
77	Pd-Yb/SiO_2[g]	Surface area of SiO_2 > 200	Continuous	150	1	-	-	0.65[f]	Cyclohexanone/cycloxanol ratio (1.3)	

[a] Reaction time
[b] Conversion
[c] Initial pressure
[d] Amorphous-silica-alumina
[e] Phenol molar flow rate is 1.6×10^{-3} mol h^{-1}
[f] Fractional conversion
[g] Phenol molar flow rate is 3.1×10^{-3} mol h^{-1}

2.1.2 HDO mechanism of cresol

Cresol is another phenolic compound which has been used as model compound for study of bio-oil HDO. Based on the position of methyl group, *o*-cresol, *m*-cresol and *p*-cresol are the three isomers of cresol molecule. Like phenol, hydroxyl group (-OH) is the only oxygen-containing group of cresol. Hydrogenolysis of $C_{aromatic}$-OH bond producing toluene (as aromatic product) and ring hydrogenation of cresol followed by rapid dehydration forming methylcyclohexane (as methylcycloalkane product) are the two main reaction pathways that occur in HDO of cresol (Scheme 2.4) (Laurent & Delmon, 1993). Toluene and methylcyclohexane which have high octane number are the two valuable products formed from HDO of cresol (Wan et al., 2012). In comparison with phenol molecule, the presence of methyl group in cresol molecule favors aromatic production in HDO process (Massoth et al., 2006). Various isomers of cresol behave differently in hydrodeoxygenation reaction. Massoth et al. (2006) reported that *o*-cresol had lower conversion compared with *m*- and *p*-cresol probably due to the steric hindrance to adsorption of *o*-cresol with methyl group adjacent to the hydroxyl group. Meanwhile, type of catalyst could change overall pathway of cresols HDO. The lowest unoccupied molecular orbital of $C_{aromatic}$-OH is antibonding and the surfaces which transfer electron to this orbital promote the cleavage of $C_{aromatic}$-OH bond (Whiffen & Smith, 2010). Catalysts with high electron density facilitate the above mentioned electron transfer improving catalytic activity. An overview of catalysts and operating conditions applied in HDO of cresols is presented in Table 2.2.

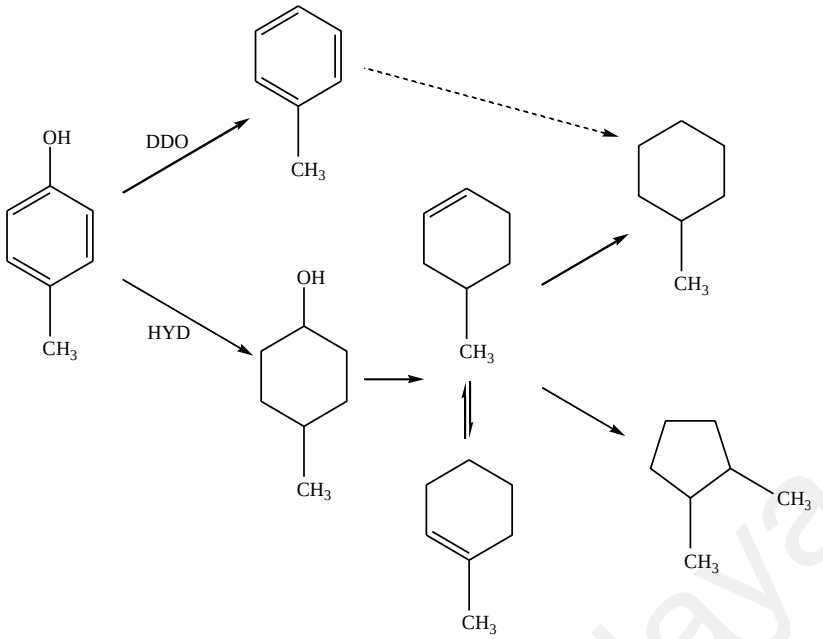

Scheme 2.4: Simple reaction scheme of HDO of *p*-cresol (Laurent & Delmon, 1993).

Table 2.2: Overview of catalysts and operating conditions applied in HDO processing of cresols.

Entry	Catalyst	S_{BET} (m^2/g)	Cresol Isomers	Reactor	T (°C)	P (bar)	t[a] (h)	Solvent	Conv.[b] (%)	Product Selectivity	Ref.
1	Pt/C	764	*p*-Cresol	Batch	300	83	1	Water	~98	Toluene (~45 C%) 4-Methylcyclohexanol (~2) Methylcyclohexane (~53)	(Wan et al., 2012)
2	Pt/C	764	*p*-Cresol	Batch	300	83	1	*n*-Heptane	~99	Toluene (~2) 4-Methylcyclohexanol (~92) Methylcyclohexane (~6)	
3	Pt/Al_2O_3	106	*p*-Cresol	Batch	300	83	1	Water	~96	Toluene (~50) 4-Methylcyclohexanol (~22) Methylcyclohexane (~28)	
4	Pt/Al_2O_3	106	*p*-Cresol	Batch	300	83	1	*n*-Heptane	~100	4-Methylcyclohexanol (~20) Methylcyclohexane (~80)	
5	Pd/C	-	*p*-Cresol	Batch	300	83	1	Water	~69	Toluene (~20) 4-Methylcyclohexanol (~64) Methylcyclohexane (~16)	
6	Pd/C	-	*p*-Cresol	Batch	300	83	1	*n*-Heptane	~99	4-Methylcyclohexanol (~88) Methylcyclohexane (~12)	
7	Pd/Al_2O_3	-	*p*-Cresol	Batch	300	83	1	Water	~30	Toluene (~9) 4-Methylcyclohexanol (~90) Methylcyclohexane (~1)	
8	Pd/Al_2O_3	-	*p*-Cresol	Batch	300	83	1	*n*-Heptane	~99	4-Methylcyclohexanol (~30) Methylcyclohexane (~70)	
9	Ru/C	-	*p*-Cresol	Batch	300	83	1	Water	~50	Toluene (~12) 4-Methylcyclohexanol (~68) Methylcyclohexane (~6)	
10	Ru/C	-	*p*-Cresol	Batch	300	83	1	*n*-Heptane	~100	4-Methylcyclohexanol (~78) Methylcyclohexane (~18)	
11	Ru/Al_2O_3	-	*p*-Cresol	Batch	300	83	1	Water	~30	Toluene (~12) 4-Methylcyclohexanol (~72) Methylcyclohexane (~4)	
12	Ru/Al_2O_3	-	*p*-Cresol	Batch	300	83	1	*n*-Heptane	~94	Toluene (~7) 4-methylcyclohexanol (~54) Methylcyclohexane (~22)	

'**Table 2.2,** continued'

Entry	Catalyst	S_{BET} (m^2/g)	Cresol Isomers	Reactor	T (°C)	P (bar)	t[a] (h)	Solvent	Conv.[b] (%)	Product Selectivity	Ref.
13	$CoMo/Al_2O_3$	-	*p*-Cresol	Batch	300	83	1	*n*-Heptane	~35	Toluene (~98) Methylcyclohexane (~2)	
14	$NiMo/Al_2O_3$	-	*p*-Cresol	Batch	300	83	1	*n*-Heptane	~20	Toluene (~26) Methylcyclohexane (~74)	
15	NiW/Al_2O_3	-	*p*-Cresol	Batch	300	83	1	*n*-Heptane	~10	Toluene (~46) Methylcyclohexane (~54)	
16	MoP	8.8	*p*-Cresol	Batch	325	41.4	5	Decalin	~60	Toluene (~58%) Hydrogenated products (~42)	(Whiffen & Smith, 2010)
17	MoP	8.8	*p*-Cresol	Batch	350	44	5	Decalin	~94	Toluene (~50) Hydrogenated products (~50)	
18	MoS_2	4.3	*p*-Cresol	Batch	325	41.4	5	Decalin	~35	Toluene (~70) Hydrogenated products (~30)	
19	MoS_2	4.3	*p*-Cresol	Batch	350	44	5	Decalin	~60	Toluene (~82) Hydrogenated products (~15) Isomerization products (~3)	
20	MoO_2	4.8	*p*-Cresol	Batch	325	41.4	5	Decalin	~34	Toluene (~64) Hydrogenated products (~36)	
21	MoO_2	4.8	*p*-Cresol	Batch	350	44	5	Decalin	~60	Toluene (~68) Hydrogenated products (~26) Isomerization products (~6)	
22	MoO_3	0.3	*p*-Cresol	Batch	325	41.4	5	Decalin	~80	Toluene (~60) Hydrogenated products (~32) Isomerization products (~8)	
23	MoO_3	0.3	*p*-Cresol	Batch	350	44	5	Decalin	~100	Toluene (~60) Hydrogenated products (~18) Isomerization products (~22)	
24	MoP	8	*p*-Cresol	Batch	350	44	5	Decalin	45	Toluene (49%) Methylcylcohexane (50) Dimethylcyclopentane (1)	(Whiffen, Smith, & Straus, 2012)

‘**Table 2.2,** continued’

Entry	Catalyst	S_{BET} (m^2/g)	Cresol Isomers	Reactor	T (°C)	P (bar)	t[a] (h)	Solvent	Conv.[b] (%)	Product Selectivity	Ref.
25	MoP prepared with citric acid and calcinated at 550 °C	112	*p*-Cresol	Batch	350	44	5	Decalin	71	Toluene (51) Methylcylcohexane (47) Dimethylcyclopentane (2)	
26	MoP prepared with citric acid and calcinated at 600 °C	75	*p*-Cresol	Batch	350	44	5	Decalin	56	Toluene (56) Methylcylcohexane (42) Dimethylcyclopentane (2)	
27	Pt/Al_2O_3 (0.5 wt% Pt)	-	*m*-Cresol	Continuous	260	1	-	-	9.3	Methylcyclohexanol (19.4%) Toluene (61.6) Methylcyclohexane (17.6) Phenol (1.4)	(Foster, Do, & Lobo, 2012)
28	Pt/Al_2O_3 (1.0 wt% Pt)	-	*m*-Cresol	Continuous	260	1	-	-	18	Methylcyclohexanol (16.4) Toluene (69.7) Methylcyclohexane (12.9) Phenol (0.6)	
29	Pt/Al_2O_3 (1.7 wt% Pt)	-	*m*-Cresol	Continuous	260	1	-	-	38.3	Methylcyclohexanol (16.6) Toluene (66.8) Methylcyclohexane (13.7) Methylcyclohexene (0.3) Phenol (0.2)	
30	$Pt/F\text{-}Al_2O_3$	-	*m*-Cresol	Continuous	260	1	-	-	63	Methylcyclohexanol (1.4) Toluene (82.3) Methylcyclohexane (16) Phenol (0.3)	
31	$Pt/K\text{-}Al_2O_3$	-	*m*-Cresol	Continuous	260	1	-	-	25.7	Methylcyclohexanol (16.3) Toluene (77.6) Methylcyclohexane (4.4) Methylcyclohexene (1.1) Phenol (0.5)	

'**Table 2.2,** continued'

Entry	Catalyst	S_{BET} (m^2/g)	Cresol Isomers	Reactor	T (°C)	P (bar)	t[a] (h)	Solvent	Conv.[b] (%)	Product Selectivity	Ref.
32	K-Pt/Al_2O_3	-	*m*-Cresol	Continuous	260	1	-	-	25.1	Methylcyclohexanol (11.7) Toluene (73) Methylcyclohexane (14.4) Methylcyclohexene (0.8)	
33	Pt/SiO_2	-	*m*-Cresol	Continuous	260	1	-	-	54.9	Methylcyclohexanol (16.6) Toluene (77.9) Methylcyclohexane (4.2) Methylcyclohexene (1) Phenol (0.2)	
34	Pt/K-SiO_2	-	*m*-Cresol	Continuous	260	1	-	-	13.5	Methylcyclohexanol (84.6) Toluene (5) Methylcyclohexane (6.3) Methylcyclohexene (3.4) Phenol (0.6)	
35	K-Pt/SiO_2	-	*m*-Cresol	Continuous	260	1	-	-	16.4	Methylcyclohexanol (90) Toluene (1.3) Methylcyclohexane (5) Methylcyclohexene (3.1) Phenol (0.5)	
36	Ga/HBeta (2.9 wt% Ga)	580	*m*-Cresol	Continuous	450	1	-	-	82.78	Benzene (12.62%) Toluene (27.85) Xylene (11.88) Other hydrocarbons C_2-C_6 (2.22) Phenol (16.65) Oxygen-containing compounds (26.06)	(Ausavasukhi, Huang, To, Sooknoi, & Resasco, 2012)
37	Ga/SiO_2 (2.9 wt% Ga)	370	*m*-Cresol	Continuous	450	1	-	-	4.49	Benzene (3.40) Toluene (7.19) Phenol (62.88) Oxygen-containing compounds (9.08)	

'**Table 2.2,** continued'

Entry	Catalyst	S_{BET} (m^2/g)	Cresol Isomers	Reactor	T (°C)	P (bar)	t[a] (h)	Solvent	Conv.[b] (%)	Product Selectivity	Ref.
38	Ga/HZSM-5 (2.8 wt% Ga)	510	*m*-Cresol	Continuous	450	1	-	-	40.32	Benzene (3.08) Toluene (22.06) Xylene (2.13) Other hydrocarbons C_2-C_6 (2.23) Phenol (49.38) Oxygen-containing compounds (20.29)	
39	$CoMoS/Al_2O_3$	235	*m*-Cresol	Continuous	300	28.5	-	-	~25	Aromatic/hydrogenated compounds ratio (~0.6)	(Massoth et al., 2006)
40	$CoMoS/Al_2O_3$	235	*p*-Cresol	Continuous	300	28.5	-	-	~27	Aromatic/hydrogenated compounds ratio (~0.75)	
41	$CoMoS/Al_2O_3$	-	*o*-Cresol	Batch	300	50	4	Dodecane	23	Toluene (65 mol% of product) Cyclohexene, cyclohexanol, methylcyclohexane, and methylcyclohexene (3)	(Jongerius et al., 2012)
42	$CoMoS/Al_2O_3$	-	*p*-Cresol	Batch	300	50	4	Dodecane	22	Toluene (60) Cyclohexene, cyclohexanol, methylcyclohexane, and methylcyclohexene (6)	

[a] Reaction time
[b] Conversion

2.1.3 HDO mechanism of guaiacol

Guaiacol with two oxygen functionalities (phenolic functional group (-OH) and methoxy functional group (-OCH_3)) is an attractive model compound of bio-oil for HDO survey (Bredenberg, Huuska, & Toropainen, 1989; Furimsky, 2000; Guehenneux, Baussand, Brothier, Poletiko, & Boissonnet, 2005). The $C_{aromatic}$-OH bond of phenolic group is stronger than the C-O bond of methoxy group, and its rupture happens at highly strict conditions (high temperature and pressure). In HDO of guaiacol, methoxy group undergoes two reactions (Scheme 2.5): demethylation (DME) which occurs by the cleavage of C-O bond of -OCH_3 group leading to production of catechol and methane (as byproduct), and direct demethoxylation (DMO) which happens by the rupture of $C_{aromatic}$-O bond resulting in formation of phenol and methanol (as byproduct). Oxygen atom of phenolic group is also eliminated through two different routes: cleavage of the bond between aromatic ring carbon atom and phenol group oxygen atom as well as aromatic ring hydrogenation followed by deletion of -OH group (Bykova et al., 2011; Bykova et al., 2012). Guaiacol type molecules in bio-oil are the main agents for coke formation (Centeno, Laurent, & Delmon, 1995). Hydrotreating of guaiacol without the presence of catalyst yields oxygen-containing compounds such as catechol, phenol and cresol indicating the necessity of catalyst use for complete deoxygenation of guaiacol (Forchheim, Hornung, Kempe, Kruse, & Steinbach, 2012; Mukundan, Konarova, Atanda, Ma, & Beltramini, 2015; Wahyudiono, Sasaki, & Goto, 2008). Product selectivities obtained from HDO of guaiacol at different reaction conditions is presented in Table 2.3.

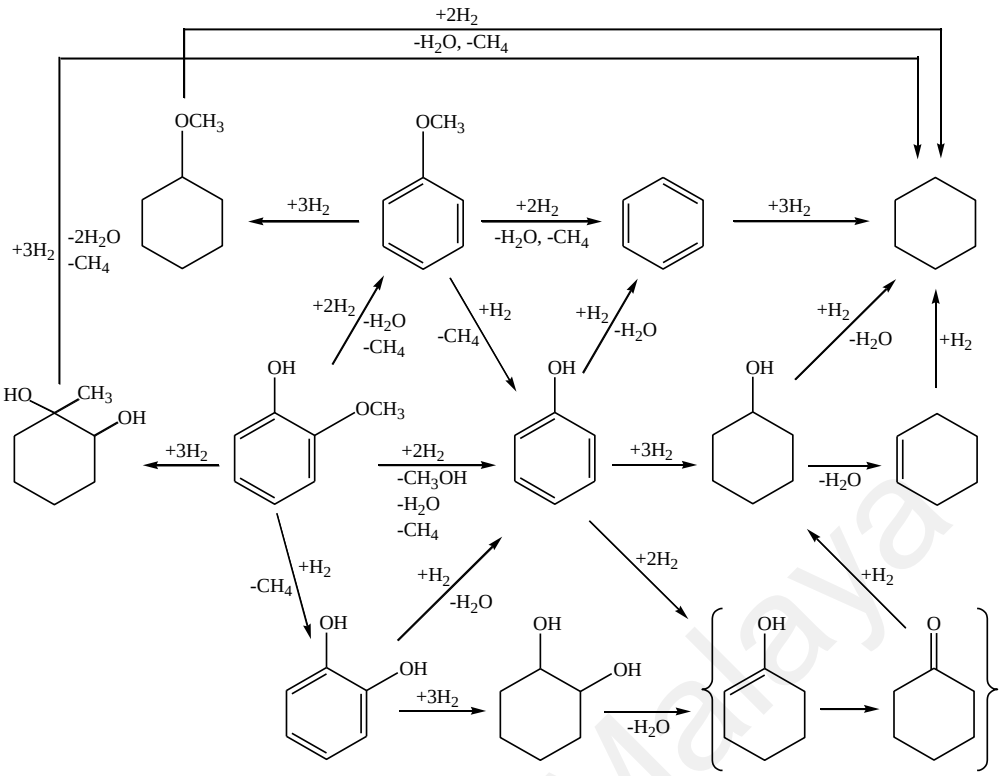

Scheme 2.5: General scheme of guaiacol conversion pathways (Bykova et al., 2012).

To study the role of catalyst type in reaction selectivity of guaiacol HDO, hydrodeoxygenation of guaiacol over Pt, Rh, Pd and Ru noble metal catalysts supported on Al_2O_3, SiO_2-Al_2O_3 and nitric acid treated carbon black (NAC) were conducted in a batch reactor at 250 °C and 40 bar hydrogen pressure (Lee et al., 2012). Cyclohexane selectivity in HDO of guaiacol over these catalysts demonstrates a different reaction route from the common pathway of this process (guaiacol → phenol → hydrodeoxygenated products) (Puente, Gil, Pis, & Grange, 1999; Filley & Roth, 1999; Olcese et al., 2012; Sepúlveda et al., 2011; Ghampson et al., 2012; Zhao et al., 2011). Phenol was not produced and 2-methoxycyclohexanol, cyclohexanol and cyclohexanone were intermediate products (Scheme 2.6). Non-production of phenol was attributed to the high hydrogenation capability of noble metal catalysts. In fact, the mechanism of guaiacol HDO in this study included two sequential steps; hydrogenation of guaiacol benzene ring followed by demethoxylation and dehydroxylation of oxygenates. Noble metals hydrogenate the aromatic ring and acid sites of support catalyze hydrogenolysis reaction.

However, at different experimental conditions (continuous reactor at 300 °C, 1.4 bar) over Pt/Al_2O_3, it was shown that the cleavage of $C_{aromatic}$-O bond of guaiacol due to direct hydrogenolysis led to phenol and anisole as primary products (Nimmanwudipong et al., 2011b). The high selectivity towards phenol shows that demethoxylation was more favorable than dehydroxylation in direct deoxygenation pathway. Meanwhile, presence of methylated compounds such as 3-methylcatechol and methylguaiacols indicates that transalkylation (methyl group transfer) route also occurred in HDO of guaiacol over Pt/Al_2O_3. Methylation reaction is taken place on the acidic alumina support.

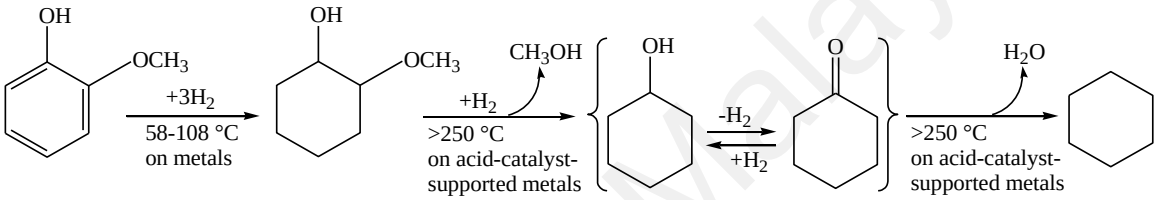

Scheme 2.6: Proposed reaction pathway for conversion of guaiacol to cyclohexane over Pt, Rh, Pd, and Ru catalysts supported on Al_2O_3, SiO_2-Al_2O_3, and NAC (Lee et al., 2012).

Table 2.3: Overview of catalysts and operating conditions applied in HDO processing of guaiacol.

Entry	Catalyst	S_{BET} (m^2/g)	Reactor	T (°C)	P (bar)	t[a] (h)	Conv.[b] (%)	Product Selectivity	Ref.
1	Ni/SiO_2 (64.2 wt% Ni)	38	Batch	320	170	1	96.7	Saturated cyclic C_5–C_7 hydrocarbons and benzene (3.6 mol%) Saturated cyclic oxygen-containing C_5 and C_6 hydrocarbons (95.9) Phenol and anisole (0.5)	(Bykova et al., 2011)
2	Ni/SiO_2 (55.4 wt% Ni)	216	Batch	320	170	1	97.5	Saturated cyclic C_5–C_7 hydrocarbons and benzene (93.1) Saturated cyclic oxygen-containing C_5 and C_6 hydrocarbons (1.5) Phenol and anisole (2.2)	
3	$NiCuLa/ZrO_2$–SiO_2	66	Batch	320	170	1	85.6	Saturated cyclic C_5–C_7 hydrocarbons and benzene (92.9) Saturated cyclic oxygen-containing C_5 and C_6 hydrocarbons (3) Phenol and anisole (2.2)	
4	$NiCu/CeO_2$–ZrO_2	82	Batch	320	170	1	94.2	Saturated cyclic C_5–C_7 hydrocarbons and benzene (1.7) Saturated cyclic oxygen-containing C_5 and C_6 hydrocarbons (97.9) Phenol and anisole (0.4)	
5	$NiCu/Al_2O_3$	109	Batch	320	170	1	80.2	Saturated cyclic C_5–C_7 hydrocarbons and benzene (61.8) Saturated cyclic oxygen-containing C_5 and C_6 hydrocarbons (35.6) Phenol and anisole (1.2)	
6	$NiCu/SiO_2$	142	Batch	320	170	1	87	Saturated cyclic C_5–C_7 hydrocarbons and benzene (83.6) Saturated cyclic oxygen-containing C_5 and C_6 hydrocarbons (8.2) Phenol and anisole (3.5)	

'**Table 2.3,** continued'

Entry	Catalyst	S_{BET} (m^2/g)	Reactor	T (°C)	P (bar)	t[a] (h)	Conv.[b] (%)	Product Selectivity	Ref.
7	Ni_2P/SiO_2	309	Continuous	300	1	-	80	Phenol (30%) Benzene (60) Anisole (10)	(Zhao et al., 2011)
8	Co_2P/SiO_2	307	Continuous	300	1	-	70	Phenol (32) Benzene (52) Anisole (1) C_3–C_5 hydrocarbons (15)	
9	Fe_2P/SiO_2	233	Continuous	300	1	-	64	Phenol (94) Anisole (6)	
10	WP/SiO_2	147	Continuous	300	1	-	60	Phenol (100)	
11	MoP/SiO_2	207	Continuous	300	1	-	54	Phenol (28) Benzene (53) Toluene (4) C_3–C_5 hydrocarbons (15)	
12	Pt/ZrO_2	17	Batch	100	80	5	10	Cyclohexanol (~65 mol%) 1-Methyl-1,2-cyclohexanediol (~15) 1,2-Dimethoxybenzene (~15) Cyclohexane (~1)	(Gutierrez et al., 2009)
13	Pd/ZrO_2	17	Batch	100	80	5	13.7	Cyclohexanol (~40%) 1-Methyl-1,2-cyclohexanediol (~37) 1,2-Dimethoxybenzene (~20) Cyclohexane (~2)	
14	Rh/ZrO_2	20	Batch	100	80	5	98.9	Cyclohexanol (~12) 1-Methyl-1,2-cyclohexanediol (~72) 1,2-Dimethoxybenzene (~3)	
15	$PdPt/ZrO_2$	16	Batch	100	80	5	5.2	Cyclohexanol (~73) 1-Methyl-1,2-cyclohexanediol (~4) 1,2-Dimethoxybenzene (~17)	
16	$RhPd/ZrO_2$	21	Batch	100	80	5	32.7	Cyclohexanol (~32) 1-Methyl-1,2-cyclohexanediol (~44) 1,2-Dimethoxybenzene (~8) Cyclohexane (~0.05)	

'**Table 2.3,** continued'

Entry	Catalyst	S_{BET} (m^2/g)	Reactor	T (°C)	P (bar)	t[a] (h)	Conv.[b] (%)	Product Selectivity	Ref.
17	$RhPt/ZrO_2$	23	Batch	100	80	5	98.7	Cyclohexanol (~7) 1-Methyl-1,2-cyclohexanediol (~91)	
18	$CoMoS/Al_2O_3$	-	Batch	100	80	5	13.8	Cyclohexanol (~73) 1,2-Dimethoxybenzene (~17)	
19	MoS_2	82	Continuous	300	40	-	~55	Cyclohexane (~25%) Methylcyclopentane (~16) Benzene (~18) Cyclohexene (trace) Cyclohexylbenzene (trace)	(Bui, Laurenti, Afanasiev, et al., 2011)
20	MoS_2/Al_2O_3	250	Continuous	300	40	-	~13	Cyclohexene (~5.8) Benzene (~1.8) Cyclohexylbenzene (~1) Methyl-containing products (~4.8) Cyclohexane (~1)	
21	CoMoS	110	Continuous	300	40	-	~50	Benzene (~42) Cyclohexene (~2) Cyclohexane (~6) Toluene (~2)	
22	$CoMoS/Al_2O_3$	230	Continuous	300	40	-	~13	Methyl-containing products (~6.3) Cyclohexene (~2.8) Benzene (~1.8) Cyclohexane (~2)	
23	MoS_2/Al_2O_3	230	Continuous	300	40	-	~25	Catechol (~51%) Methylcatechol (~18) Phenol (~9) Cresol (~9) Oxygen-free products (~2) Heavy compounds (~7) Light compounds (~4)	(Bui, Laurenti, Delichère, et al., 2011)

'**Table 2.3,** continued'

Entry	Catalyst	S_{BET} (m^2/g)	Reactor	T (°C)	P (bar)	t[a] (h)	Conv.[b] (%)	Product Selectivity	Ref.
24	MoS_2/TiO_2	120	Continuous	300	40	-	~25	Catechol (~20) Phenol (~60) Cresol (~7) Oxygen-free products (~4) Light compounds (~9)	
25	MoS_2/ZrO_2	94	Continuous	300	40	-	~25	Catechol (~37) Phenol (~45) Cresol (~4) Oxygen-free products (~5) Light compounds (~9)	
26	$CoMoS/Al_2O_3$	190	Continuous	300	40	-	~90	Catechol (~10) Methylcatechol (~4) Phenol (~34) Cresol (~28) Oxygen-free products (~15) Heavy compounds (~4) Light compounds (~5)	
27	$CoMoS/TiO_2$	112	Continuous	300	40	-	100	Catechol (~1) Methylcatechol (trace) Phenol (~61) Cresol (~6) Oxygen-free products (~18) Light compounds (~14)	
28	$CoMoS/ZrO_2$	90	Continuous	300	40	-	100	Catechol (~1) Phenol (~55) Cresol (~2) Oxygen-free products (~30) Light compounds (~12)	
29	Ni/SiO_2	216	Batch	320	170	1	97.5	Aliphatics C_5–C_7 and benzene (90.9 mol%) Oxygen-containing aliphatics C_5–C_7 (1.4) Phenol, anisole and methoxy-methylphenol (2.1) Products of aromatic ring condensation (3.1)	(Bykova et al., 2012)

'**Table 2.3,** continued'

Entry	Catalyst	S_{BET} (m^2/g)	Reactor	T (°C)	P (bar)	t[a] (h)	Conv.[b] (%)	Product Selectivity	Ref.
30	$NiCu/SiO_2$	142	Batch	320	170	1	87.1	Aliphatics C_5–C_7 and benzene (72.7) Oxygen-containing aliphatics C_5–C_7 (7.1) Phenol, anisole and methoxy-methylphenol (3) Products of aromatic ring condensation (4.2)	
31	$NiCu/CeO_2$-ZrO_2	82	Batch	320	170	1	94.2	Aliphatics C_5–C_7 and benzene (1.6) Oxygen-containing aliphatics C_5–C_7 (92.5) Phenol, anisole and methoxy-methylphenol (0.4)	
32	$NiCu/Al_2O_3$	109	Batch	320	170	1	80.3	Aliphatics C_5–C_7 and benzene (49.9) Oxygen-containing aliphatics C_5–C_7 (28.9) Phenol, anisole and methoxy-methylphenol (0.9) Products of aromatic ring condensation (1.1)	
33	$NiCu/ZrO_2$-SiO_2-La_2O_3	66	Batch	320	170	1	85.6	Aliphatics C_5–C_7 and benzene (80.1) Oxygen-containing aliphatics C_5–C_7 (2.7) Phenol, anisole and methoxy-methylphenol (1.9) Products of aromatic ring condensation (1.6)	
34	Pt/Al_2O_3	120	Batch	250	40[c]	1	100	Yield of product (mol%): Cyclohexane (23) Cyclohexanol (19) Cyclohexanone (6) 2-Methoxycyclohexanol (26)	(Lee et al., 2012)
35	Pt/SiO_2-Al_2O_3	626	Batch	250	40[c]	1	50	Cyclohexane (17)	
36	Pt/nitric-acid-treated carbon black	290	Batch	250	40[c]	1	100	Cyclohexane (14) Cyclohexanol (15) Cyclohexanone (1) 2-Methoxycyclohexanol (44)	
37	Ru/Al_2O_3	119	Batch	250	40[c]	1	100	Cyclohexane (22) Cyclohexanol (35) 2-Methoxycyclohexanol (7)	
38	Ru/SiO_2-Al_2O_3	518	Batch	250	40[c]	1	100	Cyclohexane (60) Cyclohexanol (8)	

'**Table 2.3,** continued'

Entry	Catalyst	S_{BET} (m^2/g)	Reactor	T (°C)	P (bar)	t[a] (h)	Conv.[b] (%)	Product Selectivity	Ref.
39	Ru/nitric-acid-treated carbon black	210	Batch	250	40[c]	1	100	Cyclohexane (12) Cyclohexanol (19) 2-Methoxycyclohexanol (60)	
40	Rh/Al_2O_3	122	Batch	250	40[c]	1	100	Cyclohexane (25) Cyclohexanol (8) Cyclohexanone (1) 2-Methoxycyclohexanol (9)	
41	Rh/SiO_2-Al_2O_3	569	Batch	250	40[c]	1	100	Cyclohexane (57)	
42	Rh/nitric-acid-treated carbon black	238	Batch	250	40[c]	1	100	Cyclohexane (20) Cyclohexanol (6) Cyclohexanone (1) 2-Methoxycyclohexanol (41)	
43	Pd/Al_2O_3	114	Batch	250	40[c]	1	100	Cyclohexane (19) Cyclohexanol (13) 2-Methoxycyclohexanol (13)	
44	Pd/SiO_2-Al_2O_3	520	Batch	250	40[c]	1	100	Cyclohexane (46)	
45	Pd/nitric-acid-treated carbon black	240	Batch	250	40[c]	1	54	Cyclohexane (1) Cyclohexanol (1) 2-Methoxycyclohexanol (41)	
46	MoN/Al_2O_3 (ammonia as nitriding agent)	191	Batch	300	50	4	66	At 10% guaiacol conversion: Phenol (1%) Catechol (26)	(Ghampson et al., 2012)
47	MoN/Al_2O_3 (N_2/H_2 as nitriding agent)	183	Batch	300	50	4	62	At 10% guaiacol conversion: Phenol (2) Catechol (26)	
48	MoN/SBA-15 (ammonia as nitriding agent)	418	Batch	300	50	4	44	At 10% guaiacol conversion: Phenol (26) Catechol (6)	
49	MoN/SBA-15 (N_2/H_2 as nitriding agent)	397	Batch	300	50	4	40	At 10% guaiacol conversion: Phenol (22) Catechol (9)	

'**Table 2.3,** continued'

Entry	Catalyst	S_{BET} (m^2/g)	Reactor	T (°C)	P (bar)	t[a] (h)	Conv.[b] (%)	Product Selectivity	Ref.
50	CoMoN/SBA-15 (ammonia as nitriding agent)	387	Batch	300	50	4	24	At 10% guaiacol conversion: Phenol (12%) Catechol (6%)	
51	CoMoN/Al_2O_3 (ammonia as nitriding agent)	182	Batch	300	50	4	58	At 10% guaiacol conversion: Phenol (5) Catechol (22)	
52	Re/ZrO_2 (sulfided in H_2/H_2S mixture)	77	Batch	300	50	~4	~50	Yield of product (%): Catechol (~10) Phenol (~34) Cyclohexane (~4) Cyclohexene (~4) Benzene (~1)	(Ruiz et al., 2010)
53	Re/ZrO_2 (sulfided in N_2/H_2S mixture)	77	Batch	300	50	~4	~70	Catechol (~18) Phenol (~46) Cyclohexane (~4) Cyclohexene (~5) Benzene (~2)	
54	Re/ZrO_2 (sulfated support)	79	Batch	300	50	~4	~10	Catechol (~7) Phenol (~3) Cyclohexane (~1)	
55	Ni_2P/Al_2O_3	90	Continuous	300	1	-	99.6	Yield of product (C%): Benzene (30.9) Phenol (13.7) Cresol (1.5)	(Wu et al., 2013)
56	Ni_2P/ZrO_2	47	Continuous	300	1	-	96.5	Benzene (32.4) Phenol (25.5) Cresol (1.3) Catechol (0.3)	
57	Ni_2P/SiO_2	127	Continuous	300	1	-	99.5	Benzene (71.9) Phenol (1.9) Cresol (0.1)	

'**Table 2.3,** continued'

Entry	Catalyst	S_{BET} (m^2/g)	Reactor	T (°C)	P (bar)	t[a] (h)	Conv.[b] (%)	Product Selectivity	Ref.
58	MoS_2/C	126	Batch	300	50[c]	5	~55	Phenol (52 mol%) Cyclohexane (4.2) Cyclohexene (8) Cyclohexanol (5) Anisole (0.3) Cresol (1.2) Benzene (0.4) Catechol (1.8)	(Mukundan et al., 2015)
59	Pt/MgO	-	Continuous	250	69	-	62.9	Cyclopentane (25%) Cyclohexanol (39) Cyclohexanone (24) Phenol (0.6) Methylcyclohexanol (0.6) 1,2-Dimethoxybenzene (1)	(Nimmanwudipong et al., 2014)

[a] Reaction time
[b] Conversion
[c] Initial pressure

2.1.4 HDO mechanism of anisole

Anisole with an isolated methoxy group (-OCH_3) is another phenolic compound applied for study of bio-oil HDO. A bifunctional catalyst consisting acid and metal is required for hydrogenolysis and hydrocracking of $C_{aromatic}$-O-C_{methyl} bonds in anisole molecule (Huuska, 1986). HDO of anisole could proceed via two common reaction pathways (Scheme 2.7): (i) demethylation of anisole to phenol followed by hydrogenolysis and ring hydrogenation of phenol to benzene and cyclohexane, (ii) transalkylation to cresols, toluene and xylenols. Since $C_{aromatic}$-O bond is stronger than C_{methyl}-O bond in anisole molecule, the possibility of direct cleavage of methoxy group is weak (Loricera et al., 2011). In a study held for anisole HDO over sulfided $CoMo/Al_2O_3$ catalyst, it was inferred that the two reactions of demethylation and methyl transfer occurred on different active sites of catalyst (Massoth et al., 2006; Viljava et al., 2000). Generally, acidic sites of catalyst participate in anisole demethylation. An overview of products selectivity obtained by HDO of anisole using different types of catalyst and operating conditions is presented in Table 2.4.

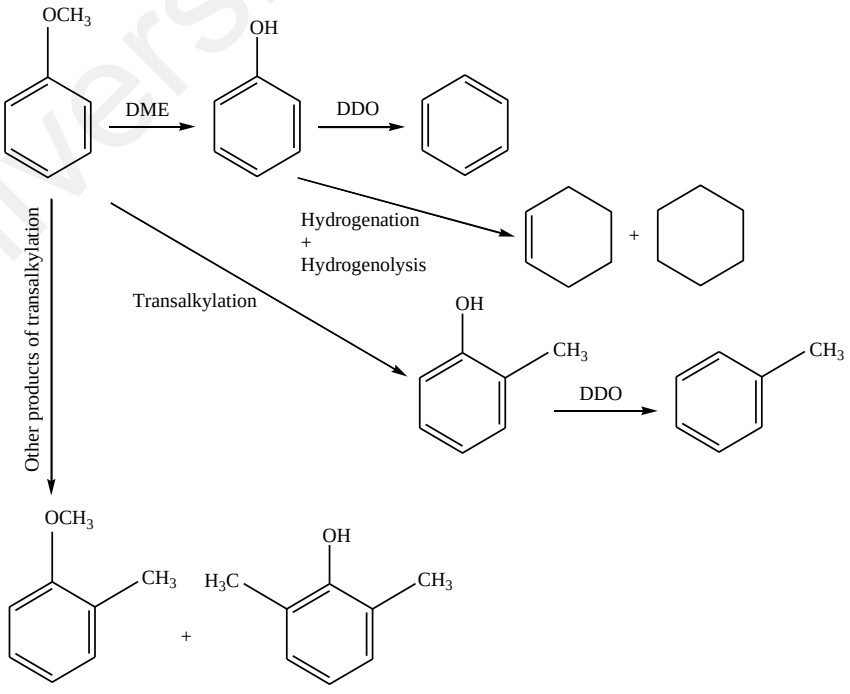

Scheme 2.7: HDO network of anisole (Viljava et al., 2000).

Table 2.4: Overview of catalysts and operating conditions applied in HDO processing of anisole.

Entry	Catalyst	Reactor	T (°C)	P (bar)	Conv.[a] (%)	Product Selectivity	Ref.
1	Pt/Al_2O_3	Continuous	300	1.4	14	Phenol (65 mol%) *o*-Cresol (15) Benzene (4.4) Cyclohexanone (3.3) 2,6-Dimethylphenol (2.4) 2-Methylanisole (0.77) *p*-Cresol (0.22) 4-Methylanisole (0.13)	(Runnebaum et al., 2010)
2	$NiCu/Al_2O_3$	Continuous	300	10	78.6	Cyclohexane (24.3 mol%) Benzene (59.9) Methylcyclohexane (8.8) Toluene (2.9) Cyclohexanole (2.3) Cyclohexanone (1.8)	(Ardiyanti et al., 2012)
3	$CoMoS/Al_2O_3$	Batch	250	34.5	-	Phenol, benzene and cyclohexane (~82 wt%) *o*-Cresol, toluene and methylcyclohexane (~18)	(Hurff & Klein, 1983)
4	$CoMoS/Al_2O_3$	Batch	300	50	58	Benzene (10 mol% of product) Phenol (64) Methylated products (10) Cyclohexene, cyclohexanol, methylcyclohexane, and methylcyclohexene (3)	(Jongerius et al., 2012)
5	Rh/SiO_2	Continuous	300	10	53.4	Aliphatic/aromatic products molar ratio (0.22)	(Yakovlev et al., 2009)
6	Rh/CeO_2	Continuous	300	10	100	Aliphatic/aromatic products molar ratio (0.30)	
7	Rh/ZrO_2	Continuous	300	10	99.6	Aliphatic/aromatic products molar ratio (0.88)	
8	$Rh/CoSiO_3$	Continuous	300	10	82	Aliphatic/aromatic products molar ratio (0.81)	
9	$RhCo/Al_2O_3$	Continuous	300	10	98	Aliphatic/aromatic products molar ratio (1.68)	
10	$RhCo/SiO_2$	Continuous	300	10	99	Aliphatic/aromatic products molar ratio (0.30)	
11	Co/SiO_2	Continuous	300	10	10.3	Aliphatic/aromatic products molar ratio (0.03)	
12	Ni/SiO_2	Continuous	300	10	92.8	Aliphatic/aromatic products molar ratio (1.44)	
13	Ni/Cr_2O_3	Continuous	300	10	90.2	Aliphatic/aromatic products molar ratio (1.53)	
14	Ni/Al_2O_3	Continuous	300	10	80	Aliphatic/aromatic products molar ratio (3.02)	
15	Ni/ZrO_2	Continuous	300	10	26	Aliphatic/aromatic products molar ratio (0.12)	

‘**Table 2.4,** continued’

Entry	Catalyst	Reactor	T (°C)	P (bar)	Conv.[a] (%)	Product Selectivity	Ref.
16	$NiCu/Al_2O_3$	Continuous	300	10	99.6	Aliphatic/aromatic products molar ratio (4.81)	
17	$NiCu/ZrO_2$	Continuous	300	10	63.5	Aliphatic/aromatic products molar ratio (0.20)	
18	$CoMoS/Al_2O_3$	Continuous	300	10		Phenol (41 mol%) Benzene (23) Cyclohexane (5) Cresol isomers (30)	
19	$CoMoS/Al_2O_3$	Continuous	250	15	88.2	Phenol (48.4%) Benzene (7.5) Toluene (4.0) *o*-Cresol (24.7) *o*-Methylanisole (1.4) 2,6-Xylenol (10.8)	(Viljava et al., 2000)
20	$CoMoS/Al_2O_3$	Continuous	300	15	96.8	Phenol (40.8) Benzene (22.8) Cyclohexane and cyclohexene (4.3) Toluene (9.7) *o*-Cresol (12.2) 2,6-Xylenol (3.7)	
21	MoP/SiO_2	Continuous	300	15	17.8	Phenol (~75 mol%) Cyclohexane (~5) Benzene (~4.5)	(Li et al., 2011)
22	Ni_2P/SiO_2	Continuous	300	15	76.8	Phenol (~5) Cyclohexane (~90) Benzene (~5)	
23	$NiMoP/SiO_2$	Continuous	300	15	28.6	Phenol (~3) Cyclohexane (~81) Benzene (~16%)	

'**Table 2.4,** continued'

Entry	Catalyst	Reactor	T (°C)	P (bar)	Conv.[a] (%)	Product Selectivity	Ref.
24	Pt/HBeta (1 wt% Pt)	Continuous	400	1	~99	Yield of product (%): Phenol (0.1) Cresols (0.2) C_{1-2} (6) C_3 (0.4) C_{4-9} (1.6) Benzene (51.2) Toluene (27.6) Xylenes (10.6) C_{9+} aromatics (1.7)	(Zhu et al., 2011)
25	CoMoWS/SBA-15	Continuous	310	30	38	Phenol (60.1%) *o*-Cresol (25.9) *o*-Xylenol (11.2) *o*-Methylanisole (1.7) Benzene (1.0)	(Loricera et al., 2011)
26	CoMoWS/1 wt% P/SBA-15	Continuous	310	30	38	Phenol (62.7) *o*-Cresol (24.4) *o*-Xylenol (10.7) *o*-Methylanisole (1.7) Benzene (0.5)	
27	CoMoWS/SBA-16	Continuous	310	30	38	Phenol (60.8) *o*-Cresol (25.1) *o*-Xylenol (10.8) *o*-Methylanisole (1.8) Benzene (1.5)	
28	CoMoWS/1 wt% P/SBA-16	Continuous	310	30	38	Phenol (65.9) *o*-Cresol (22) *o*-Xylenol (8.4) *o*-Methylanisole (2.3) Benzene (1.4)	

[a] Conversion

2.2 Effective parameters on reaction selectivity of catalytic HDO of phenol, cresol, guaiacol and anisole

2.2.1 Catalyst promoters

Use of multi-component catalysts seems to be highly useful for selective hydrodeoxygenation of phenols to high-value hydrocarbons. Due to the high activity of transition metals in reactions including hydrogen, several elements of this metal group have been vastly used as catalyst for hydrodeoxygenation of phenolic compounds. Supported or unsupported transition metals have been used as both hydrogenation catalyst and promoter in HDO process. The addition of promoters to metal catalysts has been studied in order to determine their effects on catalytic activity and reaction selectivity. In HDO of anisole over bimetallic NiCu catalyst, the ratio of aliphatic to aromatic hydrocarbons in product stream was higher than that over mono-Ni catalyst demonstrating that the bimetallic active sites in $NiCu/Al_2O_3$ were more efficient for aromatic ring hydrogenation compared with single Ni active sites in Ni/Al_2O_3 (Ardiyanti et al., 2012). Gutierrez et al. (2009) showed that combining Rh with Pt or Pd noble metals enhanced catalytic activity and guaiacol conversion due to the efficient interaction between these metals leading to higher hydrogen adsorption which facilitates hydrogenation process; conversion of about 10% on monometallic catalyst was enhanced to 32.7% on RhPd and 98.7% on RhPt (see Table 2.3, entries 12-17). However, the combination of Pd and Pt led to lower active surface area which caused lower guaiacol conversion and catalytic activity compared with individual Pd and Pt catalysts. Promoters affect reaction selectivity through the influence on physical (i.e. surface area, pore volume and particle size) and chemical (i.e. type of active sites) properties of catalyst. The influence of different promoters on the performance of HDO catalysts is illustrated in the following subsections.

2.2.1.1 Effect of promoters on catalyst structure

A major effect of promoters on catalyst is change of catalyst structure. For instance, introduction of promoter Co into Ni-Mo-B destroyed the shell structure of catalyst and caused more uniform and smaller particles (Wang, Yang, Luo, & Liu, 2010). Study of the promoting effect of Mo in Co-Mo-B amorphous catalyst displayed that the increase of Mo content decreased catalyst surface area due to small BET surface area of Mo oxides (W. Wang, Y. Yang, H. Luo, T. Hu, & Liu, 2011). Meanwhile, it was shown that lanthanum (La) addition in an appropriate amount increased the amorphous degree of Ni-W-B catalyst due to enhanced interaction between hydrogenation active site of Ni^0 and B^0 which results in agglomeration of catalyst particles (Wang, Yang, Luo, Peng, & Wang, 2011). However, excess content of La reduced the amorphous degree since large atom of La in catalyst acts as dispersing agent and could intercept particle agglomeration. In HDO of phenol over Ni-W-B, free hydrogen activated on Ni site was more involved in benzene ring hydrogenation of phenol molecule activated on WO_3 Brønsted acid site than cleavage of $C_{aromatic}$-OH bond of phenol. By addition of La into catalyst composition, this mechanism was not changed, phenol conversion decreased, deoxygenation rate increased and cyclohexanol, cyclohexene and cyclohexane were the main products.

Yoosuk et al. studied the effect of the addition of Ni (2012a) and Co (2012b) promoters on the activity of unsupported sulfided molybdenum amorphous catalyst in HDO of phenol. Nickel and cobalt addition leads to the formation of Ni-Mo-S and Co-Mo-S structures with weaker metal-sulfur bond strength in comparison with the Mo-S catalyst without promoter. Hence, the elimination of sulfur atom which leads to formation of sulfur vacancies (active sites) on the edge of MoS_2 slabs can easily occur in amorphous NiMoS and CoMoS. Moreover, promoted catalysts had better hydrogen activation capability. However, Ni and Co differently alter catalyst properties and product selectivities. Ni addition into MoS_2 catalyst led to an increase in phenol conversion

(Yoosuk et al., 2012a). In the presence of Ni promoter, cyclohexane was the selective product and HDO process showed a strong favor toward HYD route. Ni addition can also form metallic-like brim sites (fully sulfided metallic edges and active sites for HYD reaction pathway) next to MoS_2 slabs. Reduction of surface area, pore volume, number of large pores and number of layers in stacks are typical changes in amorphous MoS_2 catalyst structure due to addition of Ni promoter. Nickel metal also changes catalyst morphology to crystalline structure. Long slabs of MoS_2 became smaller and more curved by Ni addition due to the formation of smaller particles. Edge planes and basal planes of MoS_2 layers are two models of active sites in Mo sulfide catalysts (Eijsbouts, Heinerman, & Elzerman, 1993; Hensen et al., 2001; Iwata et al., 1998; Schweiger, Raybaud, Kresse, & Toulhoat, 2002; Yoosuk et al., 2012b). Formation of large particles in catalyst prevents the prevalence of edge planes available for exposure to reactants. Also, Mo sulfide catalyst with bent basal planes have higher catalytic activity than that with flat basal planes. In fact, formation of small particles and predominance of bent basal planes in MoS_2 layers are the positive effects of Ni promoter. However, cobalt metal in MoS_2 catalyst acted as inhibitor of formation of crystalline MoS_2 (Yoosuk et al., 2012b). By adding cobalt as promoter, phenol conversion strongly increased and reaction selectivity shifted toward DDO route (see Table 2.1, entries 59 and 60). Addition of Co as promoter into amorphous MoS_2 decreased catalyst surface area and pore volume and also led to shorter slabs in the stacks of catalyst. In catalytic HDO of guaiacol over molybdenum sulfide catalyst, addition of cobalt promoter led to remarkable increase in guaiacol conversion, catalytic activity and final oxygen-free products (Bui, Laurenti, Afanasiev, et al., 2011). HDO reaction was proceeded through DME and both DME and DMO routes over non-promoted and promoted molybdenum sulfide catalysts, respectively. On MoS_2 catalyst, catechol was formed as the primary product followed by formation of phenol, methylcyclopentane, benzene and cyclohexane (as the major product). In the case of using

CoMoS, phenol and catechol were the primary products and benzene (as the main product), cyclohexane, cyclohexene and toluene were produced as final products. Higher acidity of MoS_2 compared with CoMoS resulted in greater amount of heavy methyl-substitution compounds production which harden the deoxygenation.

2.2.1.2 Effect of promoters on catalyst active site

Promoters are influential on catalytic activity and reaction selectivity through affecting type and dispersion of catalyst active sites. For instance, large radius atom of Mo acts as dispersing agent in molybdenum-promoted Co-Mo-B catalyst (Wang, Yang, Luo, Hu, & Liu, 2011). Higher content of Mo in initial material decreases Co diffusion and inhibits agglomeration resulting in increase in the Co content of catalyst surface. High content of Co on catalyst surface is beneficial to adsorb enough hydrogen and supply sufficient free hydrogen while high content of MoO_2 on catalyst surface is beneficial to provide enough Brønsted acid sites to activate oxy-groups.

In guaiacol HDO, incorporation of Co into unsupported molybdenum nitride catalyst (Mo_2N) enhanced the selectivity of benzene, cyclohexane and cyclohexene as deoxygenated products (Ghampson et al., 2012). Cobalt addition into this catalyst resulted in formation of γ-Mo_2N and Co_3Mo_3N active phases which lead to increase of deoxygenation activity. Higher production of oxygen-free compounds over cobalt modified catalyst is caused by Co_3Mo_3N active sites. Unlike unsupported Mo_2N which was promoted by addition of cobalt, Co incorporation reduced catalytic activity of molybdenum nitride catalysts supported on alumina, mesoporous SBA-15 silica and activated carbon (AC) and did not cause any positive effect on HDO of guaiacol (Ghampson et al., 2012; Ghampson et al., 2012). The reason of this negative effect is that the Co_3Mo_3N active sites of deoxygenation were not completely generated on supported CoMoN catalysts and in the case of using CoMoN/AC, the concentration of cobalt in the

internal part of catalyst was higher than that in the external part of support. High quantity of Co on surface of catalyst can enhance the number of active sites while high concentration of Co in the pores of catalyst reduces the accessibility of reactants to Co and also causes a restriction in diffusivity of reactants into the inner part of support. Incorporation of copper into nickel oxide catalysts supported on Al_2O_3, CeO_2-ZrO_2, SiO_2-ZrO_2-La_2O_3 and SiO_2 facilitated the reduction of nickel oxide phases and increased catalytic activity due to decrease of coke formation rate (Bykova et al., 2011; Bykova et al., 2012; Yakovlev et al., 2009). Copper promoter addition into Ni/Al_2O_3 catalyst reduced the formation of Ni spinels ($NiAl_2O_4$) which decreased the rate of formation of active nickel metal (Ni^0) (Ardiyanti et al., 2012).

Addition of promoter into catalyst composition in an optimum value have positive effect on HDO reaction rate while, an excess amount of promoter covers HDO active sites leading to decrease in catalytic activity. Ni addition into MoS_2 catalyst led to an increase in phenol conversion and maximum conversion of 96.2% was achieved at Ni/(Mo+Ni) molar ratio of 0.3 (Yoosuk et al., 2012a). At molar ratios above 0.3, a bulk phase of NiS was formed which covers the active part of promoted Mo sites and reduces phenol conversion. In HDO of phenol over Ni-Mo-B catalyst, it was revealed that the selectivity towards cyclohexane was increased by the addition of Co up to an optimum level due to enhancement of hydrogenation-dehydration (see Table 2.1, entries 33-36) (Wang, Yang, Luo, & Liu, 2010). By further addition of Co, selectivity towards cyclohexane decreased since Ni active sites are covered by excess cobalt oxide leading to suppression of hydrogen adsorption on catalyst surface. In another work held by Zanuttini et al. (2015) for catalytic HDO of *m*-cresol over Pt/γ-Al_2O_3, it was shown that product distribution was strongly dependant on the amount of Pt loading (0.05-1.70 wt%). Direct deoxygenation of *m*-cresol to toluene was improved at high Pt loadings due to sufficient amount of metal active sites in catalyst structure. However, at low loadings of Pt and higher ratio of acid

to metal sites, selectivity towards cracking reactions was favorably enhanced compared with hydrogenolysis mechanism.

In addition to metal promoters, non-metal elements could also be considered as promoters of HDO catalysts. Transition metal phosphide catalysts are another type of catalysts which are efficient in hydroprocessing (Oyama, 2003; Oyama, Gott, Zhao, & Lee, 2009). Nickel-, iron-, molybdenum-, cobalt- and tungsten-phosphide catalysts supported on neutral silica were applied for HDO of guaiacol in a packed bed reactor at 300 °C and atmospheric pressure (Zhao et al., 2011). Metal sites dispersion and catalytic activity of these phosphide catalysts decreased in the order MoP/SiO_2 > Ni_2P/SiO_2 > WP/SiO_2 > Fe_2P/SiO_2 > Co_2P/SiO_2 and Ni_2P/SiO_2 > Co_2P/SiO_2 > Fe_2P/SiO_2 > WP/SiO_2 > MoP/SiO_2, respectively. The dominant pathway in guaiacol HDO over the transition metal phosphides was catechol formation via demethylation of guaiacol followed by phenol production via removing the -OH functional group of catechol and subsequently benzene formation by direct hydrogenolysis of phenol. Benzene and phenol were the main products of guaiacol HDO over phosphide catalysts. High capability of phosphide in production of phenol instead of catechol leads to low coke formation over phosphide-containing catalysts because the potential of catechol for coke generation is higher than phenol. Meanwhile, reaction selectivity of anisole HDO over Ni_2P/SiO_2, MoP/SiO_2 and $NiMoP/SiO_2$ catalysts at 300 °C and 15 bar hydrogen pressure was toward demethylation, hydrogenolysis and hydrogenation resulting in phenol, benzene and cyclohexane as the main products (see Table 2.4, entries 21-23) (Li et al., 2011). HDO activity of catalysts decreased in the order Ni_2P/SiO_2 > $NiMoP/SiO_2$ > MoP/SiO_2. High active Ni and Mo metal sites of these phosphide catalysts acted as Lewis acid sites. These bifunctional active sites participated in hydrogenolysis/hydrogenation and demethylation reactions through their roles as metal sites and acid sites, respectively. The high active Ni site was more effective than Mo site, and both these sites were more active than P-OH group as

Brønsted acid site. Furthermore, Yang et al. (2009) studied the promoting effect of phosphorus in sulfided CoMo/MgO catalyst for HDO of phenol (see Table 2.1, entries 43 and 44). Phenol hydrotreatment over sulfided CoMo/MgO catalyst for 60 min led to a liquid product consisting 83.3% phenol, 3.2% cyclohexylbenzene, 7.5% cyclohexylphenol and a trace amount of benzene (0.01%). The mechanism suggested for this reaction is depicted in Scheme 2.8. To enhance the activity of CoMo/MgO, phosphorus was added into catalyst structure promoting the formation of MoS_2 active site. 60 min treatment of phenol over sulfided CoMoP/MgO at 350 °C resulted in a liquid product containing 64.8% phenol, 6.4% cyclohexylbenzene, 13% cyclohexylphenol and 13.2% benzene. Decrease of coke formation, increase of Mo dispersion and also formation of new Brønsted and Lewis acid sites on surface of catalyst were the positive effects achieved by addition of phosphorus into CoMo/MgO catalyst.

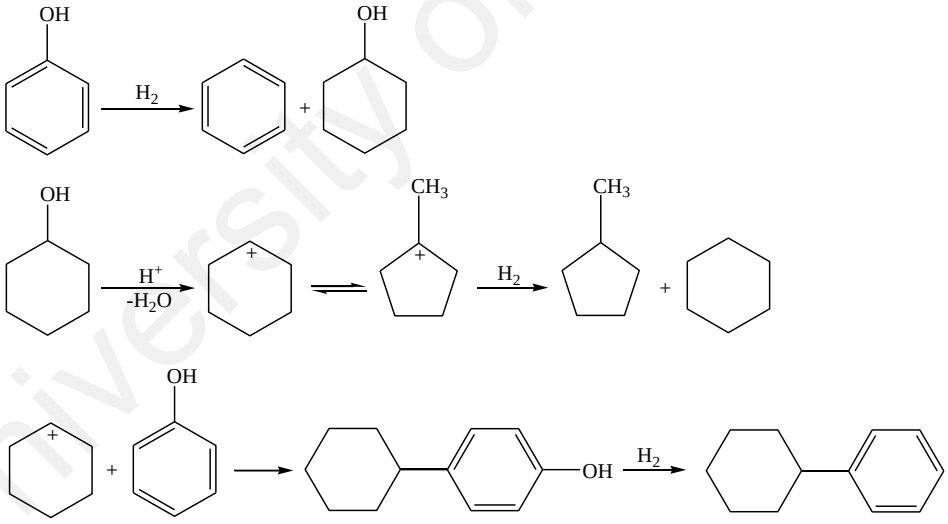

Scheme 2.8: Phenol hydrotreating mechanism for formation of cyclohexylbenzene, cyclohexylphenol and benzene over CoMo/MgO (Yang et al., 2009).

2.2.2 Catalyst support

Selection of a suitable support is an important catalyst design parameter in HDO process since materials used as catalyst support play a key role in product selectivity of HDO reaction (Centeno et al., 1995; Nikulshin, Salnikov, Varakin, & Kogan, 2015). A supported catalyst allows the catalytically active phase to be spread over the large internal

surface of the support material. Heterogeneous catalysts are usually supported by reactive and neutral materials to have higher metal dispersion, catalytic activity and structural stability under harsh operating conditions of HDO process. In HDO of guaiacol, alumina- and SBA-15 silica-supported Mo nitride catalyst was shown to have higher activity than unsupported Mo nitride catalyst due to the improvement of particle dispersion and electronic interaction as well as higher accessibility of active sites to reactants caused by the porosity of supports (Ghampson et al., 2012). Supports with different properties such as acidity-basicity, pore structure and surface area may differently change the catalyst activity. Different performance of Pt supported on γ-Al_2O_3, SiO_2 and HBeta in HDO of *m*-cresol revealed that pore structure and acid density of support are highly effective on catalytic activity; HBeta zeolite with higher density of acid sites and microporous structure led to lower activity (Zanuttini, Costa, Querini, & Peralta, 2014). High density of acid sites favors cracking mechanisms and coke formation. Meanwhile, micropores are easily blocked by coke deposits leading to limited access of reactants to the active sites. Apart from catalyst activity, reaction pathway could also be affected by catalyst support. For instance, CoMoS catalyst supported on different materials of Al_2O_3, TiO_2 and ZrO_2 exhibited different reaction pathways in guaiacol HDO (Scheme 2.9) (Bui, Laurenti, Delichère, & Geantet, 2011). Demethylation and methylation, demethylation and hydrogenation as well as demethoxylation and direct deoxygenation were the dominant reaction pathways observed in guaiacol HDO over CoMoS/Al_2O_3, CoMoS/TiO_2 and CoMoS/ZrO_2, respectively. Alumina, activated carbon, silica, zirconia and zeolites are some examples of supports which have been used for the preparation of catalysts used in HDO of phenol, cresol, guaiacol and anisole. The influence of different catalyst supports on catalytic performance and reaction selectivity of HDO of phenols is reviewed in this section.

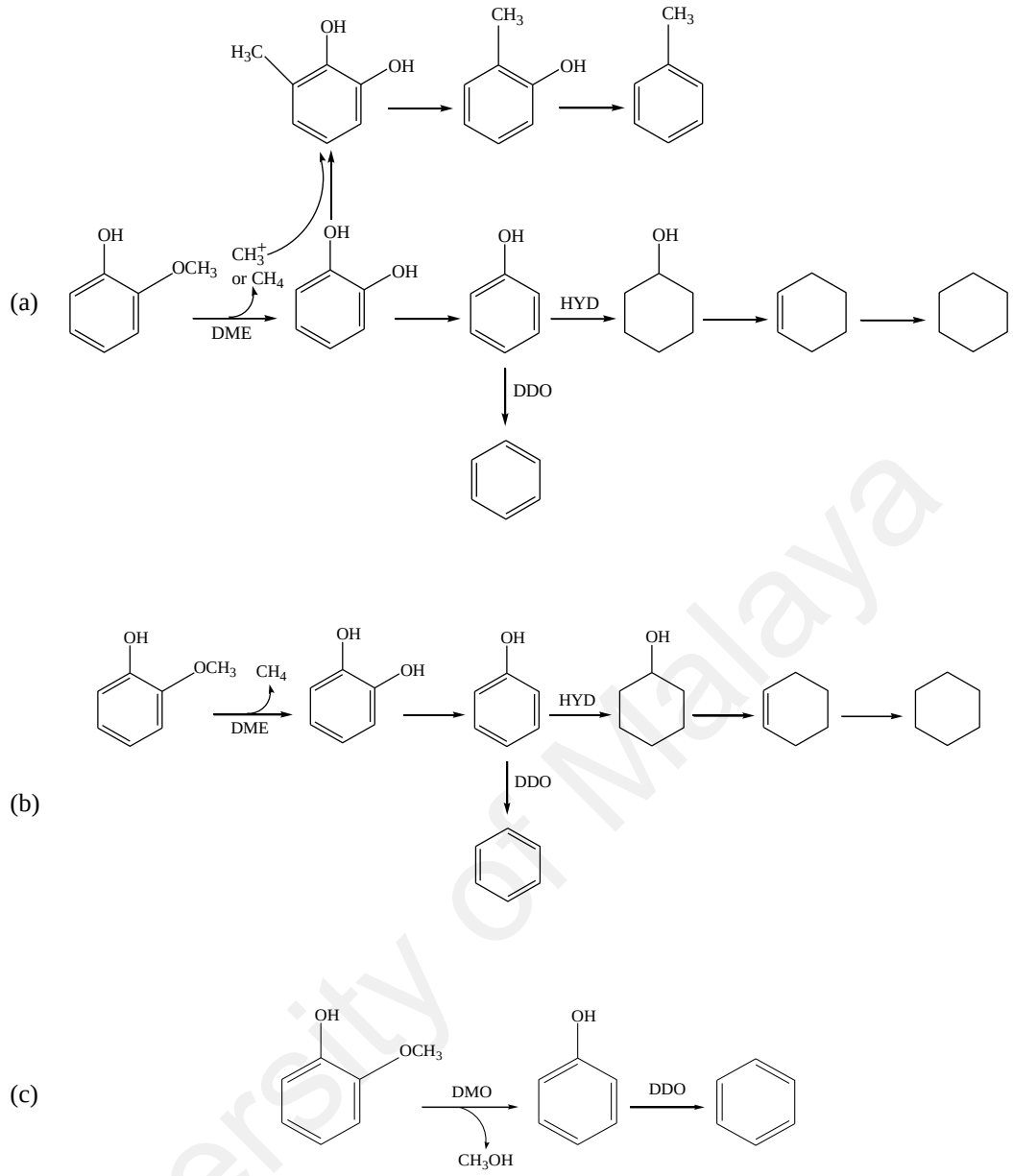

Scheme 2.9: Principal reaction network for guaiacol HDO occurring on (a) $CoMoS/Al_2O_3$; (b) $CoMoS/TiO_2$; (c) $CoMoS/ZrO_2$ (Bui, Laurenti, Delichère, & Geantet, 2011).

The effect of support nature on product selectivity was investigated using Pd catalyst (1-10 wt%) supported on mesoporous CeO_2 and ZrO_2 for HDO of phenol in a continuous fixed bed reactor at atmospheric pressure (Velu et al., 2003). At 180 °C and about 80% phenol conversion, the product obtained over Pd/CeO_2 was a mixture of cyclohexanone (~50%), cyclohexanol (~35%) and cyclohexane (~15%), while cyclohexanone (more than 90%) was the only remarkable compound produced by phenol HDO over Pd/ZrO_2 (see Table 2.1, entries 61, 63, 67 and 68). This difference in product selectivity between

Pd/ZrO_2 and Pd/CeO_2 is due to different adsorption positions of phenol on these catalysts caused by different acid-base properties of their supports. Over Pd/ZrO_2 and Pd/CeO_2, phenol is adsorbed on catalyst surface via non-planar and co-planar positions, respectively (Scheme 2.10). Phenol is adsorbed on basic sites via non-planar position resulting in high selectivity towards cyclohexanone, while acidic sites adsorb phenol molecule through co-planar mode producing more cyclohexanol and cyclohexane. In a study held by Ruiz et al. (2010), the basic nature of zirconia was changed to acidic through sulfidation of ZrO_2. It was observed that ReS_2/ZrO_2-sulfated catalyst had better dispersion of active sites compared with ReS_2/ZrO_2 whilst, guaiacol HDO reaction rate over the latter catalyst was higher than that on the former. Higher acidic strength resulted from the presence of sulfate groups in sulfated support led to better dispersion of metal in ReS_2/ZrO_2-sulfated. The high activity of ReS_2/ZrO_2 is related to its structure; ReS_2/ZrO_2-sulfated had monolayer patches of ReS_2 on support while, ReS_2/ZrO_2 had lamellar structure of sulfided Re with higher thickness. High thickness of ReS_2 layers provides higher sulfur vacancies as catalytic active sites. In guaiacol HDO at 300 °C, 50 bar and over the two Re-based catalysts, phenol and catechol were the main products whereas, deoxygenated products such as cyclohexane, cyclohexene, hexane and benzene were formed in very low content.

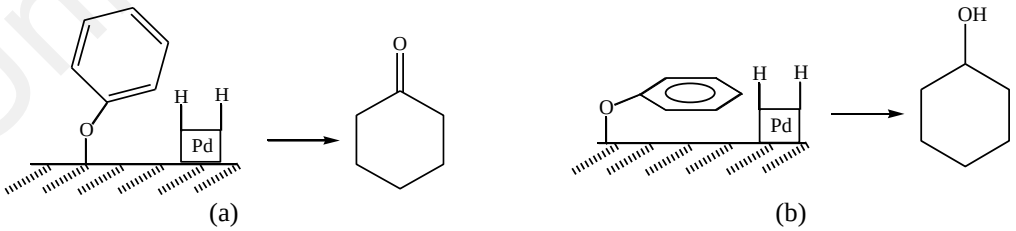

Scheme 2.10: Non-planar adsorption of phenol producing cyclohexanone (a); Co-planar adsorption of phenol producing cyclohexanol (b) (Velu et al., 2003).

Alumina has been widely used as catalyst or support in industrial catalytic reactions (Pines & Haag, 1960). Intrinsic acidity of alumina support could lead to high catalytic activity through its role in enhancing the dehydration reaction in hydrodeoxygenation

process. The overall HDO reaction of *m*-cresol over Pt/Al_2O_3 catalyst is proceeded through hydrogenation and dehydration routes catalyzed by metal and acid functions, respectively (Scheme 2.11) (Foster et al., 2012). Toluene and methylcyclohexane were the main oxygen-free products formed over Pt catalyst supported on Al_2O_3. It was reported that alumina treatment with base K_2CO_3 and acid NH_4F changes the reaction activity of Pt/Al_2O_3 catalyst (see Table 2.2, entries 27-35). Basic treatment of alumina leads to the deactivation of dehydration active sites due to the blockage of these phases caused by replacement of H^+ of support Brønsted acid sites by K^+. Increase of the acidity of support enhances the HDO rate due to the improvement of dehydration reaction. However, high acidity of alumina leads to high production of coke which deactivates catalyst rapidly. In HDO of guaiacol over Mo nitride catalysts supported on Al_2O_3, DME route was the major pathway due to high acidic properties of alumina and catechol resulted from DME route is a main intermediate compound which causes coke production (Ghampson et al., 2012). Meanwhile, it was reported by Bui et al. (Bui, Laurenti, Afanasiev, & Geantet, 2011; Bui, Laurenti, Delichère, & Geantet, 2011) that in HDO of guaiacol over MoS_2/Al_2O_3 and CoMoS/Al_2O_3, the acidic property of alumina results in production of methyl-substituted compounds which lead to difficult deoxygenation (see Table 2.3, entries 23-28).

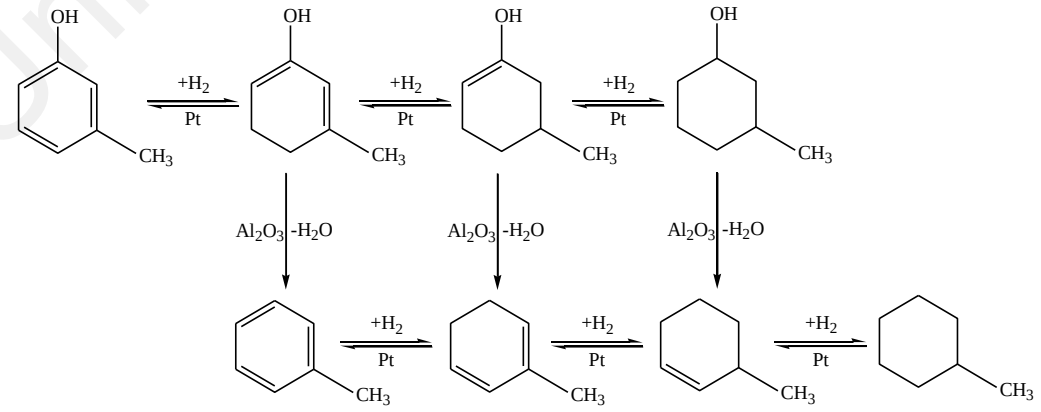

Scheme 2.11: Proposed reaction network for *m*-cresol conversion over Pt/Al_2O_3 (Foster et al., 2012).

Mesostructure silica is considered as a highly advantageous support for several types of functional groups (Angelos, Johansson, Stoddart, & Zink, 2007). Uniform channels, large pore size, high surface area and high thermal stability are great characteristics of silica materials as support (Ren, Yue, Gu, & He, 2010). Large pore size of mesoporous silica enhances mass transfer of reactant molecules. Generally, the interaction between active sites and silica support is effectively strong and can remarkably change catalytic property (Min, Santra, & Goodman, 2003). In fact, weak metal-support interaction leads to sintering which results in catalyst deactivation. The mesoporous silica SBA-15 and SBA-16 are considered proper catalyst supports for HDO process because of their high ratio of surface/volume, changeable framework composition and high thermal stability (Loricera et al., 2011). Hydrodeoxygenation of anisole on sulfided CoMoW catalyst and its modified form (by phosphate with concentrations of 0.5 or 1.0 wt%) supported on mesoporous silica SBA-15 and SBA-16 was carried out in a continuous packed bed reactor under 310 °C and 30 bar (see Table 2.4, entries 25-28) (Loricera et al., 2011). The capability of SBA-16 in dispersion of $MoWS_2$ active sites was higher than SBA-15. Modifying the catalyst with phosphate can lead to the reduction of both total catalyst acidity (due to the high interaction between Mo(W) ions and Brønsted acid P-OH groups) and catalyst deactivation caused by coke and water (Loricera et al., 2011; Stanislaus, Absi-Halabi, & Al-Doloma, 1988). Catalytic activity of samples was decreased in the order CoMoW(0.5 wt% P)/SBA-16 > CoMoW/SBA-15 ≈ CoMoW/SBA-16 ≈ CoMoW(1.0 wt% P)/SBA-15 > CoMoW(0.5 wt% P)/SBA-15 > CoMoW(1.0 wt% P)/SBA-16. Except CoMoW(0.5 wt% P)/SBA-16 catalyst, phosphate incorporation led to the decrease of interaction between metal and support resulting in the formation of large metal sulfide species which can block support pores. The similar activity of non-modified catalysts supported on SBA-15 and SBA-16 illustrated that the morphology of these supports is not influential on catalytic activity (Loricera et al., 2011). Splitting of

C_{methyl}-O bond occurs on both metal sulfides and acid sites of support. The acidic function of sulfided CoMoW/SBA-15(16) catalysts was more effective than their metallic function. Product selectivity in this process indicates two reaction routes: anisole demethylation which leads to phenol and methyl transfer to benzene ring which leads to *o*-cresol and *o*-xylenol formation. In a comparison between alumina and silica supported catalysts, it was reported by Foster et al. (2012) that activity of Pt/SiO_2 in HDO of *m*-cresol is higher than that of Pt/Al_2O_3 with the same product selectivity. Also in HDO of guaiacol over MoN/SBA-15 and MoN/Al_2O_3 catalysts, DMO and DME were the major pathways on mesoporous silica- and alumina-supported catalysts, respectively (Ghampson et al., 2012). Density of acid sites in alumina supported catalyst was four times higher than that supported on SBA-15 silica leading to higher coke formation. Although the conversion of guaiacol on MoN/SBA-15 was lower than MoN/Al_2O_3, the lower amount of hydrogen utilization and coke formation were the two benefits of Mo nitride catalyst supported on mesoporous silica.

Solid acid zeolites are another type of support materials used for HDO catalysts. Indeed, zeolites could be used as both catalyst and support which participate in acid-catalyzed reactions and affect reaction selectivity. A mixture of Pd/C (hydrogenation function) and HZSM-5 as Brønsted solid acid (dehydration function) was shown to be a high potential catalyst for hydrodeoxygenation of phenol (Zhao & Lercher, 2012); at 200 °C, 50 bar and reaction time of 2 h, complete conversion of phenol led to 100 C% cycloalkanes selectivity. Meanwhile, catalytic transformation of phenol over Ni/HZSM-5 was carried out through hydrogenation and dehydration mechanisms proceeded over Ni metal and HZSM-5 support, respectively (Song et al., 2015). In HDO of anisole in a packed bed reactor at 400 °C and atmospheric pressure using Pt noble metal catalyst supported on HBeta zeolite, Brønsted acid sites of HBeta catalyzed transalkylation reaction leading to phenol, cresols and xylenols as major products (Zhu et al., 2011). Demethylation,

hydrodeoxygenation and hydrogenation routes were sequentially catalyzed by Pt metal sites of catalyst to produce phenol, benzene and cyclohexane. A comparison between bifunctional Pt/HBeta catalyst and monofunctional HBeta and Pt/SiO_2 catalysts exhibited that catalytic activity of Pt/HBeta catalyst in both transalkylation and HDO routes was higher and the amount of hydrogen used by this catalyst was lower (Scheme 2.12). Besides, Pt supported on acidic mesoporous ZSM-5 zeolite exhibited remarkable capability in hydrodeoxygenation of mixed isomers of cresol (above 93% deoxygenation degree) (Wang et al., 2012). Gallium metal supported on HBeta and HZSM-5 zeolites was used for catalyzing HDO of *m*-cresol (Ausavasukhi et al., 2012). At similar gallium loading, HDO activity of Ga/HBeta was higher than that of Ga/HZSM-5 (see Table 2.2, entries 36-38). Different activity of the two zeolites is related to the difference in their pore size. The pore size of Beta zeolite is larger than that of ZSM-5 causing higher diffusion of large molecules of *m*-cresol into Beta zeolite. In contrast to HBeta and HZSM-5, SiO_2 is not a suitable support to stabilize gallium species and its low acidity leads to lower activity in HDO of *m*-cresol. Due to the easy adsorption of *m*-cresol on the surface of catalysts supported on zeolites, a surface pool of oxygen-containing compounds is probably formed in these catalysts (Ausavasukhi et al., 2012; Ausavasukhi, Sooknoi, & Resasco, 2009). The surface pool of oxygen-containing compounds is an intermediate which can be converted to phenol, heavy oxygen-containing compounds, benzene, toluene, xylene and light C_2-C_6 hydrocarbons.

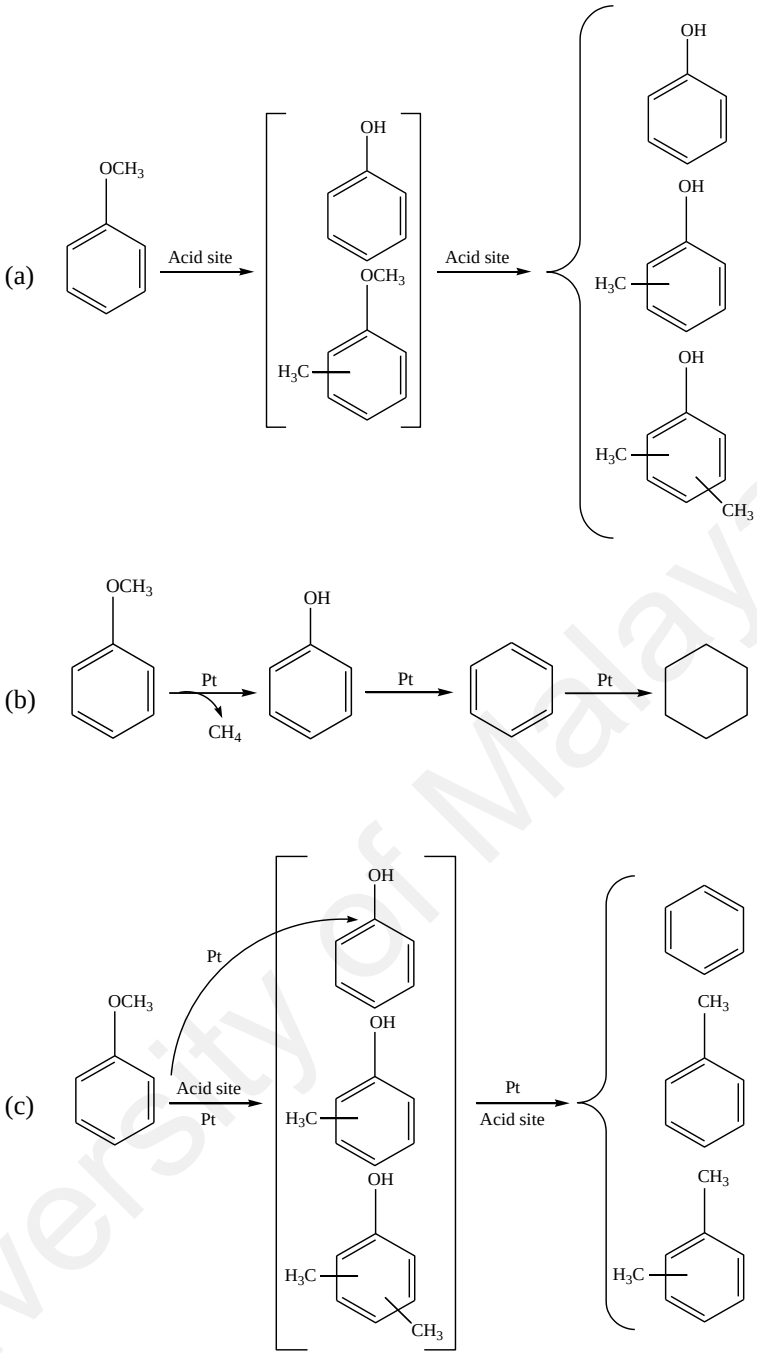

Scheme 2.12: Proposed reaction pathways of anisole HDO over (a) HBeta; (b) 1% Pt/SiO_2; (c) 1% Pt/HBeta (Zhu et al., 2011).

Activated carbon could be a suitable choice as catalyst support for hydrodeoxygenation of oxygen-containing compounds due to the low activity of activated carbon for coke generation. Centeno et al. (1995) indicated that using low acidic supports such as activated carbon instead of alumina could promote the activity of CoMoS catalyst. Large surface area of activated carbon in comparison with alumina, silica and amorphous-silica-

alumina (ASA) is considered as a positive property for high dispersion of metal active sites (Zhao et al., 2011). Besides, Nikulshin et al. (2015) showed that in guaiacol HDO, catalytic activity of CoMoS supported on carbon-coated alumina (CCA) was higher than that supported on alumina. Lower acidity of carbon-coated alumina, lower CoMoS phase size and higher CoMoS content caused enhanced activity of CoMoS/CCA compared with CoMoS/alumina. Selective hydrodeoxygenation of phenol to cyclohexane was reported to be similar for all Pd, Pt, Rh and Ru catalysts supported on carbon. Using Pd/C in neutral water at 200 °C for 0.5 h, phenol conversion and cyclohexanol selectivity were reported to be 100% and 98 C%, respectively. While under the same reaction conditions, Pd supported on Al_2O_3, SiO_2 and ASA led to about 90% phenol conversion, and selectivities toward cyclohexanol and cyclohexanone were approximately 70 and 30 C%, respectively. Al_2O_3, SiO_2 and ASA as Lewis acid supports have the potential of stabilizing cyclohexanone intermediate (Liu, Jiang, Han, Liang, & Zhou, 2009; Zhao et al., 2011). Stabilization of cyclohexanone production suppresses further hydrogenation and cyclohexane production. High stability of carbon in non-neutral solutions compared with Al_2O_3, SiO_2 and ASA leads to enhanced performance of carbon supported catalysts in basic and acidic solutions compared with those supported on Al_2O_3, SiO_2 and ASA.

2.2.3 Solvent

Catalytic activity and reaction selectivity of HDO of phenols can be promoted by type of reaction solvent. The same reaction carried out in different solvents gives a completely different performance in terms of activity and selectivity. Catalytic aqueous-phase hydrodeoxygenation of phenol over palladium supported on C, Al_2O_3, SiO_2 and ASA was studied using different solvents such as H_2O, NaOH-H_2O, CH_3COOH-H_2O and H_3PO_4-H_2O at 50 bar hydrogen pressure (see Table 2.1, entries 4-7 and 11-19) (Zhao et al., 2011). In the case of using carbon as catalyst support, alkaline solution resulted in the same

phenol conversion and product selectivity as neutral water (phenol conversion 100% and cyclohexanol selectivity 98 C%). Whilst, acidic solutions changed product selectivity of Pd/C in favor of cyclohexane (75 C% in acetic acid-water solution with pH=2.6 and 85 C% in phosphoric acid-water solution with pH=2.1). Higher acidity of solvent leads to higher cyclohexane production. In the case of using Pd/Al_2O_3, Pd/SiO_2 and Pd/ASA, catalytic activity was reduced by replacing neutral water with basic solution. The weak decomposition of amorphous inorganic oxides in alkaline solution and also aggregation of Pd particles leads to low content of Pd on the surface of these catalysts reducing hydrogenation activity. The results obtained from all catalysts show that acidic solvent is more suitable than neutral water for cyclohexane selectivity. Yan et al. (2010) and Panneman and Beenackers (1992) reported that water as solvent has negative effect on dehydration of cyclohexanol to cyclohexene.

Activity of noble metal catalysts (Pd, Pt and Ru) supported on C and Al_2O_3 as well as conventional catalysts of $CoMo/Al_2O_3$, $NiMo/Al_2O_3$ and NiW/Al_2O_3 was investigated in HDO of *p*-cresol using water and supercritical *n*-heptane as solvent (see Table 2.2, entries 1-15) (Wan et al., 2012). In water solvent, Pt catalysts exhibited highest HDO activity and selectivity towards toluene and methylcyclohexane. While due to high sensitivity of conventional catalysts to water which blocks active sites of these catalysts, HDO almost did not occur in water using CoMo, NiMo and NiW catalysts supported on Al_2O_3. Conversion of *p*-cresol over Pt, Pd and Ru noble metal catalysts was approximately complete and toluene selectivity was low in supercritical *n*-heptane. Using *n*-heptane as solvent, $CoMo/Al_2O_3$ exhibited the greatest activity and toluene selectivity (97%) among the three conventional catalysts. At HDO reaction conditions of 300 °C, 83 bar pressure and batch reaction time of 1 h, mass transfer limitation was observed in water. However, in supercritical *n*-heptane, both reactant and hydrogen gas are totally miscible and pore diffusion is highly improved. Therefore, there was not any mass transfer limitation in *n*-

heptane. In fact, high hydrogen accessibility in supercritical *n*-heptane led to hydrogenation of benzene ring to 4-methylcyclohexanol while in water, low accessibility of hydrogen resulted in hydrogenolysis pathway and toluene production. Apart from the effect of solvent on hydrogen accessibility, solvent polarity can also affect product selectivity of *p*-cresol HDO. In a polar solvent like water, *p*-cresol prefers to be vertically adsorbed on catalyst surface with its hydroxyl group (Scheme 2.13, I). Therefore, the reaction proceeds by hydrogenolysis pathway for toluene production. On the other hand, in non-polar solvent such as *n*-heptane, *p*-cresol prefers to be adsorbed on catalyst surface with its benzene ring resulting in ring hydrogenation and 4-methylcyclohexanol production (Scheme 2.13, II).

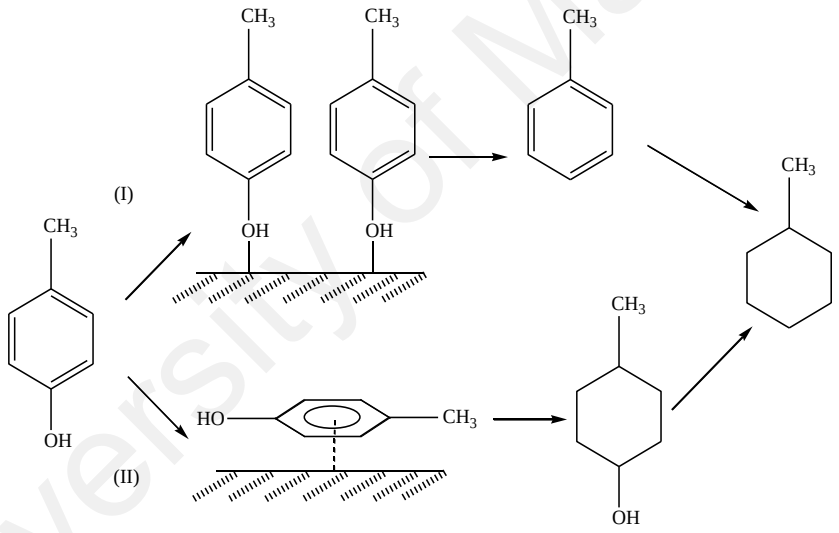

Scheme 2.13: Proposed reaction mechanisms for hydroprocessing of *p*-cresol in polar solvent (I) and non-polar solvent (II) (Wan et al., 2012).

2.2.4 Catalyst preparation procedure

The performance of catalysts in hydrodeoxygenation of phenolic compounds of bio-oil to high-value hydrocarbons is strongly dependent on the method of catalyst preparation. Method of catalyst preparation determines the homogeneity, metal dispersion, resistance toward sintering and structural properties of catalysts which are highly effective on catalytic activity. There are several different ways to prepare HDO catalysts such as impregnation, precipitation, sol-gel, etc. Selection of a suitable method for catalyst

synthesis is considered as an important step in selective hydrodeoxygenation of phenolic compounds. The effect of two different preparation methods of impregnation and sol-gel on the performance of CeO_2-ZrO_2, SiO_2-ZrO_2-La_2O_3 and SiO_2 supported nickel oxide catalysts in guaiacol HDO was studied by Bykova et al. (2011; 2012) The overall catalytic reaction of guaiacol HDO over nickel oxide catalysts is based on three main routes. (i) Formation of 1-methylcyclohexane-1,2-diol due to migration of methyl group to the aromatic ring and hydrogenation of aromatic ring. (ii) Phenol formation due to both demethylation and partial deoxygenation of guaiacol followed by hydrogenation of aromatic ring of phenol to cyclohexanone and cyclohexanol which are reduced to produce cyclohexane. (iii) Benzene formation through elimination of both methoxy and phenolic functional groups and further hydrogenation of benzene to cyclohexane. The reaction selectivity over NiCu/CeO_2-ZrO_2 and Ni/SiO_2 catalysts prepared by impregnation was toward alicyclic C_5-C_7 hydrocarbons, cyclohexanol, cyclohexanone and 1-methylcyclohexane-1,2-diol. However, on these catalysts, cyclohexane and benzene formation was low and cyclohexanone was the main product. On the other hand, NiCu/SiO_2, NiCu/ZrO_2-SiO_2-La_2O_3 and Ni/SiO_2 catalysts prepared by sol-gel method were very selective for alicyclic hydrocarbons (especially cyclohexane) formation. Although, the conversion of guaiacol on all catalysts was higher than 80%, those prepared by sol-gel method had the highest deoxygenation degree (92-97%). Catalyst analysis exhibited that the catalysts prepared by sol-gel method were highly active due to the great content of fine particles of reduced Ni films on the surface of silicate structure. These catalysts had lamellar structure leading to high specific surface area of nickel active sites and in turn high catalytic activity.

Five different structures of MoS_2 catalyst obtained by different preparation procedures were examined for HDO of phenol in a batch reactor under 320-370 °C and 28 bar H_2 (Yang, Luo, Tong, Smith, & Tye, 2008): MoS_2 derived by in situ decomposition of

molybdenum naphthenate (MoNaph), MoS_2 derived by in situ decomposition of ammonium heptamolybdate tetrahydrate (AHM), commercial crystalline MoS_2, exfoliated MoS_2 dispersed in water (TDM-W) and exfoliated MoS_2 dispersed in decalin (TDM-D). In the whole range of reaction temperature (320-370 °C), catalytic activity decreased in the order AHM > TDM-D > MoNaph > crystalline > TDM-W. AHM derived MoS_2 catalyst had larger BET surface area and smaller particle size (in terms of average stack height, slab length and number of stack layers). This means that MoS_2 catalyst derived from AHM has high dispersion in reaction solution, and much more active sites are involved in HDO reaction. The HDO activity of MoNaph derived MoS_2 catalyst was lower than that of AHM derived one since MoNaph was not completely decomposed during catalyst preparation. The main products of phenol HDO over AHM derived MoS_2 catalyst were benzene, cyclohexylbenzene and 4-cyclohexylphenol indicating that MoS_2 catalyst derived from AHM favored DDO reaction route. Furthermore, the activity of TDM-W is lower than that of TDM-D since TDM-W catalyst particles are conglomerated after being transferred from the polar solvent of water into the non-polar solvent of *n*-hexadecane at the beginning of HDO reaction.

To enhance the production of high-value hydrocarbons in HDO of phenols, it is important to develop a catalyst possessing large surface area. Larger catalyst surface area results in higher dispersion of catalytic active sites and in turn enhanced conversion and reaction rate. Apart from the selection of a suitable catalyst support with high surface area, one way to increase catalyst surface area is the use of proper additive in catalyst preparation step. Additives can affect catalyst structure by formation of new compounds in the catalyst. Use of citric acid as an additive for preparation of MoP was revealed to be effective on catalyst morphology and *p*-cresol HDO (Whiffen et al., 2012). Catalyst surface which was coarse without using citric acid became flat by addition of citric acid into catalyst precursors (Cheng et al., 2007; Whiffen et al., 2012). Also by the use of citric

acid, catalyst surface area was increased. Elemental analysis of MoP catalysts prepared with or without citric acid exhibited that citric acid addition leads to the presence of C as citrate compound. Carbon can improve catalyst structure by restricting metal crystallites accumulation and enhancing metal dispersion in catalyst. Generally, on MoP catalysts prepared with or without citric acid, toluene, methylcyclohexane and trace quantity of 1,3-dimethylcyclopentane were produced from hydrogenolysis, hydrogenation and isomerization of *p*-cresol, respectively. In the case of using MoP prepared with citric acid, direct hydrogenolysis pathway was dominant over hydrogenation pathway while in the case of using MoP prepared without citric acid, the rate of both pathways were approximately the same.

Type of metal precursor used for catalyst preparation is another preparation factor which affects catalytic activity. Different chemical composition of metal precursors leads to the presence of different elements in catalyst structure which can change the quality of active metal dispersion. The performance of Ru/C catalyst prepared from ruthenium precursors of $Ru(NO)(NO_3)_3$, $RuCl_3$ and $Ru(acac)_3$ in HDO of phenol was compared with that of commercial Ru/C (see Table 2.1, entries 23-30) (Wildschut et al., 2010). At 250 °C, 100 bar H_2 pressure and 4.3 h operation time, hydrogenation-dehydration was the only reaction mechanism and no benzene was detected in product. It was observed that the highest yield of cyclohexane produced through hydrogenation was obtained by the commercial Ru/C. Ru/C prepared from $RuCl_3$ produced more cyclohexane compared with the catalyst prepared from $Ru(acac)_3$. Hydrogenation activity of the catalyst made of $Ru(NO)(NO_3)_3$ was remarkably low probably due to nitrogen remaining on catalyst. This result is in accordance with that obtained in hydrogenation of phenol over Pd/C prepared from $Pd(NO_3)_2$ as a nitrate precursor of palladium (Díaz et al., 2007). Nitrogen had negative effect on catalyst performance due to poor distribution of metal active sites in catalyst. Nitrogen presence in catalyst precursor led to higher deposition of metal on

catalyst external surface as compared with bulk phase resulting in poor distribution of metal active sites and in turn lower hydrogenation activity. On the other hand, the catalyst prepared from $RuCl_3$ as Ru precursor led to high hydrogenation activity due to the presence of Cl^- which participates positively in active site preparation (Wildschut et al., 2010).

In addition, tungstic acid (H_2WO_4) and two heteropolyacids of phosphotungstic acid ($H_3PW_{12}O_{40}$) and silicotungstic acid ($H_4SiW_{12}O_{40}$) were used as precursors of tungsten for the preparation of oxide catalysts of Ni-W, Ni-W(P) and Ni-W(Si), respectively (Echeandia et al., 2010). The acidity of Ni-W oxide catalysts decreased in the order Ni-W > Ni-W(P) > Ni-W(Si). Although the potential of all Ni-W catalysts in phenol HDO was suitable, the catalysts prepared from heteropolyacids exhibited higher activity in HDO process. The dispersion of metal oxides on the surface of Ni-W(P) and Ni-W(Si) was better than that on the surface of Ni-W. Also, surface exposure of Ni as the active sites for hydrogenation was higher in Ni-W(P) and Ni-W(Si) catalysts compared to Ni-W meaning that the use of heteropolyacids as precursors of tungsten species resulted in more favorable properties in catalyst structure than the use of tungstic acid.

As metal precursor is effective on performance of HDO catalysts, chemical source of non-metal components of catalyst is also influential on catalytic activity and product selectivity of reaction. Chemical source of catalyst components can control the reaction selectivity through affecting catalyst structure and catalytic active phases. For instance, it was shown that type of materials utilized for nitridation of nitride metal catalysts and sulfidation of sulfide metal catalysts is mainly effective on catalytic activity and reaction selectivity of these types of HDO catalysts (Ghampson et al., 2012; Ruiz et al., 2010). Unsupported molybdenum nitride catalysts (Mo_2N) nitridated by thermal conversion in NH_3 (ammonolysis) and/or thermal conversion in mixture of N_2/H_2 (reduction/nitridation) were used in guaiacol transformation (Ghampson et al., 2012). The

catalyst prepared by ammonolysis had higher surface area and reaction rate compared with that prepared through reduction/nitridation. The source of nitrogen applied for nitridation was effective on type of active phases in catalyst. γ-Mo_2N which is highly active phase for hydrodeoxygenation was the dominant nitride phase in the catalyst nitrided by NH_3. High concentration of γ-Mo_2N as well as high atomic ratio of N/Mo were the reasons for high activity of catalyst nitrided through ammonolysis. On the other hand, nitridation of catalyst by the mixture of N_2/H_2 reduced catalyst activity due to the presence of β-$Mo_2N_{0.78}$, MoO_2 and Mo phases. β-$Mo_2N_{0.78}$ is resulted from the transformation of γ-Mo_2N leading to the decrease of hydrodeoxygenation active phase of γ-Mo_2N. MoO_2 and Mo metal lead to formation of molybdenum nitrides with low surface area. It should be mentioned that interaction between chemical source and catalyst support is also effective on catalytic performance of catalyst. For instance, nitridation of Mo catalysts supported on Al_2O_3 and mesoporous SBA-15 silica through ammonolysis was more effective on catalytic activity than reduction/nitridation method (see Table 2.3, entries 46-51) (Ghampson et al., 2012), while in comparison with ammonolysis method, nitridation of Mo supported on activated carbon by reduction/nitridation method resulted in higher catalytic activity due to the better scattering of Mo oxynitrides (Ghampson et al., 2012). Also, sulfiding Re/ZrO_2 catalyst using gas flow of H_2S mixed with either N_2 or H_2 indicated that type of sulfidation mixture (H_2/H_2S and N_2/H_2S) influenced catalytic activity via its effect on catalyst structure (Ruiz et al., 2010). N_2/H_2S sulfidation mixture led to higher reaction rate due to the decomposition of lamellar structure of ReS_2 into spherical shape. Meanwhile in HDO of guaiacol, N_2/H_2S sulfidation mixture led to higher content of active sites on support surface followed by an increase in both DMO reaction rate and phenol/catechol ratio in product (see Table 2.3, entries 52-54).

Sometimes, catalysts are reduced by reducing agents to become activated before the use in HDO process. Reduction time of catalyst in preparation step is also influential on

catalytic activity of HDO catalysts. Transformation of guaiacol on Mo_2N/Norit catalyst reduced by hydrogen gas at 400 °C for 4, 6 and 8 h illustrated that the reduction time of 6 h resulted in the maximum HDO activity (Sepúlveda et al., 2011). Increase of the reduction time from 4 h to 6 h promoted the elimination of surface oxygen functional groups and led to the enhancement of reactants accessibility to Mo_2N species. Whilst, further increase of reduction time led to decrease of catalytic activity due to the appearance of NH_x surface species as well as H and Mo unsaturated species resulted from the cleavage of Mo-N bond by H_2. Unsaturated species of Mo react with oxygen present on support surface or on subsurface of Mo_2N leading to high formation of Mo oxynitrides and decrease of catalytic activity.

2.2.5 Operating conditions

Temperature is highly effective on reaction selectivity of exothermic HDO by affecting the stability of intermediates and their consequent conversion. The difference in hydrogen availability on catalyst surface is the reason for different product selectivities obtained at different temperatures. At temperatures higher than optimum value, hydrogenation activity is decreased due to the reduction of hydrogen adsorption which is an exothermic reaction. High availability of hydrogen is suitable for hydrogenation reaction due to higher hydrogen consumption in hydrogenation pathway compared with hydrogenolysis route. Therefore at high temperature, more hydrogenolysis is taken place in comparison with hydrogenation. It was revealed that in HDO of phenol over sulfided catalysts, DDO and HYD routes are the dominant reaction pathways occurred at high and low temperatures, respectively (Yang et al., 2008; Yoosuk et al., 2012b). Yang et al. (2009) showed that increase of reaction temperature up to 450 °C enhanced catalyst activity of CoMoP/MgO and benzene selectivity; phenol conversion over CoMoP/MgO and selectivity of benzene were increased from 2 and 1% at 300 °C to 89.8 and 64% at 450

°C, respectively. Ni-W oxide catalyst supported on activated carbon was used for HDO of phenol at four different temperatures (150, 200, 250 and 300 °C) and operating pressure of 15 bar (see Table 2.1, entries 49-52) (Echeandia et al., 2010). At 150 °C, the activation of tungsten sites and adsorption of phenol was low and high yield of cyclohexanol was obtained. Cyclohexanol was also shown to be highly stable at low temperature of 150 °C in HDO of phenol over Pd/C combined with H_3PO_4 (see Table 2.1, entries 9 and 10) (Zhao et al., 2011). Increase of temperature in the range of 150-300 °C was shown to enhance the activity of Ni-W oxide catalyst (Echeandia et al., 2010). Besides, by increase of reaction temperature up to 250 °C, phenol conversion was increased and product selectivity was shifted toward cyclohexane. By increase of temperature from 250 to 300 °C, production of cyclohexane was decreased while production of benzene, methylcyclopentane and cyclohexene was increased indicating that at temperatures from 250 to 300 °C, hydrogenation activity was decreased over Ni-W catalyst.

Temperature dependence of catalytic activity and product selectivity of guaiacol HDO showed that increase of operating temperature (350-450 °C) promotes catalytic activity of Fe/SiO_2 catalyst but has no effect on product selectivity (Olcese et al., 2012). However, in HDO of guaiacol over $NiCu/ZrO_2$-SiO_2-La_2O_3 at 280, 320 and 360 °C, increase of reaction temperature led to the reduction of guaiacol conversion (Bykova et al., 2012). High temperature provided high potential for polymerization of oxygen-containing organics. Therefore, coke formation was increased due to the coverage of catalyst active sites by large molecular compounds resulting in less conversion of guaiacol. It was reported that low and high temperatures were more selective toward oxygen-containing aliphatics and cyclohexane/benzene, respectively. In addition, dependency of product selectivity of guaiacol HDO over Rh/SiO_2-Al_2O_3 catalyst to reaction temperature exhibited that by increasing temperature from room temperature to 250 °C, at 58-108 °C, guaiacol was completely hydrogenated and was mostly converted to 2-

methoxycyclohexanol (Lee et al., 2012). Further heating the reaction system (to 250 °C) led to higher production of partially deoxygenated compounds such as cyclohexanol, cyclohexanone and fully deoxygenated compound of cyclohexane. Temperatures higher than 250 °C were suitable for production of fully deoxygenated compound of cyclohexane. HDO of guaiacol over Rh/ZrO_2, $PtRh/ZrO_2$ and $PdRh/ZrO_2$ catalysts in a batch reactor at different temperatures (300, 350 and 400 °C) and 50 bar H_2 pressure included hydrogenation of aromatic ring (yielding 2-methoxycyclohexanol and 2-methoxycyclohexanone) followed by demethoxylation and dehydroxylation producing cyclohexane (Lin, Li, Wan, Lee, & Liu, 2011). Increase of reaction temperature from 300 to 400 °C enhanced the yield of cyclohexane. Besides, in HDO of *m*-cresol using MoO_3 in a packed-bed reactor, it was shown that increase of reaction temperature form 300 to 400 °C reduced activity of MoO_3 catalyst due to the change of active phase of MoO_3 to inactive phase of MoO_2 (Prasomsri, Shetty, Murugappan, & Román-Leshkov, 2014). At 400 °C, complete conversion of MoO_3 to MoO_2 occurred after 0.5 h reaction time and up to 80% of catalyst activity was reduced after 3 h. However, different behaviour was observed at lower temperature of 320 °C; MoO_3 was changed to an oxycarbohydride phase ($MoO_xC_yH_z$) with low amount of MoO_2 after 1.5 h. It was mentioned that carburisation of MoO_3 to $MoO_xC_yH_z$ stabilizes active phase of MoO_3 and prevents from formation of inactive phase of MoO_2.

Product distribution in HDO of phenolic compounds is a function of reaction temperature due to the temperature dependence of activation energies for different reaction routes taken place in HDO process. High operating temperature is needed for reaction mechanisms with high activation energy. In catalytic HDO of anisole over Pt/Al_2O_3, demethylation to phenol, demethoxylation to benzene and transalkylation to methylphenols were reported to occur at reaction temperatures in the range of 300-400 °C (Saidi et al., 2015). It was shown that the activation energy for oxygen removing

mechanism was lower than that for transalkylation mechanism. Therefore, selectivity towards deoxygenation was favored at lower operating temperatures.

In addition to temperature, pressure is another operating factor influential on selective HDO of phenols. High pressure of hydrogen is usually required to accelerate catalyst reduction and to enhance the efficiency of HDO process. In HDO of *m*-cresol over Pt/Al_2O_3 in a continuous fixed bed reactor at 260 °C, the increase of hydrogen pressure (0.5-1 bar) enhanced both *m*-cresol conversion (from 38 to 74%) and methylcyclohexane selectivity (Foster et al., 2012). The effect of hydrogen partial pressure (0-0.9 bar) on catalytic activity of Fe/SiO_2 was investigated in atmospheric hydrodeoxygenation of guaiacol for selective production of benzene and toluene (products of complete HDO) instead of phenol (product of partial HDO) (Olcese et al., 2012). It was revealed that conversion of guaiacol in the atmosphere with no hydrogen and 0.2 bar H_2 partial pressure was 30 and 70%, respectively. Guaiacol conversion was approximately constant in hydrogen partial pressure range of 0.2-0.9 bar. Increase of H_2 partial pressure from 0.2 to 0.9 bar slightly increased the production of benzene and toluene. The maximum conversion of 74% and benzene and toluene production of 38 C% were achieved at H_2 partial pressure 0.9 bar. In another work held by Saidi et al. (2015), increase of reaction pressure in a fixed-bed tubular microflow reactor from 8 to 14 and 20 bar reduced conversion of anisole from 48 to 30 and 29%, respectively. However, pressure increase improved selectivity of HDO products. Selectivity towards benzene and phenol was increased, while selectivity towards methylphenols and hexamethylbenzene was decreased. Investigation of pressure influence on product distribution of HDO of phenols using mixed catalysts of Pd/C and ZSM-5 zeolite in a batch reactor showed that for hydrogen pressure in the range of 30-50 bar, HDO activity remained almost unchanged, and selectivity of cycloalkane was 90% at reaction time of 0.5 h (Zhao & Lercher, 2012). For the pressures below 20 bar, yields of cycloalkane and cycloketone were 76 and 10%,

respectively. By decrease of hydrogen pressure to 10 bar, reactant conversion was decreased to 80% and product selectivity towards cycloalkane and cycloketone was 12 and 75%, respectively. It was deduced that low hydrogen pressure stabilizes formation of cycloketone and hinders production of cycloalkane.

2.2.6 Co-feeding

Conventional hydrotreating catalysts are based on sulfided molybdenum in combination with a promoting metal such as cobalt or nickel. Typically, the catalysts are made in an inactive oxide form of active metals which have to be sulfided in order to reach their active forms. The catalysts are sulfided by the reaction of their active metals with hydrogen sulfide which can be produced from a reaction between the sulfur available in sulfiding agent and hydrogen (Eqs. 2-1, 2-2 and 2-3). A defined quantity of sulfur is required to maintain the catalysts in their active form. Since during the HDO reaction over sulfided catalysts, sulfur leaching from catalyst surface can happen, the addition of sulfiding agent during the reaction seems to be essential for maintaining the sulfided state of catalyst. H_2S/H_2 mixture gas or CS_2 as a precursor for H_2S are common sulfiding agents which have been utilized in HDO process. However, addition of sulfiding agent reduces catalytic activity and remarkably changes product selectivity. In fact, the adsorption of thiol group on catalyst surface leads to obstruction of the sites of hydrogen chemisorption decreasing the activity of catalyst for HDO reactions (Gland, Kollin, & Zaera, 1988).

$$MoO_3 + 2H_2S + H_2 \rightarrow MoS_2 + 3H_2O \quad (2.1)$$

$$CoO + H_2S \rightarrow CoS + H_2O \quad (2.2)$$

$$3NiO + 2H_2S + H_2 \rightarrow Ni_3S_2 + 3H_2O \quad (2.3)$$

The addition of sulfiding agent into HDO feed remarkably decreases initial activity of sulfided $CoMo/Al_2O_3$ catalyst but does not have clear positive or negative effect on catalyst stability (Şenol, Ryymin, Viljava, & Krause, 2007; Viljava et al., 2000). In the

absence of sulfiding agent, sulfided $CoMo/Al_2O_3$ is much more selective toward benzene than cyclohexane and cyclohexene. However by addition of sulfiding agent, direct hydrogenolysis of phenol to benzene is strongly suppressed even in a very low amount of H_2S. While, hydrogenation-hydrogenolysis conversion of phenol to alicyclic products is the same in the absence and presence of H_2S (up to an optimum value) in feed stream. Therefore, selective inhibition of DDO reaction route by H_2S addition can be considered as an effective way for enhanced production of alicyclic products. The selective inhibition of hydrogenolysis route by H_2S illustrates that sulfided $CoMo/Al_2O_3$ contains at least two types of active sites which are different in sensitivity to sulfur (Viljava et al., 2000). Direct hydrogenolysis reaction is activated by sulfur anion vacancies present in MoS_2 which is the active site for HDO reactions in molybdenum sulfide catalysts; phenol is adsorbed on sulfur anion vacancies through its oxygen atom resulting in production of benzene and water. By addition of H_2S, this route is inhibited as the result of competitive adsorption of phenol and H_2S on sulfur anion vacancies. Higher electron affinity of hydrogenolysis active sites compared with hydrogenation sites leads to adsorption of H_2S on hydrogenolysis sites and selective inhibition of hydrogenolysis route. However, addition of H_2S inhibits both reaction routes of HYD and DDO in phenol hydrodeoxygenation over sulfided $NiMo/Al_2O_3$ catalyst (Şenol, Ryymin, Viljava, & Krause, 2007). Meanwhile in HDO of guaiacol over sulfided Re/ZrO_2, inhibitory effect of high concentration of CS_2 sulfiding agent was the same as H_2S leading to decrease of reaction rate and increase of catechol selectivity (Ruiz et al., 2010).

Addition of sulfiding agent can have negative effect by being a cause for formation of sulfur containing byproducts. By addition of H_2S, cyclohexanethiol is produced as a byproduct during phenol HDO over $CoMo/Al_2O_3$ and $NiMo/Al_2O_3$ (Şenol, Ryymin, Viljava, & Krause, 2007). Cyclohexanethiol can be produced through nucleophilic substitution reactions catalyzed by acid (Scheme 2.14). The existing mobile SH^- groups

on catalyst surface are able to act as nucleophiles and dispose catalysts for substitution reactions (Mijoin, Pommier, Richard, & Pérot, 2001; Şenol, Ryymin, Viljava, & Krause, 2007). The concentration of nucleophiles is a principal parameter in acid-catalyzed nucleophilic substitution reactions. Therefore, the production of thiol in the presence of sulfiding agent can be attributed to the increase in the number of SH^- groups of catalyst surface caused by H_2S addition.

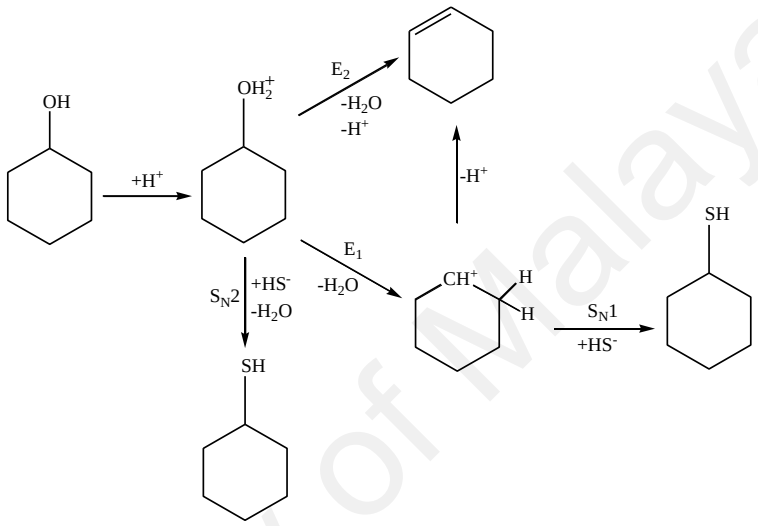

Scheme 2.14: Hydrogenation of cyclohexanol to form cyclohexene and cyclohexanethiol by elimination (E_1 and E_2) and nucleophilic substitution (S_N1 and S_N2) reactions, respectively (Şenol, Ryymin, Viljava, & Krause, 2007).

A reductant agent is usually mixed with oxygenates in order to facilitate the removal of oxygen. The reductant agent is decomposed into hydrogen molecule or prepares active hydrogen atoms to participate in hydrogenation/hydrogenolysis and hydrogen transfer reactions. The effect of co-feeding reductant agent of *α*-terpinene on catalytic activity and product selectivity was studied in HDO of guaiacol over vanadium oxide on alumina (Filley & Roth, 1999). Co-feeding *α*-terpinene with guaiacol led to easier oxygen elimination and higher yield of phenol as well as lower amount of coke generation. High tendency of V_2O_5/Al_2O_3 to phenol production is due to the oxophilic behavior of vanadium as well as its high potential to undergo changes of oxidation state. Vanadium is considered as a suitable catalyst for deoxygenation of the aromatic compounds containing oxygen atoms placed in 1,2-positions. Alumina support of vanadium oxide

catalyst had impressive role in catechol production from guaiacol. In HDO of guaiacol co-fed with α-terpinene over V_2O_5/Al_2O_3, vanadium is reduced by α-terpinene and the organic compound of *p*-cymene is formed as the product of oxidation of α-terpinene (Scheme 2.15a). The reduced vanadium is bound to catechol via one of its oxygen atoms (Scheme 2.15b). The total scheme of guaiacol HDO (combination of Schemes 2.15a and 2.15b) is depicted in Scheme 2.15c.

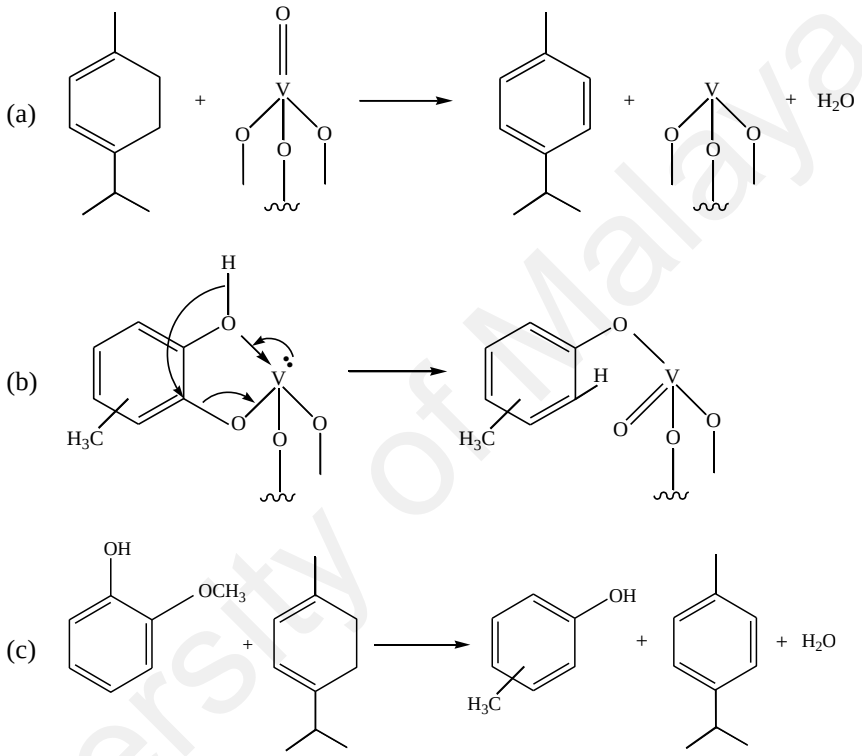

Scheme 2.15: *p*-Cymene formation due to reduction of vanadium by α-terpinene (a); The adsorption of oxygen atom of catechol by V(III) (b); The total scheme of guaiacol HDO on V_2O_5/Al_2O_3 catalyst (c) (Filley & Roth, 1999).

Co-feeding a hydrodesulfurization (HDS) feed with bio-based HDO feed leads to direct production of a partially bio-sourced fuel. In such systems, both HDS and HDO reactions are competitively proceeded. Straight run gas oil (SRGO, a residue in petroleum refineries) was co-fed with guaiacol in HDO process over CoMo catalyst supported on alumina (Bui, Toussaint, Laurenti, Mirodatos, & Geantet, 2009; Pinheiro, Hudebine, Dupassieux, & Geantet, 2009). In a trickle bed reactor under 40 bar, temperature of below 320 °C and LHSV (liquid hourly space velocity) of 2 h^{-1}, guaiacol was preferentially

transformed into phenolic compounds and conversion of sulfur-containing molecules was inhibited (Bui et al., 2009). Intermediate phenolic products of guaiacol HDO were more adsorbed on hydrogenation and/or hydrogenolysis sites of catalyst compared with sulfur-containing compounds. In fact, at temperatures lower than 320 °C, the HDO feed acted as inhibitor for HDS reaction while HDS could occur after complete conversion of phenolic intermediates into deoxygenated compounds. Similarly, by co-feeding 4,6-dimethyldibenzothiophene (4,6-DMDBT) with guaiacol over ReS_2/SiO_2 and ReS_2/Al_2O_3 catalysts, the adsorption of guaiacol molecules on catalytic active sites was more than 4,6-DMDBT molecules (Sepúlveda, Escalona, García, Laurenti, & Vrinat, 2012). Without co-feeding 4,6-DMDBT, ReS_2/Al_2O_3 had higher total rate of guaiacol conversion due to stronger acidity of alumina and ReS_2/SiO_2 had higher HDO rate (larger amount of oxygen-free products) due to lower acidity of silica. By co-feeding 4,6-DMDBT with guaiacol, total rate of guaiacol conversion over ReS_2/SiO_2 was increased while HDO rate on this catalyst was decreased. On the other hand, both rates of guaiacol conversion and HDO were increased over ReS_2/Al_2O_3 by 4,6-DMDBT addition. Adsorption of 4,6-DMDBT on ReS_2/Al_2O_3 blocks Lewis acid sites of support which are active phases for demethylation route. Thus, less accessibility of support acid sites leads to lower selectivity towards DME pathway and catechol production as well as enhanced selective conversion of guaiacol to phenol via DMO followed by more hydrogenation of phenol to oxygen-free compounds.

2.3 Deactivation of HDO catalysts

In heterogeneous catalysis, loss of catalyst activity with time-on-stream is called deactivation. The knowledge about deactivation mechanisms and effective parameters on catalyst deactivation could help in designing more effective HDO process with high yield of desired products. Lower catalyst deactivation leads to longer catalyst lifetime and

higher selectivity towards deoxygenated products (González-Borja & Resasco, 2011; Romero et al., 2009; Wildschut et al., 2009; Wildschut et al., 2010; Wildschut et al., 2009; Wildschut et al., 2010). Catalyst stability is a key catalyst characteristic which determines its applicability in commercial scale. Generally, deactivation of HDO catalysts is caused by coking, poisoning, thermal degradation and sintering.

2.3.1 Deactivation caused by coke

The main challenge of HDO process is the rapid loss of catalyst activity due to formation of coke which is a competing reaction with production of aromatics and alicyclics. Polymerization and polycondensation are two main reactions resulting in coke generation which blocks catalytic active sites and reduces their accessibility for reactants (Bykova et al., 2014). Coke deposition on catalyst surface is strongly dependent on type of reactants and intermediates. Unsaturated oxygenates such as aromatic fragments have high tendency to produce coke through polymerization on catalyst surface (Furimsky & Massoth, 1999). Phenols are considered as a potential group of bio-oil compounds for coke production in HDO reaction (González-Borja & Resasco, 2011; Graça et al., 2011; Popov et al., 2010). In comparison to phenol, cresol and anisole, guaiacol with two oxygen atoms bonded to benzene ring causes highest coke formation (Elliott, 2007; Foster et al., 2012; González-Borja & Resasco, 2011; Hurff & Klein, 1983; Laurent, Centeno, & Delmon, 1994; Mu et al., 2014; Popov et al., 2010; Romero et al., 2009; Wildschut et al., 2009; Wildschut et al., 2010; Wildschut et al., 2009; Wildschut et al., 2010). Oxygenated compounds with more than one oxygen atom have high affinity for coke formation through polymerization mechanism (Popov et al., 2013). Catechol which is produced as an intermediate in HDO of guaiacol is also a strong agent for coke generation (Puente et al., 1999; Elliott, 2007; Filley & Roth, 1999; Foster et al., 2012; Mu et al., 2014; Olcese et al., 2012; Sepúlveda et al., 2011; Ghampson et al., 2012; Zhao et al.,

2011). In catalytic HDO of guaiacol over Ru/C and Pt/C, naphthalene which was produced from ring condensation mechanism and its larger condensed ring derivatives were reported as the main cause for rapid catalyst deactivation (Gao, Schweitzer, Hwang, & Varma, 2014).

In addition, deactivation of catalyst by coke is dependent on catalyst properties such as acidity. Generally, higher acidity of catalyst (including both Lewis and Brønsted acid sites) leads to higher coke formation (Bykova et al., 2014). Lewis acid sites bind reactant species to catalyst surface, and Brønsted acid sites give proton to reactant molecules to form carbocations which are known to be coke precursor (Furimsky & Massoth, 1999; Li et al., 2015). In a study held by Zanuttini et al. (2014) for HDO of *m*-cresol over Pt/SiO_2, Pt/Al_2O_3 and Pt/HBeta catalysts, Brønsted acid sites were reported to have the highest impact on catalyst deactivation by coking, and coke yield was shown to be reduced by decrease in density of Brønsted acid sites. Pt/SiO_2 had lower total density of acid sites compared with Pt/Al_2O_3, but coke formation on Pt/SiO_2 was higher than that over Pt/Al_2O_3. This was due to the presence of Brønsted acid sites in Pt/SiO_2, while Pt/Al_2O_3 had only Lewis acid sites. In comparison to Pt/SiO_2 and Pt/Al_2O_3, faster deactivation of Pt/HBeta was observed which was due to the high density of Brønsted acids of zeolite support. Meanwhile, based on literature reports, catalysts supported on alumina suffer from deactivation through coking owing to the presence of strong acid sites on this support. Enhanced HDO activity was obtained in guaiacol transformation over CoMoS supported on carbon-coated alumina compared with alumina (Nikulshin et al., 2015). Coverage of alumina by carbon reduced total acidity of catalyst and resulted in lower coke formation. Eq. (2-4) was given to estimate degrees of catalyst deactivation in guaiacol conversion and HDO using a fixed bed microreactor:

$$Dd_{Gua} = \left(\frac{x_{Gua}^{init} - x_{Gua}^{s}}{x_{Gua}^{init}}\right).100\% \text{ and} \quad (2.4)$$

$$Dd_{HDO} = \left(\frac{x_{HDO}^{init} - x_{HDO}^{s}}{x_{HDO}^{init}}\right).100\%$$

where Dd_{Gua}, Dd_{HDO}, x_{Gua}^{init}, x_{HDO}^{init}, x_{Gua}^{s} and x_{HDO}^{s} are catalyst deactivation degree in guaiacol conversion, catalyst deactivation degree in guaiacol HDO, initial guaiacol conversion, initial guaiacol HDO, steady-state guaiacol conversion and steady-state guaiacol HDO, respectively. Experimental data showed that degree of catalyst deactivation was a function of carbon amount used for coating the alumina support. Dd_{Gua} and Dd_{HDO} for CoMo/Al_2O_3, CoMo/C/Al_2O_3 (2 wt% C) and CoMo/C/Al_2O_3 (5.6 wt% C) were 46, 33, 31% and 69, 19, 4%, respectively. These data indicate that increase of carbon content in catalyst support (or decrease of catalyst acidity) resulted in reduction of catalyst deactivation degree. This result is in agreement with that reported by Sun et al. (2013) who showed that substitution of alumina support with carbon enhanced catalyst stability in HDO of phenolic compounds since strong reaction of phenolic compounds and acidic sites of alumina leads to rapid deactivation of catalyst by formation of coke precursors.

Apart from catalyst properties, operating parameters such as temperature and pressure are influential on coke yield of HDO. Low hydrogen pressure and low reaction temperature favor the condensation/polymerization reactions rather than hydrogenation reaction. Indeed, hydrogen regenerates active oxygen vacancy sites and prevents from site blocking by carbonaceous species (Prasomsri, Nimmanwudipong, & Román-Leshkov, 2013). Reaction temperature could be optimized for reduced coke yield. Increase of reaction temperature could result in lower coke yield due to hydrogenation of coke deposited on catalyst to stable products (Gualda & Kasztelan, 1996). However, temperatures higher than optimum value lead to high coke formation due to generation of hard coke with low volatility and solubility which is difficult to be desorbed from catalyst surface (Li et al., 2013; Li et al., 2015; Yakovlev et al., 2009). In phenol HDO over Pd/HY-Al_2O_3, high

coke formation and rapid catalyst deactivation was observed at temperatures higher than 250 °C (Echeandia et al., 2014). In catalytic HDO of phenol over Ni/Na-Y, effect of reaction temperature on degree of catalyst deactivation and initial conversion of phenol was quantitatively studied using an empirical model as follow (Shin & Keane, 2000):

$$x = x_{initial}\exp(-\alpha\Delta t) \quad (2.5)$$

where α (h^{-1}), $x_{initial}$ and t (h) refer to catalyst deactivation degree, initial conversion of phenol and reaction time, respectively. Increase of reaction temperature from 200 to 300 °C increased deactivation degree of Ni/Na-Y catalyst. Increase of reaction temperature led to higher pore blockage of catalyst due to higher amount of coke deposited on catalyst.

In addition to acid sites, metal active sites could also cause coke formation in HDO of phenolic compounds. However, deactivation rate of metal and acid sites of catalyst by coke deposition is different; in catalytic HDO of *m*-cresol over bifunctional catalysts of Pt/Al_2O_3 and Pt/HBeta, deactivation of acid sites was faster than that of metal sites (Zanuttini et al., 2014). Deactivation degree of Fe/SiO_2 catalyst in guaiacol HDO carried out in a fixed bed reactor was determined by fitting experimental data with an empirical model (Eq. 2-6) (Olcese, Francois, Bettahar, Petitjean, & Dufour, 2013).

$$k = k^0\exp(\alpha t) \quad (2.6)$$

Here, k (kmol s^{-1} kg^{-1}), k^0 (kmol s^{-1} kg^{-1}), α (min^{-1}) and t (min) are reaction rate, initial reaction rate, deactivation coefficient and time on stream, respectively. Deactivation coefficient values for guaiacol conversion, phenol transformation to benzene and cresol conversion to toluene (HDO mechanisms) were in the range of 4.6-5.03 × 10^{-3} min^{-1}, while deactivation coefficient value for guaiacol transformation to cresol (transalkylation mechanism) was 7.29 × 10^{-3} min^{-1}. Modification of structural properties of catalyst could enhance catalyst durability by decrease of coke formation over metal active sites. For instance, coke formation on metal Ni catalyst was remarkably suppressed by addition of Cu into catalyst structure leading to reformation of metal active phase by formation of

NiCu alloy (Lee, Lee, Joo, & Jung, 2004). Meanwhile, in a study held by Bykova et al. (2014), catalyst deactivation through coke formation was decreased by addition of P and Mo to nickel based catalyst of $NiCu/SiO_2$-ZrO_2. The P and Mo additives changed the distance between Ni sites and thus hindered polymerization mechanism and coke formation.

2.3.2 Deactivation caused by poisoning

Catalyst poisoning caused by strong chemisorption of reactants, products or impurities on catalytic sites is considered as another main cause for catalyst deactivation during HDO reactions. In catalytic HDO of guaiacol over Ni/ZrO_2, rapid deactivation of catalyst occurred by co-feeding 0.05 wt% sulfur (Mortensen et al., 2014). Complete loss of activity was observed due to formation of inactive phase of nickel sulfide. Catalysts based on nickel have high potential to be deactivated by sulfur. Conventional hydrotreating catalysts such as NiMoS and CoMoS are rapidly deactivated by oxygenated compounds and water (Zhao, Kasakov, He, & Lercher, 2012). Water which is used as solvent or produced through HDO reactions can lead to catalyst deactivation by being adsorbed on catalytic active sites (Badawi et al., 2011; Busetto et al., 2011; Elliott & Hart, 2009; Gutierrez et al., 2009; Joshi & Lawal, 2012; Loricera et al., 2011; Romero et al., 2009; Şenol, Viljava, & Krause, 2007; Xiong et al., 2011). Water causes oxidation of active metals (Li et al., 2011; Wan et al., 2012; Wang, Yang, Luo, Peng, & Wang, 2011; Whiffen & Smith, 2010; Yoosuk et al., 2012a; Zhao et al., 2011) and agglomeration of particles and in turn loss of catalytic activity (Albers, Pietsch, & Parker, 2001). It was reported by Mortensen et al. (2015) that catalyst deactivation rate by the water used as solvent is higher than that by the water produced from HDO reaction. In a study held by Olcese et al. (2013) for guaiacol HDO, oxidation of iron by phenols, water and carbon oxides was the main cause for deactivation of Fe supported on silica and activated carbon. In HDO

of bio-oil carried out by Laurent and Delmon (1994), it was shown that high content of water leads to deactivation of sulfided $NiMo/Al_2O_3$ catalyst through oxidizing nickel species. Meanwhile, Li et al. (2011) reported that Ni_2P catalyst was deactivated by water through oxidization of active phase of phosphide to less active phases of phosphate or oxy-phosphide. It was also reported that water results in change of active phase of Mo_2C to inactive phase of MoO_2 in HDO of phenol (Mortensen et al., 2015) and anisole (Lee, Kumar, Wang, & Bhan, 2015). However, Prasomsri et al. (2013) pointed out that water addition did not increase deactivation rate of MoO_3 catalyst used in HDO of phenolic compounds. MoO_3 showed high tolerance to poisoning with water. Badawi et al. (2011) also reported that water was not the main cause for deactivation of Mo/Al_2O_3 catalyst in HDO of phenol, and addition of Co into catalyst structure decreased deactivating effect of water. Furthermore, in catalytic HDO of phenolic compounds over bimetallic catalyst of Pd/Fe_2O_3, Pd addition to Fe catalyst decreased Fe oxidation by water and catalyst deactivation rate due to the electronic interactions of Pd-Fe which facilitate the desorption of intermediates/products form catalyst active sites (Hensley et al., 2014; Hensley, Wang, & McEwen, 2015). Traditional hydrotreating catalysts supported on alumina are rapidly deactivated at high concentration of water due to the instability of alumina in contact with water (Busetto et al., 2011; Elliott & Hart, 2009; Gutierrez et al., 2009; Joshi & Lawal, 2012; Kobayashi et al., 2012; Romero et al., 2009; Şenol, Viljava, & Krause, 2007; Xiong et al., 2011). Water converts alumina to boemite (AlO(OH)) leading to oxidation of metal catalysts and catalyst deactivation. Therefore, selection of a suitable support with high tolerance to water can increase the lifetime of HDO catalyst. For instance, use of hydrophobic activated carbon as support hinders catalyst deactivation caused by water (Echeandia et al., 2010; Ghampson et al., 2012). Moreover, the increase of water concentration can change product selectivity; according to chemical equilibrium of the reaction of cyclohexanol dehydration, the increase of water content decreases

cyclohexanol dehydration and as a consequence leads to decrease of oxygen-free products (Bykova et al., 2011; Bykova et al., 2012; Li et al., 2011; Yakovlev et al., 2009; Zhao et al., 2011; Zhao et al., 2011). Loricera et al. (2011) pointed out that modifying the surface chemistry of CoMoW/SBA-16 with 0.5 wt% phosphate prevents catalyst deactivation by water and coke in HDO of anisole.

2.3.3 Deactivation caused by thermal degradation

Thermal degradation causes catalyst deactivation through sintering or chemical transformation of active phases. Morphological changes of catalyst due to sintering and agglomeration result in particle growth and reduction of catalytic activity (Albers et al., 2001). Loss of catalytic surface area caused by both crystallite growth of catalytic sites and pore breakdown on crystallites of active sites as well as loss of support area due to support breakdown generally occur by sintering phenomenon. In catalytic HDO of guaiacol over Pt, Pd, Rh and Ru supported on activated carbon, increase of reaction temperature from 275 to 325 °C resulted in decrease of catalyst surface area due to metal crystallite growth and collapse of support structure (Gao et al., 2014). Reduction of catalyst surface area results in lower catalytic activity since the amount of active sites available for reactant molecules is reduced. Average sizes of metal particles was increased due to sintering of catalysts; average sizes of Pt/C and Ru/C were increased from 2.40 ± 0.54 and 2.56 ± 0.47 nm to 2.67 ± 0.62 and 2.87 ± 0.63 nm, respectively. In addition to sintering, chemical transformation of active phases to inactive phases could occur as a result of thermal degradation of catalyst during HDO process. For instance, in HDO of lignin-derived oxygenates (phenol, *m*-cresol, anisole and guaiacol) over MoO_3, increase of reaction temperature from 300 to 400 °C caused strong deactivation of catalyst due to the change of active MoO_3 to inactive MoO_2; at 400 °C and after 0.5 h reaction time, MoO_3 was completely converted to MoO_2 (Prasomsri et al., 2014). However, at

temperatures below 350 °C, MoO_3 was changed to oxycarbohydride-containing phases ($MoO_xC_yH_z$) with minor impurity of MoO_2. In fact, conversion of MoO_3 to $MoO_xC_yH_z$ which occurs via surface carburization in the presence of a carbon source like phenolic compounds leads to stabilization of MoO_3 and reduction of MoO_2 formation. First order deactivation model (Eq. 2-7) was used to determine catalyst deactivation degree by experimental data obtained from *m*-cresol HDO over MoO_3 at different reaction temperatures (Prasomsri et al., 2014).

$$\ln \ln \left(\frac{1}{1-x}\right) = k_{Deact} t + C \tag{2.7}$$

Where x, k_{Deact} (h^{-1}) and t (h) refer to fractional conversion, first order deactivation rate constant and time, respectively. At 400 °C, rapid deactivation of catalyst occurred and deactivation constants of 0.898 and 0.156 h^{-1} were achieved for reaction time regimes of 0-4 and 4-7 h, respectively. At reaction temperatures below 350 °C, catalyst deactivation was slow; deactivation constants at temperatures of 300, 320 and 350 °C were 0.048, 0.058 and 0.149 h^{-1}, respectively.

2.3.4 Deactivation caused by desulfurization

In the case of using sulfided HDO catalysts, desulfurization also results in catalyst deactivation in addition to coke formation and water poisoning (Bowker et al., 2011; Busetto et al., 2011; Bykova et al., 2014; C. Chen et al., 2015; Elliott & Hart, 2009; Hong et al., 2014; Joshi & Lawal, 2012; Romero et al., 2009; Şenol, Viljava, & Krause, 2007; Xiong et al., 2011). Considering the low content of sulfur in bio-oil and in order to compensate sulfur leaching from catalyst surface and maintain sulfided state of catalyst, co-feeding a sulfiding agent seems to be necessary. Sulfiding agent in an optimum value can maintain catalytic activity of sulfided catalysts. However, at values higher than the optimum value, sulfur of sulfiding agent acts as an inhibitor of HDO reaction. Sulfur as competitor of oxygen-containing compounds is adsorbed on catalyst and deactivates the

catalyst by decreasing the concentration of coordinatively unsaturated active sites (CUSs) of catalyst (Ferrari, Maggi, Delmon, & Grange, 2001; Viljava et al., 2000). By adsorption of sulfur-containing compounds on the CUSs, sulfur is present in final product composition. For sulfided HDO catalysts, very high temperature also leads to rapid catalyst deactivation caused by high concentration of water generation, large amount of sulfur loss and high yield of coke formation (Zakzeski et al., 2010).

2.4 Transfer hydrogenation of phenol

Severe operating conditions of HDO of bio-oil to high value chemicals make it difficult to industrialize the process. Flammability of molecular hydrogen in contact with air leads to hard control of high pressure of hydrogen in large scale industrial applications of HDO process. Besides, high price of hydrogen gas production and compression as well as the difficulties related to its transportation and storage limit the application of hydrogen gas (Panagiotopoulou & Vlachos, 2014; Patil & Sasson, 2015). Therefore, replacing hydrogen gas with liquid hydrogen donors (H-donor) as alternative source of hydrogen is highly attractive. Hydrogen released from H-donor compounds could be reacted with hydrogen acceptors on catalytic active sites. Catalytic reduction of a molecule using hydrogen atom transferred from donor molecule is called transfer hydrogenation (Gao, Jaenicke, & Chuah, 2014; Villaverde, Garetto, & Marchi, 2015; Wang & Rinaldi, 2012). Transfer hydrogenation occurs at less severe operating condition compared with hydrogenation using hydrogen gas. The precise mechanism of catalytic transfer hydrogenation is not yet clear. Generally, hydrogenation could occur in two mechanisms: (i) decomposition of H-donor to hydrogen molecule which is activated on catalytic active sites for involving in hydrogenation reaction; (ii) transfer of hydrogen atom from H-donor molecule to acceptor on catalytic sites. The general reaction between donor (DH_x) and acceptor (A) is supposed to be like Eq. (2-21) (Brieger & Nestrick, 1974).

$$DH_x + nA \xrightarrow{Catalyst} nAH_x + D \quad (2.8)$$

The compound used as hydrogen donor should have high reduction potential through which hydrogen transfer could occur in mild operating conditions. Meanwhile, compounds formed via hydrogen release of H-donors should be easily separated from final products obtained from transfer hydrogenation process. So far, hydroaromatics (Baraniec-Mazurek & Mianowski, 2010; Zhang & Yoshida, 2001), unsaturated hydrocarbons (Ikeshita, Kihara, Sonoda, & Ogawa, 2007; Quinn, Razzano, Golden, & Gregg, 2008), alcohols (Elie, Clausen, & Geiger, 2012; Farhadi, Kazem, & Siadatnasab, 2011; Radhakrishan, Do, Jaenicke, Sasson, & Chuah, 2011; Xiang, Li, Lu, Ma, & Zhang, 2010), acids (Koike, Murata, & Ikariya, 2000; Yu, Wu, Ramarao, Spencer, & Ley, 2003; Zhang, Blazecka, Bruendl, & Huang, 2009) and formate salts (Cortez, Aguirre, Parra-Hake, & Somanathan, 2009; Gao et al., 2014; Prasad et al., 2005) have been used as hydrogen donor for transfer hydrogenation reactions. Among all types of donors, alcohols are most attractive since they are non-corrosive and act as both reactants and solvents, and also their dehydrogenation products (aldehydes and ketones) are easily separated from final products (Panagiotopoulou & Vlachos, 2014). Secondary alcohols such as 2-propanol, 2-butanol, 2-pentanol, 2-heptanol and 2-octanol are more efficient than primary alcohols such as ethanol, 1-propanol and 1-butanol in transfer hydrogenation reactions (Villaverde et al., 2015). Methanol, ethanol, 2-propanol and 2-butanol were examined in transfer hydrogenation of phenol over RANEY® Ni (Wang & Rinaldi, 2012); complete conversion of phenol was only achieved by the use of 2-propanol and 2-butanol, while methanol and ethanol led to catalyst deactivation (see Table 2.5, entries 1-8). Contradictory data achieved using different types of alcohols were assigned to different interactions between catalyst and donors. Adsorption of methanol and ethanol on Ni surface splits the O-H bond producing an H-adatom and surface alkoxy groups which block the surface of RANEY® Ni and deactivate the catalyst. On the other hand, 2-

propanol adsorption on Ni surface cleaves both O-H and α-C-H bonds releasing two atoms of H which are adsorbed on the catalyst surface and acetone is produced instead of alkoxy groups. These reactions lead to the loading of catalyst surface with H-atoms and keep the catalyst surface unblocked for transfer hydrogenation. In addition to alcohols, formic acid, a major product of biomass processing, has high potential to be used as hydrogen donor in hydrogenation (Zhang et al., 2014). Formic acid is an inexpensive, environmentally non-malignant and easy to handle hydrogen source (Wienhöfer, Westerhaus, Junge, & Beller, 2013). Formate salts are also considered as important H-donors since they are highly capable for hydrogen production, stable and easily accessible. Furthermore, bicarbonate which is produced from dehydrogenation of formate could be converted back to formate at mild conditions (Gao et al., 2014). In transfer hydrogenation of phenol over Pd/C catalyst, hydrogen donor of sodium format/water was reported to result in the selectivities of 98.1 and 1.9% for cyclohexanone and cyclohexanol, respectively, at 63.6% phenol conversion (Cheng et al., 2012). Potassium formate was also used in transfer hydrogenation of phenol over Pd/C catalyst which resulted in 85% phenol conversion and ~100% cyclohexanone selectivity (Patil & Sasson, 2015).

In addition to H-donors, catalyst characteristics have also remarkable effect on deoxygenation efficiency of transfer hydrogenation process. So far, homogeneous catalysts have been vastly used in transfer hydrogenation reactions (Indra, Maity, Bhaduri, & Lahiri, 2013; Wu et al., 2006; Zhou, Wu, Yang, & Xiao, 2012). Difficult reusability of homogeneous catalysts and the necessity for a base or ligand in homogeneous catalysis make it difficult to handle these catalytic systems. Heterogeneous catalysts do not have such problems and are more appropriate for industrial application. Heterogeneous catalysts of Pd/C, Pd/Al_2O_3, $Pd\text{-}La/\text{-}Al_2O_3$, Ru/C, RANEY Ni and $Ni\text{-}Cu/Al_2O_3$ were used in transfer hydrogenation of phenols, aldehydes, ketones and bio-oil

(Gao et al., 2014; Liu et al., 2013; Patil & Sasson, 2015; Kannapu, Mullen, Elkasabi, & Boateng, 2015; Xu et al., 2015). It is generally supposed that both the reactions of hydrogen liberation from H-donor and hydrogen consumption by acceptor simultaneously occur on the same catalytic active sites. Therefore, an efficient catalyst for transfer hydrogenation reaction should have high potential for adsorption of both hydrogen donor and acceptor molecules. For instance, in transfer hydrogenation of phenol using formic acid as H-donor, Pd supported on AC had higher activity compared with Pd supported on MIL-101, TiO_2, Al_2O_3 and TiO_2-AC due to the facilitating effect of activated carbon on adsorption of both phenol and formic acid (see Table 2.5, entries 12-16) (Zhang et al., 2014). At 65.6% phenol conversion over Pd/AC, the use of formic acid as hydrogen donor led to production of cyclohexanone and cyclohexanol with selectivities of 96.3 and 3.7%, respectively (Zhang et al., 2014). Meanwhile, the rates of hydrogen release from H-donor and hydrogen consumption by acceptor should be synergistic since the hydrogenation of acceptor molecule occurs by the hydrogen liberated from H-donor molecule. Higher rate of hydrogen liberation compared with hydrogen consumption results in inefficient consumption of released hydrogen while a fraction of generated hydrogen is not involved in hydrogenation reaction. On the other hand, too slow rate of hydrogen release by H-donor in comparison with hydrogen consumption by acceptor could lead to reduction in hydrogenation of acceptor molecule due to the polymerization of acceptor prior to its hydrogenation on catalytic active sites. Further understanding of the interaction between catalyst and H-donor is essential for development of transfer hydrogenation of bio-oil/bio-oil model compounds.

Table 2.5: Transfer hydrogenation of phenol at different conditions.

Entry	H-donor	Catalyst	T (°C)	t (h)	Conv. (%)	Selectivity (%)		Ref.
						Cyclohexanone	Cyclohexanol	
1	2-Propanol	RANEY® Ni	80	3	100	0.4	99.3	(Wang & Rinaldi, 2012)
2	2-Propanol	RANEY® Ni	120	3	100	0.7	98.7	
3	2-Butanol	RANEY® Ni	80	3	100	1.1	98.2	
4	2-Butanol	RANEY® Ni	120	3	100	0.8	98.8	
5	Methanol	RANEY® Ni	80	3	18	5.3	93.5	
6	Methanol	RANEY® Ni	120	3	21	4.8	94.1	
7	Ethanol	RANEY® Ni	80	3	15	7.1	92.9	
8	Ethanol	RANEY® Ni	120	3	20	5.1	91.7	
9	HCOONa	Pd/C	80	2	32.2	99.8	0.2	(Cheng et al., 2012)
10	HCOONa	Pd/C	80	5	63.6	98.1	1.9	
11	Formic acid	Pd/C (commercial)	50	4	56	98.6	1.4	(Zhang et al., 2014)
12	Formic acid	Pd/AC	50	4	65.6	96.3	3.7	
13	Formic acid	Pd/MIL-101	50	4	37.9	98.2	1.8	
14	Formic acid	Pd/TiO_2	50	4	24.7	99.2	0.8	
15	Formic acid	Pd/Al_2O_3	50	4	18.1	99.4	0.6	
16	Formic acid	Pd/TiO_2-AC	50	4	47.3	96.4	3.6	
17	2-Methyltetrahydrofuran	RANEY® Ni	80	3	15	7.9	91.2	
18	Methanol	Ni/SiO_2	0	5 min	20	-	100	(Rahman & Jonnalagadda, 2009)
19	HCOOK	Pd/C	100	5	85	>99	0	(Patil & Sasson, 2015)
20	HCOOK	Pd/C	100	6	>99	>99	0	
21	HCOOK	Pd/C	100	7	>99	95	5	
22	HCOOK	Pd/C	100	14	>99	75	25	
23	HCOOK	Pd/C	70	6	94	97	3	
24	HCOOK	Pd/C	50	6	19	>99	0	

CHAPTER 3: MATERIALS AND METHODS

3.1 Materials

Phenol (C_6H_6O, ≥99%), *m*-cresol (C_7H_8O, ≥98%), *o*-cresol (C_7H_8O, ≥99%), guaiacol ($C_7H_8O_2$, natural, ≥98%), decalin (cis-trans, 98%, reagent grade), tetralin (≥97%, reagent grade), 2-isopropylphenol ($C_9H_{12}O$, ≥98%), nickel (II) nitrate hexahydrate (crystallized, ≥97%) and iron (III) nitrate nonahydrate (ACS reagent, ≥98%) were purchased from Sigma-Aldrich. Ethyl acetate was procured from R&M Chemicals. All the chemicals were used as received without any purification. Purified hydrogen and nitrogen were supplied from Linde Malaysia Sdn. Bhd.

3.2 Commercial catalysts

Pd/C (10 wt% Pd loading, matrix activated carbon support) and Pt/C (10 wt% Pt loading, matrix activated carbon support) were obtained from Sigma-Aldrich. Prior to catalytic activity measurements, Pd/C was pretreated by hydrogen gas at 300 °C and 20 bar for 1 h. Pt/C was used as received and without further pretreatment. Beta (CP814C, SiO_2/Al_2O_3 molar ratio of 38), ZSM-5 (CBV3024E, SiO_2/Al_2O_3 molar ratios of 30, 50 and 80) and HY (CBV720, SiO_2/Al_2O_3 molar ratios of 30 and 60) zeolites were purchased from Zeolyst International. Prior to catalytic activity measurements, all the zeolites were calcined in air at 550 °C overnight.

3.3 Modified catalysts

Ni/HZSM-5, Ni/HY, Ni/HBeta, Fe/HBeta and NiFe/HBeta were used as modified catalyst in this study. HZSM-5 and HBeta were obtained by calcination of the ammonium form of ZSM-5 and Beta zeolites at 550 °C (with heating rate of 3 °C/min) overnight (Zhu et al., 2011). The 5 wt% Ni/HZSM-5, 5 wt% Ni/HY, 5 wt% Ni/HBeta, 5 wt% Fe/HBeta,

2.5 wt% Ni-2.5 wt% Fe/HBeta (NiFe-5/HBeta) and 5 wt% Ni-5 wt% Fe/HBeta (NiFe-10/HBeta) catalysts were prepared by incipient wetness impregnation method using aqueous solutions of nickel (II) nitrate hexahydrate and iron (III) nitrate nonahydrate. The concentrations of nickel and iron salts in the aqueous solutions used for 5 wt% metal loading were 0.82 and 0.87 M, respectively. After impregnation, the sample was dried at 100 °C for 12 h and then calcined in air at 550 °C (with heating rate of 3 °C/min) overnight. Prior to the reaction, catalyst was reduced by hydrogen at 450 °C and 35 bar for 2 h.

3.4 BET surface area and porosity analysis

BET surface area, pore volume and pore size distribution of fresh or spent catalysts were determined by N_2 isothermal (-196 °C) adsorption-desorption using Micromeritics ASAP 2020 surface area and porosity analyzer. Before textural analysis, the samples were outgassed at 180 °C under vacuum for 4 h.

3.5 X-ray flouresence (XRF) analysis

X-ray flouresence (XRF) instrument (PANalytical Axios^{mAX}) was used to determine inorganic contents of catalyst samples.

3.6 X-ray diffraction (XRD) analysis

X-ray diffraction (XRD) patterns of catalysts were recorded at 25 °C using Rigaku Miniflex diffractometer with Cu Kα (λ=1.54 Å) radiation. The working voltage and current of X-ray tube were 45 kV and 40 mA, respectively. Scans were collected over a 2θ range of 5° to 80° with a step size of 0.026° and scan rate of 0.05°/s.

3.7 Temperature-programmed desorption of ammonia (NH_3-TPD)

The acidity of catalysts was studied by temperature programmed desorption of ammonia (NH_3-TPD) on Micromeritics ChemiSorb 2720 instrument using mixed gas of 10%NH_3/90%He. 200 mg of each sample was loaded in TPD cell and heated from ambient temperature to 550 °C with a heating rate of 20 °C/min and was held at 550 °C for 1 h in a stream of He (20 ml/min). Then, the sample was cooled down to 170 °C and ammonia was adsorbed after change of gas from pure He to 10%NH_3/90%He for 30 min. The sample was purged with He for 30 min to remove physisorbed molecules. Ammonia desorption measurement was carried out from 50 °C with the heating rate of 10 °C/min using He carrier gas (20 ml/min).

3.8 Temperature-programmed desorption of hydrogen (H_2-TPD)

H_2-TPD analysis of catalysts was carried out to determine the desorption temperature of hydrogen species adsorbed on the catalysts. H_2-TPD was performed using the same instrument as with NH_3-TPD. 200 mg of each sample was reduced with mixed gas of 5%H_2/95%N_2 (20 ml/min) at 450 °C for 1 h and then cooled down to ambient temperature. After hydrogen adsorption for 30 min, gas flow was changed to He (20 ml/min). After TCD (thermal conductivity detector) signal was stable, H_2-TPD was conducted at a heating rate of 10 °C/min. The desorbed hydrogen was recorded by TCD.

3.9 Catalytic activity measurement

3.9.1 Catalytic hydrogenation of phenol, cresol and guaiacol over physically mixed catalysts of Pd/C and zeolite solid acids

Hydrogenation of phenol, *o*-cresol, *m*-cresol and guaiacol was conducted in an autoclave batch reactor (Figure 3.1) equipped with a magnetic drive stirrer and water cooling coil (1000 ml volume, maximum temperature and pressure of 500 °C and 100 bar,

respectively). Before reaction, mixed catalysts of Pd/C (0.6 g) and calcined zeolite (1 g) was pretreated by hydrogen gas at 300 °C and 20 bar for 1 h. Then, the system was cooled to ambient temperature and pressure was released to atmosphere. Reactant (12 g) and H_2O (140 ml) were loaded into the reactor under the inert atmosphere of nitrogen. Hydrogen gas was charged-discharged for four times to displace the nitrogen. Afterward, reactor was pressurized with hydrogen gas to 15 bar and heating was started (20 °C/min). Reaction was carried out at 275 °C and stirring speed of 500 rpm. In the beginning of the reaction, total pressure of the system was decreased (from 70 to 66 bar at 275 °C) due to the high activity of catalysts for hydrogenation reaction leading to high hydrogen consumption. After a short while, rate of pressure reduction was decreased due to the decrease of hydrogen consumption rate with the reaction time, and pressure of the reactor was fixed at 64 bar till the end of reaction. After 2 h reaction, reactor was rapidly cooled to ambient temperature and products were collected.

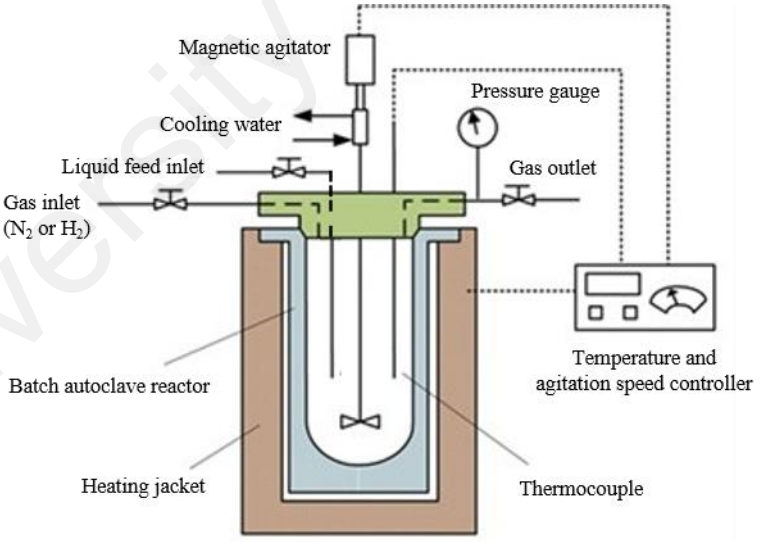

Figure 3.1: Autoclave batch reactor used for hydrotreatment of phenolic model compounds of bio-oil.

3.9.2 Catalytic HDO of simulated phenolic bio-oil over bifunctional metal/acid catalysts of Ni/HBeta, Fe/HBeta and NiFe/HBeta

The main purpose of this work was to develop a bifunctional metal/acid catalyst which is efficient for both hydrogenolysis and hydrogenation of phenolic compounds. Phenol and a simulated phenolic bio-oil consisting of phenol (50 wt%), *o*-cresol (25 wt%) and guaiacol (25 wt%) were selected as bio-oil model compounds for hydrogenation study using inexpensive mono- and bimetallic catalysts of Ni/HZSM-5, Ni/HY, Ni/HBeta, Fe/HBeta and NiFe/HBeta. Catalytic HDO of the simulated phenolic bio-oil over these catalysts was studied for the first time in this work. All experiments were conducted in an autoclave batch reactor equipped with a magnetic drive stirrer and water cooling coil. Catalyst (2 or 4 g) was pretreated with hydrogen at 450 °C and 35 bar for 2 h. After cooling down the reactor to ambient temperature and releasing the reactor pressure to atmosphere, reactor was charged with reactant (phenol, 2 g or bio-oil, 4 g) and water (100 ml) under the inert atmosphere of nitrogen. Hydrogen gas was charged-discharged for four times to displace nitrogen. Afterward, reactor was pressurized with hydrogen gas to 16 bar (HDO of phenol was conducted over Ni/HBeta and Fe/HBeta at different hydrogen pressures of 6, 11 and 16 bar) and heating was started (20 °C/min). Reaction was performed at 300 °C and stirring speed of 800 rpm for 4 h. For temperature dependence study of HDO of simulated bio-oil over NiFe-10/HBeta, the reaction was carried out at different temperatures of 220, 260, 300 and 340 °C. Meanwhile, the effect of methanol as solvent on the HDO reaction of simulated phenolic bio-oil over NiFe-10/HBeta was investigated by using water to methanol ratios of 100/0, 50/50 and 0/100 v/v.

3.9.3 Using decalin and tetralin as hydrogen source for transfer hydrogenation of renewable lignin-derived phenolics over Pd/C and Pt/C catalysts

This work was the first attempt for the study of the fisibility of using decalin and tetralin as hydrogen source for transfer hydrogenation of phenolic model compounds of bio-oil over Pd/C and Pt/C catalysts. Hydrogenation/transfer hydrogenation of phenol, *o*-cresol, guaiacol and simulated bio-oil were conducted in an autoclave batch reactor equipped with a magnetic drive stirrer and water cooling coil. The reaction procedures are as follows:

(i) Hydrogenation with hydrogen gas over Pt/C catalyst. No pretreatment was carried out prior to the reaction over Pt/C. Pt/C (0.6 g), reactant (12 g) and water (100 g) were loaded into the reactor. Hydrogen gas was charged-discharged for four times to displace the air. Afterward, reactor was pressurized with hydrogen gas (16 bar: 0.58 mol) and heating was started (20 °C/min). Reaction was carried out for 4 hours at 275 °C and stirring speed of 500 rpm. For kinetic study, the mentioned reactions were also carried out in different reaction times of 0.5, 1.0, 1.5, 2.0, 2.5, 3.0 and 3.5 h.

(ii) Hydrogenation with hydrogen gas over Pd/C catalyst. Before the reaction, 0.6 g of Pd/C was pretreated by hydrogen gas at 300 °C and 20 bar for 1 h. Then, the system was cooled down to ambient temperature and pressure was released to atmosphere. Reactant (12 g) and water (100 g) were loaded into the reactor under the inert atmosphere of nitrogen. Hydrogen gas was charged-discharged for four times to displace the nitrogen. Afterward, reactor was pressurized with hydrogen gas (16 bar: 0.58 mol) and heating was started. Reaction was carried out for 4 hours at 275 °C and stirring speed of 500 rpm.

(iii) Transfer hydrogenation with decalin/tetralin over Pt/C. Pt/C (0.6 g), reactant (12 g), water (50 g) and decalin or tetralin (50 g) were loaded into the reactor.

Nitrogen gas was charged-discharged for four times to displace the air. Then, heating was started and the reaction was carried out for 4 hours at 275 °C and stirring speed of 500 rpm. Meanwhile, different ratios of water to decalin or water to tetralin (0/100, 25/75, 50/50, 75/25 g/g) were employed for investigation of the effect of water content on hydrogenation efficiency. For kinetic study, the mentioned reactions were also carried out in different reaction times of 0.5, 1.0, 1.5, 2.0, 2.5, 3.0 and 3.5 h.

(iv) Transfer hydrogenation with decalin/tetralin over Pd/C. Before the reaction, 0.6 g of Pd/C was pretreated by hydrogen gas at 300 °C and 20 bar for 1 h. Then, the system was cooled down to ambient temperature and pressure was released to atmosphere. Reactant (12 g), water (50 g) and decalin or tetralin (50 g) were loaded into the reactor under the inert atmosphere of nitrogen. Then, heating was started and the reaction was carried out for 4 hours at 275 °C and stirring speed of 500 rpm.

3.10 Product analysis

After each reaction, the reactor was rapidly cooled down to ambient temperature and products were collected for further analysis. Solid catalysts were separated from liquid product by vacuum filtration. Organic phase of product was separated by use of ethyl acetate as solvent and analyzed by GC-MS (Shimadzu QP 2010, DB-5 30 m × 0.25 mm × 0.25 µm) coupled with flame ionization and mass spectrometry detection. The GC was equipped with a split injector with a split ratio of 1:50 at 290 °C. Pure helium gas (99.995%) was used as carrier gas at flow rate of 1.26 ml/min. The GC oven program started at 40 °C for 3 min, and then heated at 5 °C/min to 280 °C and held for 15 min. The products were identified by using NIST (National Institute of Standards and Technology) library. 2-Isopropylphenol was used as internal standard for quantitative

analysis of product samples based on the equation of $C_x = C_{is}\ (A_x/A_{is})$ which C_x, C_{is}, A_x and A_{is} are concentration of component x, concentration of internal standard, peak area of component x and peak area of internal standard, respectively. Conversion and product selectivity were calculated as follows:

$$Conversion\ (mol\%) = \frac{Mole\ of\ consumed\ reactant}{Mole\ of\ initial\ reactant} \times 100 \quad (3.1)$$

$$Selectivity\ (mol\%) = \frac{Mole\ of\ a\ certain\ product}{Mole\ of\ initial\ reactant} \times 100 \quad (3.2)$$

$$Selectivity\ (wt\%) = \frac{Weight\ of\ a\ certain\ product}{Weight\ of\ total\ products} \times 100 \quad (3.3)$$

3.11 Catalyst regeneration

Catalyst regeneration method comprises (i) washing the spent catalyst to remove organic species adsorbed on catalyst surface and drying the washed catalyst (Zhao, Kasakov, He, & Lercher, 2012); (ii) calcination of the dried catalyst in an oxygen-containing gas for combustion and removal of the carbonaceous deposits (Sun & Nowowiejski, 2011); and (iii) in situ reduction of the calcined catalyst with a hydrogen-containing gas (Sun & Nowowiejski, 2011). In order to test catalyst activity in recycling experiments, NiFe-10/HBeta catalyst separated from liquid product by vacuum filtration was washed with acetone and water to remove organic species adsorbed on catalyst surface (Zhao, Kasakov, He, & Lercher, 2012). Afterward, the catalyst was dried in ambient air at 110 °C for 8 h followed by an overnight calcination in air at 550 °C (with heating rate of 3 °C/min). The regenerated catalyst was used in subsequent hydrodeoxygenation reaction after being reduced at 450 °C and 35 bar for 2 h.

In order to test catalytic activity of Pt/C in recycling experiments, the catalyst separated from liquid product by vacuum filtration was washed with acetone and water to remove organic species adsorbed on catalyst surface. Afterward, the catalyst was dried in ambient

air at 100 °C for 12 h. The regenerated catalyst was analyzed by nitrogen isothermal adsorption-desorption, XRF and XRD methods.

3.12 Coke quantification

Coke content deposited on the spent catalysts was determined by thermogravimetric analysis (TGA) using a PerkinElmer STA 6000 Simultaneous Thermal Analyzer. Under synthetic air flow of 100 ml/min, samples were heated from 30 to 750 °C with the rate of 5 °C/min and kept at final temperature for 30 min. The weight loss below 300 °C was assigned to desorption of water and volatile components, and the weight loss in temperature range of 300-750 °C was considered as the amount of coke deposited on catalyst.

CHAPTER 4: RESULTS AND DISCUSSION

4.1 Catalytic hydrogenation of phenol, cresol and guaiacol over physically mixed catalysts of Pd/C and zeolite solid acids

4.1.1 Physicochemical characteristics of catalysts

Textural properties of 10 wt% Pd/C catalyst and zeolite solid acids (HZSM-5 (Si/Al of 30, 50 and 80) and HY (Si/Al of 30 and 60)) determined by N_2 isothermal adsorption-desorption are presented in Table 4.1. The BET surface area of all catalysts is high (>290 m^2/g) and the micropore surface area of all catalysts predominates on external surface area. The increase of Si/Al ratio in all the zeolites led to higher BET surface area and pore volume. As depicted in Figure 4.1, all the catalysts showed type IV of adsorption isotherm with hysteresis loop H4. The H4 hysteresis loop and nearly horizontal curve of isotherms demonstrate that Pd/C and zeolite solid acids are mostly microporous. Meanwhile, the distribution of meso scale pores in catalysts determined by BJH desorption pore size distribution (Figure 4.2) exhibits that Pd/C has a very broad pore size distribution between 3 and 60 nm. HY zeolites have two pore size distributions of 3-4 nm (very narrow) and 4-50 nm (very broad) which the dominant part of pores have a diameter in the range of 3-4 nm. HZSM-5 (30) and HZSM-5 (50) have also a bimodal distribution with maximum peaking at 3-10 and 3-4 nm, respectively. Substantial part of the mesopore volume found in HZSM-5 (80) was in the range of 3-10 nm.

Table 4.1: Textural properties of 10 wt% Pd/C and zeolite solid acids.

Catalyst	Pd/C	HZSM-5 (Si/Al=30)	HZSM-5 (Si/Al=50)	HZSM-5 (Si/Al=80)	HY (Si/Al=30)	HY (Si/Al=60)
BET surface area (m^2/g)	694	291	326	345	645	664
Micropore surface area (m^2/g)	390	192	216	214	487	487
External surface area (m^2/g)	304	99	110	131	158	177
Pore volume (cm^3/g)	0.53	0.19	0.20	0.21	0.43	0.44
Micropore volume (cm^3/g)	0.19	0.09	0.10	0.10	0.24	0.24
Mesopore volume (cm^3/g)	0.34	0.10	0.10	0.11	0.19	0.20

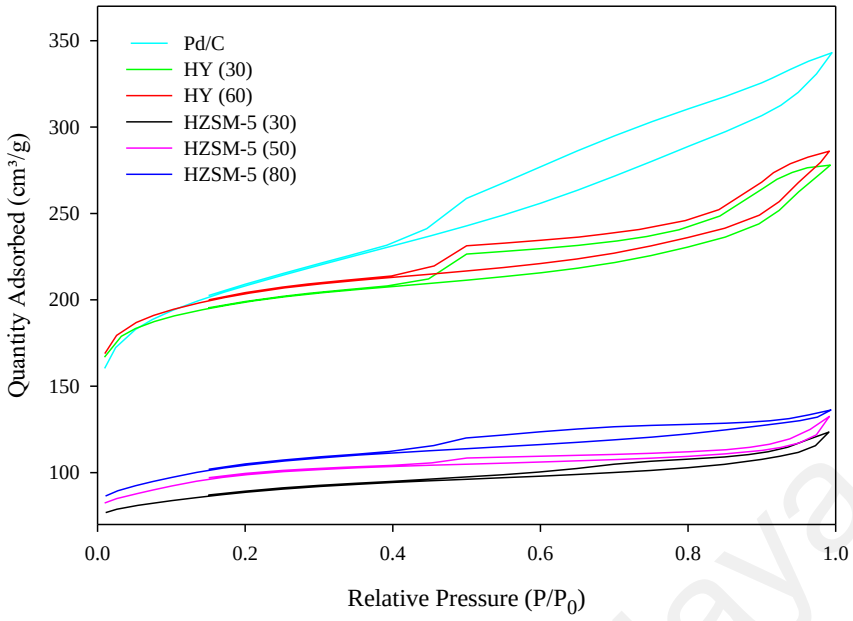

Figure 4.1: Nitrogen adsorption-desorption isotherms of Pd/C, HY and HZSM-5 catalysts.

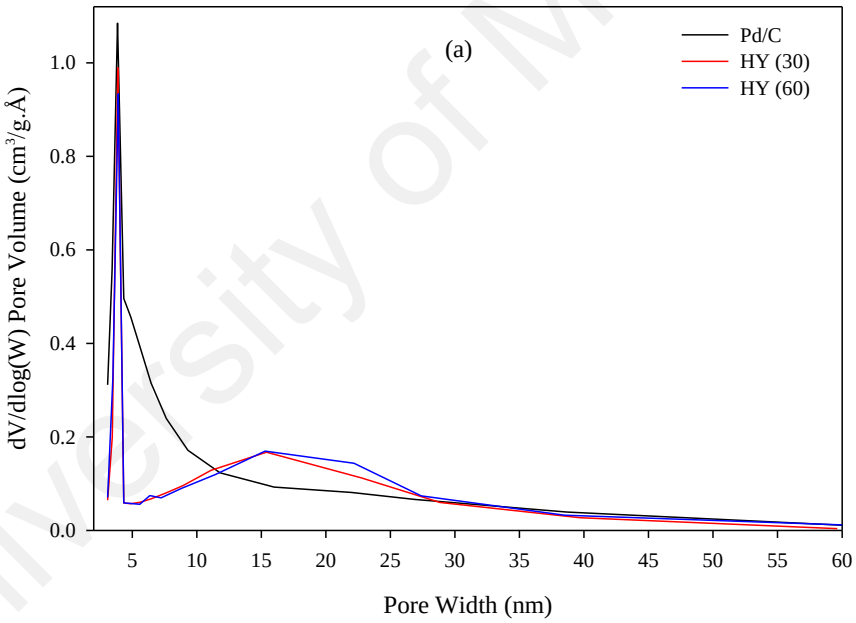

Figure 4.2: Pore size distribution (from BJH desorption data); Halsey plot with Faas correction: (a) Pd/C and HY zeolites (b) HZSM-5 zeolites.

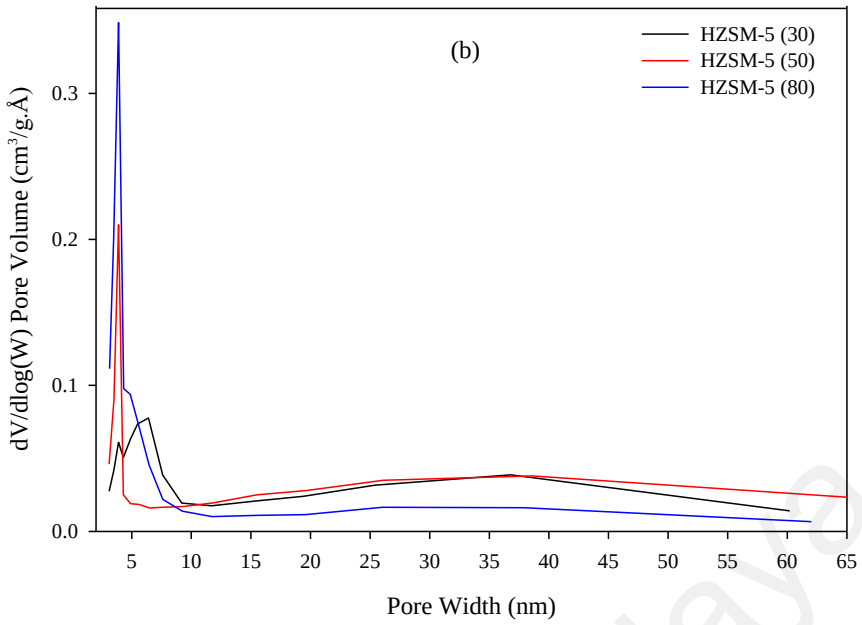

'**Figure 4.2,** continued'

The NH_3-TPD curves of HZSM-5 and HY zeolites are shown in Figure 4.3. It can be seen from this figure that HZSM-5 (50) and HZSM-5 (80) have two ammonia desorption peaks at low and high temperature regions (Table 4.2) which belong to weak and strong acid sites, respectively (Echeandia et al., 2014; Mortensen et al., 2013). These acid sites could be both types of Lewis and Brønsted acids (He et al., 2014; Jin & Li, 2009; Katada & Niwa; Kim, Choi, & Ryoo, 2010; Zhao et al., 2010). Jin and Li (Jin & Li, 2009) professed that Lewis acid sites are dominant at desorption temperature range of 200-300 °C while at 300-450 °C, Brønsted acid sites are the major acid sites of ZSM-5. Desorption temperature is associated to the strength of interaction between ammonia and acid sites; high temperature is required for separation of ammonia adsorbed on strong acid sites. By the increase of Si/Al ratio from 50 to 80, both the low- and high-temperature desorption peaks shifted to lower temperatures which means that the acid strength is decreased. HZSM-5 (30) has only one broad desorption peak at low-temperature (221 °C) indicating that its acidic strength is low. Since standard condition volume of ammonia desorbed per gram of catalyst typically signifies the concentration of acid sites (Dayton, Pavani, Carpenter, & Von, 2014), HZSM-5 (30) has higher density of acid sites compared with

HZSM-5 (50) and HZSM-5 (80) (Table 4.2). TPD analysis of HY (30) and HY (60) zeolites resulted in only one ammonia desorption peak in the temperatures of 315 and 330 °C, respectively. By increase of Si/Al ratio in HY zeolites, desorption peak moved to higher temperature indicating that acidity is strengthened. Based on a theoretical analysis, Brønsted acid strength of zeolites (≡Si-OH-Al≡) depends on the composition of second coordination sphere around the spanning OH group; the strongest Brønsted acid site is the one with six Si^{4+} species in the second coordination sphere around OH group and replacing the Si^{4+} by Al^{3+} decreases the acid strength (Primo & Garcia, 2014). According to the high-temperature desorption peak, it can be concluded that the acid strength of zeolites follows the trend: HZSM-5 (50) ≈ HZSM-5 (80) > HY (60) > HY (30).

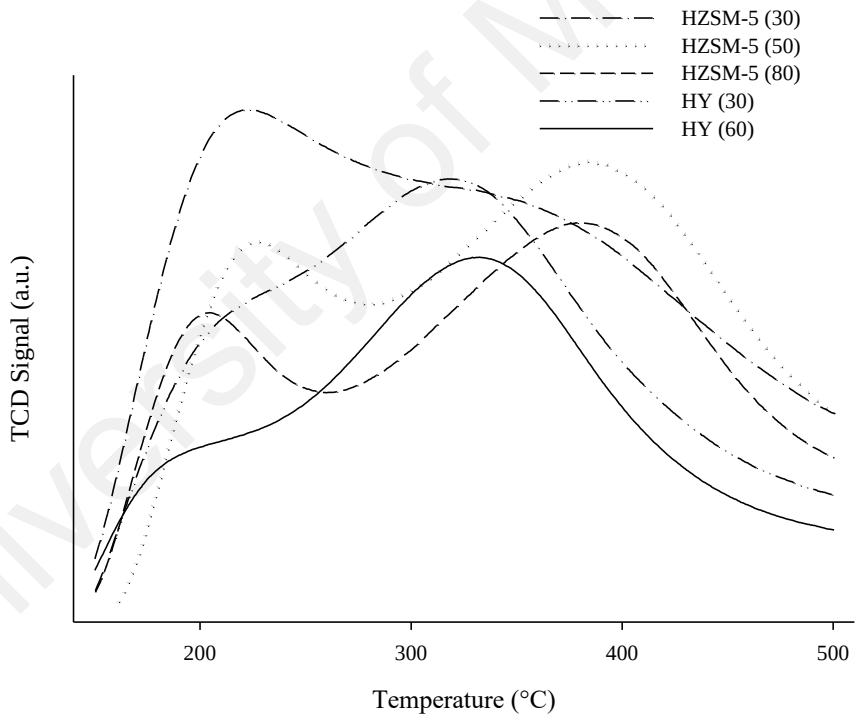

Figure 4.3: NH_3-TPD curves of HZSM-5 and HY zeolites with different Si/Al ratios.

Table 4.2: Ammonia desorption temperature and amount of desorbed ammonia from zeolite acid sites obtained by TPD analysis.

Zeolites	**HZSM-5 (30)**	**HZSM-5 (50)**		**HZSM-5 (80)**		**HY (30)**	**HY (60)**
Desorption peak temperature (°C)	221	225	382	203	378	315	330
Volume of desorbed ammonia (ml/g STP)	6.247	1.592	3.219	1.276	2.810	4.822	3.136

4.1.2 Catalytic hydrogenation of phenol

Reactant conversion and product distribution obtained from catalytic hydrogenation of phenol over Pd/C catalyst and combined catalysts of Pd/C and zeolite solid acids are presented in Table 4.3. Using mixture of Pd/C and zeolite led to higher phenol conversion compared with the use of Pd/C alone. Maximum phenol conversion of 96.89 mol% was achieved over mixed catalyst of Pd/C-HZSM-5 (80) while phenol was converted only 48.05 mol% over Pd/C. By increase in density of acid sites in both zeolites of HZSM-5 and HY (decrease of Si/Al ratio), phenol conversion decreased. This could be due to the fact that higher density of acid sites causes higher formation of coke and zeolite deactivation (Echeandia et al., 2014).

Reaction mechanisms of phenol hydrogenation on Pd/C or mixed catalysts of Pd/C and zeolite is depicted in scheme 4.1. Over Pd/C, hydrogenation of benzene ring of phenol was the main reaction pathway producing cyclohexanone and cyclohexanol (path I); cyclohexanol is the end product since it is not dehydrated in the absence of Brønsted acid sites. The addition of zeolite solid acids to Pd/C led to dehydration of cyclohexanol to cyclohexene (not detected in product samples) and further hydrogenation of cyclohexene on metal catalyst producing cyclohexane as oxygen-free product (path II). Except HY (30), other zeolites dehydrated all produced cyclohexanol to cyclohexene. Low hydrogen pressure of 15 bar in phenol hydrogenation stabilized the production of cyclohexanone intermediate. Our result is in accordance with that of Zhao and Lercher (2012) who noted that low hydrogen pressure in phenol hydrodeoxygenation stabilizes cycloketone intermediate and decreases cycloalkane formation. Meanwhile, our data reveal that zeolites cannot be involved in hydrogenation mechanism; no conversion of phenol was observed in hydrogenation of phenol over HZSM-5 (80) and HY (60) catalysts without Pd/C, indicating that zeolites do not possess proper active sites for activation of hydrogen molecules to be involved in hydrogenation reaction. In addition, benzene formation was

only observed over mixed catalysts of Pd/C-HY (30) and Pd/C-HZSM-5 (30). The proposed reaction pathway for benzene production (path III) is as follows: phenol decarbonylation to cyclopentadiene which is converted to naphthalene via Diels-Alder mechanism (Egsgaard, Ahrenfeldt, Ambus, Schaumburg, & Henriksen, 2014; Nitsch et al., 2013), naphthalene hydrogenation to tetralin, tetralin ring-opening/isomerization to alkyl benzene and dealkylation of alkyl benzene to benzene. High density of acid sites in HY (30) (4.822 ml/g) and HZSM-5 (30) (6.247 ml/g) resulted in dealkylation of alkyl benzene and production of benzene. Selectivity towards benzene in the presence of HY (30) and HZSM-5 (30) was 2.34 and 3.12 mol%, respectively. As depicted in Table 4.3, HZSM-5 was more efficient than HY for catalytic transformation of phenol to cyclohexane. In the case of using HZSM-5 (80), phenol hydrogenation occurred via two reaction pathways; i) the common pathway of ring hydrogenation of phenol to cyclohexanone and cyclohexanol with subsequent dehydration of cyclohexanol to cyclohexene followed by further hydrogenation of cyclohexene to cyclohexane (paths I and II), ii) phenol hydrogenation to cyclohexanol and subsequent production of 2-cyclohexylphenol through electrophilic aromatic substitution (EAS) of phenol with cyclohexyl cation followed by further hydrogenation of 2-cyclohexylphenol to 2-cyclohexylcyclohexanone and dicyclohexane (paths I and IV) (Hong, Miller, Agrawal, & Jones, 2010). In fact, Brønsted acid sites of zeolite catalyze the alkylation of phenol with cyclohexanol to form 2-cyclohexylphenol (Zhao, Camaioni, & Lercher, 2012). Generally, alkylation of phenol by cyclohexanol and production of bicyclic compounds is possible over combined catalysts of acid zeolite and palladium (Zhao, Camaioni, & Lercher, 2012). One significant factor for possibility of alkylation reaction is molar ratio of phenol to Pd which should be sufficient to proceed alkylation. At low ratios of phenol to Pd, phenol undergoes hydrogenation rather than alkylation, while at high phenol to Pd ratios and sufficient concentration of cyclohexanol, phenol could be alkylated. Zhao et al.

(2012) reported that at low phenol to Pd molar ratio of 564, only 2.1 C% selectivity of bicyclic products was achieved. In our work, the ratio of phenol to Pd is very low (~227) which prevents the alkylation mechanism and only by the use of Pd/C mixed with HZSM-5 (80), very low concentrations of bicyclic products were observed. Furthermore, the possibility of phenol alkylation has reverse dependency on density of acid sites; higher density of acid sites favors dehydration reaction rather than alkylation (Zhao, Camaioni, & Lercher, 2012). Therefore, bicyclic compounds were only produced over HZSM-5 (80) which has lower density of acid sites compared with HZSM-5 (50) and HZSM-5 (30) (Table 4.2).

Table 4.3: Hydrogenation of phenol over mixed catalysts of Pd/C and zeolite solid acids.

Catalyst	**Pd/C-HZSM-5 (80)**	**Pd/C-HZSM-5 (50)**	**Pd/C-HZSM-5 (30)**	**Pd/C-HY (60)**	**Pd/C-HY (30)**	**Pd/C**
Conversion (mol%)	96.89	68.24	49.00	53.15	50.27	48.05
Product compounds	Product selectivity (mol%): (mole of product compound / mole of total product) × 100					
Benzene	-	-	3.12	-	2.34	-
Cyclohexanone	70.71	75.99	76.86	87.09	85.94	83.86
Cyclohexanol	-	-	-	-	1.14	14.35
Cyclohexane	22.83	22.14	19.97	11.11	10.40	-
Dicyclohexane	3.25	-	-	-	-	-
2-cyclohexylcyclohexanone	0.85	-	-	-	-	-
2-cyclohexylphenol	0.57	-	-	-	-	-
Tetralin	1.80	1.88	0.20	1.90	0.24	1.97

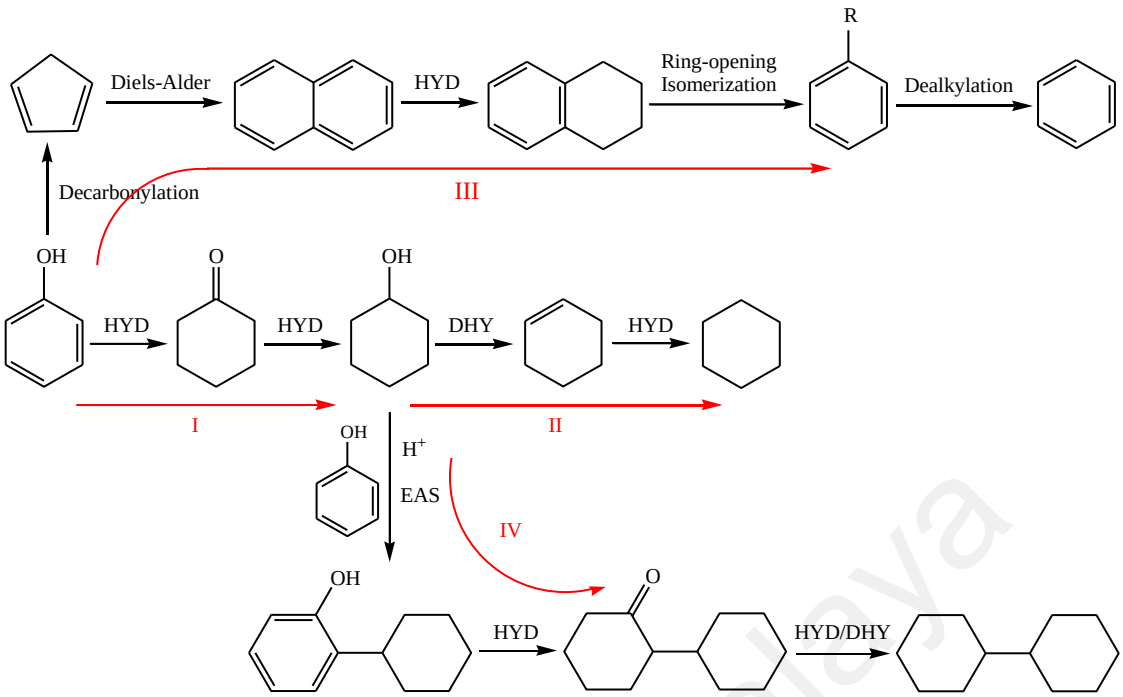

Scheme 4.1: Reaction pathways of phenol hydrogenation over Pd/C and Pd/C mixed with HZSM-5 or HY zeolites; HDO: hydrodeoxygenation, HYD: hydrogenation, DHY: dehydration, EAS: electrophilic aromatic substitution.

4.1.3 Catalytic hydrogenation of cresol

Results obtained from hydrogenation of *o*-cresol and *m*-cresol over 10 wt% Pd/C and zeolite solid acids are presented in Tables 4.4 and 4.5. Compared with phenol molecule, the presence of methyl group in cresol favors aromatic production. This is in agreement with the results reported by Massoth et al. (2006) who showed that higher aromatic yield is achieved from hydrogenation of methyl-substituted phenols rather than phenol over sulfided $CoMo/Al_2O_3$ catalyst. Generally, conversion of *o*-cresol was lower than that of *m*-cresol; maximum conversion of *m*-cresol was 76.23 mol% which was achieved over Pd/C-HY (60) while maximum conversion of *o*-cresol was only 50.65 mol% obtained by Pd/C-HZSM-5 (50). Lower conversion of *o*-cresol, with the methyl group adjacent to hydroxyl group, could be due to the steric hindrance to adsorption of *o*-cresol on catalytic active sites. Hydrogenation of *o*-cresol (scheme 4.2) was proceeded through pathways of direct hydrodeoxygenation of cresol to toluene (path III), cresol alkylation to 2,6-dimethylphenol (path IV), and hydrogenation of benzene ring to 2-methylcyclohexanone/2-methylcyclohexanol (path I) followed by dehydration of 2-

methylcyclohexanol to methylcyclohexane (path II). In addition to the above mentioned reaction mechanisms for hydrogenation of *o*-cresol, *m*-cresol seems to be hydrogenated through some more reaction pathways resulting in some different products (Table 4.5). The proposed reaction mechanisms for hydrogenation of *m*-cresol are depicted in scheme 4.3. The results obtained in this work indicate that the effects of addition of zeolite solid acids to Pd/C on product selectivity are dependent on the methyl group position in cresol molecule. For instance, zeolite addition did not have negative effect on toluene selectivity in hydrogenation of *o*-cresol while in *m*-cresol hydrogenation, zeolite addition led to the decrease of toluene production (except HZSM-5 (30)) due to dehydration, demethylation and alkylation reactions which competitively occur to produce methylcyclohexane, phenol and 2-ethylphenol, respectively.

In *o*-cresol transformation, catalytic activity of mixed catalysts of Pd/C and zeolite solid acids decreased in the order Pd/C-HZSM-5 (50) > Pd/C-HY (30) > Pd/C-HY (60) > Pd/C-HZSM-5 (80) > Pd/C-HZSM-5 (30) > Pd/C. Hydrogenation of benzene ring of *o*-cresol to 2-methylcyclohexanone and 2-methylcyclohexanol (scheme 4.2, path I) was the dominant reaction mechanism over Pd/C, while the addition of HZSM-5 led to dehydration of 2-methylcyclohexanol and formation of methylcyclohexane as oxygen-free product (path II). Lower density of acid sites in HZSM-5 zeolites led to higher selectivity of methylcyclohexane over mixed catalysts. However, HY zeolites were not selective to the production of methylcyclohexane. This is in agreement with the results obtained by Zhao et al. (2010) who demonstrated that ketone was selectively formed over HY zeolite in hydrodeoxygenation of 4-*n*-propylphenol. As is depicted in scheme 4.2, HDO of *o*-cresol to toluene is another reaction mechanism over Pd/C and mixed catalysts (path III). The addition of HZSM-5 strongly affected the selectivity towards toluene while HY did not have remarkable effect on HDO selectivity. It is also inferred from Table 4.4 that toluene selectivity is not a function of density and strength of zeolite acid sites. The

results show that Brønsted acid sites of zeolites were not efficient for dehydration of 2-methylcyclohexanol to methylcyclohexane. Meanwhile, the combination of zeolite solid acids with Pd/C catalyst led to alkylation of *o*-cresol (path IV) which occurs concurrently with hydrogenation and hydrodeoxygenation reactions.

The study of catalytic hydrogenation of *m*-cresol over Pd/C and mixed catalysts of Pd/C-zeolite revealed that conversion of *m*-cresol decreased in the order Pd/C-HY (60) > Pd/C-HZSM-5 (50) > Pd/C-HZSM-5 (80) > Pd/C-HY (30) > Pd/C-HZSM-5 (30) > Pd/C. Direct hydrodeoxygenation (scheme 4.3, path I) and benzene ring hydrogenation (path II) were the only reaction mechanisms in hydrogenation of *m*-cresol over Pd/C. Selectivity towards toluene reduced in the order Pd/C-HZSM-5 (30) > Pd/C-HY (30) > Pd/C > Pd/C-HZSM-5 (80) > Pd/C-HY (60) > Pd/C-HZSM-5 (50). Dehydration of 3-methylcyclohexanol to methylcyclohexane (path III) was activated by zeolite addition and maximum selectivity of methylcyclohexane was obtained in the presence of HZSM-5 (50) which has highest strength of acidity compared with other zeolites. Meanwhile, addition of HZSM-5 zeolites and HY (60) resulted in demethylation of *m*-cresol to phenol followed by phenol hydrogenation and cyclohexanone formation (path IV). Phenol alkylation to 2-ethylphenol and further hydrogenation of 2-ethylphenol to 2-ethylcyclohexanone also occurred (path V). High density of acid sites in HZSM-5 (30) and HY (30) favored 2-ethylphenol production. Unlike *m*-cresol, demethylation mechanism did not occur in transformation of *o*-cresol illustrating that the methyl group adjacent to hydroxyl group prevents dealkylation reaction on zeolite acid site. Production of large molecule compounds over HY (60) might be due to the large pore size of this zeolite which allows formation of such large molecules through aromatic ring condensation or isomerization reactions.

Table 4.4: Hydrogenation of *o*-cresol over mixed catalysts of Pd/C and zeolite solid acids.

Catalyst	**Pd/C-HZSM-5 (80)**	**Pd/C-HZSM-5 (50)**	**Pd/C-HZSM-5 (30)**	**Pd/C-HY (60)**	**Pd/C-HY (30)**	**Pd/C**
Conversion (mol%)	38.16	50.65	35.90	39.38	47.75	35.20
Product compounds	Product selectivity (mol%): (mole of product compound / mole of total product) × 100					
Toluene	29.58	29.52	29.84	19.98	18.24	16.23
Methylcyclohexane	2.59	2.09	1.83	-	-	-
2-Methylcyclohexanone	66.24	67.33	66.92	79.07	80.63	79.80
2-Methylcyclohexanol	-	-	-	-	0.33	3.96
2,6-Dimethylphenol	1.58	1.06	1.41	0.95	0.80	-

Table 4.5: Hydrogenation of *m*-cresol over mixed catalysts of Pd/C and zeolite solid acids.

Catalyst	**Pd/C-HZSM-5 (80)**	**Pd/C-HZSM-5 (50)**	**Pd/C-HZSM-5 (30)**	**Pd/C-HY (60)**	**Pd/C-HY (30)**	**Pd/C**
Conversion (mol%)	48.02	66.95	39.63	76.23	42.00	39.58
Product compounds	Product selectivity (mol%): (mole of product compound / mole of total product) × 100					
Toluene	15.30	9.26	20.57	14.47	18.63	19.51
Methylcyclohexane	1.48	2.87	0.22	0.20	0.97	-
Phenol	6.80	11.19	1.24	1.00	-	-
Cyclohexanone	2.33	3.16	1.00	1.25	-	-
3-Methylcyclohexanone	73.61	73.40	76.50	80.79	79.73	80.00
3-Methylcyclohexanol	-	-	-	-	0.16	1.29
2-Ethylphenol	-	-	0.38	0.08	0.52	-
2-Ethylcyclohexanone	-	-	-	0.12	-	-
1,1'-Bicyclopentyl	0.64	-	-	-	-	-
1-Butylcyclohexene	0.34	-	-	-	-	-
1,1'-Bicyclohexyl, 4,4'-dimethyl-	-	-	-	0.20	-	-
1-Phenyl-1-cyclohexylethane	-	-	-	0.14	-	-
4,4'-Dimethylbiphenyl	-	-	-	1.76	-	-
Cyclohexylbenzene	-	-	0.12	-	-	-

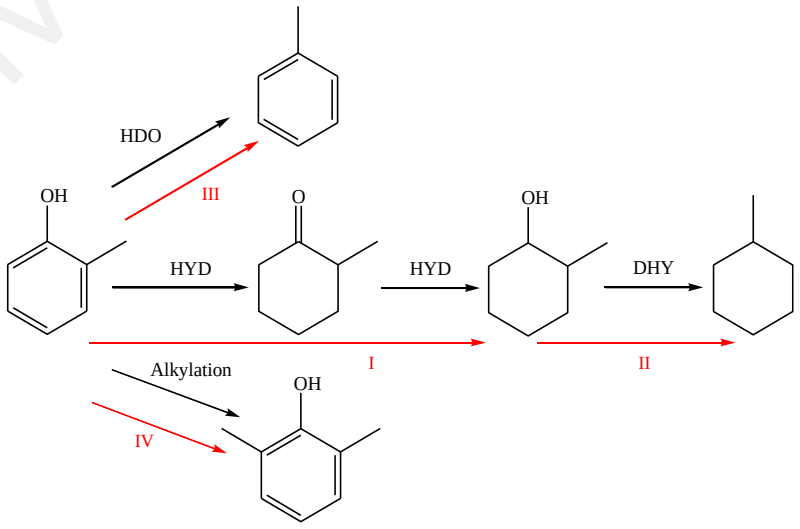

Scheme 4.2: Mechanisms of hydrogenation of *o*-cresol over combined catalysts of Pd/C and zeolite solid acids.

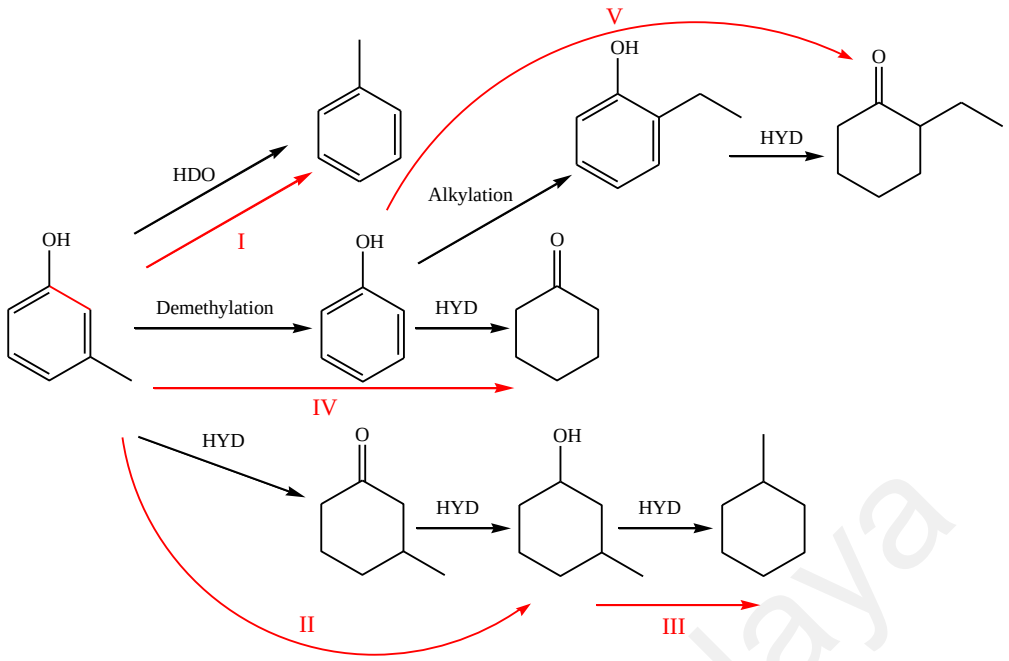

Scheme 4.3: Mechanisms of hydrogenation of *m*-cresol over combined catalysts of Pd/C and zeolite solid acids.

4.1.4 Catalytic hydrogenation of guaiacol

The addition of HZSM-5 and HY zeolites to Pd/C caused enhanced catalytic performance in transformation of guaiacol (Table 4.6). Compered to HY zeolite, HZSM-5 showed higher catalytic activity, and complete conversion of guaiacol was achieved over mixed catalysts of Pd/C-HZSM-5 (80). Phenol, cyclohexanone and cyclopentanone were the highly selective products of guaiacol hydrodeoxygenation over Pd/C. Reaction mechanisms of guaiacol hydrogenation on Pd/C is depicted in scheme 4.4. Benzene ring hydrogenation and dehydroxylation of guaiacol took place to form 2-methoxycyclohexanone (path I) and anisole (path II), respectively. Concurrently, demethoxylation of guaiacol occurred to produce phenol (path III) which was transformed to cyclohexanone/cyclohexanol (path IV), *o*-cresol/2-methylcyclohexanone (path V) and *o*-cresol/toluene (path VI) through hydrogenation, methylation-hydrogenation and methylation-dehydroxylation reactions, respectively. *o*-Cresol could be produced via methylation of phenol with methanol which is formed through demethoxylation of guaiacol. Unusual production of cyclopentanone from guaiacol

deoxygenation might be due to ring hydrogenation, ring opening/closing and decarbonylation reactions of catechol (path VII) (Nimmanwudipong et al., 2012). Ring opening reaction is supposed to be catalyzed by metal catalyst (McVicker, 2002; Nimmanwudipong et al., 2012). Since catechol was not detected in product analysis, it can be considered as an intermediate product which was completely consumed during the reaction. In comparison with HY zeolite, HZSM-5 remarkably improved the selectivity towards phenol, and HZSM-5 with higher density of acid sites led to higher phenol selectivity. On the other hand, cyclopentanone formation notably decreased by the addition of HZSM-5 to Pd/C while HY did not show remarkable effect on the selectivity of cyclopentanone. Except HY (60), addition of all other zeolites caused a reduction in dehydroxylation reaction and anisole production. Meanwhile, low concentration or absence of 2-methoxycyclohexanone in product composition observed in guaiacol hydrogenation over Pd/C mixed with zeolites illustrates that the addition of zeolite solid acids to metal catalyst resulted in the reduction of benzene ring hydrogenation of guaiacol.

Table 4.6: Hydrogenation of guaiacol over mixed catalysts of Pd/C and zeolite solid acids.

Catalyst	**Pd/C-HZSM-5 (80)**	**Pd/C-HZSM-5 (50)**	**Pd/C-HZSM-5 (30)**	**Pd/C-HY (60)**	**Pd/C-HY (30)**	**Pd/C**
Conversion (mol%)	100.00	93.95	92.08	62.79	56.43	37.38
Product compounds	Product selectivity (mol%): (mole of product compound / mole of total product) × 100					
Phenol	61.07	66.87	71.08	33.61	33.03	31.91
Cyclohexanone	30.90	23.62	20.50	37.03	40.84	27.23
Cyclohexanol	-	-	-	-	-	4.62
Cyclohexane	0.24	0.37	0.09	0.21	0.20	-
Toluene	1.11	1.21	1.22	2.20	3.32	2.88
Cyclopentanone	2.91	2.88	3.12	16.37	17.35	17.97
Anisole	3.36	4.44	3.15	9.89	5.02	8.85
o-Cresol	0.39	0.62	0.78	-	0.16	0.20
2-Methylcyclohexanone	0.01	-	-	0.51	0.08	0.15
2-Methoxycyclohexanone	-	-	-	0.19	-	6.21

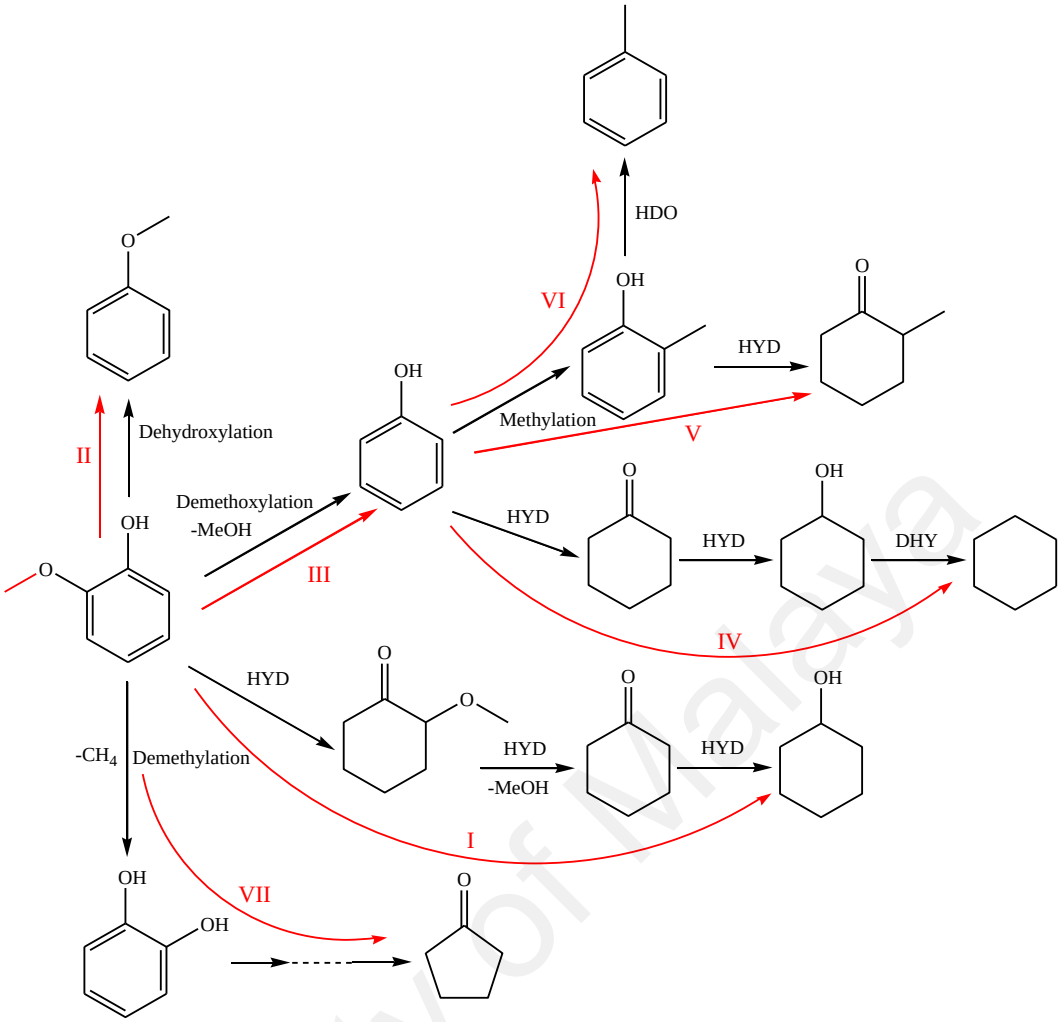

Scheme 4.4: Reaction mechanisms of guaiacol hydrogenation over 10 wt% Pd/C catalyst and combined catalysts of Pd/C and zeolite solid acids.

4.2 Catalytic hydrodeoxygenation of simulated phenolic bio-oil to cycloalkanes and aromatic hydrocarbons over bifunctional metal/acid catalysts of Ni/HBeta, Fe/HBeta and NiFe/HBeta

4.2.1 Physicochemical characteristics of catalysts

Physicochemical properties of HBeta, 5 wt% Ni/HBeta, 5 wt% Fe/HBeta, 2.5 wt% Ni-2.5 wt% Fe/HBeta (NiFe-5/HBeta) and 5 wt% Ni-5 wt% Fe/HBeta (NiFe-10/HBeta) catalysts determined by N_2 isothermal adsorption-desorption, X-ray flouresence (XRF), NH_3-TPD and H_2-TPD are presented in Table 4.7. Pore volume of HBeta was higher than that of metal impregnated HBeta; the metal species loaded on catalyst occupy space inside the catalyst pores and reduce the pore volume. Besides, metal loading resulted in

reduction of BET surface area which only occurred in micropores. Ni loading on HBeta support resulted in lower reduction of catalyst surface area and pore volume compared to Fe loading. However, higher surface area and volume of micropores compared to those of mesopores indicate that all catalysts are mainly microporous. XRD patterns of catalysts depicted in Figure 4.4 reveal that crystalline structure of HBeta was relatively unchanged by metal impregnation. Reflections found at 2θ values of 37.43°, 43.46° and 63.20° pertain to NiO phase, and diffraction peaks observed at 2θ = 35.92°, 57.50° and 63.07° represent Fe_2O_3 phase.

Table 4.7: Physicochemical properties of HBeta, Ni/HBeta, Fe/HBeta and NiFe/HBeta catalysts.

Catalyst	HBeta	Ni/HBeta	Fe/HBeta	NiFe-5/HBeta	NiFe-10/HBeta
S_{BET}[a] (m^2/g)	502	463	445	455	417
S_{micro}[b] (m^2/g)	384	329	301	310	283
V_{micro}[b] (cm^3/g)	0.188	0.154	0.144	0.147	0.126
V_{meso}[c] (cm^3/g)	0.106	0.117	0.121	0.122	0.124
V_{total}[d] (cm^3/g)	0.294	0.271	0.265	0.269	0.250
Metal loading[e] (wt%)		4.94	4.97	Ni: 2.48/Fe: 2.49	Ni: 4.95/Fe: 4.98
Density of acid sites[f] (mmol/g)	0.71	0.53	0.48	0.50	0.38
Relative H_2 desorption amount[g]		1.00	0.71	1.16	1.82

[a] Calculated in the range of relative pressure (P/P_0) = 0.05-0.25
[b] Evaluated by t-plot method
[c] $V_{meso} = V_{total} - V_{micro}$
[d] Total pore volume evaluated at $P/P_0 = 0.99$
[e] Determined by XRF method
[f] Determined by NH_3-TPD analysis
[g] Based on the area under H_2-TPD curves at temperature below 400 °C; H_2 desorption amount of Ni/HBeta was designated as 1.00

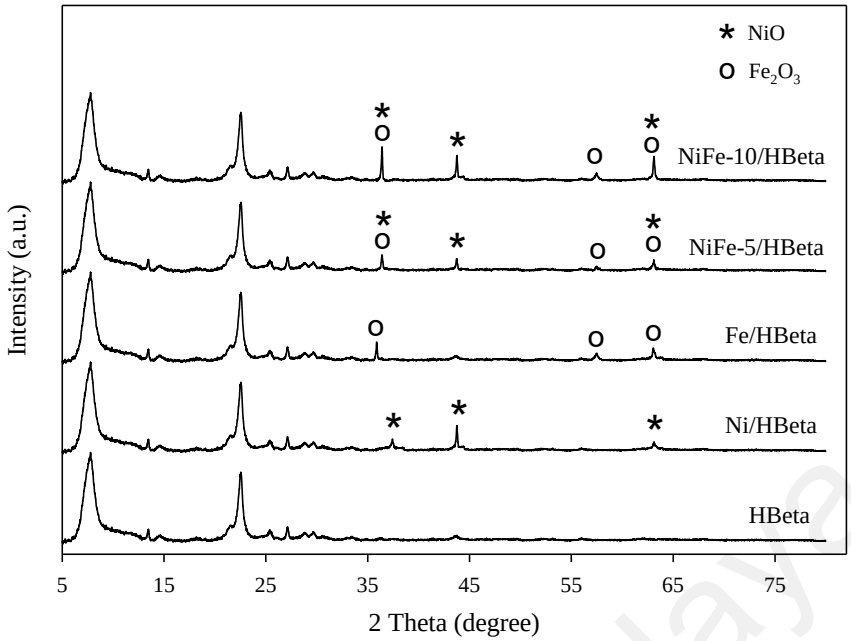

Figure 4.4: XRD patterns of HBeta, Ni/HBeta, Fe/HBeta and NiFe/HBeta.

Strength distribution of acid sites of bare HBeta support and metal impregnated HBeta determined by NH_3-TPD analysis is shown in Figure 4.5. The amount of ammonia desorbed from catalyst corresponds to total acid content (shown in Table 4.7). Higher temperature required for desorption of ammonia from strong acid sites is due to more intense interaction between ammonia and strong acid sites. As depicted in Figure 4.5, HBeta support has two ammonia desorption peaks at 232 and 328 °C which belong to weak and strong acid sites, respectively. Ni, Fe, NiFe-5 and NiFe-10 impregnation over HBeta zeolite resulted in single desorption peaks at 292, 326, 307 and 384 °C, respectively, indicating that strength of acidity of catalysts decreased in the order NiFe-10/HBeta > Fe/HBeta > NiFe-5/HBeta > Ni/HBeta. Change of acidic strength distribution of HBeta by metal oxides loading indicates that introduction of metal into HBeta led to removal of weak acid sites. Since the area under desorption peak signifies the relative concentration of acid sites, bimetallic catalyst of NiFe-10/HBeta has lower acid density compared with NiFe-5/HBeta, Ni/HBeta and Fe/HBeta which have nearly similar density of acid sites (Table 4.7). The peak area of metal-impregnated HBeta was lower than that of HBeta indicating the reduction in the density of acid sites as a result of metal loading.

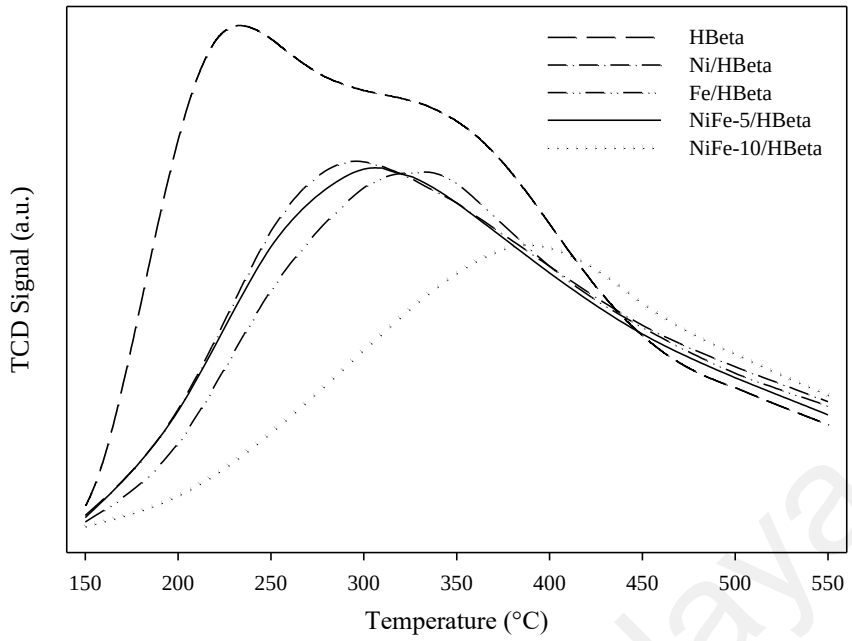

Figure 4.5: NH_3-TPD curves of HBeta, Ni/HBeta, Fe/HBeta and NiFe/HBeta.

H_2-TPD analysis of catalysts was conducted to determine their relative catalytic activities (shown in Table 4.7 and Figure 4.6). Higher hydrogen amount desorbed from catalyst signifies higher catalytic activity, since the area of H_2-TPD peak is correlated to the amount of metal active species (Yingxin, Jixiang, & Jiyan, 2007). Generally, desorption of hydrogen species chemisorbed on metal sites occurs at temperatures below 400 °C (Chen, Sun, Wang, & Zhang, 2009; Li et al., 2011). High temperature is required for desorption of hydrogen species strongly adsorbed on catalyst. As shown in H_2-TPD profiles presented in Figure 4.6, desorption peak occurred at 177 °C for Ni/HBeta. However, desorption peak of Fe/HBeta appeared at higher temperature (200 °C) indicating that desorption of hydrogen from Fe species requires more energy than hydrogen desorption from Ni species. Besides, the hydrogen desorption peaks of bimetallic catalysts of NiFe-5/HBeta and NiFe-10/HBeta were observed at 162 and 168 °C, respectively. Considering the area under desorption peaks, the amount of hydrogen desorption from catalysts decreased in the order NiFe-10/HBeta > NiFe-5/HBeta > Ni/HBeta > Fe/HBeta. Lower temperature for hydrogen desorption and higher desorbed hydrogen observed for bimetallic catalyst of NiFe/HBeta compared to those for

monometallic catalysts of Ni/HBeta and Fe/HBeta indicate the synergistic effect of Ni and Fe which facilitates hydrogen release from catalyst surface. Our data (shown in the following section) indicate that NiFe-10/HBeta catalyst with the highest hydrogen desorption ratio of 1.82 and the lowest acid site density of 0.38 mmol/g resulted in highest HDO efficiency for conversion of the simulated phenolic bio-oil to cycloalkanes and aromatic hydrocarbons.

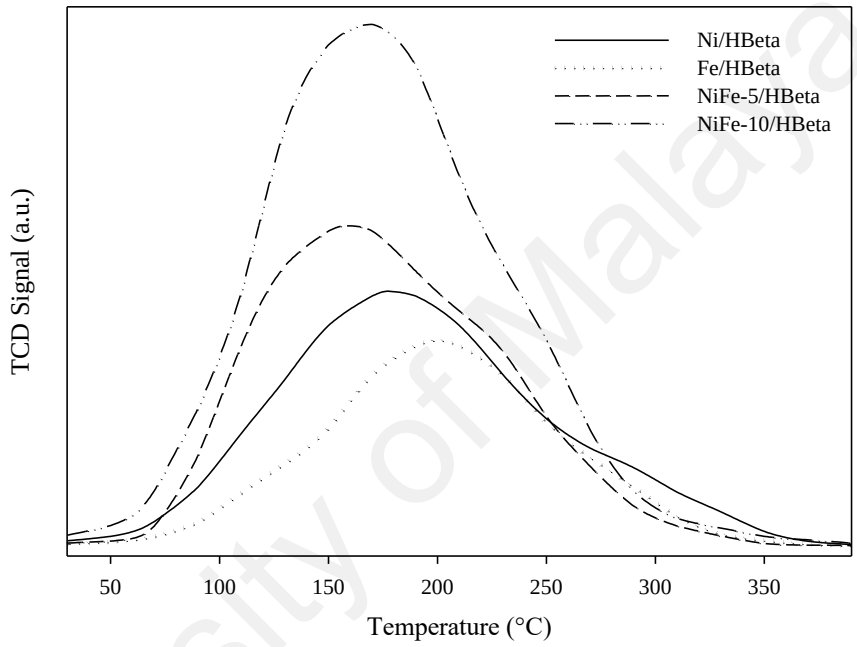

Figure 4.6: H_2-TPD profiles of Ni/HBeta, Fe/HBeta and NiFe/HBeta.

4.2.2 HDO of simulated phenolic bio-oil over Ni/HBeta, Fe/HBeta and NiFe/HBeta

5 wt% nickel metal supported on HZSM-5, HY and HBeta zeolites were used for HDO of phenol at reaction conditions of phenol, 2 g; water, 100 ml; catalyst, 2 g; temperature, 300 °C; reaction time, 4 h and rpm, 800. Higher phenol conversion and selectivity towards deoxygenated products were obtained over Ni/HBeta compared to Ni/HZSM-5 and Ni/HY; phenol conversion and selectivity of oxygen-free products over Ni/HBeta, Ni/HZSM-5 and Ni/HY were 58.77, 51.04, 23.45 wt% and 37.91, 28.13, 14.07 wt%, respectively. Different performance of the catalysts could be due to the difference in pore size of the zeolite supports; pore sizes of ZSM-5, Beta and Y zeolites are 5.1×5.5/5.3×5.6,

6.6×6.7/5.6×5.6 and 7.4×7.4 Å, respectively (Jae et al., 2011; Mihalcik, Mullen, & Boateng, 2011). Lower activity of Ni/HZSM-5 compared with Ni/HBeta might be due to the smaller pore size of HZSM-5 which could reduce the diffusion rate of reactants/intermediates inside catalyst channels. Meanwhile, large pores of HY could be the cause for low activity of Ni/HY since high internal pore space of HY results in high degree of polymerization and coke formation. The coke deposits could cover catalyst active sites leading to their low accessibility for reactants. Therefore, HBeta with medium pore size was selected as catalyst support for further catalytic HDO experiments in this research. In addition, prolonging the reaction time of HDO of phenol over Ni/HBeta catalyst to 5 and 6 h did not considerably change hydrocarbon yield, and reaction time of 4 h was selected for the experiments in this work.

Distribution of products obtained from hydrodeoxygenation of simulated phenolic bio-oil over mono- and bimetallic catalysts of Ni/HBeta, Fe/HBeta, NiFe-5/HBeta and NiFe-10/HBeta at 300 °C is shown in Table 4.8. Scheme 4.5 presents the overall reaction network proposed for transformation of the simulated phenolic bio-oil through HDO over these metal/acid bifunctional catalysts. As can be seen from the data in Table 4.8, selectivity of products is a strong function of catalyst type. No measurable conversion of phenolic compounds of the simulated bio-oil occurred over HBeta in the presence of hydrogen illustrating that HBeta does not contain suitable active sites for activation of hydrogen molecules to be involved in hydrodeoxygenation. Over Ni/HBeta, selectivities towards phenolic compounds (phenol, cresol and guaiacol), cycloalkanes and aromatic hydrocarbons were 55.88, 21.39 and 7.12 wt%, respectively. Higher selectivity towards saturated cyclic compounds compared to aromatic hydrocarbons indicates that the reaction was favorably proceeded through hydrogenation of benzene ring of phenolics over nickel metal. This is in agreement with the result of study held by Bykova et al. (2012) showing that the main product obtained from guaiacol HDO over Ni/SiO_2 catalyst

was cyclohexane. Cyclohexane, cyclopentane, methylcyclopentane and methylcyclohexane were the main cycloalkanes produced through HDO of the phenolic bio-oil over Ni/HBeta. On the other hand, Fe/HBeta was an efficient catalyst for hydrogenolysis (direct deoxygenation) of the simulated bio-oil to aromatic hydrocarbons; aromatic hydrocarbons selectivity of 20.21 wt% was obtained using Fe/HBeta. Benzene, toluene, xylene and trimethylbenzene were the main aromatic products. Selectivities towards phenolic compounds (phenol, cresol and guaiacol) and cycloalkanes produced over Fe/HBeta were 69.28 and 0.95 wt%, respectively. Similar to our results, Fe active site was shown to be efficient for hydrogenolysis in a study held by Olcese et al. (2012) for guaiacol HDO over Fe/SiO_2 catalyst. Nie et al. (2014) also reported that Fe/SiO_2 was suitable for toluene production from *m*-cresol. In order to compare the selectivities of Ni/HBeta and Fe/HBeta towards hydrogenation and hydrogenolysis, HDO of phenol was conducted over these catalysts at 300 °C and different hydrogen pressures of 6, 11 and 16 bar. Phenol molecule is converted to benzene and cyclohexanone/cyclohexanol through hydrogenolysis and benzene ring hydrogenation mechanisms, respectively. The produced cyclohexanol could be transformed to cyclohexene and methylcyclopentane through dehydration and isomerization pathways, respectively, which concurrently occur over acid sites of zeolite support. Further hydrogenation of cyclohexene over metal sites forms cyclohexane. Similar reaction pathway for conversion of phenol to cyclohexane and methylcyclopentane was reported in a study held by Zhang et al. (2013) for HDO of phenol over Ni/HZSM-5. Over both catalysts of Ni/HBeta and Fe/HBeta, rise of hydrogen pressure from 6 to 16 bar resulted in enhanced phenol conversion (Figure 4.7). However, pressure dependency of phenol conversion over Ni/HBeta was higher than that over Fe/HBeta. Over Ni/HBeta and at low pressure of 6 bar, selectivity towards benzene was higher than cycloalkanes (weight ratio of cycloalkanes to benzene: 0.85). By increase of pressure to 11 and 16 bar, weight ratio of cycloalkanes to benzene was increased to 1.5

and 4, respectively, illustrating that reaction selectivity over Ni active sites is a strong function of the amount of available hydrogen. However, over Fe/HBeta and at low hydrogen pressure of 6 bar, the cycloalkanes to benzene ratio was 0.035 which was slightly increased to 0.05 by rise of hydrogen pressure to16 bar. This indicates that Fe favorably proceeded the reaction through hydrogenolysis mechanism to produce benzene at either low or high hydrogen pressure. As depicted in Table 4.8, co-impregnation of Ni and Fe on HBeta support (NiFe-5/HBeta) did not change the intrinsic catalytic behavior of nickel and iron active sites in HDO of the simulated phenolic bio-oil; both hydrogenation and hydrogenolysis mechanisms were proceeded over bimetallic catalyst of NiFe-5/HBeta, demonstrating that loading of both Ni and Fe active sites on HBeta did not cause negative interactive effect on transformation of phenolic compounds of the simulated bio-oil. Selectivities towards oxygen-free compounds over Ni/HBeta, Fe/HBeta and NiFe-5/HBeta were 32.19, 23.82 and 36.20 wt%, respectively. Enhanced HDO efficiency of bimetallic catalyst of NiFe-5/HBeta compared to that of monometallic catalysts of Ni/HBeta and Fe/HBeta is due to the synergistic effect between the two metals. The H_2-TPD results presented in Table 4.7 also indicate the synergistic effect between Ni and Fe; co-impregnation of Ni and Fe on HBeta resulted in enhanced adsorption of hydrogen by metal oxide phases which leads to higher conversion of phenolic compounds.

Meanwhile, catalytic performance of bimetallic catalyst of NiFe/HBeta was considerably improved by the increase of nickel and iron loadings (Table 4.8). It can be seen from the HDO results that increase of metal loading of the bimetallic catalyst from 2.5 wt% Ni and 2.5 wt% Fe to 5 wt% Ni and 5 wt% Fe resulted in higher HDO activity due to the increase in the amount of available metal active sites (refer to H_2-TPD results in Table 4.7). Total selectivity of oxygen-free products including both aromatic hydrocarbons and cycloalkanes obtained over NiFe-10/HBeta was 53.59 wt%. The aromatic hydrocarbons

selectivity of Ni/HBeta, Fe/HBeta, NiFe-5/HBeta and NiFe-10/HBeta was 7.12, 20.21, 15.91 and 29.48 wt%, respectively. Meanwhile, the cycloalkanes selectivity of Ni/HBeta, Fe/HBeta, NiFe-5/HBeta and NiFe-10/HBeta was 21.39, 0.95, 16.50 and 21.66 wt%, respectively. As shown in Table 4.8, selectivity towards methylcyclopentane over NiFe-10/HBeta is lower than that over Ni/HBeta and NiFe-5/HBeta. This could be due to lower density of acid sites of NiFe-10/HBeta compared to that of Ni/HBeta and NiFe-5/HBeta (Figure 4.5); methylcyclopentane is produced through isomerization of cyclohexanol on zeolite acid sites. As can be seen from the data in Table 4.8, by increase of metal loading from 5 to 10 wt% in the bimetallic catalyst of NiFe/HBeta, the selectivity of cycloalkanes had a lower increase compared to selectivity of aromatic hydrocarbons. This could be due to the fact that dehydration of cycloalcohol intermediates to cycloalkanes occurs over the acid sites of catalyst, and replacement of NiFe-5/HBeta with NiFe-10/HBeta with lower density of acid sites which is caused by higher metal loading favored aromatic hydrocarbons production rather than cycloalkanes production. It could be inferred that bimetallic catalyst of NiFe/HBeta is an efficient catalyst for hydrodeoxygenation of phenolic compounds since both hydrogenolysis and hydrogenation reactions could concurrently occur over this catalyst resulting in high conversion of phenolic compounds and production of both aromatic hydrocarbons and cycloalkanes.

Table 4.8: Catalytic performance of Ni/HBeta, Fe/HBeta and NiFe/HBeta in HDO of simulated bio-oil.

Catalyst	**Ni/HBeta**	**Fe/HBeta**	**NiFe-5/HBeta**	**NiFe-10/HBeta**
Selectivity in organic liquid (wt%)				
Oxygenates	67.81	76.18	63.80	46.41
Phenol	27.33	42.88	35.46	25.24
Cresol	17.96	17.20	14.93	8.23
Guaiacol	10.59	9.20	5.80	3.15
Cyclohexanone	2.00		1.44	2.68
Cyclohexanol	1.02		0.52	0.31
Cyclopentanone	0.08			
Methylcyclohexanone	0.49			
2,6-Dimethylphenol	4.68	2.06	2.83	2.25
Anisole	1.72	0.23	0.53	0.96
Catechol	0.99	3.61	1.38	2.55
Methylcatechol	0.95	1.00	0.91	1.04

‘**Table 4.8,** continued’

Catalyst	Ni/HBeta	Fe/HBeta	NiFe-5/HBeta	NiFe-10/HBeta
Cycloalkanes	21.39	0.95	16.50	21.66
Cyclohexane	14.60	0.87	12.81	18.93
Cyclopentane	0.40			
Methylcyclopentane	5.12	0.08	3.02	2.73
Methylcyclohexane	1.27		0.67	
Aromatic hydrocarbons	7.12	20.21	15.91	29.48
Benzene	4.11	12.03	9.48	10.53
Toluene	1.36	4.66	3.72	10.92
Xylene	0.98	1.65	1.07	2.47
Trimethylbenzene	0.67	1.87	1.64	5.56
Other hydrocarbons	3.68	2.66	3.79	2.45

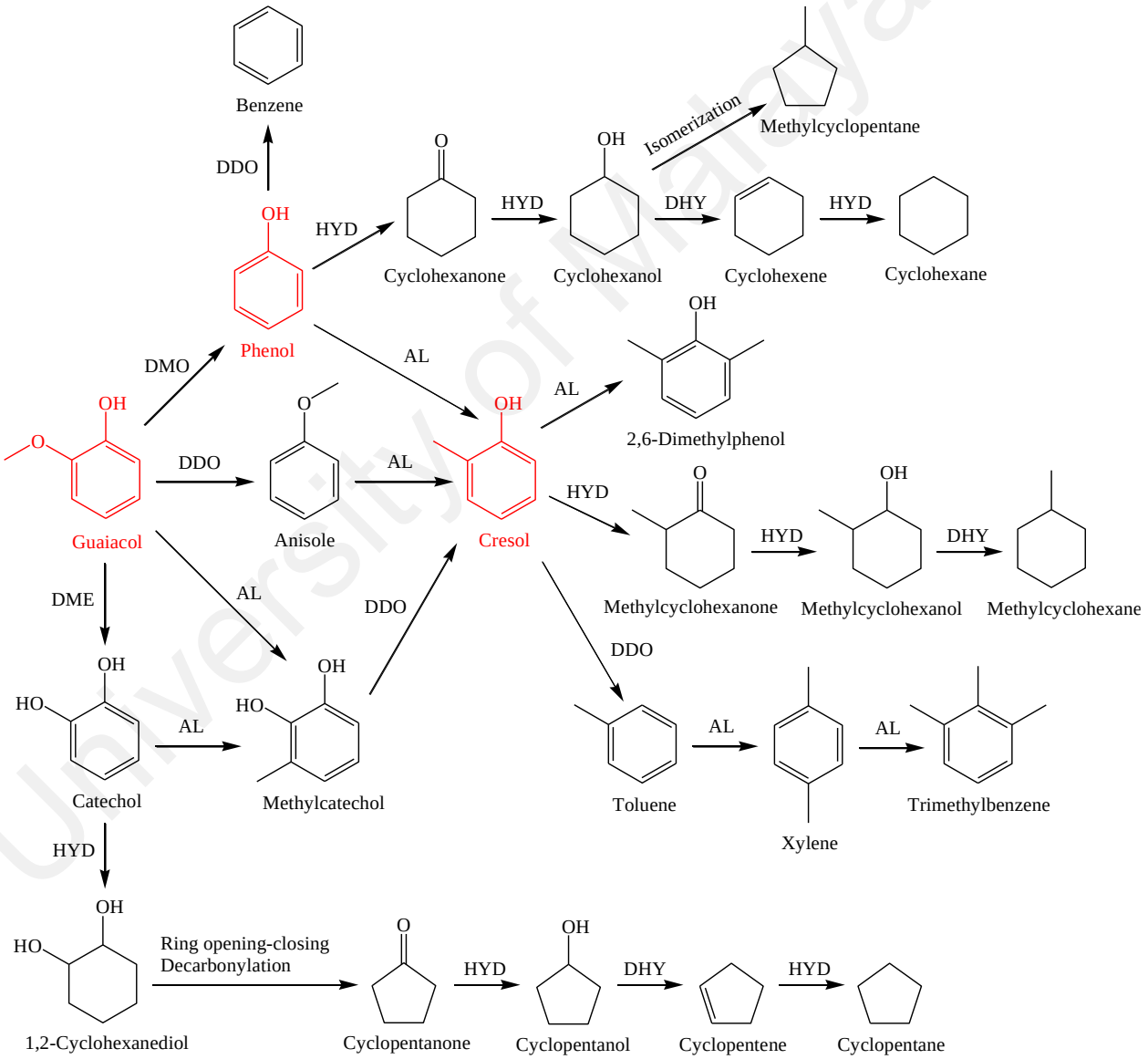

Scheme 4.5: Proposed reaction mechanism for catalytic HDO of simulated phenolic bio-oil over Ni/HBeta, Fe/HBeta and NiFe/HBeta catalysts; HYD: hydrogenation, DDO: direct deoxygenation (hydrogenolysis), DMO: demethoxylation, DME: demethylation, AL: alkylation, DHY: dehydration.

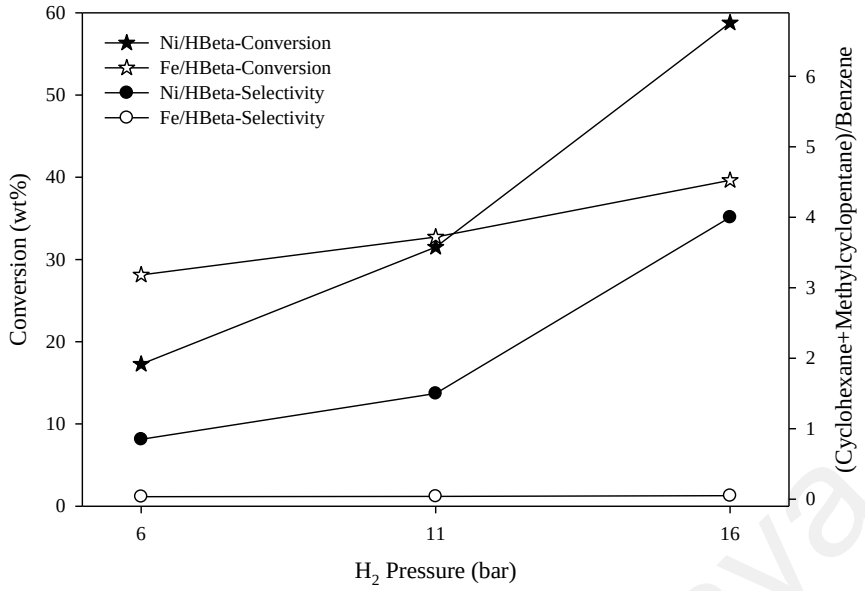

Figure 4.7: Pressure dependency of phenol conversion and (cyclohexane + methylcyclopentane)/benzene ratio over Ni/HBeta and Fe/HBeta catalysts. Reaction conditions: phenol, 2 g; water, 100 ml; catalyst, 2 g; temperature, 300 °C; reaction time, 4 h and rpm, 800.

Formation and deposition of coke which blocks catalytic active sites and hinders their accessibility to reactants is considered as a main cause for catalyst deactivation (Fisk et al., 2009; Wildschut et al., 2010; Xiong et al., 2011). Coke contents of the spent catalysts of Ni/HBeta, Fe/HBeta, NiFe-5/HBeta and NiFe-10/HBeta determined by TGA analysis were 2.31, 3.97, 2.91 and 6.09 wt%, respectively. Catalyst acidity and type of intermediates/products formed in HDO of phenolic compounds are usually considered as major causes for coke generation on bifunctional metal/acid catalysts. Data presented in this work show that strength of acid sites as well as selectivity towards catechol and aromatic hydrocarbons were effective on the amount of coke deposited on catalyst. Since the coke content and strength of acidity of catalysts decreased in the same order of NiFe-10/HBeta > Fe/HBeta > NiFe-5/HBeta > Ni/HBeta, it could be concluded that the amount of coke formed over catalyst was increased by increase of acid strength of catalyst. Meanwhile, higher coke contents of Fe/HBeta and NiFe-10/HBeta could be due to higher formation of catechol on these catalysts; catechol produced as an intermediate in HDO of guaiacol is recognized as a strong cause for coke generation (Puente et al., 1999; Elliott, 2007; Filley & Roth, 1999; Foster et al., 2012; Olcese et al., 2012; Sepúlveda et al., 2011;

Ghampson et al., 2012; Zhao et al., 2011). Besides, high selectivity towards aromatic hydrocarbons over Fe active sites could lead to the formation of polycyclic aromatic hydrocarbons which act as coke precursor (Dufour, Masson, Girods, Rogaume, & Zoulalian, 2011; Olcese et al., 2012).

The results of recycling of NiFe-10/HBeta catalyst shown in Table 4.9 indicate that catalytic activity of catalyst was slightly reduced in the second and third runs signifying that this catalyst maintained its stability during the first three runs. Use of catalyst for two recycled runs did not considerably reduced BET surface area and pore volume. Meanwhile, XRF analysis of the spent catalysts showed that leaching of metals from catalyst was negligible after two times of reusing NiFe-10/HBeta. However, considerable decrease in conversion of phenolic compounds and selectivity of oxygen-free products was observed at third and fourth recycle runs. Lower activity of catalyst at third and fourth recycle runs could be caused by higher loss of metal active sites and change of textural properties of catalyst during these two recycle runs. After five runs, Ni and Fe loadings were reduced from 4.95 and 4.98 wt% to 3.81 and 4.05 wt%, respectively. Comparison between XRD results of fresh and spent catalyst (Figure 4.8) shows that the intensity of diffraction peaks related to metal oxides was considerably decreased by five times using NiFe-10/HBeta, indicating that a fraction of metal active sites was leached from catalyst structure. Meanwhile, after five times use, surface area and pore volume of NiFe-10/HBeta were reduced from 417 and 0.250 to 296 m^2/g and 0.161 cm^3/g, respectively (Table 4.9). Reduction of catalyst surface area and pore volume results in lower catalytic activity since the amount of active sites available for reactant molecules is reduced.

Table 4.9: Selectivity of phenolic and oxygen-free products of fresh and reused NiFe-10/HBeta as well as physical properties of regenerated NiFe-10/HBeta.

Run	Selectivity of phenolic compounds[a] (wt%)	Selectivity of oxygen-free products (wt%)	Ni loading[b] (wt%)	Fe loading[b] (wt%)	S_{BET}[c] (m^2/g)	Pore volume[d] (cm^3/g)
1	36.62	53.59	4.95	4.98	412	0.246
2	38.09	48.96	4.93	4.95	404	0.238
3	40.01	45.42	4.86	4.89	389	0.226
4	47.18	30.53	4.33	4.46	368	0.213
5	69.25	9.36	3.81	4.05	296	0.161

[a] Selectivity of phenol, cresol and guaiacol in product sample.
[b] Determined by XRF method
[c] Calculated in the range of relative pressure (P/P_0) = 0.05-0.25
[d] Total pore volume evaluated at P/P_0 = 0.99

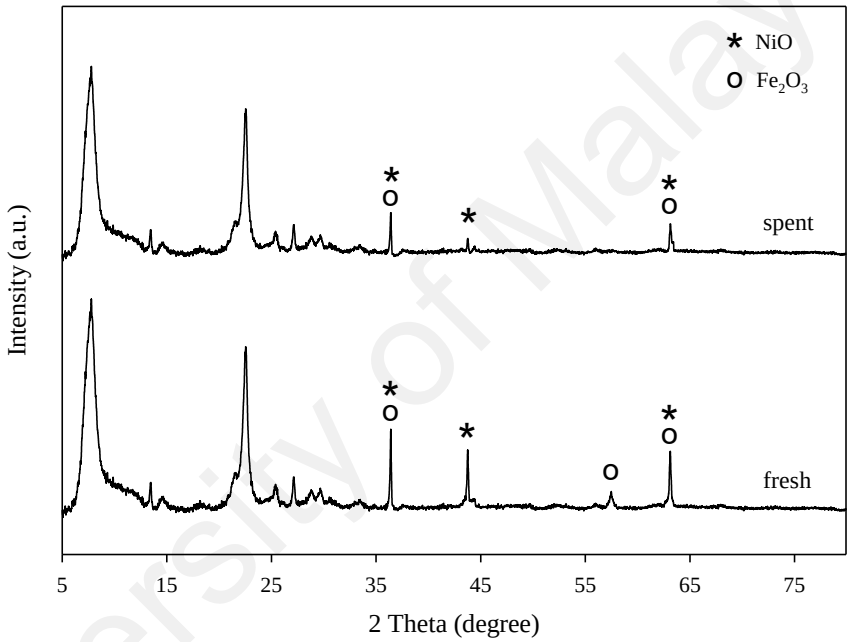

Figure 4.8: XRD patterns of fresh and five times used NiFe-10/HBeta catalyst.

4.2.3 Temperature dependence of product distribution of simulated bio-oil HDO over NiFe-10/HBeta

Products selectivity and coke formation over NiFe-10/HBeta in HDO of simulated phenolic bio-oil at different reaction temperatures are shown in Table 4.10. Selectivities towards cycloalkanes and aromatic hydrocarbons were very low at 220 °C. Increase of reaction temperature to 300 °C resulted in increase of selectivities towards hydrocarbon products mainly aromatic hydrocarbons. This indicates that reaction temperature should be sufficiently high for efficient deoxygenation. However, further temperature increase

to 340 °C decreased the selectivity of oxygen-free products. The reason for this might be the exothermic nature of hydrogen adsorption on catalyst (Ojagh, Creaser, Tamm, Hu, & Olsson, 2015); at temperatures higher than optimum value, hydrogen adsorption on catalyst could be reduced resulting in lower hydrodeoxygenation activity. It can be seen from Table 4.10 that selectivity of cycloalkanes had much more reduction than that of aromatic hydrocarbons by increase of reaction temperature from 300 to 340 °C; the ratio of cycloalkanes to aromatic hydrocarbons was 0.73 and 0.40 at 300 and 340 °C, respectively. This is due to the fact that higher hydrogen is required for formation of cycloalkanes which might be less available to reactants at elevated temperature resulting in shift of the reaction pathway from hydrogenation to hydrogenolysis. Our data are in agreement with the results of the study held by Wan et al. (2012) for catalytic HDO of *p*-cresol over Pt/Al_2O_3 showing that increase of reaction temperature in the range of 250-300 °C resulted in enhanced hydrogenolysis and reduced hydrogenation due to lower hydrogen coverage on catalyst surface at elevated temperature. As shown in Table 4.10, coke content deposited on catalyst was increased by the increase of reaction temperature from 220 to 340 °C; higher temperature leads to enhanced polymerization of oxygen containing compounds and higher formation of coke precursors (Bykova et al., 2012; Yakovlev et al., 2009).

Table 4.10: Temperature dependence of products selectivity and coke formation over NiFe-10/HBeta in HDO of simulated phenolic bio-oil.

Temperature (°C)	**220**	**260**	**300**	**340**
Selectivity in organic liquid (wt%)				
Oxygenates	88.16	71.61	46.41	62.03
Cycloalkanes	4.51	12.74	21.66	9.99
Aromatic hydrocarbons	6.00	13.61	29.48	24.75
Other hydrocarbons	1.33	2.04	2.45	3.23
Coke content (wt%)				
	4.62	5.54	6.09	6.53

4.2.4 Effect of methanol solvent on HDO of simulated phenolic bio-oil over NiFe-10/HBeta

In this section, the effect of methanol as solvent on reaction selectivity of hydrodeoxygenation of the simulated bio-oil over NiFe-10/HBeta is compared with that of water. The reason for selection of methanol to be examined as solvent was its higher hydrogen solubility compared with water; the solubility of 1 bar hydrogen at 25 °C in water and methanol was 7.8×10^{-7} and 3.5×10^{-6} mol/cm^3, respectively (He et al., 2014). Meanwhile, use of methanol as solvent could be useful due to its low boiling point which makes it easy to be separated from final product. As shown in Table 4.11, addition of methanol to water with the ratio of 50:50 v/v resulted in decrease of selectivity towards oxygen-free products. Both hydrogenation and hydrogenolysis activities of NiFe-10/HBeta catalyst were significantly reduced using the mixture of methanol and water as solvent. The reduction of selectivity towards cyclohexane and detection of methoxycyclohexanol, 1,1′-dimethoxycyclohexane and methoxycyclohexane in the product sample obtained from the simulated bio-oil HDO in presence of methanol indicate that the acetal reaction between methanol and cyclohexanone had occurred (scheme 4.6). During the acetalization reaction, cyclohexanone is protonated by Brønsted acid sites (H^+ ions of HBeta zeolite), and then the protonated cyclohexanone is combined with methanol molecule to form hemiacetal of methoxycyclohexanol (Thomas, Prathapan, & Sugunan, 2005; Thomas et al., 2011). Methoxycyclohexanol could react with another molecule of methanol to produce the acetal of 1,1′-dimethoxycyclohexane. Moreover, the methoxycyclohexanol molecule could be dehydrated over the acid sites of HBeta to form 1-methoxycyclohexene which undergoes hydrogenation over metallic sites of catalyst to produce methoxycyclohexane. Similar reaction pathways for cyclohexanone transformation to 1-methoxycyclohexene and 1,1′-dimethoxycyclohexane was reported in a study held by He et al. (2014) for hydrogenation of cyclohexanone in methanol using

combined catalysts of Pd/C and HZSM-5. In the case of using methanol as the only solvent, hydrogenation of cyclohexanone to cyclohexane was completely suppressed. Our data reveal that reaction selectivity of HDO of bio-oil could be strongly affected by the type of the solvent; methanol was not a suitable solvent due to its involvement in the reaction, and water resulted in much enhanced catalytic activity for hydrodeoxygenation of phenolic compounds. It could be inferred that use of a solvent like methanol which has reactivity over acidic catalyst is not suitable for catalytic hydrodeoxygenation of phenolics over zeolites.

Table 4.11: The effect of solvent type on product distribution of HDO of simulated phenolic bio-oil over NiFe-10/HBeta. Reaction conditions: simulated bio-oil, 4 g; solvent, 100 ml; catalyst, 4 g; temperature, 300 °C; reaction time, 4 h and rpm, 800.

Solvent type	**Water**	**Water:methanol (50:50 v/v)**	**Methanol**
Selectivity in organic liquid (wt%)			
Oxygenates	46.41	68.80	89.23
Phenol	25.24	30.17	36.86
Cresol	8.23	11.36	10.69
Guaiacol	3.15	5.12	7.97
Cyclohexanone	2.68	1.44	3.45
Cyclohexanol	0.31	0.16	
2,6-Dimethylphenol	2.25	3.98	4.38
Anisole	0.96	1.03	1.29
Catechol	2.55	1.46	0.66
Methylcatechol	1.04	1.51	2.08
Methoxycyclohexanol		2.15	3.92
Methoxycyclohexane		8.47	14.41
1,1′-Dimethoxycyclohexane		1.95	3.52
Cycloalkanes	21.66	8.72	
Cyclohexane	18.93	8.72	
Methylcyclopentane	2.73		
Aromatic hydrocarbons	29.48	18.15	5.71
Benzene	10.53	2.01	
Toluene	10.92	4.70	0.12
Xylene	2.47	1.34	0.83
Trimethylbenzene	5.56	10.10	4.76
Other hydrocarbons	2.45	4.33	5.06

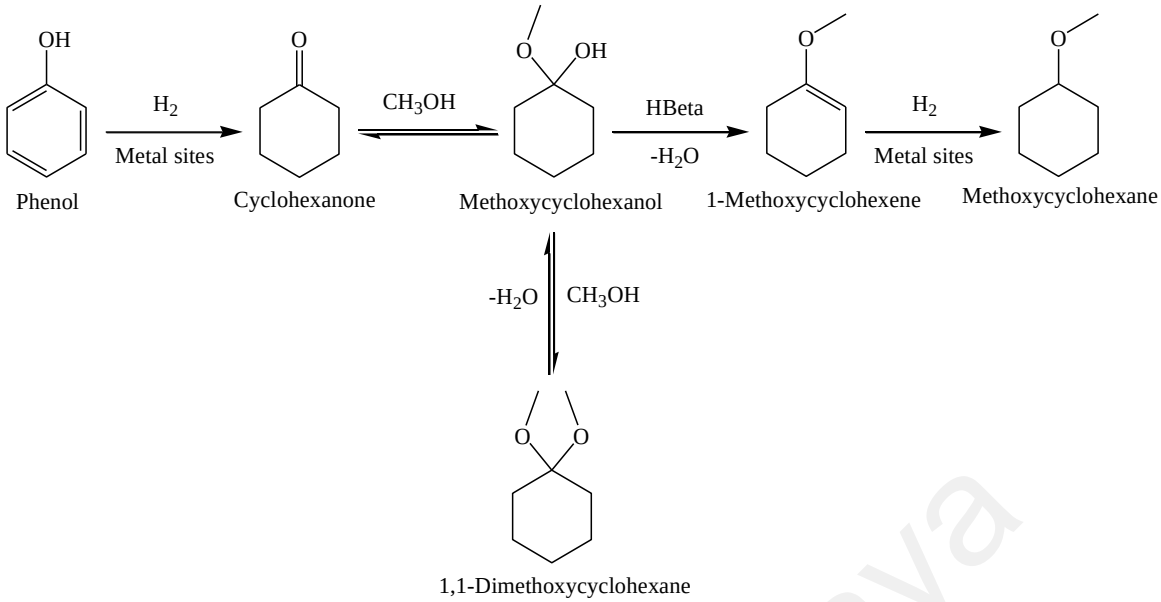

Scheme 4.6: Acetal reaction occurred during catalytic HDO of simulated phenolic bio-oil over NiFe-10/HBeta using methanol as solvent.

4.3 Using decalin and tetralin as hydrogen source for transfer hydrogenation of renewable lignin-derived phenolics over activated carbon supported Pd and Pt catalysts

4.3.1 Physicochemical characteristics of catalysts

BET surface areas of 10 wt% Pd/C and 10 wt% Pt/C catalysts were 694 and 1078 m^2/g, respectively (Table 4.12). The ratio of micropore area to external surface area of Pd/C and Pt/C catalysts was 1.28 and 0.26, respectively. As depicted in Figure 4.9, both catalysts showed type IV adsorption isotherm with hysteresis loop H3 and H4 for Pt/C and Pd/C, respectively. The H3 hysteresis type indicates very wide distribution of pore size and dominant presence of mesoporosity in Pt/C. The H4 hysteresis loop and nearly horizontal curve of isotherms of Pd/C demonstrate the dominant microporous surface area in this catalyst. Bulk XRF analysis of Pd/C and Pt/C catalysts showed that the amounts of palladium (9.96 wt%) and platinum (10.07 wt%) loaded on activated carbon carrier were close to the nominal commercial value of 10 wt%.

Table 4.12: Chemical and textural properties of Pd/C and Pt/C catalysts: specific surface area (S_{BET}), micropore surface area (S_{micro}), micropore and mesopore volume (V_{micro} and V_{meso}), total pore volume (V_{total}), average pore width (D) and metal content.

Catalyst	S_{BET} (m^2/g)	S_{micro} (m^2/g)	V_{micro} (cm^3/g)	V_{meso} (cm^3/g)	V_{total} (cm^3/g)	D (nm)[a]	Metal loading (wt%)[b]
Pd/C	694	390	0.19	0.34	0.53	7.14	9.96
Pt/C	1078	224	0.10	0.72	0.82	7.22	10.07

[a] Average pore width derived from adsorption branches of isotherms through BJH method
[b] Determined by XRF method

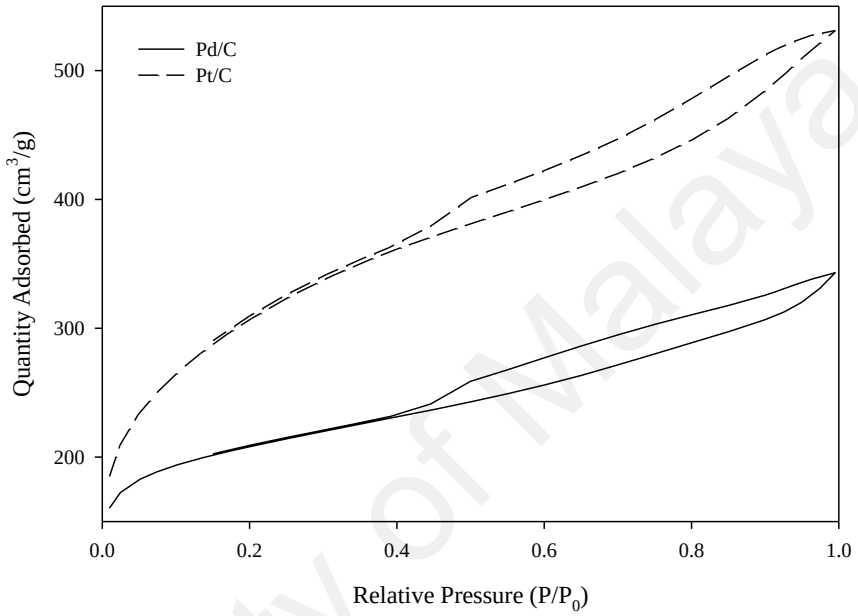

Figure 4.9: Nitrogen adsorption-desorption isotherms of Pd/C and Pt/C catalysts.

The XRD pattern of 10 wt% Pd/C shows the peaks for tetragonal palladium oxide phase found at 2θ values of 34.3° (intense reflection), 42.8°, 55.3° and 72.4° (Figure 4.10). As depicted in Figure 4.10, XRD analysis of 10 wt% Pt/C shows reflections at 2θ values of 39.5° (intense reflection), 46°, 67.1° and 80.7° which belong to cubic platinum particles. Broad diffraction peaks of the samples indicate small-sized particles of palladium oxide and platinum. Meanwhile, the average crystallite sizes of Pd/C and Pt/C catalysts determined from XRD peak broadening using the Scherrer equation ($D = 0.9\lambda/\beta \cos \theta$; D: crystallite size; λ: X-ray wavelength; β: line broadening full width at half maximum (FWHM); and θ: Bragg's angle) are 57.82 and 40.76 nm, respectively.

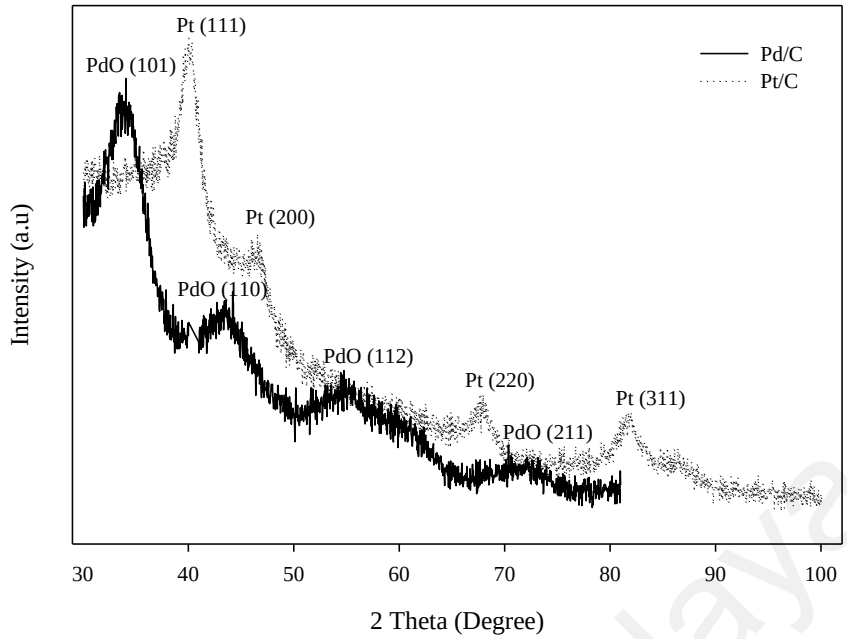

Figure 4.10: XRD patterns of Pd/C and Pt/C catalysts.

4.3.2 Mechanism of dehydrogenation of decalin and tetralin

Generally, hydrogen donor compounds are thermally and catalytically transformed to produce hydrogen required for hydrogenation reaction. Decalin and tetralin are adsorbed on catalytic active sites and hydrogen atoms are simultaneously released to be involved in hydrogenation reaction through transfer hydrogenation mechanism (Biniwale, Kariya, & Ichikawa, 2005). The activated hydrogen on metal catalyst might be used in hydrogenation reaction through two mechanisms: (i) direct involvement in hydrogenation reaction over metal catalysts, (ii) hydrogen spillover from metal sites to carbon support and subsequent participation of the hydrogen atoms on carbon support in hydrogenation reaction. In order to study the mechanism of catalytic dehydrogenation of decalin and tetralin, the dehydrogenation experiments were carried out over Pd/C and Pt/C at 275 °C for 4 h reaction time (water to donor ratio of 50/50 g/g and catalyst amount of 0.6 g). Since the mechanism of dehydrogenation of decalin and tetralin largely prevented over acid sites of zeolites, decalin and tetralin cannot be used as hydrogen donor over zeolite catalysts. Conversions of decalin and tetralin over Pd/C were 67.23 and 80.44 mol%, which were increased to 71.09 and 92.21 mol% over Pt/C, respectively (Table 4.13).

Higher conversion of H-donors over Pt/C might be due to the larger pore size of this catalyst compared to Pd/C (mesoporous Pt/C versus microporous Pd/C) which facilitates the accessibility of the interior surface of the catalyst by reacting molecules. The presence of aromatic compounds of tetralin and naphthalene in product composition of decalin transformation confirms hydrogen production from decalin. By conversion of one mole of decalin to one mole of tetralin or one mole of naphthalene, three or five moles of hydrogen are released, respectively. Dehydrogenation of decalin occurs through two steps: tetralin production from decalin dehydrogenation followed by naphthalene production via tetralin dehydrogenation. Since tetralin dehydrogenation to naphthalene occurs faster than decalin dehydrogenation to tetralin, tetralin selectivity is lower than naphthalene selectivity (Wang, Shah, Huggins, & Huffman, 2006). Similarly, hydrogen release from tetralin is evidenced by naphthalene production; dehydrogenation of tetralin to naphthalene results in two moles of hydrogen. Tetralin dehydrogenation resulted in naphthalene selectivities of 93.45 and 90.90 mol% over Pd/C and Pt/C, respectively. In addition to tetralin dehydrogenation to naphthalene, hydrogenation of tetralin to decalin also occurred and higher decalin selectivity (9.10 mol%) was obtained over Pt/C catalyst. Wang et al. (2006) reported that slow desorption of aromatic compounds produced by dehydrogenation of decalin and tetralin from catalyst surface could lead to reduction in conversion rate of decalin and tetralin. The data illustrate that Pt/C was more efficient than Pd/C for dehydrogenation of decalin and tetralin. Higher conversions of decalin and tetralin over Pt/C catalyst indicate that the affinity of these H-donor compounds for Pt/C was higher than that for Pd/C. Meanwhile, Pt/C and Pd/C resulted in higher catalytic activity for transformation of tetralin compared to decalin. This could be due to the higher tendency of tetralin to be adsorbed on metal active sites compared to decalin; since aromatic cycles have higher tendency to be adsorbed on metal active sites compared to saturated cycles, the adsorption of tetralin with one aromatic cycle is higher than that of

decalin (Ninomiya, Tanabe, Sotowa, Yasukawa, & Sugiyama, 2008; Ninomiya, Tanabe, Uehara, Sotowa, & Sugiyama, 2006; Wang et al., 2006).

Table 4.13: Product selectivity of dehydrogenation of decalin and tetralin over Pd/C and Pt/C catalysts. Reaction conditions: H-donor, 50 g; water, 50 g; catalyst, 0.6 g; temperature, 275 °C; reaction time, 4 h and rpm, 500.

H-donor	**Decalin**		**Tetralin**	
Catalyst	**Pt/C**	**Pd/C**	**Pt/C**	**Pd/C**
H-donor conversion (mol%)				
	71.09	67.23	92.21	80.44
Product selectivity (mol%)				
Tetralin	26.47	28.57		
Naphthalene	73.53	71.43	90.90	93.45
Decalin			9.10	6.55

The addition of phenol, *o*-cresol and guaiacol as hydrogen acceptor to decalin and tetralin decreased the conversion of H-donors due to the competitive adsorption of acceptor and donor molecules on catalytic sites (Table 4.14). The results show that catalytic performance of Pt/C and Pd/C in decalin conversion in the presence of guaiacol was lower than that when phenol and *o*-cresol were used as hydrogen acceptor; reactions that occurred in guaiacol transformation led to more inhibitory effect on decalin dehydrogenation. Similar to decalin dehydrogenation, the inhibitory effect of guaiacol on tetralin transformation was higher than that of phenol and *o*-cresol. This could be due to the fact that guaiacol and its products through hydrogenation reaction (such as catechol) are known as coke precursors which cause catalyst deactivation (Olcese et al., 2012; Sepúlveda et al., 2011; Ghampson et al., 2012; Zhao et al., 2011). In addition to H-donor conversion, product selectivity of dehydrogenation of H-donors was also affected by the addition of phenolic compounds. In decalin dehydrogenation, the selectivity towards naphthalene was remarkably decreased in the presence of phenolics. However, in tetralin dehydrogenation, addition of phenolics led to increase in naphthalene selectivity due to reduction in tetralin hydrogenation to decalin.

Table 4.14: Product selectivity (mol%) and dehydrogenation conversion (mol%) of decalin and tetralin over Pt/C and Pd/C catalysts in presence of phenol, *o*-cresol and guaiacol. Reaction conditions: H-donor, 50 g; water, 50 g; phenolic compounds, 12 g; catalyst, 0.6 g; temperature, 275 °C; reaction time, 4 h and rpm, 500.

Hydrogen acceptor	**Phenol**		***o*-Cresol**		**Guaiacol**	
Catalyst	**Pt/C**	**Pd/C**	**Pt/C**	**Pd/C**	**Pt/C**	**Pd/C**
Decalin conversion	56.27	50.12	57.18	50.27	51.07	49.30
Product selectivity						
Tetralin	38.01	40.92	39.35	41.10	38.37	40.13
Naphthalene	61.99	59.08	60.65	58.90	61.63	59.87
H_2 release from decalin (mol)[a]	0.77	0.67	0.78	0.68	0.70	0.67
Tetralin conversion	80.98	68.53	81.35	73.06	75.18	66.67
Product selectivity						
Naphthalene	95.85	99.02	96.39	98.23	95.46	99.67
Decalin	3.15	0.98	3.61	1.77	4.54	0.33
H_2 release from tetralin (mol)[b]	0.58	0.51	0.59	0.54	0.54	0.50

[a] Estimated from the stoichiometric reaction of decalin decomposition to hydrogen considering the average organic yield of 90% for all experiments.
[b] Estimated from the stoichiometric reaction of tetralin decomposition to hydrogen considering the average organic yield of 99% for all experiments.

4.3.3 Transfer hydrogenation of phenol, *o*-cresol and guaiacol

Blank reactions of hydrogenation of phenol, *o*-cresol and guaiacol using H_2 gas, decalin and tetralin as hydrogen source without using catalyst were carried out to investigate the product distribution of transformation of both H-donors and phenolic compounds (Table 4.15). Low conversion of phenol, *o*-cresol and guaiacol was obtained in absence of catalyst. Meanwhile, higher conversion of all phenolic compounds in hydrogenation reaction using H_2 gas occurred compared to hydrogenation using H-donors due to low conversion of donors (up to 7 and 12 mol% for decalin and tetralin, respectively) which leads to low hydrogen formation. Data presented in Table 4.15 show that the hydrogenation conversion of phenolics by the use of tetralin was higher than that of phenolics using decalin. In phenol hydrogenation using H_2 gas, cyclohexanone and cyclohexanol were detected in product composition while cyclohexanone was the only product obtained from hydrogenation of phenol using decalin and tetralin. In *o*-cresol hydrogenation, demethylation of *o*-cresol to phenol was the dominant reaction mechanism in presence of each of hydrogen sources, and higher phenol selectivity was observed using H-donors. In guaiacol hydrogenation, catechol which is formed via

guaiacol demethylation was the only product of hydrogenation reaction using H-donors, while in guaiacol hydrogenation using H_2 gas, phenol with 6 mol% selectivity was also produced through guaiacol demethoxylation.

Table 4.15: Product selectivity obtained from hydrogenation of phenol, *o*-cresol and guaiacol in absence of catalyst. Reaction conditions: H_2 gas, 16 bar; H-donor, 50 g; water, 100 g for hydrogenation and 50 g for transfer hydrogenation; phenolic compounds, 12 g; temperature, 275 °C; reaction time, 4 h and rpm, 500.

Reactant	**Phenol**			***o*-Cresol**			**Guaiacol**		
Hydrogen source	**H_2 gas**	**Decalin**	**Tetralin**	**H_2 gas**	**Decalin**	**Tetralin**	**H_2 gas**	**Decalin**	**Tetralin**
Reactant conversion (mol%)									
	6.33	2.02	2.53	6.49	1.78	2.96	9.06	2.17	4.22
Product selectivity (mol%)									
Cyclohexanone	92.15	100	100						
Cyclohexanol	7.85								
Methylcyclohexanone				42.98	24.51	29.05			
Methylcyclohexanol				2.39	0.48				
Phenol				54.63	75.01	70.95	6		
Catechol							94	100	100

Pt/C and Pd/C catalysts were used for hydrogenation/transfer hydrogenation of phenol, *o*-cresol and guaiacol using pure hydrogen and decalin/tetralin as gas and liquid sources of hydrogen. Tetralin was previously reported as a potential hydrogen donor for catalytic transfer hydrogenation of bio-oil (Su-Ping, 2003; Zhang, Yan, Li, & Ren, 2005) and guaiacol (Afifi, Chornet, Thring, & Overend, 1996). Over Pt/C and Pd/C catalysts and in presence of pure hydrogen gas, phenol conversion was 100 and 83.32 mol%, respectively (Table 4.16). Hydrogenation of benzene ring of phenol to cyclohexanone and cyclohexanol was the main reaction mechanism over these two catalysts (scheme 4.7). Cyclohexanol and cyclohexanone are consumed as intermediate for production of adipic acid and caprolactam which are used to produce fibers and resins based on nylon 66 and nylon 6, respectively. The molar ratio of cyclohexanone to cyclohexanol over Pt/C and Pd/C was 2.62 and 5.27, respectively. Higher phenol conversion and cyclohexanol selectivity on Pt/C catalyst shows its higher potential for phenol hydrogenation compared to Pd/C. When decalin was used as hydrogen source, catalytic performance of Pt/C in phenol hydrogenation was significant; phenol conversion was 100 mol% and cyclohexanone and cyclohexanol selectivities were 30.95 and 69.05 mol%, respectively. High selectivity of cyclohexanol indicates the influential interaction between the hydrogen donor of decalin, hydrogen acceptor of phenol and Pt/C. However, catalytic performance of Pd/C in phenol hydrogenation by the use of decalin as hydrogen source was notably low and selectivity of cyclohexanol was only 10.77 mol%. On the other hand, use of tetralin as hydrogen source led to low phenol conversion over both Pt/C (85.40 mol%) and Pd/C (36.20 mol%) catalysts. In fact, tetralin acts as competitor with phenol to be adsorbed on catalytic active sites and reduces phenol conversion. Higher selectivity of cyclohexanol over Pt/C compared with Pd/C indicates that Pt/C is more efficient for phenol hydrogenation by providing better accessibility of hydrogen atoms released from H-donor compounds. Considering the fact that lower amount of hydrogen is liberated

from tetralin compared to decalin, another experiment of transfer hydrogenation of phenol over Pt/C was carried out with higher initial amount of tetralin (tetralin to water ratio of 60/60 g/g) which resulted in the amount of released hydrogen (~0.76 mol) approximately the same as the amount of hydrogen generated from decalin (~0.77 mol). However, it was observed that with similar amounts of hydrogen released from decalin and tetralin, higher hydrogenation efficiency was achieved in presence of decalin. This indicates that the competitive adsorption of donor and acceptor on catalyst active sites is of more significant impact compared with the amount of released hydrogen.

The reusability of Pt/C catalyst was investigated in transfer hydrogenation of phenol using decalin as hydrogen source. High catalytic activity of Pt/C was observed in the first three runs; phenol conversions of 100, 96.25 and 88.11 mol% were obtained in the first, second and third runs, respectively. However, a significant decrease in phenol conversion was observed at fourth (49.80 mol%) and fifth (46.63 mol%) runs. Nitrogen isothermal adsorption-desorption analysis of fresh and five times used Pt/C showed that textural properties of catalyst was changed; after five times use, BET surface area and pore volume of Pt/C were reduced from 1078 and 0.82 to 798 m^2/g and 0.60 cm^3/g, respectively. Meanwhile, XRF analysis of the spent catalyst indicated that Pt loading was reduced from 10.07 to 7.91 wt% after five runs. Therefore, change of textural properties of catalyst and leaching of Pt from catalyst structure could be considered as effective causes for catalyst deactivation.

Table 4.16: Product selectivity obtained from hydrogenation/transfer hydrogenation of phenol over Pt/C and Pd/C catalysts.

Hydrogen source	**H_2 gas**		**Decalin**		**Tetralin**	
Catalyst	**Pt/C**	**Pd/C**	**Pt/C**	**Pd/C**	**Pt/C**	**Pd/C**
Phenol conversion (mol%)						
	100.00	83.32	100.00	57.30	85.40	36.20
Product selectivity (mol%)						
Cyclohexanone	72.40	84.07	30.95	89.23	38.78	92.64
Cyclohexanol	27.60	15.96	69.05	10.77	61.22	7.36

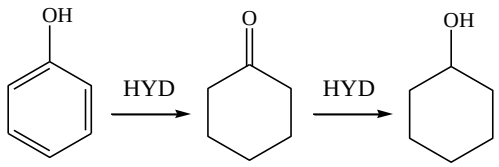

Scheme 4.7: Reaction mechanism of phenol hydrogenation over Pt/C and Pd/C using H_2 gas, decalin and tetralin as hydrogen source; HYD: hydrogenation.

Similar to the results obtained in hydrogenation/transfer hydrogenation of phenol, competitive adsorption of H-donor and *o*-cresol molecules on metal active sites led to lower conversion of *o*-cresol in presence of H-donors compared to H_2 gas (Table 4.17). Hydrogenation of *o*-cresol with a methyl group adjacent to the hydroxyl group over Pd/C and Pt/C catalysts resulted in production of aromatic hydrocarbon of toluene via direct deoxygenation of *o*-cresol (scheme 4.8, path I). Over both catalysts, selectivity towards toluene in hydrogenation using H_2 gas was higher than that in hydrogenation in presence of decalin and tetralin. Besides, hydrogenation of benzene ring of *o*-cresol to methylcyclohexanone (scheme 4.8, path II) followed by further hydrogenation to methylcyclohexanol (scheme 4.8, path III) occurred during hydrogenation/transfer hydrogenation of *o*-cresol. Maximum methylcyclohexanol selectivity was observed over Pt/C using hydrogen donors.

Table 4.17: Product selectivity obtained from hydrogenation/transfer hydrogenation of *o*-cresol over Pt/C and Pd/C catalysts.

Hydrogen source	**H_2 gas**		**Decalin**		**Tetralin**	
Catalyst	**Pt/C**	**Pd/C**	**Pt/C**	**Pd/C**	**Pt/C**	**Pd/C**
o-Cresol conversion (mol%)						
	97.30	68.60	88.05	49.13	61.12	16.96
Product selectivity (mol%)						
Methylcyclohexanone	65.92	77.41	28.02	73.60	40.55	87.05
Methylcyclohexanol	10.91	4.12	50.04	8.36	48.19	4.43
Toluene	23.17	18.47	21.94	18.04	11.26	8.52

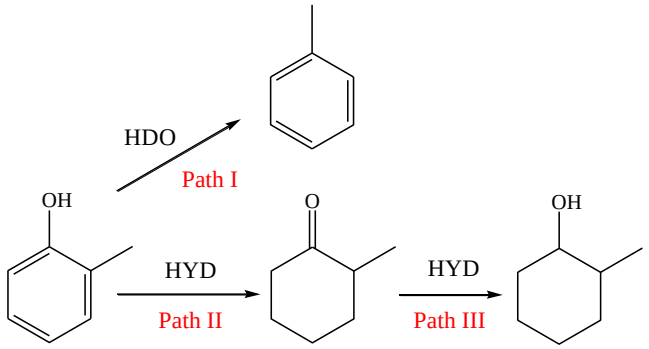

Scheme 4.8: Reaction mechanism of *o*-cresol hydrogenation over Pt/C and Pd/C using H_2 gas, decalin and tetralin as hydrogen source; HYD: hydrogenation, HDO: hydrodeoxygenation.

Catalytic activity and product selectivity of hydrogenation/transfer hydrogenation of guaiacol over Pt/C and Pd/C catalysts are presented in Table 4.18. Catalytic activity of Pt/C was higher than that of Pd/C and this difference was remarkable when decalin and tetralin were used as hydrogen source. By the use of pure hydrogen gas and Pt/C catalyst, guaiacol demethoxylation to phenol and further hydrogenation of phenol to cyclohexanone and cyclohexanol were the main reaction mechanisms (scheme 4.9, paths I and II). Meanwhile, demethylation of guaiacol to catechol and subsequent ring hydrogenation, ring opening-closing and decarbonylation reactions of catechol were proceeded to produce cyclopentanone which was partly hydrogenated to cyclopentanol (paths III, IV and V). Since catechol was not detected in product sample, it could be considered as an intermediate compound which is completely converted during the reaction. In comparison with Pt/C, Pd/C led to the enhanced selectivities of cyclopentanone and cyclopentanol. Also, 1,2-cyclohexanediol formation from ring hydrogenation of catechol (path IV) was observed over Pd/C when H_2 gas was used. On the other hand, over Pt/C and when decalin and tetralin were used as hydrogen source, an enhanced hydrogenation of cycloketones of cyclopentanone and cyclohexanone was observed particularly in cyclohexanone hydrogenation to cyclohexanol. This could be due to the synergistic interaction between Pt/C and hydrogen donors which facilitates the accessibility of hydrogen atoms for hydrogenation reactions. Moreover, the mechanisms of guaiacol dehydroxylation to anisole (path VI), further hydrogenation of benzene ring

of anisole to methoxycyclohexane (path VII) and ring hydrogenation of catechol to 1,2-cyclohexanediol (path IV) occurred over Pt/C in presence of H-donors. Over Pd/C, the hydrogen atoms provided by decalin were involved in production of phenol, cyclohexanone and cyclohexanol. In addition, hydrogenation of benzene ring of guaiacol to 2-methoxycyclohexanone (path VIII) was only observed on Pd/C catalyst. In guaiacol transformation over Pt/C and Pd/C catalysts, use of decalin or tetralin as hydrogen donor resulted in similar type of reaction mechanisms and products, but product selectivities were different (Table 4.18).

Table 4.18: Product selectivity obtained from hydrogenation/transfer hydrogenation of guaiacol over Pt/C and Pd/C catalysts.

Hydrogen source	**H_2 gas**		**Decalin**		**Tetralin**	
Catalyst	**Pt/C**	**Pd/C**	**Pt/C**	**Pd/C**	**Pt/C**	**Pd/C**
Guaiacol conversion (mol%)						
	100	80.04	95.15	49.80	62.00	15.62
Product selectivity (mol%)						
Cyclopentanone	4.47	10.03	3.32		3.70	
Cyclopentanol	0.56	3.83	1.87		0.83	
Phenol	44.43	2.03	7.86	60.21	12.79	85.20
Cyclohexanone	25.31	63.28	19.57	25.08	20.86	13.77
Cyclohexanol	25.51	5.83	63.73	13.93	38.55	0.76
Anisole		0.18	0.68		0.96	
2-Methoxycyclohexanone				0.78		0.26
Methoxycyclohexane			0.15		0.25	
1,2-Cyclohexanediol		14.80	3.50		22.05	

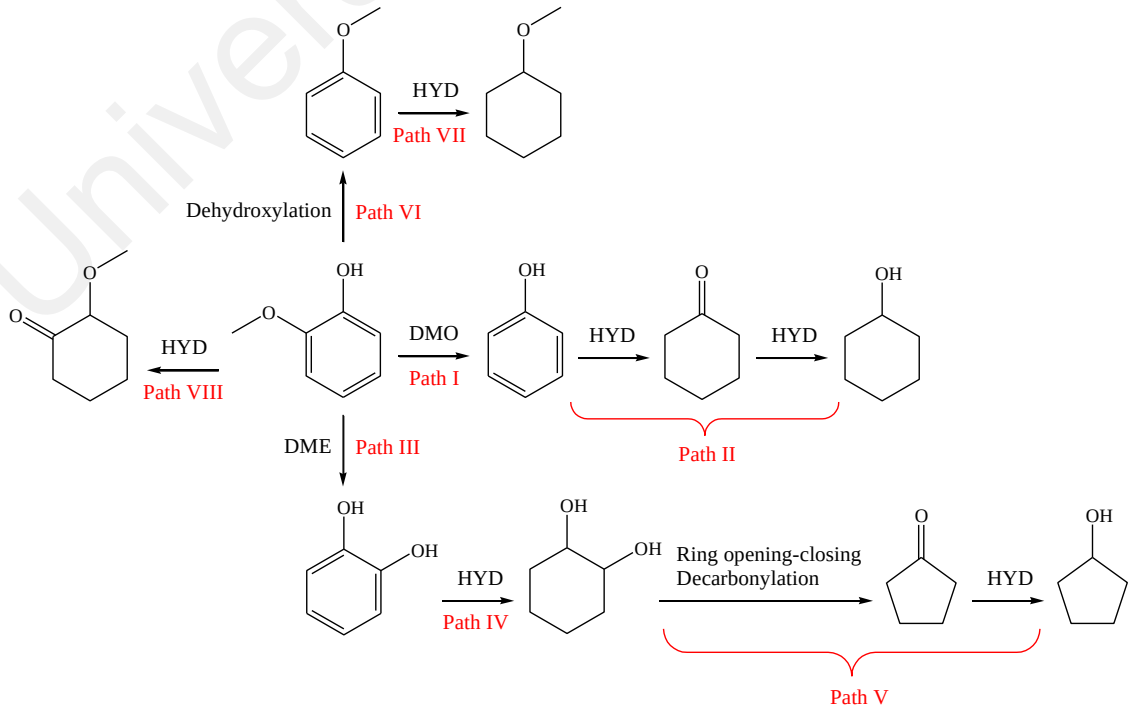

Scheme 4.9: Reaction mechanism of guaiacol hydrogenation over Pt/C and Pd/C using H_2 gas, decalin and tetralin as hydrogen source; DMO: demethoxylation, HYD: hydrogenation, DME: demethylation.

The exact mechanism of transfer hydrogenation of phenolics by decalin and tetralin is still unclear. Two reaction pathways could be proposed for transfer hydrogenation of the phenolics: (i) abstraction of the hydrogen atoms of the H-donors by activated acceptors, (ii) formation of dihydrogen which can be activated on metal catalysts and be involved in hydrogenation of the acceptors. By the use of H-donor compounds instead of hydrogen gas for hydrogenation of phenol, *o*-cresol and guaiacol, both the mechanisms of H-donor dehydrogenation and phenol/*o*-cresol/guaiacol hydrogenation competitively occurred on metal active sites of catalyst. Therefore, the two reactions are affected by each other probably decreasing the overall reaction activity. Dehydrogenation of decalin and tetralin could be decelerated by the adsorption of phenolic compounds on catalyst active sites leading to decrease of transfer hydrogenation activity. On the other hand, the transfer of activated hydrogen from metal catalyst to phenol, *o*-cresol and guaiacol could be hindered by the adsorption of hydrogen donor molecules on active sites. The intensity of these effects depends on reaction conditions particularly catalyst type. Data analysis of this study showed that use of hydrogen donor compounds remarkably decreased catalytic conversion of phenol, *o*-cresol and guaiacol over Pd/C catalyst. However, catalytic conversion of the phenolic compounds over Pt/C catalyst was considerable in the presence of decalin and tetralin; phenol conversion of 100 and 85.40 mol%, *o*-cresol conversion of 88.05 and 61.12 mol% as well as guaiacol conversion of 95.15 and 62 mol% were achieved in transfer hydrogenation using decalin and tetralin, respectively.

4.3.4 Kinetic study of hydrogenation/transfer hydrogenation of phenol, *o*-cresol and guaiacol over Pt/C catalyst

Kinetic study of hydrogenation/transfer hydrogenation of phenol, *o*-cresol and guaiacol was conducted using Pt/C catalyst and different hydrogen sources. The effects of

hydrogen sources on hydrogenation rate of phenolic compounds are depicted in Figs. 4.11a-4.13a. The comparison between these figures demonstrates that lower conversion of phenolics was achieved when H-donors were used as hydrogen source; the competitive adsorption of phenolics and H-donors on catalyst active sites causes lower conversion. As it was mentioned in previous section, cyclohexanone and cyclohexanol were the only compounds produced from hydrogenation/transfer hydrogenation of phenol. As shown in Figure 4.11b, at reaction times below 2.5 h, selectivity of cyclohexanone in the presence of H-donors was higher than that in the presence of H_2 gas since the amount of hydrogen released from donors is limited leading to low hydrogenation efficiency. However, at reaction times higher than 2.5 h, H_2 gas resulted in lower hydrogenation efficiency compared to H-donors due to consumption of initially charged hydrogen and reduction in the amount of available hydrogen. Lower selectivity towards cyclohexanone in presence of decalin indicates that the rate of cyclohexanone hydrogenation to cyclohexanol is higher in presence of decalin compared to tetralin. By increase of reaction time (0.5 to 4 h), the selectivity towards cyclohexanone was decreased indicating that higher reaction time results in higher cyclohexanone hydrogenation. In hydrogenation/transfer hydrogenation of *o*-cresol, methylcyclohexanone selectivity was decreased by increase of reaction time due to conversion of methylcyclohexanone to methylcyclohexanol (Figure 4.12b). In hydrogenation/transfer hydrogenation of guaiacol, cyclohexanone selectivity was increased by increase of reaction time upto a peak time which was 3 and 2.5 h for H_2 gas/tetralin and decalin, respectively (Figure 4.13b). Further increase of reaction time decreased cyclohexanone selectivity and increased cyclohexanol selectivity. Before peak time, the rate of cyclohexanone formation is higher than the rate of its conversion to cyclohexanol, and after peak time, the rate of cyclohexanone consumption for cyclohexanol formation is higher than the rate of cyclohexanone formation.

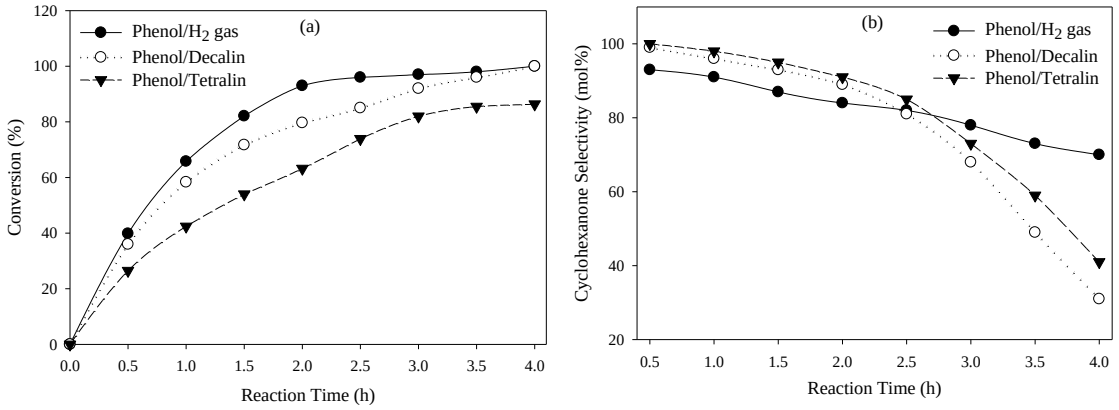

Figure 4.11: Catalytic conversion (a) and cyclohexanone selectivity (b) in hydrogenation/transfer hydrogenation of phenol over Pt/C catalyst.

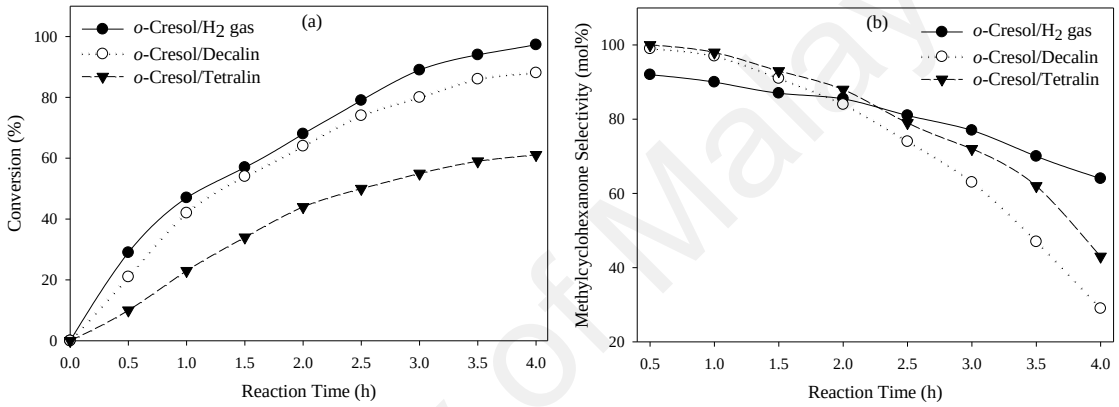

Figure 4.12: Catalytic conversion (a) and methylcyclohexanone selectivity (b) in hydrogenation/transfer hydrogenation of *o*-cresol over Pt/C catalyst.

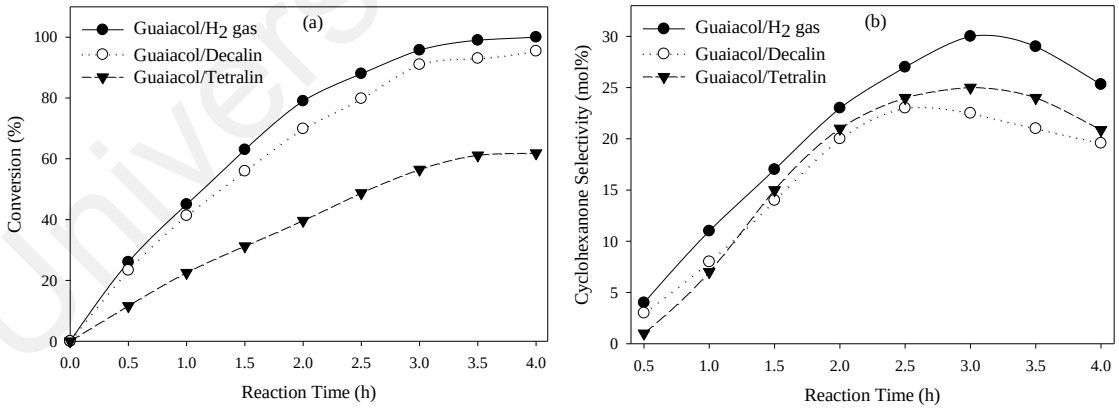

Figure 4.13: Catalytic conversion (a) and cyclohexanone selectivity (b) in hydrogenation/transfer hydrogenation of guaiacol over Pt/C catalyst.

4.3.5 Role of water solvent in transfer hydrogenation of phenol using decalin and tetralin over Pt/C catalyst

The influence of water solvent on transfer hydrogenation of phenol over Pt/C catalyst was studied by employing the water to donor ratios of 0/100, 25/75, 50/50 and 75/25 g/g with total weight of 100 g. It was observed that the addition of non-donor solvent of water to H-donors of decalin and tetralin could cause higher phenol conversion (Table 4.19). As mentioned before, high interaction between donor and Pt active sites could be a cause for prevention of interaction between phenol molecules and catalytic active sites leading to lower hydrogenation efficiency. The addition of water solvent to H-donor improved the hydrogenation efficiency of the system due to the decrease of interaction between donor and Pt active sites and increase of the chance of phenol molecules to reach the active sites. When water was used as solvent, the rate of transfer hydrogenation of phenol was enhanced and maximum conversion of phenol was achieved at water/donor ratio of 50/50 g/g. Further increase of water content or decrease of H-donor content (water to donor ratio of 75/25 g/g) caused a reduction in phenol conversion and hydrogenation efficiency. In fact, low content of H-donor results in low amount of hydrogen required for hydrogenation reaction.

Table 4.19: Impact of water content on catalytic activity of Pt/C in transfer hydrogenation of phenol. Reaction conditions: Pt/C, 0.6 g; phenol, 12 g; total weight of water and decalin/tetralin, 100 g; temperature, 275 °C; reaction time, 4 h and rpm, 500.

Water/H-donor (g/g)	H-donor conversion (mol%)	Phenol conversion (mol%)	Cyclohexanone selectivity (mol%)	Cyclohexanol selectivity (mol%)
H-donor: decalin				
0/100	77.60	27.80	68.14	31.86
25/75	62.00	67.23	41.00	59.00
50/50	56.27	100.00	30.95	69.05
75/25	40.22	42.00	31.90	68.10
H-donor: tetralin				
0/100	95.45	10.10	71.90	28.10
25/75	83.30	46.30	48.89	51.11
50/50	80.98	85.40	38.78	61.22
75/25	71.10	34.00	38.90	61.10

4.3.6 Transfer hydrogenation of simulated bio-oil consisting of phenol, *o*-cresol and guaiacol

Mixture of phenol (70 wt%), *o*-cresol (15 wt%) and guaiacol (15 wt%) was used as simulated bio-oil in order to study the feasibility of using decalin and tetralin as hydrogen source for hydrogenation of phenolic bio-oil. Product distribution obtained from transfer hydrogenation of simulated bio-oil using decalin and tetralin over Pd/C and Pt/C is compared with that obtained using H_2 gas (Table 4.20). High selectivities of phenol, *o*-cresol and guaiacol over Pd/C compared to Pt/C indicate that Pt/C is more efficient than Pd/C for bio-oil transformation through transfer hydrogenation mechanism. These results are in agreement with those obtained from transfer hydrogenation of phenol, *o*-cresol and guaiacol which were discussed in the section 4.3.3. By the use of H_2 gas, cyclohexanone was the dominant product achieved in bio-oil hydrogenation over both catalysts. Using decalin and tetralin as hydrogen source over Pt/C, cyclohexanol was the main product indicating higher performance of Pt/C in conversion of cyclohexanone to cyclohexanol through transfer hydrogenation compared to hydrogenation mechanism. Maximum cyclohexanol production was achieved over Pt/C using decalin as H-donor. However over Pd/C, cyclohexanone had the highest selectivity using each of hydrogen sources. The data presented in Table 4.20 reveal that tetralin leads to lower hydrogenation efficiency compared to decalin. In comparison to decalin with two saturated cycle, the aromatic cycle in tetralin structure causes high tendency for adsorption on catalytic active sites leading probably to non-appropriate rates of hydrogen release from tetralin and hydrogen consumption by oxygenates. Since the hydrogenation of acceptor molecule is proceeded by the hydrogen liberated from H-donor molecule, a synergistic rate between hydrogen release and hydrogen consumption is needed. Higher rate of hydrogen liberation compared to hydrogen consumption leads to inefficient consumption of released hydrogen while a fraction of generated hydrogen is not involved in hydrogenation

reaction. On the other hand, too slow rate of hydrogen release by H-donor in comparison with hydrogen consumption by acceptor could result in decrease of hydrogenation of acceptor molecule due to the polymerization of acceptor prior to its hydrogenation on catalytic active sites. In summary, the study of transfer hydrogenation of simulated bio-oil over Pd/C and Pt/C using decalin and tetralin as hydrogen source clearly showed that decalin and tetralin could be considered as suitable alternatives for hydrogen gas in bio-oil hydrogenation.

Table 4.20: Product selectivity obtained from hydrogenation/transfer hydrogenation of bio-oil over Pd/C and Pt/C catalysts. Reaction conditions: simulated bio-oil, 12 g; catalyst, 0.6 g; water, 50 g; H-donor, 50 g; temperature, 275 °C; reaction time, 4 h and rpm, 500.

Hydrogen source	**H_2 gas**		**Decalin**		**Tetralin**	
Catalyst	**Pt/C**	**Pd/C**	**Pt/C**	**Pd/C**	**Pt/C**	**Pd/C**
Selectivity in organic liquid (mol%)						
Phenol	2.90	11.71		13.61	8.81	24.38
Cresol		2.02		4.68	2.96	3.50
Guaiacol				4.09	1.46	2.21
Cyclohexanone	56.80	70.04	29.03	63.41	38.31	62.11
Cyclohexanol	32.52	9.64	61.69	8.46	45.77	4.91
Cyclopentanone	0.39	1.93	1.71	0.78	0.38	
Cyclopentanol	0.89	0.55	0.26	0.34	0.10	
Anisole		0.50	0.11	0.37	0.11	0.28
Methoxycyclohexanone				1.22		0.71
Methoxycyclohexane			0.87		0.02	
1,2-Cyclohexanediol	0.10	1.10	2.40	2.85	1.60	0.79
Methylcyclohexanone	1.37	0.69	0.54	0.09	0.06	1.06
Methylcyclohexanol	1.08		2.94		0.13	
Toluene	2.63	1.02				
Catechol			0.40	0.10	0.33	0.05
Methylcatechol			0.05			
Other hydrocarbons	1.32	0.80				

CHAPTER 5: CONCLUSIONS AND RECOMMENDATIONS FOR FUTURE STUDIES

5.1 Conclusions

5.1.1 Effective parameters on selective catalytic hydrodeoxygenation of phenolic compounds of pyrolysis bio-oil to high-value hydrocarbons

Several researches have been done in order to explore efficient catalytic systems for selective hydrodeoxygenation of bio-oil phenolic compounds to high-value hydrocarbons. Phenols are highly stable in HDO reaction and their oxygen removal is difficult due to the strong bond between $C_{aromatic}$ and O. HDO reaction could be proceeded through different pathways leading to the formation of different products. Selective hydrodeoxygenation of phenols to valuable hydrocarbons is a strong function of catalyst properties and operating conditions. The effects of promoters, support materials, catalyst preparation method, operating conditions, solvent and co-feeding on catalytic performance and reaction selectivity of HDO of phenol, cresol, guaiacol and anisole have been reviewed in this work. Generally, multifunctional catalysts are more suitable than monofunctional catalysts in HDO of phenols. Metals applied in HDO process should have high potential for activating both oxygenates and hydrogen molecules. Selection of metals which are in good interaction with each other can improve the dispersion of active sites in catalyst and prevent their agglomeration. From this review, it is inferred that metal promoters like Mo, Ni, Co, La and Cu as well as non-metal promoter of phosphorus increase the selectivity towards oxygen-free products in HDO of phenol, guaiacol and anisole. Use of an appropriate support could enhance the interaction between reactants and catalyst surface and reduce coke formation. A support with high surface area like activated carbon can cause more active functional groups on catalyst surface and better dispersion of metal active sites leading to enhanced catalytic activity. Although acidic

supports such as alumina and zeolites can improve HDO rate, but the high coke formation caused by these supports reduces catalyst lifetime. Method of catalyst preparation is influential on catalytic performance and reaction selectivity by affecting catalyst properties such as active metal dispersion, particle size and morphology. Since hydrodeoxygenation and hydrogen adsorption are exothermic reactions, reaction temperature is needed to be optimized in order not to restrict these reactions. Besides, high hydrogen pressure is required to improve the efficiency of HDO process. The solvent selected for HDO of phenols should improve the miscibility of both oxygenates and hydrogen and eliminate mass transfer limitations in order to increase diffusion rate of reactants in catalyst.

5.1.2 Catalytic hydrogenation of phenol, cresol and guaiacol over physically mixed catalysts of Pd/C and zeolite solid acids

The influence of density and strength of acid sites on transformation of different phenolic reactants was studied in a physically mixed catalyst system. In hydrogenation of phenol, *o*-cresol, *m*-cresol and guaiacol, the combination of 10 wt% Pd/C catalyst with HZSM-5 (Si/Al of 30, 50 and 80) or HY (Si/Al of 30 and 60) zeolites resulted in enhanced catalytic activity compared to the use of Pd/C alone. Zeolites containing strong acid sites showed better catalytic performance for transformation of phenol, *o*-cresol, *m*-cresol and guaiacol. Zeolite solid acids led mostly to the reactions of alkylation, dealkylation and dehydration of cyclic alcohols. In phenol hydrogenation over the combined catalysts, Brønsted acid sites were mainly involved in dehydration of cyclohexanol to form cyclohexane as an oxygen-free product. Hydrogenation reaction selectivity of phenol molecules containing methyl (*o*-cresol and *m*-cresol) or methoxy (guaiacol) groups is entirely different from that of the simple phenol molecule. As can be concluded from the data obtained in this work, the presence of methyl and methoxy groups in cresol and

guaiacol structures favors direct hydrodeoxygenation mechanism in the hydrogenation reaction. Meanwhile, the position of methyl group and spatial structure of cresol molecules affects the product selectivity of hydrogenation reaction. In conversion of *o*-cresol, selectivity towards toluene was enhanced by the use of mixed catalysts, while in *m*-cresol hydrogenation, zeolites led to dealkylation and phenol production and decrease of hydrodeoxygenation. The presence of methoxy group in guaiacol structure resulted in dehydroxylation reaction and anisole production. Demethoxylation was the dominant reaction mechanism in guaiacol transformation over the combined catalysts.

5.1.3 Catalytic hydrodeoxygenation of simulated phenolic bio-oil to cycloalkanes and aromatic hydrocarbons over bifunctional metal/acid catalysts of Ni/HBeta, Fe/HBeta and NiFe/HBeta

In this study, HDO of a simulated phenolic bio-oil consisting of phenol (50 wt%), *o*-cresol (25 wt%) and guaiacol (25 wt%) was carried out over bifunctional metal/acid catalysts of Ni/HBeta, Fe/HBeta, NiFe-5/HBeta and NiFe-10/HBeta. Bimetallic catalyst of NiFe/HBeta showed higher HDO activity compared to monometallic catalysts of Ni/HBeta and Fe/HBeta due to the synergistic effect between Ni and Fe; the selectivities towards oxygen-free products over Ni/HBeta, Fe/HBeta, NiFe-5/HBeta and NiFe-10/HBeta were 32.19, 23.82, 36.20 and 53.59 wt%, respectively. Cycloalkanes (21.39 wt%) and aromatic hydrocarbons (20.21 wt%) were the dominant hydrocarbons produced over monometallic catalysts of Ni/HBeta and Fe/HBeta, respectively. Bimetallic catalyst of NiFe/HBeta was shown to be an efficient catalyst for transformation of phenolic compounds to oxygen-free products through both hydrogenolysis and hydrogenation reactions. Analysis of coke deposited on spent catalysts indicated that NiFe-10/HBeta and Fe/HBeta resulted in higher coke formation compared to Ni/HBeta and NiFe-5/HBeta due to higher strength of acidity and higher selectivities towards aromatic hydrocarbons and

catechol. Reusability test of NiFe-10/HBeta for HDO of the simulated bio-oil showed slight reduction in catalytic activity during the first two recycled runs. However, further recycling of NiFe-10/HBeta led to considerable catalyst deactivation due to leaching of metal sites from catalyst structure and change of catalyst textural properties. Meanwhile, temperature dependence study of the simulated bio-oil HDO over NiFe-10/HBeta showed that catalytic activity and hydrocarbons selectivity were increased by rise of reaction temperature from 220 to 300 °C. However, further increase of reaction temperature to 340 °C had negative effect on catalytic performance of NiFe-10/HBeta due to the low availability of activated hydrogen and higher coke formation. Furthermore, it was revealed in this work that deoxygenation efficiency of NiFe-10/HBeta catalyst was remarkably reduced by replacing water with methanol as solvent. The common pathway of phenol HDO (phenol → cyclohexanone → cyclohexanol → cyclohexane) was suppressed by the use of methanol; methanol was involved in acetal reaction with cyclohexanone intermediate to produce methoxylated compounds. It could be inferred from this study that bimetallic catalysts with synergistic effect between the metals could be effective for enhanced HDO of the phenolic compounds present in bio-oil.

5.1.4 Using decalin and tetralin as hydrogen source for transfer hydrogenation of renewable lignin-derived phenolics over activated carbon supported Pd and Pt catalysts

In this study, decalin and tetralin were used as liquid hydrogen source for hydrogenation of renewable lignin-derived phenolic compounds (phenol, *o*-cresol and guaiacol) and a simulated phenolic bio-oil over activated carbon supported Pd and Pt catalysts. The results obtained in this work clearly indicate that in comparison with Pd/C, Pt/C has more efficient catalytic performance for transfer hydrogenation of the phenolic compounds using decalin or tetralin as hydrogen source. Two competing reactions of

dehydrogenation of H-donor and hydrogenation of phenolics concurrently occurred on metal active sites of catalysts. Competitive adsorption of H-donor and acceptor compounds on catalyst active sites could result in reduced conversion of phenolic compounds. The conversions of phenol, *o*-cresol and guaiacol were lower in the presence of tetralin compared to the case of using decalin as H-donor. The presence of benzene ring in tetralin molecule enhances tetralin adsorption on catalytic active sites leading to the decrease in adsorption of phenolic compounds. Conversions of phenol, *o*-cresol and guaiacol over Pt/C using decalin as hydrogen source were almost as high as those achieved by use of hydrogen gas. Using non-donor solvent of water in transfer hydrogenation of phenol led to the enhanced hydrogenation efficiency due to the decrease of interaction between catalyst active phases and H-donors, and the increase of interaction between phenol and catalytic sites. The highest hydrogenation activity was observed at the water to donor ratio of 50/50 g/g.

5.2 Recommendations for future studies

Considering the fact that HDO could be proceeded through a variety of reaction pathways which result in formation of different products, further researches are needed in order to develop efficient catalysts and to optimize reaction conditions for selective hydrodeoxygenation of phenolic compounds to high-value hydrocarbons. The following recommendations are suggested for further research on catalytic transformation of phenolic model compounds of bio-oil to high-value chemicals through hydrogenation:

- Exploration of functionality of different metals for selective conversion of phenolic compounds into hydrocarbons of aromatics and alicyclics through hydrogenolysis and hydrogenation reactions, respectively.
- Optimization of ratio of metal to acid sites in bifunctional metal/acid catalysts.

- Use of pore- and acid-modified activated carbon as catalyst support; supports with mild acidity and mesopore structure could improve HDO efficiency.
- Study of the effect of solvent type on synergistic rates of hydrogen release from H-donor and hydrogen consumption by acceptor in transfer hydrogenation of phenolic model compounds of bio-oil.

REFERENCES

Afifi, A. I., Chornet, E., Thring, R. W., & Overend, R. P. (1996). The aryl ether bond reactions with H-donor solvents: guaiacol and tetralin in the presence of catalysts. *Fuel, 75*(4), 509-516. doi: http://dx.doi.org/10.1016/0016-2361(95)00199-9

Albers, P., Pietsch, J., & Parker, S. F. (2001). Poisoning and deactivation of palladium catalysts. *Journal of Molecular Catalysis A: Chemical, 173*(1–2), 275-286. doi: http://dx.doi.org/10.1016/S1381-1169(01)00154-6

Angelos, S., Johansson, E., Stoddart, J. F., & Zink, J. I. (2007). Mesostructured silica supports for functional materials and molecular machines. *Advanced Functional Materials, 17*(14), 2261-2271. doi: 10.1002/adfm.200601217

Ardiyanti, A. R., Khromova, S. A., Venderbosch, R. H., Yakovlev, V. A., & Heeres, H. J. (2012). Catalytic hydrotreatment of fast-pyrolysis oil using non-sulfided bimetallic Ni-Cu catalysts on a δ-Al_2O_3 support. *Applied Catalysis B: Environmental, 117-118*, 105-117. doi: 10.1016/j.apcatb.2011.12.032

Ausavasukhi, A., Huang, Y., To, A. T., Sooknoi, T., & Resasco, D. E. (2012). Hydrodeoxygenation of *m*-cresol over gallium-modified beta zeolite catalysts. *Journal of Catalysis, 290*, 90-100. doi: 10.1016/j.jcat.2012.03.003

Ausavasukhi, A., Sooknoi, T., & Resasco, D. E. (2009). Catalytic deoxygenation of benzaldehyde over gallium-modified ZSM-5 zeolite. *Journal of Catalysis, 268*(1), 68-78. doi: 10.1016/j.jcat.2009.09.002

Badawi, M., Paul, J. F., Cristol, S., Payen, E., Romero, Y., Richard, F., Brunet, S., Lambert, D., Portier, X., Popov, A., Kondratieva, E., Goupil, J. M., Fallah, J. E., Gilson, J. P., Mariey, L., Travert, A., & Maugé, F. (2011). Effect of water on the stability of Mo and CoMo hydrodeoxygenation catalysts: A combined experimental and DFT study. *Journal of Catalysis, 282*(1), 155-164. doi: 10.1016/j.jcat.2011.06.006

Baraniec-Mazurek, I., & Mianowski, A. (2010). Liquid fuel from waste polyolefins part I: Thermal and pressure degradation of waste polyolefins in tetralin as H-donor model system. *Chemical Engineering Journal, 163*(3), 284-292. doi: 10.1016/j.cej.2010.07.066

Biniwale, R. B., Kariya, N., & Ichikawa, M. (2005). Dehydrogenation of cyclohexane over Ni based catalysts supported on activated carbon using spray-pulsed reactor and enhancement in activity by addition of a small amount of Pt. *Catalysis Letters, 105*(1-2), 83-87. doi: 10.1007/s10562-005-8009-x

Bowker, R. H., Smith, M. C., Pease, M. L., Slenkamp, K. M., Kovarik, L., & Bussell, M. E. (2011). Synthesis and hydrodeoxygenation properties of ruthenium phosphide catalysts. *ACS Catalysis, 1*(8), 917-922. doi: 10.1021/cs200238v

Bredenberg, J. B. s., Huuska, M., & Toropainen, P. (1989). Hydrogenolysis of differently substituted methoxyphenols. *Journal of Catalysis, 120*(2), 401-408. doi: http://dx.doi.org/10.1016/0021-9517(89)90279-0

Brieger, G., & Nestrick, T. J. (1974). Catalytic transfer hydrogenation. *Chemical Reviews, 74*(5), 567-580. doi: 10.1021/cr60291a003

Bui, V. N., Laurenti, D., Afanasiev, P., & Geantet, C. (2011). Hydrodeoxygenation of guaiacol with CoMo catalysts. Part I: Promoting effect of cobalt on HDO selectivity and activity. *Applied Catalysis B: Environmental, 101*(3-4), 239-245. doi: 10.1016/j.apcatb.2010.10.025

Bui, V. N., Laurenti, D., Delichère, P., & Geantet, C. (2011). Hydrodeoxygenation of guaiacol. *Applied Catalysis B: Environmental, 101*(3-4), 246-255. doi: 10.1016/j.apcatb.2010.10.031

Bui, V. N., Toussaint, G., Laurenti, D., Mirodatos, C., & Geantet, C. (2009). Co-processing of pyrolisis bio oils and gas oil for new generation of bio-fuels: Hydrodeoxygenation of guaïacol and SRGO mixed feed. *Catalysis Today, 143*(1-2), 172-178. doi: 10.1016/j.cattod.2008.11.024

Busetto, L., Fabbri, D., Mazzoni, R., Salmi, M., Torri, C., & Zanotti, V. (2011). Application of the Shvo catalyst in homogeneous hydrogenation of bio-oil obtained from pyrolysis of white poplar: New mild upgrading conditions. *Fuel, 90*(3), 1197-1207. doi: 10.1016/j.fuel.2010.10.036

Bykova, M. V., Bulavchenko, O. A., Ermakov, D. Y., Lebedev, M. Y., Yakovlev, V. A., & Parmon, V. N. (2011). Guaiacol hydrodeoxygenation in the presence of Ni-containing catalysts. *Catalysis in Industry, 3*(1), 15-22. doi: 10.1134/s2070050411010028

Bykova, M. V., Ermakov, D. Y., Kaichev, V. V., Bulavchenko, O. A., Saraev, A. A., Lebedev, M. Y., & Yakovlev, V. A. (2012). Ni-based sol–gel catalysts as promising systems for crude bio-oil upgrading: Guaiacol hydrodeoxygenation study. *Applied Catalysis B: Environmental, 113-114*, 296-307. doi: 10.1016/j.apcatb.2011.11.051

Bykova, M. V., Ermakov, D. Y., Khromova, S. A., Smirnov, A. A., Lebedev, M. Y., & Yakovlev, V. A. (2014). Stabilized Ni-based catalysts for bio-oil hydrotreatment: Reactivity studies using guaiacol. *Catalysis Today, 220-222*, 21-31. doi: 10.1016/j.cattod.2013.10.023

Centeno, A., Laurent, E., & Delmon, B. (1995). Influence of the support of CoMo sulfide catalysts and of the addition of potassium and platinum on the catalytic performances for the hydrodeoxygenation of carbonyl, carboxyl, and guaiacol-type molecules. *Journal of Catalysis, 154*(2), 288-298. doi: http://dx.doi.org/10.1006/jcat.1995.1170

Chen, C., Chen, G., Yang, F., Wang, H., Han, J., Ge, Q., & Zhu, X. (2015). Vapor phase hydrodeoxygenation and hydrogenation of *m*-cresol on silica supported Ni, Pd and Pt catalysts. *Chemical Engineering Science, 135*, 145-154. doi: 10.1016/j.ces.2015.04.054

Chen, J., Sun, L., Wang, R., & Zhang, J. (2009). Hydrodechlorination of chlorobenzene over Ni_2P/SiO_2 catalysts: Influence of Ni_2P loading. *Catalysis Letters, 133*(3-4), 346-353. doi: 10.1007/s10562-009-0191-9

Cheng, H., Liu, R., Wang, Q., Wu, C., Yu, Y., & Zhao, F. (2012). Selective reduction of phenol derivatives to cyclohexanones in water under microwave irradiation. *New Journal of Chemistry, 36*(4), 1085-1090. doi: 10.1039/c2nj20990j

Cheng, R., Shu, Y., Li, L., Zheng, M., Wang, X., Wang, A., & Zhang, T. (2007). Synthesis and characterization of high surface area molybdenum phosphide. *Applied Catalysis A: General, 316*(2), 160-168. doi: 10.1016/j.apcata.2006.08.036

Cortez, N. A., Aguirre, G., Parra-Hake, M., & Somanathan, R. (2009). New heterogenized C_2-symmetric bis(sulfonamide)-cyclohexane-1,2-diamine-$Rh^{III}Cp^*$ complexes and their application in the asymmetric transfer hydrogenation (ATH) of ketones in water. *Tetrahedron Letters, 50*(19), 2228-2231. doi: 10.1016/j.tetlet.2009.02.183

Dayton, D. C., Pavani, M. S., Carpenter, J. R., & Von, H. M. (2014). Catalyst compositions and use thereof in catalytic biomass pyrolysis: Google Patents, EP2928594 A1.

de la Puente, G., Gil, A., Pis, J. J., & Grange, P. (1999). Effects of support surface chemistry in hydrodeoxygenation reactions over CoMo/activated carbon sulfided catalysts. *Langmuir, 15*(18), 5800-5806. doi: 10.1021/la981225e

De Miguel Mercader, F., Koehorst, P. J. J., Heeres, H. J., Kersten, S. R. A., & Hogendoorn, J. A. (2011). Competition between hydrotreating and polymerization reactions during pyrolysis oil hydrodeoxygenation. *AIChE Journal, 57*(11), 3160-3170. doi: 10.1002/aic.12503

Díaz, E., Mohedano, A. F., Calvo, L., Gilarranz, M. A., Casas, J. A., & Rodríguez, J. J. (2007). Hydrogenation of phenol in aqueous phase with palladium on activated carbon catalysts. *Chemical Engineering Journal, 131*(1-3), 65-71. doi: 10.1016/j.cej.2006.12.020

Dufour, A., Masson, E., Girods, P., Rogaume, Y., & Zoulalian, A. (2011). Evolution of aromatic tar composition in relation to methane and ethylene from biomass pyrolysis-gasification. *Energy & Fuels, 25*(9), 4182-4189. doi: 10.1021/ef200846g

Echeandia, S., Arias, P. L., Barrio, V. L., Pawelec, B., & Fierro, J. L. G. (2010). Synergy effect in the HDO of phenol over Ni–W catalysts supported on active carbon:

Effect of tungsten precursors. *Applied Catalysis B: Environmental, 101*(1-2), 1-12. doi: 10.1016/j.apcatb.2010.08.018

Echeandia, S., Pawelec, B., Barrio, V. L., Arias, P. L., Cambra, J. F., Loricera, C. V., & Fierro, J. L. G. (2014). Enhancement of phenol hydrodeoxygenation over Pd catalysts supported on mixed HY zeolite and Al_2O_3. An approach to O-removal from bio-oils. *Fuel, 117*, 1061-1073. doi: 10.1016/j.fuel.2013.10.011

Egsgaard, H., Ahrenfeldt, J., Ambus, P., Schaumburg, K., & Henriksen, U. B. (2014). Gas cleaning with hot char beds studied by stable isotopes. *Journal of Analytical and Applied Pyrolysis, 107*, 174-182. doi: 10.1016/j.jaap.2014.02.019

Eijsbouts, S., Heinerman, J. J. L., & Elzerman, H. J. W. (1993). MoS_2 structures in high-activity hydrotreating catalysts: I. Semi-quantitative method for evaluation of transmission electron microscopy results. Correlations between hydrodesulfurization and hydrodenitrogenation activities and MoS_2 dispersion. *Applied Catalysis A: General, 105*(1), 53-68. doi: http://dx.doi.org/10.1016/0926-860X(93)85133-A

Elie, M. R., Clausen, C. A., & Geiger, C. L. (2012). Reduction of benzo[*a*]pyrene with acid-activated magnesium metal in ethanol: a possible application for environmental remediation. *Journal of Hazardous Materials, 203-204*, 77-85. doi: 10.1016/j.jhazmat.2011.11.089

Elliott, D. C. (2007). Historical developments in hydroprocessing bio-oils. *Energy & Fuels, 21*(3), 1792-1815. doi: 10.1021/ef070044u

Elliott, D. C., & Hart, T. R. (2009). Catalytic hydroprocessing of chemical models for bio-oil. *Energy & Fuels, 23*(2), 631-637. doi: 10.1021/ef8007773

Farhadi, S., Kazem, M., & Siadatnasab, F. (2011). NiO nanoparticles prepared via thermal decomposition of the bis(dimethylglyoximato)nickel(II) complex: A novel reusable heterogeneous catalyst for fast and efficient microwave-assisted reduction of nitroarenes with ethanol. *Polyhedron, 30*(4), 606-613. doi: 10.1016/j.poly.2010.11.037

Ferrari, M., Maggi, R., Delmon, B., & Grange, P. (2001). Influences of the hydrogen sulfide partial pressure and of a nitrogen compound on the hydrodeoxygenation activity of a CoMo/carbon catalyst. *Journal of Catalysis, 198*(1), 47-55. doi: 10.1006/jcat.2000.3103

Filley, J., & Roth, C. (1999). Vanadium catalyzed guaiacol deoxygenation. *Journal of Molecular Catalysis A: Chemical, 139*(2–3), 245-252. doi: http://dx.doi.org/10.1016/S1381-1169(98)00202-7

Fisk, C. A., Morgan, T., Ji, Y., Crocker, M., Crofcheck, C., & Lewis, S. A. (2009). Bio-oil upgrading over platinum catalysts using in situ generated hydrogen. *Applied Catalysis A: General, 358*(2), 150-156. doi: 10.1016/j.apcata.2009.02.006

Forchheim, D., Hornung, U., Kempe, P., Kruse, A., & Steinbach, D. (2012). Influence of RANEY nickel on the formation of intermediates in the degradation of lignin. *International Journal of Chemical Engineering, 2012*, 1-8. doi: 10.1155/2012/589749

Foster, A. J., Do, P. T. M., & Lobo, R. F. (2012). The synergy of the support acid function and the metal function in the catalytic hydrodeoxygenation of *m*-cresol. *Topics in Catalysis, 55*(3-4), 118-128. doi: 10.1007/s11244-012-9781-7

Furimsky, E. (2000). Catalytic hydrodeoxygenation. *Applied Catalysis A: General, 199*(2), 147-190. doi: http://dx.doi.org/10.1016/S0926-860X(99)00555-4

Furimsky, E., & Massoth, F. E. (1999). Deactivation of hydroprocessing catalysts. *Catalysis Today, 52*(4), 381-495. doi: http://dx.doi.org/10.1016/S0920-5861(99)00096-6

Gao, D., Schweitzer, C., Hwang, H. T., & Varma, A. (2014). Conversion of guaiacol on noble metal catalysts: Reaction performance and deactivation studies. *Industrial & Engineering Chemistry Research, 53*(49), 18658-18667. doi: 10.1021/ie500495z

Gao, Y., Jaenicke, S., & Chuah, G.-K. (2014). Highly efficient transfer hydrogenation of aldehydes and ketones using potassium formate over AlO(OH)-entrapped ruthenium catalysts. *Applied Catalysis A: General, 484*, 51-58. doi: 10.1016/j.apcata.2014.07.010

Ghampson, I. T., Sepúlveda, C., Garcia, R., Frederick, B. G., Wheeler, M. C., Escalona, N., & DeSisto, W. J. (2012). Guaiacol transformation over unsupported molybdenum-based nitride catalysts. *Applied Catalysis A: General, 413-414*, 78-84. doi: 10.1016/j.apcata.2011.10.050

Ghampson, I. T., Sepúlveda, C., Garcia, R., Radovic, L. R., Fierro, J. L. G., DeSisto, W. J., & Escalona, N. (2012). Hydrodeoxygenation of guaiacol over carbon-supported molybdenum nitride catalysts: Effects of nitriding methods and support properties. *Applied Catalysis A: General, 439-440*, 111-124. doi: 10.1016/j.apcata.2012.06.047

Gland, J. L., Kollin, E. B., & Zaera, F. (1988). Adsorbed sulfhydryl (SH) on the molybdenum(100) surface. *Langmuir, 4*(1), 118-120. doi: 10.1021/la00079a020

González-Borja, M. A. n., & Resasco, D. E. (2011). Anisole and guaiacol hydrodeoxygenation over monolithic Pt–Sn catalysts. *Energy & Fuels, 25*(9), 4155-4162. doi: 10.1021/ef200728r

Graça, I., Lopes, J. M., Ribeiro, M. F., Ramôa Ribeiro, F., Cerqueira, H. S., & de Almeida, M. B. B. (2011). Catalytic cracking in the presence of guaiacol. *Applied Catalysis B: Environmental, 101*(3-4), 613-621. doi: 10.1016/j.apcatb.2010.11.002

Gualda, G., & Kasztelan, S. (1996). Initial deactivation of residue hydrodemetallization catalysts. *Journal of Catalysis, 161*(1), 319-337. doi: http://dx.doi.org/10.1006/jcat.1996.0190

Guehenneux, G., Baussand, P., Brothier, M., Poletiko, C., & Boissonnet, G. (2005). Energy production from biomass pyrolysis: A new coefficient of pyrolytic valorisation. *Fuel, 84*(6), 733-739. doi: 10.1016/j.fuel.2004.11.005

Gutierrez, A., Kaila, R. K., Honkela, M. L., Slioor, R., & Krause, A. O. I. (2009). Hydrodeoxygenation of guaiacol on noble metal catalysts. *Catalysis Today, 147*(3-4), 239-246. doi: 10.1016/j.cattod.2008.10.037

He, J., Zhao, C., & Lercher, J. A. (2014). Impact of solvent for individual steps of phenol hydrodeoxygenation with Pd/C and HZSM-5 as catalysts. *Journal of Catalysis, 309*, 362-375. doi: 10.1016/j.jcat.2013.09.009

Hensen, E. J. M., Kooyman, P. J., van der Meer, Y., van der Kraan, A. M., de Beer, V. H. J., van Veen, J. A. R., & van Santen, R. A. (2001). The relation between morphology and hydrotreating activity for supported MoS_2 particles. *Journal of Catalysis, 199*(2), 224-235. doi: 10.1006/jcat.2000.3158

Hensley, A. J. R., Hong, Y., Zhang, R., Zhang, H., Sun, J., Wang, Y., & McEwen, J.-S. (2014). Enhanced Fe_2O_3 reducibility via surface modification with Pd: Characterizing the synergy within Pd/Fe catalysts for hydrodeoxygenation reactions. *ACS Catalysis, 4*(10), 3381-3392. doi: 10.1021/cs500565e

Hensley, A. J. R., Wang, Y., & McEwen, J.-S. (2015). Phenol deoxygenation mechanisms on Fe(110) and Pd(111). *ACS Catalysis, 5*(2), 523-536. doi: 10.1021/cs501403w

Hong, D. Y., Miller, S. J., Agrawal, P. K., & Jones, C. W. (2010). Hydrodeoxygenation and coupling of aqueous phenolics over bifunctional zeolite-supported metal catalysts. *Chem Commun (Camb), 46*(7), 1038-1040. doi: 10.1039/b918209h

Hong, Y., Zhang, H., Sun, J., Ayman, K. M., Hensley, A. J. R., Gu, M., Engelhard, M. H., McEwen, J. S., & Wang, Y. (2014). Synergistic catalysis between Pd and Fe in gas phase hydrodeoxygenation of *m*-cresol. *ACS Catalysis, 4*(10), 3335-3345. doi: 10.1021/cs500578g

Hurff, S. J., & Klein, M. T. (1983). Reaction pathway analysis of thermal and catalytic lignin fragmentation by use of model compounds. *Industrial & Engineering Chemistry Fundamentals, 22*(4), 426-430. doi: 10.1021/i100012a012

Huuska, M. K. (1986). Effect of catalyst composition on the hydrogenolysis of anisole. *Polyhedron, 5*(1–2), 233-236. doi: http://dx.doi.org/10.1016/S0277-5387(00)84915-3

Ibáñez, M., Valle, B., Bilbao, J., Gayubo, A. G., & Castaño, P. (2012). Effect of operating conditions on the coke nature and HZSM-5 catalysts deactivation in the

transformation of crude bio-oil into hydrocarbons. *Catalysis Today, 195*(1), 106-113. doi: 10.1016/j.cattod.2012.04.030

Ikeshita, K.-i., Kihara, N., Sonoda, M., & Ogawa, A. (2007). Lewis acid-catalyzed reduction of dithioacetals by 1,4-cyclohexadiene. *Tetrahedron Letters, 48*(17), 3025-3028. doi: 10.1016/j.tetlet.2007.02.119

Indra, A., Maity, P., Bhaduri, S., & Lahiri, G. K. (2013). Chemoselective hydrogenation and transfer hydrogenation of olefins and carbonyls with the cluster-derived ruthenium nanocatalyst in water. *ChemCatChem, 5*(1), 322-330. doi: 10.1002/cctc.201200448

Iwata, Y., Sato, K., Yoneda, T., Miki, Y., Sugimoto, Y., Nishijima, A., & Shimada, H. (1998). Catalytic functionality of unsupported molybdenum sulfide catalysts prepared with different methods. *Catalysis Today, 45*(1–4), 353-359. doi: http://dx.doi.org/10.1016/S0920-5861(98)00262-4

Jae, J., Tompsett, G. A., Foster, A. J., Hammond, K. D., Auerbach, S. M., Lobo, R. F., & Huber, G. W. (2011). Investigation into the shape selectivity of zeolite catalysts for biomass conversion. *Journal of Catalysis, 279*(2), 257-268. doi: 10.1016/j.jcat.2011.01.019

Jin, F., & Li, Y. (2009). A FTIR and TPD examination of the distributive properties of acid sites on ZSM-5 zeolite with pyridine as a probe molecule. *Catalysis Today, 145*(1-2), 101-107. doi: 10.1016/j.cattod.2008.06.007

Jongerius, A. L., Jastrzebski, R., Bruijnincx, P. C. A., & Weckhuysen, B. M. (2012). CoMo sulfide-catalyzed hydrodeoxygenation of lignin model compounds: An extended reaction network for the conversion of monomeric and dimeric substrates. *Journal of Catalysis, 285*(1), 315-323. doi: 10.1016/j.jcat.2011.10.006

Joshi, N., & Lawal, A. (2012). Hydrodeoxygenation of pyrolysis oil in a microreactor. *Chemical Engineering Science, 74*, 1-8. doi: 10.1016/j.ces.2012.01.052

Katada, N., & Niwa, M. Analysis of acidic properties of zeolitic and non-zeolitic solid acid catalysts using temperature-programmed desorption of ammonia. *Catalysis Surveys from Asia, 8*(3), 161-170. doi: 10.1023/b:cats.0000038534.37849.16

Kim, J., Choi, M., & Ryoo, R. (2010). Effect of mesoporosity against the deactivation of MFI zeolite catalyst during the methanol-to-hydrocarbon conversion process. *Journal of Catalysis, 269*(1), 219-228. doi: 10.1016/j.jcat.2009.11.009

Kobayashi, H., Ohta, H., & Fukuoka, A. (2012). Conversion of lignocellulose into renewable chemicals by heterogeneous catalysis. *Catalysis Science & Technology, 2*(5), 869-883. doi: 10.1039/c2cy00500j

Koike, T., Murata, K., & Ikariya, T. (2000). Stereoselective synthesis of optically active α-hydroxy ketones andanti-1,2-diols via asymmetric transfer hydrogenation of

unsymmetrically substituted 1,2-diketones. *Organic Letters, 2*(24), 3833-3836. doi: 10.1021/ol0002572

Laurent, E., Centeno, A., & Delmon, B. (1994). Coke formation during the hydrotreating of biomass pyrolysis oils: influence of guaiacol type compounds. In B. Delmon & G. F. Froment (Eds.), *Studies in Surface Science and Catalysis* (Volume 88, pp. 573-578): Elsevier.

Laurent, E., & Delmon, B. (1993). Influence of oxygen-, nitrogen-, and sulfur-containing compounds on the hydrodeoxygenation of phenols over sulfided cobalt-molybdenum/.gamma.-alumina and nickel-molybdenum/.gamma.-alumina catalysts. *Industrial & Engineering Chemistry Research, 32*(11), 2516-2524. doi: 10.1021/ie00023a013

Laurent, E., & Delmon, B. (1994). Deactivation of a sulfided NiMo/γ-Al_2O_3 during the hydrodeoxygenation of bio-oils: Influence of a high water pressure. In B. Delmon & G. F. Froment (Eds.), *Studies in Surface Science and Catalysis* (Volume 88, pp. 459-466): Elsevier.

Lee, C. R., Yoon, J. S., Suh, Y.-W., Choi, J.-W., Ha, J.-M., Suh, D. J., & Park, Y.-K. (2012). Catalytic roles of metals and supports on hydrodeoxygenation of lignin monomer guaiacol. *Catalysis Communications, 17*, 54-58. doi: 10.1016/j.catcom.2011.10.011

Lee, J.-H., Lee, E.-G., Joo, O.-S., & Jung, K.-D. (2004). Stabilization of Ni/Al_2O_3 catalyst by Cu addition for CO_2 reforming of methane. *Applied Catalysis A: General, 269*(1-2), 1-6. doi: 10.1016/j.apcata.2004.01.035

Lee, W.-S., Kumar, A., Wang, Z., & Bhan, A. (2015). Chemical titration and transient kinetic studies of site requirements in Mo_2C-catalyzed vapor phase anisole hydrodeoxygenation. *ACS Catalysis, 5*(7), 4104-4114. doi: 10.1021/acscatal.5b00713

Li, K., Wang, R., & Chen, J. (2011). Hydrodeoxygenation of anisole over silica-supported Ni_2P, MoP, and NiMoP catalysts. *Energy & Fuels, 25*(3), 854-863. doi: 10.1021/ef101258j

Li, Y., Xu, X., Zhang, P., Gong, Y., Li, H., & Wang, Y. (2013). Highly selective Pd@mpg-C_3N_4 catalyst for phenol hydrogenation in aqueous phase. *RSC Advances, 3*(27), 10973-10982. doi: 10.1039/c3ra41397g

Li, Y., Zhang, C., Liu, Y., Hou, X., Zhang, R., & Tang, X. (2015). Coke deposition on Ni/HZSM-5 in bio-oil hydrodeoxygenation processing. *Energy & Fuels, 29*(3), 1722-1728. doi: 10.1021/ef5024669

Lin, Y.-C., Li, C.-L., Wan, H.-P., Lee, H.-T., & Liu, C.-F. (2011). Catalytic hydrodeoxygenation of guaiacol on Rh-based and sulfided CoMo and NiMo catalysts. *Energy & Fuels, 25*(3), 890-896. doi: 10.1021/ef101521z

Liu, H., Jiang, T., Han, B., Liang, S., & Zhou, Y. (2009). Selective phenol hydrogenation to cyclohexanone over a dual supported Pd-Lewis acid catalyst. *Science, 326*(5957), 1250-1252. doi: 10.1126/science.1179713

Liu, R., Wang, Y., Cheng, H., Yu, Y., Zhao, F., & Arai, M. (2013). Reduction of citral in water under typical transfer hydrogenation conditions—Reaction mechanisms with evolution of and hydrogenation by molecular hydrogen. *Journal of Molecular Catalysis A: Chemical, 366*, 315-320. doi: 10.1016/j.molcata.2012.10.010

Loricera, C. V., Pawelec, B., Infantes-Molina, A., Álvarez-Galván, M. C., Huirache-Acuña, R., Nava, R., & Fierro, J. L. G. (2011). Hydrogenolysis of anisole over mesoporous sulfided CoMoW/SBA-15(16) catalysts. *Catalysis Today, 172*(1), 103-110. doi: 10.1016/j.cattod.2011.02.037

Mahfud, F. H., Ghijsen, F., & Heeres, H. J. (2007). Hydrogenation of fast pyrolyis oil and model compounds in a two-phase aqueous organic system using homogeneous ruthenium catalysts. *Journal of Molecular Catalysis A: Chemical, 264*(1-2), 227-236. doi: 10.1016/j.molcata.2006.09.022

Massoth, F. E., Politzer, P., Concha, M. C., Murray, J. S., Jakowski, J., & Simons, J. (2006). Catalytic hydrodeoxygenation of methyl-substituted phenols: Correlations of kinetic parameters with molecular properties. *The Journal of Physical Chemistry B, 110*(29), 14283-14291. doi: 10.1021/jp057332g

McVicker, G. (2002). Selective ring opening of naphthenic molecules. *Journal of Catalysis, 210*(1), 137-148. doi: 10.1006/jcat.2002.3685

Mihalcik, D. J., Mullen, C. A., & Boateng, A. A. (2011). Screening acidic zeolites for catalytic fast pyrolysis of biomass and its components. *Journal of Analytical and Applied Pyrolysis, 92*(1), 224-232. doi: 10.1016/j.jaap.2011.06.001

Mijoin, J., Pommier, C., Richard, F., & Pérot, G. (2001). Transformation of ketones over sulfided $CoMo/Al_2O_3$ catalyst — factors affecting thiol selectivity. *Journal of Molecular Catalysis A: Chemical, 169*(1–2), 171-175. doi: http://dx.doi.org/10.1016/S1381-1169(00)00553-7

Min, B. K., Santra, A. K., & Goodman, D. W. (2003). Understanding silica-supported metal catalysts: Pd/silica as a case study. *Catalysis Today, 85*(2-4), 113-124. doi: 10.1016/s0920-5861(03)00380-8

Mortensen, P. M., de Carvalho, H. W. P., Grunwaldt, J.-D., Jensen, P. A., & Jensen, A. D. (2015). Activity and stability of Mo_2C/ZrO_2 as catalyst for hydrodeoxygenation of mixtures of phenol and 1-octanol. *Journal of Catalysis, 328*, 208-215. doi: 10.1016/j.jcat.2015.02.002

Mortensen, P. M., Gardini, D., de Carvalho, H. W. P., Damsgaard, C. D., Grunwaldt, J.-D., Jensen, P. A., Wagner, J. B., & Jensen, A. D. (2014). Stability and resistance of nickel catalysts for hydrodeoxygenation: carbon deposition and effects of

sulfur, potassium, and chlorine in the feed. *Catalysis Science & Technology, 4*(10), 3672-3686. doi: 10.1039/c4cy00522h

Mortensen, P. M., Grunwaldt, J.-D., Jensen, P. A., & Jensen, A. D. (2013). Screening of catalysts for hydrodeoxygenation of phenol as a model compound for bio-oil. *ACS Catalysis, 3*(8), 1774-1785. doi: 10.1021/cs400266e

Mortensen, P. M., Grunwaldt, J. D., Jensen, P. A., Knudsen, K. G., & Jensen, A. D. (2011). A review of catalytic upgrading of bio-oil to engine fuels. *Applied Catalysis A: General, 407*(1-2), 1-19. doi: 10.1016/j.apcata.2011.08.046

Mu, W., Ben, H., Du, X., Zhang, X., Hu, F., Liu, W., Ragauskas, A. J., & Deng, Y. (2014). Noble metal catalyzed aqueous phase hydrogenation and hydrodeoxygenation of lignin-derived pyrolysis oil and related model compounds. *Bioresour Technol, 173*, 6-10. doi: 10.1016/j.biortech.2014.09.067

Mukundan, S., Konarova, M., Atanda, L., Ma, Q., & Beltramini, J. (2015). Guaiacol hydrodeoxygenation reaction catalyzed by highly dispersed, single layered MoS_2/C. *Catalysis Science & Technology, 5*(9), 4422-4432. doi: 10.1039/c5cy00607d

Nie, L., de Souza, P. M., Noronha, F. B., An, W., Sooknoi, T., & Resasco, D. E. (2014). Selective conversion of *m*-cresol to toluene over bimetallic Ni–Fe catalysts. *Journal of Molecular Catalysis A: Chemical, 388-389*, 47-55. doi: 10.1016/j.molcata.2013.09.029

Nikulshin, P. A., Salnikov, V. A., Varakin, A. N., & Kogan, V. M. (2015). The use of CoMoS catalysts supported on carbon-coated alumina for hydrodeoxygenation of guaiacol and oleic acid. *Catalysis Today*. doi: 10.1016/j.cattod.2015.07.032

Nimmanwudipong, T., Aydin, C., Lu, J., Runnebaum, R. C., Brodwater, K. C., Browning, N. D., Block, D. E., & Gates, B. C. (2012). Selective hydrodeoxygenation of guaiacol catalyzed by platinum supported on magnesium oxide. *Catalysis Letters, 142*(10), 1190-1196. doi: 10.1007/s10562-012-0884-3

Nimmanwudipong, T., Runnebaum, R. C., Block, D. E., & Gates, B. C. (2011a). Catalytic conversion of guaiacol catalyzed by platinum supported on alumina: Reaction network including hydrodeoxygenation reactions. *Energy & Fuels, 25*(8), 3417-3427. doi: 10.1021/ef200803d

Nimmanwudipong, T., Runnebaum, R. C., Block, D. E., & Gates, B. C. (2011b). Catalytic reactions of guaiacol: Reaction network and evidence of oxygen removal in reactions with hydrogen. *Catalysis Letters, 141*(6), 779-783. doi: 10.1007/s10562-011-0576-4

Nimmanwudipong, T., Runnebaum, R. C., Brodwater, K., Heelan, J., Block, D. E., & Gates, B. C. (2014). Design of a high-pressure flow-reactor system for catalytic hydrodeoxygenation: Guaiacol conversion catalyzed by platinum supported on MgO. *Energy & Fuels, 28*(2), 1090-1096. doi: 10.1021/ef4020026

Ninomiya, W., Tanabe, Y., Sotowa, K.-I., Yasukawa, T., & Sugiyama, S. (2008). Dehydrogenation of cycloalkanes over noble metal catalysts supported on active carbon. *Research on Chemical Intermediates, 34*(8-9), 663-668. doi: 10.1007/BF03036923

Ninomiya, W., Tanabe, Y., Uehara, Y., Sotowa, K.-I., & Sugiyama, S. (2006). Dehydrogenation of tetralin on Pd/C and Te-Pd/C catalysts in the liquid-film state under distillation conditions. *Catalysis Letters, 110*(3-4), 191-194. doi: 10.1007/s10562-006-0108-9

Nitsch, X., Commandré, J.-M., Clavel, P., Martin, E., Valette, J., & Volle, G. (2013). Conversion of phenol-based tars over olivine and sand in a biomass gasification atmosphere. *Energy & Fuels, 27*(9), 5459-5465. doi: 10.1021/ef400817z

Ojagh, H., Creaser, D., Tamm, S., Hu, C., & Olsson, L. (2015). Effect of thermal treatment on hydrogen uptake and characteristics of Ni-, Co-, and Mo-containing catalysts. *Industrial & Engineering Chemistry Research, 54*(46), 11511-11524. doi: 10.1021/acs.iecr.5b02510

Olcese, R., Bettahar, M. M., Malaman, B., Ghanbaja, J., Tibavizco, L., Petitjean, D., & Dufour, A. (2013). Gas-phase hydrodeoxygenation of guaiacol over iron-based catalysts. Effect of gases composition, iron load and supports (silica and activated carbon). *Applied Catalysis B: Environmental, 129*, 528-538. doi: 10.1016/j.apcatb.2012.09.043

Olcese, R. N., Bettahar, M., Petitjean, D., Malaman, B., Giovanella, F., & Dufour, A. (2012). Gas-phase hydrodeoxygenation of guaiacol over Fe/SiO_2 catalyst. *Applied Catalysis B: Environmental, 115-116*, 63-73. doi: 10.1016/j.apcatb.2011.12.005

Olcese, R. N., Francois, J., Bettahar, M. M., Petitjean, D., & Dufour, A. (2013). Hydrodeoxygenation of guaiacol, a surrogate of lignin pyrolysis vapors, over iron based catalysts: Kinetics and modeling of the lignin to aromatics integrated process. *Energy & Fuels, 27*(2), 975-984. doi: 10.1021/ef301971a

Oyama, S. (2003). Novel catalysts for advanced hydroprocessing: transition metal phosphides. *Journal of Catalysis, 216*(1-2), 343-352. doi: 10.1016/s0021-9517(02)00069-6

Oyama, S. T., Gott, T., Zhao, H., & Lee, Y.-K. (2009). Transition metal phosphide hydroprocessing catalysts: A review. *Catalysis Today, 143*(1-2), 94-107. doi: 10.1016/j.cattod.2008.09.019

Panagiotopoulou, P., & Vlachos, D. G. (2014). Liquid phase catalytic transfer hydrogenation of furfural over a Ru/C catalyst. *Applied Catalysis A: General, 480*, 17-24. doi: 10.1016/j.apcata.2014.04.018

Panneman, H. J., & Beenackers, A. A. C. M. (1992). Solvent effects on the hydration of cyclohexene catalyzed by a strong acid ion-exchange resin. 3. Effect of sulfolane

on the equilibrium conversion. *Industrial & Engineering Chemistry Research, 31*(6), 1433-1440. doi: 10.1021/ie00006a002

Patil, R. D., & Sasson, Y. (2015). Selective transfer hydrogenation of phenol to cyclohexanone on supported palladium catalyst using potassium formate as hydrogen source under open atmosphere. *Applied Catalysis A: General, 499*, 227-231. doi: 10.1016/j.apcata.2015.04.009

Pina, G., Louis, C., & Keane, M. A. (2003). Nickel particle size effects in catalytic hydrogenation and hydrodechlorination: phenolic transformations over nickel/silica. *Physical Chemistry Chemical Physics, 5*(9), 1924-1931. doi: 10.1039/b212407f

Pines, H., & Haag, W. O. (1960). Alumina: Catalyst and Support. I. alumina, its intrinsic acidity and catalytic activity1. *Journal of the American Chemical Society, 82*(10), 2471-2483. doi: 10.1021/ja01495a021

Pinheiro, A., Hudebine, D., Dupassieux, N., & Geantet, C. (2009). Impact of oxygenated compounds from lignocellulosic biomass pyrolysis oils on gas oil hydrotreatment. *Energy & Fuels, 23*(2), 1007-1014. doi: 10.1021/ef800507z

Popov, A., Kondratieva, E., Goupil, J. M., Mariey, L., Bazin, P., Gilson, J.-P., Travert, A., & Maugé, F. (2010). Bio-oils Hydrodeoxygenation: Adsorption of phenolic molecules on oxidic catalyst supports. *The Journal of Physical Chemistry C, 114*(37), 15661-15670. doi: 10.1021/jp101949j

Popov, A., Kondratieva, E., Mariey, L., Goupil, J. M., El Fallah, J., Gilson, J.-P., Travert, A., & Maugé, F. (2013). Bio-oil hydrodeoxygenation: Adsorption of phenolic compounds on sulfided (Co)Mo catalysts. *Journal of Catalysis, 297*, 176-186. doi: 10.1016/j.jcat.2012.10.005

Prasad, K., Jiang, X., Slade, J. S., Clemens, J., Repič, O., & Blacklock, T. J. (2005). New trends in palladium-catalyzed transfer hydrogenations using formic acid. *Advanced Synthesis & Catalysis, 347*(14), 1769-1773. doi: 10.1002/adsc.200505132

Prasomsri, T., Nimmanwudipong, T., & Román-Leshkov, Y. (2013). Effective hydrodeoxygenation of biomass-derived oxygenates into unsaturated hydrocarbons by MoO_3 using low H_2 pressures. *Energy & Environmental Science, 6*(6), 1732-1738. doi: 10.1039/c3ee24360e

Prasomsri, T., Shetty, M., Murugappan, K., & Román-Leshkov, Y. (2014). Insights into the catalytic activity and surface modification of MoO_3 during the hydrodeoxygenation of lignin-derived model compounds into aromatic hydrocarbons under low hydrogen pressures. *Energy & Environmental Science, 7*(8), 2660-2669. doi: 10.1039/c4ee00890a

Primo, A., & Garcia, H. (2014). Zeolites as catalysts in oil refining. *Chemical Society Reviews, 43*(22), 7548-7561. doi: 10.1039/c3cs60394f

Procházková, D., Zámostný, P., Bejblová, M., Červený, L., & Čejka, J. (2007). Hydrodeoxygenation of aldehydes catalyzed by supported palladium catalysts. *Applied Catalysis A: General, 332*(1), 56-64. doi: 10.1016/j.apcata.2007.08.009

Quinn, J. F., Razzano, D. A., Golden, K. C., & Gregg, B. T. (2008). 1,4-Cyclohexadiene with Pd/C as a rapid, safe transfer hydrogenation system with microwave heating. *Tetrahedron Letters, 49*(42), 6137-6140. doi: 10.1016/j.tetlet.2008.08.023

Radhakrishan, R., Do, D. M., Jaenicke, S., Sasson, Y., & Chuah, G.-K. (2011). Potassium phosphate as a solid base catalyst for the catalytic transfer hydrogenation of aldehydes and ketones. *ACS Catalysis, 1*(11), 1631-1636. doi: 10.1021/cs200299v

Rahman, A., & Jonnalagadda, S. B. (2009). Rapid and selective reduction of adehydes, ketones, phenol, and alkenes with Ni–boride–silica catalysts system at low temperature. *Journal of Molecular Catalysis A: Chemical, 299*(1-2), 98-101. doi: 10.1016/j.molcata.2008.10.022

Reddy Kannapu, H. P., Mullen, C. A., Elkasabi, Y., & Boateng, A. A. (2015). Catalytic transfer hydrogenation for stabilization of bio-oil oxygenates: Reduction of *p*-cresol and furfural over bimetallic Ni–Cu catalysts using isopropanol. *Fuel Processing Technology, 137*, 220-228. doi: 10.1016/j.fuproc.2015.04.023

Ren, Y., Yue, B., Gu, M., & He, H. (2010). Progress of the application of mesoporous silica-supported heteropolyacids in heterogeneous catalysis and preparation of nanostructured metal oxides. *Materials, 3*(2), 764-785. doi: 10.3390/ma3020764

Romero, Y., Richard, F., & Brunet, S. (2010). Hydrodeoxygenation of 2-ethylphenol as a model compound of bio-crude over sulfided Mo-based catalysts: Promoting effect and reaction mechanism. *Applied Catalysis B: Environmental, 98*(3-4), 213-223. doi: 10.1016/j.apcatb.2010.05.031

Romero, Y., Richard, F., Renème, Y., & Brunet, S. (2009). Hydrodeoxygenation of benzofuran and its oxygenated derivatives (2,3-dihydrobenzofuran and 2-ethylphenol) over NiMoP/Al_2O_3 catalyst. *Applied Catalysis A: General, 353*(1), 46-53. doi: 10.1016/j.apcata.2008.10.022

Ruiz, P. E., Leiva, K., Garcia, R., Reyes, P., Fierro, J. L. G., & Escalona, N. (2010). Relevance of sulfiding pretreatment on the performance of Re/ZrO_2 and Re/ZrO_2-sulfated catalysts for the hydrodeoxygenation of guayacol. *Applied Catalysis A: General, 384*(1-2), 78-83. doi: 10.1016/j.apcata.2010.06.009

Runnebaum, R. C., Lobo-Lapidus, R. J., Nimmanwudipong, T., Block, D. E., & Gates, B. C. (2011). Conversion of anisole catalyzed by platinum supported on alumina: The reaction network. *Energy & Fuels, 25*(10), 4776-4785. doi: 10.1021/ef2010699

Runnebaum, R. C., Nimmanwudipong, T., Block, D. E., & Gates, B. C. (2010). Catalytic conversion of anisole: Evidence of oxygen removal in reactions with hydrogen. *Catalysis Letters, 141*(6), 817-820. doi: 10.1007/s10562-010-0510-1

Runnebaum, R. C., Nimmanwudipong, T., Block, D. E., & Gates, B. C. (2012). Catalytic conversion of compounds representative of lignin-derived bio-oils: a reaction network for guaiacol, anisole, 4-methylanisole, and cyclohexanone conversion catalysed by Pt/γ-Al_2O_3. *Catalysis Science & Technology, 2*(1), 113-118. doi: 10.1039/c1cy00169h

Saidi, M., Rostami, P., Rahimpour, H. R., Roshanfekr Fallah, M. A., Rahimpour, M. R., Gates, B. C., & Raeissi, S. (2015). Kinetics of upgrading of anisole with hydrogen catalyzed by platinum supported on alumina. *Energy & Fuels*, *29*(8), 4990-4997. doi: 10.1021/acs.energyfuels.5b00297

Schweiger, H., Raybaud, P., Kresse, G., & Toulhoat, H. (2002). Shape and edge sites modifications of MoS_2 catalytic nanoparticles induced by working conditions: A theoretical study. *Journal of Catalysis*, *207*(1), 76-87. doi: 10.1006/jcat.2002.3508

Şenol, O. İ., Ryymin, E. M., Viljava, T. R., & Krause, A. O. I. (2007). Effect of hydrogen sulphide on the hydrodeoxygenation of aromatic and aliphatic oxygenates on sulphided catalysts. *Journal of Molecular Catalysis A: Chemical, 277*(1-2), 107-112. doi: 10.1016/j.molcata.2007.07.033

Şenol, O. İ., Viljava, T. R., & Krause, A. O. I. (2007). Effect of sulphiding agents on the hydrodeoxygenation of aliphatic esters on sulphided catalysts. *Applied Catalysis A: General, 326*(2), 236-244. doi: 10.1016/j.apcata.2007.04.022

Sepúlveda, C., Escalona, N., García, R., Laurenti, D., & Vrinat, M. (2012). Hydrodeoxygenation and hydrodesulfurization co-processing over ReS_2 supported catalysts. *Catalysis Today, 195*(1), 101-105. doi: 10.1016/j.cattod.2012.05.047

Sepúlveda, C., Leiva, K., García, R., Radovic, L. R., Ghampson, I. T., DeSisto, W. J., Fierro, J. L. G., & Escalona, N. (2011). Hydrodeoxygenation of 2-methoxyphenol over Mo_2N catalysts supported on activated carbons. *Catalysis Today, 172*(1), 232-239. doi: 10.1016/j.cattod.2011.02.061

Sharma, B. K., Suarez, P. A. Z., Perez, J. M., & Erhan, S. Z. (2009). Oxidation and low temperature properties of biofuels obtained from pyrolysis and alcoholysis of soybean oil and their blends with petroleum diesel. *Fuel Processing Technology, 90*(10), 1265-1271. doi: 10.1016/j.fuproc.2009.06.011

Shin, E.-J., & Keane, M. A. (2000). Gas-phase hydrogenation/hydrogenolysis of phenol over supported nickel catalysts. *Industrial & Engineering Chemistry Research, 39*(4), 883-892. doi: 10.1021/ie990643r

Shore, S. G., Ding, E., Park, C., & Keane, M. A. (2002). Vapor phase hydrogenation of phenol over silica supported Pd and Pd-Yb catalysts. *Catalysis Communications, 3*(2), 77-84. doi: http://dx.doi.org/10.1016/S1566-7367(02)00052-3

Smit, B., & Maesen, T. L. (2008). Towards a molecular understanding of shape selectivity. *Nature, 451*(7179), 671-678. doi: 10.1038/nature06552

Song, W., Liu, Y., Baráth, E., Zhao, C., & Lercher, J. A. (2015). Synergistic effects of Ni and acid sites for hydrogenation and C–O bond cleavage of substituted phenols. *Green Chemistry, 17*(2), 1204-1218. doi: 10.1039/c4gc01798f

Stanislaus, A., Absi-Halabi, M., & Al-Doloma, K. (1988). Effect of phosphorus on the acidity of γ-alumina and on the thermal stability of γ-alumina supported nickel—molybdenum hydrotreating catalysts. *Applied Catalysis, 39*, 239-253. doi: http://dx.doi.org/10.1016/S0166-9834(00)80952-5

Su-Ping, Z. (2003). Study of hydrodeoxygenation of bio-oil from the fast pyrolysis of biomass. *Energy Sources, 25*(1), 57-65. doi: 10.1080/00908310290142118

Sun, J., Karim, A. M., Zhang, H., Kovarik, L., Li, X. S., Hensley, A. J., McEwen, J. S., & Wang, Y. (2013). Carbon-supported bimetallic Pd–Fe catalysts for vapor-phase hydrodeoxygenation of guaiacol. *Journal of Catalysis, 306*, 47-57. doi: 10.1016/j.jcat.2013.05.020

Sun, Q., & Nowowiejski, G. B. (2011). Catalyst regeneration method: Google Patents, EP2365875 A2.

Thomas, B., Prathapan, S., & Sugunan, S. (2005). Synthesis of dimethyl acetal of ketones: design of solid acid catalysts for one-pot acetalization reaction. *Microporous and Mesoporous Materials, 80*(1-3), 65-72. doi: 10.1016/j.micromeso.2004.12.001

Thomas, B., Ramu, V. G., Gopinath, S., George, J., Kurian, M., Laurent, G., Drisko, G. L. & Sugunan, S. (2011). Catalytic acetalization of carbonyl compounds over cation (Ce^{3+}, Fe^{3+} and Al^{3+}) exchanged montmorillonites and Ce^{3+}-exchanged Y zeolites. *Applied Clay Science, 53*(2), 227-235. doi: 10.1016/j.clay.2011.01.021

Tyrone Ghampson, I., Sepúlveda, C., Garcia, R., García Fierro, J. L., Escalona, N., & DeSisto, W. J. (2012). Comparison of alumina- and SBA-15-supported molybdenum nitride catalysts for hydrodeoxygenation of guaiacol. *Applied Catalysis A: General, 435-436*, 51-60. doi: 10.1016/j.apcata.2012.05.039

Velu, S., Kapoor, M. P., Inagaki, S., & Suzuki, K. (2003). Vapor phase hydrogenation of phenol over palladium supported on mesoporous CeO_2 and ZrO_2. *Applied Catalysis A: General, 245*(2), 317-331. doi: 10.1016/s0926-860x(02)00655-5

Vilches-Herrera, M., Werkmeister, S., Junge, K., Börner, A., & Beller, M. (2014). Selective catalytic transfer hydrogenation of nitriles to primary amines using Pd/C. *Catalysis Science & Technology, 4*(3), 629-632. doi: 10.1039/c3cy00854a

Viljava, T. R., Komulainen, R. S., & Krause, A. O. I. (2000). Effect of H_2S on the stability of $CoMo/Al_2O_3$ catalysts during hydrodeoxygenation. *Catalysis Today, 60*(1–2), 83-92. doi: http://dx.doi.org/10.1016/S0920-5861(00)00320-5

Villaverde, M. M., Garetto, T. F., & Marchi, A. J. (2015). Liquid-phase transfer hydrogenation of furfural to furfuryl alcohol on Cu–Mg–Al catalysts. *Catalysis Communications, 58*, 6-10. doi: 10.1016/j.catcom.2014.08.021

Wahyudiono, Sasaki, M., & Goto, M. (2008). Kinetic study for liquefaction of tar in sub- and supercritical water. *Polymer Degradation and Stability, 93*(6), 1194-1204. doi: 10.1016/j.polymdegradstab.2008.02.006

Wan, H., Chaudhari, R. V., & Subramaniam, B. (2012). Catalytic hydroprocessing of *p*-Cresol: Metal, Solvent and mass-transfer effects. *Topics in Catalysis, 55*(3-4), 129-139. doi: 10.1007/s11244-012-9782-6

Wandas, R., Surygala, J., & Śliwka, E. (1996). Conversion of cresols and naphthalene in the hydroprocessing of three-component model mixtures simulating fast pyrolysis tars. *Fuel, 75*(6), 687-694. doi: http://dx.doi.org/10.1016/0016-2361(96)00011-7

Wang, H., Male, J., & Wang, Y. (2013). Recent advances in hydrotreating of pyrolysis bio-oil and its oxygen-containing model compounds. *ACS Catalysis, 3*(5), 1047-1070. doi: 10.1021/cs400069z

Wang, W.-y., Yang, Y.-q., Bao, J.-g., & Luo, H.-a. (2009). Characterization and catalytic properties of Ni–Mo–B amorphous catalysts for phenol hydrodeoxygenation. *Catalysis Communications, 11*(2), 100-105. doi: 10.1016/j.catcom.2009.09.003

Wang, W., Yang, Y., Luo, H., Hu, T., & Liu, W. (2010). Preparation and hydrodeoxygenation properties of Co–Mo–O–B amorphous catalyst. *Reaction Kinetics, Mechanisms and Catalysis, 102*(1), 207-217. doi: 10.1007/s11144-010-0253-4

Wang, W., Yang, Y., Luo, H., Hu, T., & Liu, W. (2011). Amorphous Co–Mo–B catalyst with high activity for the hydrodeoxygenation of bio-oil. *Catalysis Communications, 12*(6), 436-440. doi: 10.1016/j.catcom.2010.11.001

Wang, W., Yang, Y., Luo, H., & Liu, W. (2010). Characterization and hydrodeoxygenation properties of Co promoted Ni–Mo–B amorphous catalysts: influence of Co content. *Reaction Kinetics, Mechanisms and Catalysis, 101*(1), 105-115. doi: 10.1007/s11144-010-0201-3

Wang, W., Yang, Y., Luo, H., Peng, H., & Wang, F. (2011). Effect of La on Ni–W–B amorphous catalysts in hydrodeoxygenation of phenol. *Industrial & Engineering Chemistry Research, 50*(19), 10936-10942. doi: 10.1021/ie201272d

Wang, X., & Rinaldi, R. (2012). Exploiting H-transfer reactions with RANEY® Ni for upgrade of phenolic and aromatic biorefinery feeds under unusual, low-severity conditions. *Energy & Environmental Science, 5*(8), 8244-8260. doi: 10.1039/c2ee21855k

Wang, Y., Fang, Y., He, T., Hu, H., & Wu, J. (2011). Hydrodeoxygenation of dibenzofuran over noble metal supported on mesoporous zeolite. *Catalysis Communications, 12*(13), 1201-1205. doi: 10.1016/j.catcom.2011.04.010

Wang, Y., He, T., Liu, K., Wu, J., & Fang, Y. (2012). From biomass to advanced bio-fuel by catalytic pyrolysis/hydro-processing: hydrodeoxygenation of bio-oil derived from biomass catalytic pyrolysis. *Bioresource Technology, 108*, 280-284. doi: 10.1016/j.biortech.2011.12.132

Wang, Y., Shah, N., Huggins, F. E., & Huffman, G. P. (2006). Hydrogen production by catalytic dehydrogenation of tetralin and decalin over stacked cone carbon nanotube-supported Pt catalysts. *Energy & Fuels, 20*(6), 2612-2615. doi: 10.1021/ef060228t

Wei, X.-R., Liu, J., Yang, Y., & Deng, L. (2014). A general approach towards efficient catalysis in Pickering emulsions stabilized by amphiphilic RGO–Silica hybrid materials. *RSC Advances, 4*(67), 35744-35749. doi: 10.1039/c4ra07547a

Whiffen, V. M. L., & Smith, K. J. (2010). Hydrodeoxygenation of 4-methylphenol over unsupported MoP, MoS_2, and MoO_x Catalysts†. *Energy & Fuels, 24*(9), 4728-4737. doi: 10.1021/ef901270h

Whiffen, V. M. L., Smith, K. J., & Straus, S. K. (2012). The influence of citric acid on the synthesis and activity of high surface area MoP for the hydrodeoxygenation of 4-methylphenol. *Applied Catalysis A: General, 419-420*, 111-125. doi: 10.1016/j.apcata.2012.01.018

Wienhöfer, G., Westerhaus, F. A., Junge, K., & Beller, M. (2013). Fast and selective iron-catalyzed transfer hydrogenations of aldehydes. *Journal of Organometallic Chemistry, 744*, 156-159. doi: 10.1016/j.jorganchem.2013.06.010

Wiggers, V. R., Meier, H. F., Wisniewski, A., Jr., Chivanga Barros, A. A., & Wolf Maciel, M. R. (2009). Biofuels from continuous fast pyrolysis of soybean oil: a pilot plant study. *Bioresource Technology, 100*(24), 6570-6577. doi: 10.1016/j.biortech.2009.07.059

Wiggers, V. R., Wisniewski, A., Madureira, L. A. S., Barros, A. A. C., & Meier, H. F. (2009). Biofuels from waste fish oil pyrolysis: Continuous production in a pilot plant. *Fuel, 88*(11), 2135-2141. doi: 10.1016/j.fuel.2009.02.006

Wildschut, J., Arentz, J., Rasrendra, C. B., Venderbosch, R. H., & Heeres, H. J. (2009). Catalytic hydrotreatment of fast pyrolysis oil: Model studies on reaction pathways for the carbohydrate fraction. *Environmental Progress & Sustainable Energy, 28*(3), 450-460. doi: 10.1002/ep.10390

Wildschut, J., Iqbal, M., Mahfud, F. H., Cabrera, I. M., Venderbosch, R. H., & Heeres, H. J. (2010). Insights in the hydrotreatment of fast pyrolysis oil using a ruthenium on carbon catalyst. *Energy & Environmental Science, 3*(7), 962-970. doi: 10.1039/b923170f

Wildschut, J., Mahfud, F. H., Venderbosch, R. H., & Heeres, H. J. (2009). Hydrotreatment of fast pyrolysis oil using heterogeneous noble-metal catalysts. *Industrial & Engineering Chemistry Research, 48*(23), 10324-10334. doi: 10.1021/ie9006003

Wildschut, J., Melián-Cabrera, I., & Heeres, H. J. (2010). Catalyst studies on the hydrotreatment of fast pyrolysis oil. *Applied Catalysis B: Environmental, 99*(1-2), 298-306. doi: 10.1016/j.apcatb.2010.06.036

Wu, S.-K., Lai, P.-C., Lin, Y.-C., Wan, H.-P., Lee, H.-T., & Chang, Y.-H. (2013). Atmospheric hydrodeoxygenation of guaiacol over alumina-, zirconia-, and silica-supported nickel phosphide catalysts. *ACS Sustainable Chemistry & Engineering, 1*(3), 349-358. doi: 10.1021/sc300157d

Wu, X., Liu, J., Li, X., Zanotti-Gerosa, A., Hancock, F., Vinci, D., Ruan, J., & Xiao, J. (2006). On water and in air: Fast and highly chemoselective transfer hydrogenation of aldehydes with iridium catalysts. *Angewandte Chemie International Edition, 45*(40), 6718-6722. doi: 10.1002/anie.200602122

Xiang, Y., Li, X., Lu, C., Ma, L., & Zhang, Q. (2010). Water-improved heterogeneous transfer hydrogenation using methanol as hydrogen donor over Pd-based catalyst. *Applied Catalysis A: General, 375*(2), 289-294. doi: 10.1016/j.apcata.2010.01.004

Xiong, W.-M., Fu, Y., Zeng, F.-X., & Guo, Q.-X. (2011). An in situ reduction approach for bio-oil hydroprocessing. *Fuel Processing Technology, 92*(8), 1599-1605. doi: 10.1016/j.fuproc.2011.04.005

Xu, R., Ferrante, L., Briens, C., & Berruti, F. (2009). Flash pyrolysis of grape residues into biofuel in a bubbling fluid bed. *Journal of Analytical and Applied Pyrolysis, 86*(1), 58-65. doi: 10.1016/j.jaap.2009.04.005

Xu, Y., Long, J., Liu, Q., Li, Y., Wang, C., Zhang, Q., Lv, W., Zhang, X., Qiu, S., Wang, T., & Ma, L. (2015). In situ hydrogenation of model compounds and raw bio-oil over Raney Ni catalyst. *Energy Conversion and Management, 89*, 188-196. doi: 10.1016/j.enconman.2014.09.017

Yakovlev, V. A., Khromova, S. A., Sherstyuk, O. V., Dundich, V. O., Ermakov, D. Y., Novopashina, V. M., Lebedev, M. Y., Bulavchenko, O., & Parmon, V. N. (2009). Development of new catalytic systems for upgraded bio-fuels production from bio-crude-oil and biodiesel. *Catalysis Today, 144*(3-4), 362-366. doi: 10.1016/j.cattod.2009.03.002

Yan, N., Yuan, Y., Dykeman, R., Kou, Y., & Dyson, P. J. (2010). Hydrodeoxygenation of lignin-derived phenols into alkanes by using nanoparticle catalysts combined with Bronsted acidic ionic liquids. *Angewandte Chemie International Edition in English, 49*(32), 5549-5553. doi: 10.1002/anie.201001531

Yang, Y., Gilbert, A., & Xu, C. (2009). Hydrodeoxygenation of bio-crude in supercritical hexane with sulfided CoMo and CoMoP catalysts supported on MgO: A model compound study using phenol. *Applied Catalysis A: General, 360*(2), 242-249. doi: 10.1016/j.apcata.2009.03.027

Yang, Y., Luo, H. a., Tong, G., Smith, K. J., & Tye, C. T. (2008). Hydrodeoxygenation of phenolic model compounds over MoS_2 catalysts with different structures. *Chinese Journal of Chemical Engineering, 16*(5), 733-739. doi: http://dx.doi.org/10.1016/S1004-9541(08)60148-2

Yingxin, L. I. U., Jixiang, C., & Jiyan, Z. (2007). Effects of the supports on activity of supported nickel catalysts for hydrogenation of *m*-dinitrobenzene to m-phenylenediamine. *Chinese Journal of Chemical Engineering, 15*(1), 63-67. doi: http://dx.doi.org/10.1016/S1004-9541(07)60034-2

Yoosuk, B., Tumnantong, D., & Prasassarakich, P. (2012a). Amorphous unsupported Ni–Mo sulfide prepared by one step hydrothermal method for phenol hydrodeoxygenation. *Fuel, 91*(1), 246-252. doi: 10.1016/j.fuel.2011.08.001

Yoosuk, B., Tumnantong, D., & Prasassarakich, P. (2012b). Unsupported MoS_2 and $CoMoS_2$ catalysts for hydrodeoxygenation of phenol. *Chemical Engineering Science, 79*, 1-7. doi: 10.1016/j.ces.2012.05.020

Yoshikawa, T., Shinohara, S., Yagi, T., Ryumon, N., Nakasaka, Y., Tago, T., & Masuda, T. (2014). Production of phenols from lignin-derived slurry liquid using iron oxide catalyst. *Applied Catalysis B: Environmental, 146*, 289-297. doi: 10.1016/j.apcatb.2013.03.010

Yoshikawa, T., Yagi, T., Shinohara, S., Fukunaga, T., Nakasaka, Y., Tago, T., & Masuda, T. (2013). Production of phenols from lignin via depolymerization and catalytic cracking. *Fuel Processing Technology, 108*, 69-75. doi: 10.1016/j.fuproc.2012.05.003

Yu, J.-Q., Wu, H.-C., Ramarao, C., Spencer, J. B., & Ley, S. V. (2003). Transfer hydrogenation using recyclable polyurea-encapsulated palladium: efficient and chemoselective reduction of aryl ketones. *Chemical Communications*(6), 678-679. doi: 10.1039/b300074p

Zakzeski, J., Bruijnincx, P. C. A., Jongerius, A. L., & Weckhuysen, B. M. (2010). The catalytic valorization of lignin for the production of renewable chemicals. *Chemical Reviews, 110*(6), 3552-3599. doi: 10.1021/cr900354u

Zanuttini, M. S., Dalla Costa, B. O., Querini, C. A., & Peralta, M. A. (2014). Hydrodeoxygenation of *m*-cresol with Pt supported over mild acid materials. *Applied Catalysis A: General, 482*, 352-361. doi: 10.1016/j.apcata.2014.06.015

Zanuttini, M. S., Peralta, M. A., & Querini, C. A. (2015). Deoxygenation of *m*-cresol: Deactivation and regeneration of $Pt/\gamma\text{-}Al_2O_3$ catalysts. *Industrial & Engineering Chemistry Research, 54*(18), 4929-4939. doi: 10.1021/acs.iecr.5b00305

Zhang, D., Ye, F., Xue, T., Guan, Y., & Wang, Y. M. (2014). Transfer hydrogenation of phenol on supported Pd catalysts using formic acid as an alternative hydrogen source. *Catalysis Today, 234*, 133-138. doi: 10.1016/j.cattod.2014.02.039

Zhang, J., Blazecka, P. G., Bruendl, M. M., & Huang, Y. (2009). Ru-TsDPEN with formic acid/Hunig's base for asymmetric transfer hydrogenation, a practical synthesis of optically enriched N-propyl pantolactam. *The Journal of Organic Chemistry, 74*(3), 1411-1414. doi: 10.1021/jo802380j

Zhang, S., Yan, Y., Li, T., & Ren, Z. (2005). Upgrading of liquid fuel from the pyrolysis of biomass. *Bioresource Technology, 96*(5), 545-550. doi: 10.1016/j.biortech.2004.06.015

Zhang, X., Wang, T., Ma, L., Zhang, Q., & Jiang, T. (2013). Hydrotreatment of bio-oil over Ni-based catalyst. *Bioresource Technology, 127*, 306-311. doi: 10.1016/j.biortech.2012.07.119

Zhang, Z.-G., & Yoshida, T. (2001). Behavior of hydrogen transfer in the hydrogenation of anthracene over activated carbon. *Energy & Fuels, 15*(3), 708-713. doi: 10.1021/ef000253d

Zhao, C., Camaioni, D. M., & Lercher, J. A. (2012). Selective catalytic hydroalkylation and deoxygenation of substituted phenols to bicycloalkanes. *Journal of Catalysis, 288*, 92-103. doi: 10.1016/j.jcat.2012.01.005

Zhao, C., He, J., Lemonidou, A. A., Li, X., & Lercher, J. A. (2011). Aqueous-phase hydrodeoxygenation of bio-derived phenols to cycloalkanes. *Journal of Catalysis, 280*(1), 8-16. doi: 10.1016/j.jcat.2011.02.001

Zhao, C., Kasakov, S., He, J., & Lercher, J. A. (2012). Comparison of kinetics, activity and stability of Ni/HZSM-5 and Ni/Al_2O_3-HZSM-5 for phenol hydrodeoxygenation. *Journal of Catalysis, 296*, 12-23. doi: 10.1016/j.jcat.2012.08.017

Zhao, C., Kou, Y., Lemonidou, A. A., Li, X., & Lercher, J. A. (2009). Highly selective catalytic conversion of phenolic bio-oil to alkanes. *Angewandte Chemie International Edition in English, 48*(22), 3987-3990. doi: 10.1002/anie.200900404

Zhao, C., Kou, Y., Lemonidou, A. A., Li, X., & Lercher, J. A. (2010). Hydrodeoxygenation of bio-derived phenols to hydrocarbons using RANEY Ni and Nafion/SiO_2 catalysts. *Chemical Communications, 46*(3), 412-414. doi: 10.1039/b916822b

Zhao, C., & Lercher, J. A. (2012). Selective hydrodeoxygenation of lignin-derived phenolic monomers and dimers to cycloalkanes on Pd/C and HZSM-5 catalysts. *ChemCatChem, 4*(1), 64-68. doi: 10.1002/cctc.201100273

Zhao, C., Song, W., & Lercher, J. A. (2012). Aqueous phase hydroalkylation and hydrodeoxygenation of phenol by dual functional catalysts comprised of Pd/C and H/La-BEA. *ACS Catalysis*, *2*(12), 2714-2723. doi: 10.1021/cs300418a

Zhao, H. Y., Li, D., Bui, P., & Oyama, S. T. (2011). Hydrodeoxygenation of guaiacol as model compound for pyrolysis oil on transition metal phosphide hydroprocessing catalysts. *Applied Catalysis A: General*, *391*(1-2), 305-310. doi: 10.1016/j.apcata.2010.07.039

Zhou, X., Wu, X., Yang, B., & Xiao, J. (2012). Varying the ratio of formic acid to triethylamine impacts on asymmetric transfer hydrogenation of ketones. *Journal of Molecular Catalysis A: Chemical*, *357*, 133-140. doi: 10.1016/j.molcata.2012.02.002

Zhu, X., Lobban, L. L., Mallinson, R. G., & Resasco, D. E. (2011). Bifunctional transalkylation and hydrodeoxygenation of anisole over a Pt/HBeta catalyst. *Journal of Catalysis*, *281*(1), 21-29. doi: 10.1016/j.jcat.2011.03.030

LIST OF PUBLICATIONS

Journal Publications

- **Shafaghat, Hoda**, Sirous Rezaei, Pouya, & Wan Daud, Wan Mohd Ashri (2016). Using decalin and tetralin as hydrogen source for transfer hydrogenation of renewable lignin-derived phenolics over activated carbon supported Pd and Pt catalysts. *Journal of the Taiwan Institute of Chemical Engineers*, in press, doi: 10.1016/j.jtice.2016.05.032.
- **Shafaghat, Hoda**, Sirous Rezaei, Pouya, & Wan Daud, Wan Mohd Ashri (2016). Catalytic hydrodeoxygenation of simulated phenolic bio-oil to cycloalkanes and aromatic hydrocarbons over bifunctional metal/acid catalysts of Ni/HBeta, Fe/HBeta and NiFe/HBeta. *Journal of Industrial and Engineering Chemistry*, 35, 268-276.
- **Shafaghat, Hoda**, Sirous Rezaei, Pouya, & Wan Daud, Wan Mohd Ashri (2015). Effective parameters on selective catalytic hydrodeoxygenation of phenolic compounds of pyrolysis bio-oil to high-value hydrocarbons. *RSC Advances*, 5, 103999-104042.
- **Shafaghat, Hoda**, Sirous Rezaei, Pouya, & Wan Daud, Wan Mohd Ashri (2015). Catalytic hydrogenation of phenol, cresol and guaiacol over physically mixed catalysts of Pd/C and zeolite solid acids. *RSC Advances*, 5, 33990-33998.

Conference Proceeding

- **Shafaghat, Hoda**, Sirous Rezaei, Pouya, & Wan Daud, Wan Mohd Ashri. Catalytic hydrodeoxygenation and transfer hydrogenation of renewable lignin-derived phenolics. 24th European Biomass Conference and Exhibition (EUBCE), Amsterdam, The Netherlands, 6-9 June 2016.

Journal of Industrial and Engineering Chemistry 35 (2016) 268–276

Contents lists available at ScienceDirect

Journal of Industrial and Engineering Chemistry

journal homepage: www.elsevier.com/locate/jiec

Catalytic hydrodeoxygenation of simulated phenolic bio-oil to cycloalkanes and aromatic hydrocarbons over bifunctional metal/acid catalysts of Ni/HBeta, Fe/HBeta and NiFe/HBeta

Hoda Shafaghat, Pouya Sirous Rezaei, Wan Mohd Ashri Wan Daud *

Department of Chemical Engineering, Faculty of Engineering, University of Malaya, 50603 Kuala Lumpur, Malaysia

ARTICLE INFO

Article history:
Received 22 October 2015
Received in revised form 30 December 2015
Accepted 4 January 2016
Available online 8 January 2016

Keywords:
Phenolic bio-oil
Hydrogenation
Hydrogenolysis
Bifunctional catalyst
Bimetallic NiFe/HBeta

ABSTRACT

Bifunctional metal/acid catalysts of 5 wt% Ni/HBeta, 5 wt% Fe/HBeta, 2.5 wt% Ni-2.5 wt% Fe/HBeta (NiFe-5/HBeta) and 5 wt% Ni-5 wt% Fe/HBeta (NiFe-10/HBeta) were used for hydrodeoxygenation (HDO) of a simulated phenolic bio-oil consisting of phenol (50 wt%), *o*-cresol (25 wt%) and guaiacol (25 wt%). Nickel and iron metals were supported on hydrogen form Beta zeolite (HBeta) under similar ion-exchange conditions. BET surface area and acid sites density of Ni/HBeta, Fe/HBeta, NiFe-5/HBeta and NiFe-10/HBeta were 463, 445, 455, 417 m^2/g and 0.53, 0.48, 0.50, 0.38 mmol/g, respectively. Cycloalkanes (21.39 wt%) and aromatic hydrocarbons (20.21 wt%) were the dominant hydrocarbons obtained over monometallic catalysts of Ni/HBeta and Fe/HBeta through reactions of hydrogenation and hydrogenolysis, respectively. It was revealed that both hydrogenation and hydrogenolysis mechanisms were effectively proceeded over the bimetallic catalyst of NiFe/HBeta which showed enhanced HDO efficiency compared to monometallic catalysts of Ni/HBeta and Fe/HBeta due to the synergistic effect between the two metals. The effect of reaction temperature on HDO efficiency of NiFe-10/HBeta catalyst was investigated at 220, 260, 300 and 340 °C. Maximum catalytic activity and hydrocarbons selectivity was observed at 300 °C. Replacement of water with methanol as solvent in HDO of the simulated phenolic bio-oil over NiFe-10/HBeta remarkably reduced the selectivity towards hydrocarbons.

Introduction

Fast depletion of fossil fuel sources and high demand for energy consumption necessitate to find potential alternatives for fossil fuels. Lignocellulosic biomass consisting of cellulose, hemicellulose and lignin is a significant source for production of fuels and valuable chemicals [1,2]. Lignocellulosic biomass could be transformed to bio-fuel through a number of thermochemical processes such as fast pyrolysis, gasification, direct liquefaction and supercritical extraction [3–6]. Fast pyrolysis is an efficient technique for large scale exploitation of lignocellulosic biomass since it is a process without extensive capital investments [7] and results in high yield of liquid fuel (up to 70 wt%) [3,8]. The liquid fuel which is called bio-oil is considered as a noteworthy alternative for depleting fossil fuels. However, high oxygen content of biomass (about 50 wt%) [9] results in highly oxygenated bio-oil consisting reactive chemical components of phenols, carboxylic acids, aldehydes, ketones, furfurals, carbohydrates, alcohols and water (around 30 wt%) [10–15]. These oxygen containing compounds lead to undesirable properties which prevent the direct use of bio-oil as fuel. Therefore, it is essential to upgrade bio-oil. Catalytic hydrodeoxygenation (HDO) is one of the most efficient methods for bio-oil upgrading [9,11,12,16,17]. Bio-oil treatment through HDO is usually conducted at high hydrogen pressure of 50–250 bar and moderate temperature of 150–450 °C [8,18,19]. So far, several studies have been conducted for catalytic hydrodeoxygenation of bio-oil using different catalysts. Wildschut et al. studied the HDO of fast pyrolysis oil from beech wood at 350 °C and 200 bar over Ru/C, Ru/TiO_2, Ru/Al_2O_3, Pt/C and Pd/C catalysts [3,8]. Maximum oil yield and deoxygenation degree were obtained using Ru/C catalyst which were 60 and 90 wt%, respectively [8]. HDO of fast pyrolysis oil from pine wood was investigated by Ardiyanti et al. [20] at 350 °C and initial hydrogen pressure of 100 bar using $NiCu/\delta\text{-}Al_2O_3$ catalyst. In another work held by Ardiyanti et al. [21] for HDO of fast pyrolysis oil from pine wood over mono- and

* Corresponding author. Tel.: +60 3 79675297; fax: +60 3 79675319.
E-mail addresses: h.shafaghat@gmail.com (H. Shafaghat), pouya.sr@gmail.com (P.S. Rezaei), ashri@um.edu.my (W.M.A.W. Daud).

http://dx.doi.org/10.1016/j.jiec.2016.01.001
1226-086X/

RSC Advances

PAPER

Cite this: *RSC Adv.*, 2015, **5**, 33990

Catalytic hydrogenation of phenol, cresol and guaiacol over physically mixed catalysts of Pd/C and zeolite solid acids†

Hoda Shafaghat, Pouya Sirous Rezaei and Wan Mohd Ashri Wan Daud*

Received 8th January 2015
Accepted 7th April 2015

DOI: 10.1039/c5ra00367a

www.rsc.org/advances

Highly reactive phenolic compounds of pyrolysis bio-oil are recognized as a major cause of the unpleasant properties of this biofuel. Catalytic hydrodeoxygenation of phenolic compounds of bio-oil is an efficient technique for improving the quality of bio-oil. Dual function catalysts consisting of metal and acid sites are usually used for transformation of bio-oil/bio-oil model compounds to high value hydrocarbons. Metal and acid sites are generally involved in hydrogenation/hydrodeoxygenation and dehydration/hydrocracking/dealkylation/alkylation reaction mechanisms, respectively. In this work, the product selectivity of hydrogenation of phenol, *o*-cresol, *m*-cresol and guaiacol was investigated over combined catalysts of Pd/C with zeolite solid acids of HZSM-5 (Si/Al of 30, 50 and 80) and HY (Si/Al of 30 and 60). Catalytic activity and product distribution in the hydrogenation process were affected by the density and strength of zeolite acid sites. HZSM-5 (30) with only weak acid sites showed lower cyclohexane selectivity compared with HZSM-5 (50) and HZSM-5 (80) which had both weak and strong acid sites. HY (30) and HY (60) containing only strong acid sites favored production of cycloketones.

1. Introduction

Bio-oil produced through biomass pyrolysis is considered as a renewable and sustainable source of energy.[1,2] Due to the high oxygen content of biomass (around 50 wt%),[3] bio-oil is highly oxygenated consisting of reactive chemical components (phenols, carboxylic acids, aldehydes, ketones, furfurals, carbohydrates and alcohols)[4–7] and water (around 30 wt%).[8] High content of such oxygen-containing compounds in bio-oil results in undesirable properties such as high viscosity, low heating value, low thermal and chemical stabilities, corrosiveness and immiscibility with fossil fuels.[4,5,7,9–11] Therefore, bio-oil needs to be upgraded in order to be considered as a standard fuel. One of the most applicable and effective techniques for bio-oil upgrading is catalytic hydrodeoxygenation[1,3,5,6,10] which treats bio-oil at high hydrogen pressure (50–350 bar) and moderate temperature (150–450 °C).[12–14] Due to the wide variety of compounds which are present in bio-oil and involved in upgrading process, it is difficult to predict the reaction mechanism of bio-oil hydrotreating. The hydrodeoxygenation of different model compounds of bio-oil could be studied in order to find out the mechanisms of their transformation and to predict the overall reaction pathway in bio-oil hydrotreating. Since the phenolic fraction of bio-oil is highly reactive causing bio-oil instability, phenols have been widely used as bio-oil model compounds.[11,15,16]

Catalysts including both metal and acid functions are highly efficient for hydrotreating of bio-oil. Metal and acid sites accomplish hydrotreating reaction through hydrogenation/hydrogenolysis and dehydration/isomerization/alkylation/condensation mechanisms, respectively.[3,4,17] These dual functional catalysts are generally prepared by embedding metals into acidic supports. As an alternative to dual functional catalysts, supported or unsupported metal catalysts such as Pd/C and RANEY® Ni could be physically mixed with liquid (H_3PO_4) and/or solid acids (HZSM-5, sulfated zirconia, Nafion/SiO_2, Amberlyst 15) and used for hydrogenation of phenolic compounds of bio-oil.[1,3,8,16] Zhao *et al.*[8] reported that substituting liquid acid with solid acid enhances the hydrotreating efficiency of the mixed catalyst system. Brønsted acids are appropriate for hydrotreatment of oxygenated compounds due to the presence of H^+ sites in their structure which promote dehydration reaction. Zeolites contain Brønsted acid sites and have high shape selectivity and thermal/hydrothermal stability which have been widely used in acid catalyzed reactions such as isomerization, cracking and alkylation.[18] Zeolites with optimum density and strength of acid sites seem to be suitable for hydrodeoxygenation of bio-oil/bio-oil model compounds. The structural framework of zeolite includes the atoms of silicon and/or aluminium having tetrahedral coordination to four oxygen atoms.[19,20] A zeolite consisting of only SiO_4 is electrically neutral but the presence of each AlO_4 in zeolite framework

Department of Chemical Engineering, Faculty of Engineering, University of Malaya, 50603 Kuala Lumpur, Malaysia. E-mail: h.shafaghat@gmail.com; pouya.sr@gmail.com; ashri@um.edu.my; Fax: +60 3 79675319; Tel: +60 3 79675297

† Electronic supplementary information (ESI) available. See DOI: 10.1039/c5ra00367a

RSC Advances

REVIEW

Cite this: *RSC Adv.*, 2015, **5**, 103999

Effective parameters on selective catalytic hydrodeoxygenation of phenolic compounds of pyrolysis bio-oil to high-value hydrocarbons

Hoda Shafaghat, Pouya Sirous Rezaei and Wan Mohd Ashri Wan Daud*

Received 22nd October 2015
Accepted 27th November 2015

DOI: 10.1039/c5ra22137d

www.rsc.org/advances

Pyrolysis bio-oil is recognized as a renewable and carbon-neutral fuel which could be a potential alternative for depleting fossil fuels. However, bio-oil is highly oxygenated and needs to be upgraded prior to be used as fuel additive. Catalytic hydrodeoxygenation (HDO) is an efficient technique for bio-oil upgrading. The reaction pathway for HDO of bio-oil is unknown since it is a mixture of hundreds of different compounds. The study on mechanism of transformation of these compounds could be helpful to propose an overall pathway for HDO of bio-oil. Phenols which are derived from pyrolysis of lignin fraction of biomass are considered as attractive model compounds for study of bio-oil HDO since they are highly stable in HDO reaction. Reaction pathway and product selectivity in HDO of phenols are highly affected by type of catalyst promoters and supports, catalyst preparation procedure, solvent type, chemicals used as co-feed and operating conditions (*i.e.*, temperature and pressure). The effects of these factors on selective production of high-value hydrocarbons of aromatics and alicyclics from HDO of phenol, cresol, guaiacol and anisole are discussed in this review.

1. Introduction

Increase of energy request, depletion of fossil fuel resources as well as growing environmental concerns have raised the importance of finding renewable and environmentally friendly fuel resource alternatives.[1,2] Lignocellulosic biomass is a sustainable source of second generation bio-fuel which can be substituted for fossil fuel.[3–6] Fast pyrolysis of biomass is a highly favorable technology for production of high yield of liquid fuel (up to 70 wt%).[1,2,4,7–9] Liquid fuel produced from fast pyrolysis of lignocellulosic biomass (named as pyrolysis oil or bio-oil) is considered as an economical fuel.[10–12] However, bio-oil has high contents of water (15–30 wt%) and oxygen (40–55 wt%) which cause some undesirable properties such as poor chemical and thermal stability, high viscosity (poor storage stability), corrosiveness (high acidity) and low heating value.[2,5,10,13–15] These negative properties of bio-oil can be removed by elimination of its oxygen content through an upgrading process. Catalytic hydrodeoxygenation (HDO) is a noteworthy method for bio-oil upgrading performed in a heterogeneous system including solid catalyst, hydrogen gas and liquid bio-oil under severe conditions (150–450 °C, 50–350 bar).[1,4,6–8,11,14,16–19] In catalytic HDO of bio-oil, oxygen is eliminated as water and/or carbon oxides.[1,3,4,14] Selection of a suitable catalyst is the main focus of researchers for efficient hydrotreating of bio-oil. Many studies have been conducted to develop catalysts with high catalytic activity and stability, low hydrogen consumption and high selectivity toward direct removal of oxygen.[20] So far, supported and/or unsupported conventional desulfurization catalysts, noble metal and transition metal catalysts have been applied in catalytic HDO.[1,2,4,10,11,14,15,21–23] Carbon,[1,15,17] alumina,[2,3,5,11,14] zeolites,[11,13,24–26] silica,[27–32] zirconia[6,29,32–34] and titania[6,7,34] are the common materials used as catalyst support in HDO process.

The reaction pathway for HDO of bio-oil is still unknown since it contains several hundreds of various organic compounds like acids, alcohols, aldehydes, esters, ketones, sugars, phenols and phenol derivatives resulting in hundreds of concurrent reactions during HDO of bio-oil.[2,3,5,6,8,14] Therefore, investigation on the transformation of bio-oil model compounds seems to be necessary in order to attain sufficient knowledge for prediction of an overall reaction pathway for bio-oil HDO.[4,14] Generally, model compounds are selected among the most reactive bio-oil compounds which lead to bio-oil instability.[10] Since reactive phenolic compounds constitute the main fraction of bio-oil[22,27,30,35–37] and the cleavage of $C_{aromatic}$–OH bond in these compounds is difficult,[37,38] many researches have been conducted in order to find suitable catalytic systems for HDO of phenols. Furthermore, phenolic compounds of bio-oil are the major cause for formation of coke precursors and catalyst deactivation during the upgrading process.[8,39] Therefore, hydrodeoxygenation of bio-oil phenolic compounds to value-added chemicals is a research field of great significance.

Generally, HDO of phenolic compounds leads to formation of aromatic and alicyclic products through direct

Department of Chemical Engineering, Faculty of Engineering, University of Malaya, 50603 Kuala Lumpur, Malaysia. E-mail: h.shafaghat@gmail.com; pouya.sr@gmail.com; ashri@um.edu.my; Fax: +60 3 79675319; Tel: +60 3 79675297